1   Emanuel Tschopp (1, 2, 3) and Octávio Mateus (1, 2)

2   1) GeoBioTec, Faculdade de Ciências e Tecnologia, Universidade Nova de Lisboa, Monte de

3   Caparica, Portugal

4   2) Museu da Lourinhã, Rua João Luis de Moura, 95, 2530-158 Lourinhã, Portugal

5   3) Dipartimento di Scienze della Terra, Università di Torino, Italy

6

7   Corresponding author: Emanuel Tschopp, Museu da Lourinhã, Rua João Luis de Moura, 95,

8   2530-158 Lourinhã, Portugal; +393426314421, tschopp.e@gmail.com

Introduction

Overview of diplodocid sauropods

The sauropod dinosaur clade Diplodocidae includes some of the most iconic sauropods. With their greatly elongated necks and tails, diplodocids constitute one of the typical popular images of sauropod dinosaurs. The clade is historically important, having provided the first published reconstruction of an entire sauropod skeleton ('*Brontosaurus*' *excelsus*; Marsh, 1883), the first complete sauropod skull to be described (*Diplodocus*; Marsh, 1884), and the first mounted sauropod specimen (*Apatosaurus* AMNH 460; Matthew, 1905). Diplodocids range from relatively small to gigantic sauropod species (*Kaatedocus siberi* Tschopp and Mateus, 2012, to *Supersaurus vivianae* Jensen, 1985, respectively), and include the well-known genera *Apatosaurus* Marsh, 1877a, *Diplodocus* Marsh, 1878, and *Barosaurus* Marsh, 1890. Their possible first occurrence dates to the Middle Jurassic of England (*Cetiosauriscus stewarti* Charig, 1980; but see Heathcote and Upchurch, 2003, or Rauhut et al., 2005, for a differential identification of *Cetiosauriscus*). Diplodocidae reacheds a peak in diversity in the Late Jurassic, with finds from North America, Tanzania, Zimbabwe, Portugal, Spain, as well as possibly England, Georgia, and China (Upchurch and Mannion, 2009; Mannion et al., 2012). To date, no convincing evidence exists for their presence in the Cretaceous (Whitlock et al., 2011), but their probable extinction at the Jurassic-Cretaceous boundary still remains a mystery (Taylor et al., 2011).

In recent phylogenetic trees, Diplodocidae consistently forms the sister group to the clade Dicraeosauridae, with which they form Flagellicaudata, which in turn is included, together with the Rebbachisauridae, in Diplodocoidea (e.g. Upchurch, 1998; Wilson, 2002, 2005; Harris and Dodson, 2004; Upchurch et al., 2004a; Rauhut et al., 2005; Harris, 2006c; Sereno et al., 2007; Whitlock, 2011a; Carballido et al., 2012b; Mannion et al., 2012; Tschopp and Mateus, 2013b). The taxonomy of the clade was historically somewhat confused, with "Diplodocidae" being used in the same way as Diplodocoidea today (see e.g. McIntosh, 1990a, b). In the following, we use the taxonomy and definitions as clarified by Taylor and Naish (2005).

Whereas the vast majority of diplodocid species were described in the late 1800s and early 1900s, additional taxa still continue to be discovered (see Tab. 1). The high rate of early descriptions, particularly during the so-called bone wars in the late 1800s, resulted also in a high amountlarge number of species that are now considered invalid, questionable, or

41 synonymous (Taylor, 2010). Species recognition is furthermore hampered by the fact that

42 many of the holotype specimens are incomplete and fragmentary (e.g. *Diplodocus longus*

43 YPM 1920), or appear to include bones of more than one individual (e.g. *Apatosaurus ajax*

44 YPM 1860). Due to the absence of field notes or quarry maps in many of these cases, it

45 remains difficult or even impossible to confidently assign the individual bones to particular

46 animals. Given that the majority of the sites in the Upper Jurassic Morrison Formation, which

47 yielded about three quarters of the reported diplodocid genera, are multi-taxon assemblages, it

48 is possible that some of these holotype specimens include material from different species.

49 This renders meaningful diagnoses for the species and thus the identification of new material

50 highly difficult. However, the detailed studies of original material and their corresponding

51 field notes by McIntosh and Berman (1975), Berman and McIntosh (1978), McIntosh (1981,

52 1990a, 1995, 2005), and McIntosh and Carpenter (1998), provided a wealth of important

53 information concerning the composition of diplodocid holotype specimens and species

54 recognition. Nonetheless, only one study that tested the validity of single species by means of

55 phylogenetic methods has been published to date, focusing on the genus *Apatosaurus*

56 alone~~only~~ (Upchurch et al., 2004b). By using individual specimens as operational taxonomic

57 units (OTUs), Upchurch et al. (2004b) ~~succeeded in obtaining a significant result, which~~

58 generally supported the traditional view of *Apatosaurus* intrarelationships.

59 The specimen-based phylogenetic analysis is herein extended to the entire clade of

60 Diplodocidae~~,~~ and combined with the most recent analyses of diplodocoid interrelationships

61 (Whitlock, 2011a; Mannion et al., 2012; Tschopp and Mateus, 2013b). It includes all holotype

62 specimens of every single putative diplodocid species ever described (see Tab. 2). The

63 phylogenetic analysis is furthermore expanded by adding reasonably complete and articulated

64 referred specimens from various sites in the Morrison Formation (e.g. *Diplodocus* sp. AMNH

65 223, Osborn, 1899; or *Barosaurus* sp. AMNH 6341, McIntosh, 2005). Among the additional

66 OTUs are also eight specimens from the Howe Ranch in the vicinity of Shell (Bighorn Basin,

67 Wyoming), one of which is herein described for the first time and identified as a previously

68 unknown species.

69 Howe Ranch: a rediscovered diplodocid El ~~d~~Dorado

70 The Howe Ranch sites have produced a high number of partially to almost completely

71 articulated dinosaur skeletons, sometimes even with soft tissue preservation (see Brinkmann

72 and Siber, 1992; Ayer, 2000; Schwarz et al., 2007c; Tschopp, 2008; Siber and Möckli, 2009;

73 Christiansen and Tschopp, 2010; Tschopp and Mateus, 2013b). Three sites proved

74 particularly productive: the Howe Quarry, the Howe-Stephens Quarry, and the Howe-Scott

75 Quarry (Fig. 1). The Howe Quarry was first worked by Barnum Brown for the American

76 Museum of Natural History (New York, USA) in 1934, and was later relocated and

77 completely excavated by a team from the Sauriermuseum Aathal (Switzerland), led by Hans-

78 Jakob 'Kirby' Siber (Brown, 1935; Ayer, 2000; Michelis, 2004; Tschopp and Mateus, 2013b).

79 The other two sites, as well as several smaller, less productive spots at various

80 ~~stratigraphy~~stratigraphic levels within the Morrison Formation, have since been discovered

81 nearby and excavated by the SMA (Ayer, 2000; Siber and Möckli, 2009; Christiansen and

82 Tschopp, 2010; Fig. 2). All three major sites yielded well-preserved and at least partially

83 articulated diplodocid specimens, both apatosaurine and diplodocine, of varying ontogenetic

84 stages (Fig. 3; Tab. 3). Only one of these specimens has yet been formally described (even

85 including the AMNH material from 1934), and now constitutes the holotype of *Kaatedocus*

86 *siberi* (Tschopp and Mateus, 2013b).

87 Due to the good preservation of the SMA material, the addition of these specimens to a

88 specimen-based phylogenetic analysis as attempted herein is of great importance. By doing

89 so, the anatomical overlap among different OTUs is greatly increased – a very welcome fact,

90 when many of the holotypes are fragmentary and only include few bones, as is the case in

91 Diplodocidae. In particular two specimens with articulated and almost complete skulls (SMA

92 0004 and 0011) yield important new data. Although the clade Diplodocidae has produced the

93 most skulls within sauropods (Whitlock et al., 2010), only two diplodocine (CM 3452, HMNS

94 175) and three apatosaurine specimens (CM 3018/11162, CMC 7180, YPM 1860) with

95 possibly articulated skull material were reported to date (Holland, 1906, 1924; McIntosh and

96 Berman, 1975; Berman and McIntosh, 1978; Barrett et al., 2011). Other than CM 11162,

97 which is probably the skull of CM 3018 (Berman and McIntosh, 1978), none of them has yet

98 been described in detail. This renders the identification of disarticulated skull material

99 extremely difficult, and impedes specimen-based phylogenetic analyses. The new specimens

100 described herein thus finally allow detailed reassessments of fragmentary material, including

101 type skeletons and disarticulated skulls.

102 **Institutional abbreviations**

103 **AC**, Beneski Museum of Natural History, Amherst College, Amherst, Massachusetts, USA;

104 **AMNH**, American Museum of Natural History, New York City, New York, USA; **ANS**,

105 Academy of Natural Sciences, Philadelphia, Pennsylvania, USA; **BYU**, Brigham Young

106 University, Museum of Paleontology, Provo, Utah, USA; **CCG**, Chengdu College of

107 Geology, Sichuan, China; **CM**, Carnegie Museum of Natural History, Pittsburgh,

108 Pennsylvania, USA; **CMC**, Cincinnati Museum Center, Cincinnati, Ohio, USA; **CMNH**,

109 Cleveland Museum of Natural History, Cleveland, Ohio, USA; **CPT**, Conjunto

110 Paleontológico de Teruel, Dinópolis, Teruel, Spain; **DMNS**, Denver Museum of Nature and

111 Science, Denver, Colorado, USA; **DNM**, Dinosaur National Monument, Jensen, Utah, USA;

112 **FMNH**, Field Museum of Natural History, Chicago, Illinois, USA; **GCP**, Grupo Cultural

113 Paleontológico de Elche, Museo Paleontológico de Elche, Elche, Spain; **GMNH**, Gunma

114 Museum of Natural History, Gunma, Japan; **HMNS**, Houston Museum of Nature and

115 Science, Houston, TX, USA; **ISIR**, Paleontological Collection, Geology Museum, Indian

116 Statistical Institute, Calcutta, India; **IVPP**, Institute of Vertebrate Paleontology and

117 Paleoanthropology, Chinese Academy of Sciences, Beijing, China; **KUVP**, Kansas University

118 Natural History Museum, Lawrence, Kansas, USA; **LACM**, Los Angeles County Museum of

119 Natural History, Los Angeles, USA; **MACN**, Museo Argentino de Ciencias Naturales,

120 Neuquén, Argentina; **MB.R.**, Museum für Naturkunde, Berlin, Germany; **MCF**, Museo

121 Carmen Funes, Plaza Huincul, Neuquén, Argentina; **MCNV**, Museo de Ciencias Naturales,

122 Valencia, Spain; **MDS**, Museo de Dinosaurios de Salas de los Infantes, Salas de los Infantes,

123 Burgos, Spain; **MIGM**, Museu Geológico do Instituto Geológico e Mineiro de Portugal,

124 Lisboa, Portugal; **ML**, Museu da Lourinhã, Lourinhã, Portugal; **MNN**, Musée National du

125 Niger, Niamey, Republic of Niger; **MOZ**, Museo Provincial de Ciencias Naturales 'Prof. Dr.

126 Juan A. Olsacher', Zapala, Neuquén, Argentina; **MPCA**, Museo Provincial Carlos

127 Ameghino, Cipolletti, Río Negro, Argentina; **MPEF**, Museo Paleontológico Egidio Feruglio,

128 Trelew, Argentina; **MUCPv**, Museum of the University of Comahue-Patagonia, Argentina;

129 **NHMUK**, Natural History Museum, London, United Kingdom; **NMB**, Staatliches

130 Naturhistorisches Museum Braunschweig, Germany; **NMMNH**, New Mexico Museum of

131 Natural History and Science, Albuquerque, New Mexico, USA; **NSMT**, National Museum if

132 Nature and Science, Tokyo, Japan; **OMNH**, Sam Noble Oklahoma Museum of Natural

133 History, Norman, Oklahoma, USA; **PMU**, Evolutionsmuseet Paleontologi, University of

134 Uppsala, Uppsala, Sweden; **SMA**, Sauriermuseum Aathal, Aathal, Switzerland; **SMNS**,

135 Staatliches Museum für Naturkunde, Stuttgart, Germany; **Tate**, Tate Geological Museum,

136 Casper College, Casper, Wyoming, USA; **UMNH**, Utah Museum of Natural History, Salt

137   Lake City, Utah, USA; **USNM**, United States National Museum, Smithsonian Institution,

138   Washington DC, USA; **UUVP**, University of Utah, Salt Lake City, Utah, USA; **UW**,

139   University of Wyoming Geological Museum, Laramie, Wyoming, USA; **WDC**, Wyoming

140   Dinosaur Center, Thermopolis, Wyoming, USA; **YPM**, Yale Peabody Museum, New Haven,

141   Connecticut, USA; **ZDM**, Zigong Dinosaur Museum of Sichuan Province, China.

142   **Anatomical abbreviations**

143   **a**, articular; **aal**, acetabular articulation surface length; **ac**, acetabular surface; **aCd,** anterior

144   caudal vertebrae; **acdl**, anterior centrodiapophyseal lamina; **acf**, anterior condyle fossa; **acl**,

145   acromion length; **acm**, acromion; **acpl**, anterior centroparapophyseal lamina; **acr**, acromial

146   ridge; **aCV**, anterior cervical vertebrae; **adt**, anterodorsal tuberosity; **aDV,** anterior dorsal

147   vertebrae; **af**, astragalus foramen; **al**, accessory lamina; **amb**, ambiens process; **amc**,

148   amphicoelous; **amCd**, anterior-most caudal vertebrae; **amp**, amphiplatyan; **an**, angular; **anp**,

149   antotic process; **aof**, antorbital fenestra; **ap**, anterior process; **apd**, anteroposterior depth; **apf**,

150   anterior pneumatic fossa; **apl**, anteroposterior length; **aprl**, anterior process length; **apw**,

151   anteroposterior width; **ar**, anterior ramus; **as**, astragalus; **asl**, accessory spinal lamina; **asp**,

152   ascending process; **at**, atlas; **ato**, anterior tooth; **avl**, anteroventral lip; **aW**, anterior width; **ax**,

153   axis; **axr**, axial rib; **Bc,** braincase; **bic**, biconvex; **bns**, bifid neural spine; **bo**, basioccipital;

154   **bph**, basipterygoid hook; **bpr**, basipterygoid process; **bs**, basisphenoid; **bt**, basal tuber; **c**,

155   carpal; **ca**, coracoid articulation; **cal**, calcaneum; **can**, crista antotica; **cap**, capitulum; **cc**,

156   cnemial crest; **Cd**, caudal vertebra; **cdf**, centrodiapophyseal fossa; **CF**, coracoid foramen; **Ch**,

157   chevrons; **chf**, chevron facet; **cl**, centrum length; **cl-cd**, centrum length without condyle; **cmw**,

158   centrum minimum width; **co**, coracoid; **comp**, compressed; **cph**, centrum posterior height;

159   **cpol**, centropostzygapophyseal lamina; **cpr**, crista prootica; **cprf**, centroprezygapophyseal

160   fossa; **cprl**, centroprezygapophyseal lamina; **CR**, cervical ribs; **CV**, cervical vertebra; **cw**,

161   centrum width; **d**, dentary; **dapd**, distal anteroposterior depth; **das**, anterior spur on

162   diapophysis; **db**, distal blade; **dCd**, distal caudal vertebrae; **dds**, dorsal spur on diapophysis;

163   **de**, dentin; **def**, deformed; **dg**, distal groove; **dH**, distal dorsoventral height; **di**, diapophysis;

164   **dip**, distal process; **dlr**, dorsolateral ridge; **dp**, diapophysis posterior process; **dpc**,

165   deltopectoral crest; **dpcl**, length deltopectoral crest; **DR**, dorsal ribs; **dro**, distal roller; **dsf**,

166   dorsal spinal fossa; **dt**, denticles; **dtw**, distal transverse width; **DV**, dorsal vertebra; **dw**, dorsal

167   width; **ec**, epicondyle; **EFS**, external fundamental system; **emf,** external mandibular fenestra;

168   **en**, enamel; **ep**, ectopterygoid; **epi**, epipophysis; **er**, ectopterygoid ramus; **est**, estimated; **ex**,

169   exoccipital; **f**, frontal; **fe**, femur; **fh**, femoral head; **fi**, fibula; **fic**, fibular condyle; **fif**, fibular

170   facet; **Fl**, forelimb; **fm**, foramen magnum; **FS**, facial skull; **ft**, fourth trochanter; **gh**, greatest

171   height; **GL**, glenoid; **h**, humerus; **Hap**, dorsoventral height anterior process; **hc**, haemal canal;

172   **hcd**, height condyle; **hct**, height cotyle; **Hdlp**, dorsoventral height dorsolateral process;

173   **Hdmp**, dorsoventral height dorsomedial process; **hh**, humeral head; **Hl**, hindlimb; **hna**, height

174   neural arch; **hns**, height neural spine; **Hvr**, dorsoventral length ventral ramus; **hya**,

175   hypantrum; **hys**, hyposphene; **ic**, interclavicle; **icg**, intercondylar groove; **il**, ilium; **inc**,

176   incomplete; **int sprl**, interrupted spinoprezygapophyseal lamina; **ip**, iliac peduncle; **is**,

177   ischium; **isa**, ischial articular surface; **isal**, ischial articular surface length; **j**, jugal; **la**,

178   lacrimal; **L aop**, length antotic process; **Lap**, length anterior process; **lco**, lateral condyle; **L**

179   **cpr**, length crista prootica; **LJ**, lower jaw; **Ll-oc**, lateral length contributing to orbit; **lprl**,

180   lateral process length; **Lpp**, length posterior process; **lprzc**, lateral prezygapophyseal cavity;

181   **lr**, lateral ridge; **ls**, laterosphenoid; **lsc**, lateral spine cavity; **lsp**, lateral spur; **lspol**, lateral

182   spinopostzygapophyseal lamina; **Ltb**, length tooth-bearing portion; **ltf**, laterotemporal

183   fenestra; **Lv**, length ventral edge **m**, maxilla; **Ma**, manus; **maxH**, maximum dorsoventral

184   height; **maxW**, maximum transverse width; **MB**, morphotype B element; **mc**, metacarpal;

185   **mCd**, mid-caudal vertebrae; **mco**, medial condyle; **mCV**, mid-cervical vertebrae; **mDV**, mid-

186   dorsal vertebrae; **minH**, minimum dorsoventral height; **minW**, minimum transverse width;

187   **mp**, medial process; **mr**, medial ridge; **mspol**, medial spinopostzygapophyseal lamina; **msw**,

188   midshaft width; **mt**, median tubercle; **mts**, metatarsal; **n**, external nares; **na**, nasal; **naf**, neural

189   arch foramen; **nc**, neural canal; **ncs**, neurocentral synostosis; **nf**, nutrient foramen; **ns**, neural

190   spine; **o**, orbit; **oc**, occipital condyle; **of**, obturator foramen; **olf**, olfactory foramen; **opc**,

191   opisthocoelous; **opf**, optic foramen; **os**, orbitosphenoid; **p**, parietal; **pa**, palate; **pabh**,

192   preacetabular blade height; **pap**, parapophysis; **papd**, proximal anteroposterior depth; **paof**,

193   preantorbital fossa; **par bns**, parallel bifurcated neural spine; **pas**, proximal articular surface;

194   **pCd**, posterior caudal vertebrae; **pcdl**, posterior centrodiapophyseal lamina; **PcG**, pectoral

195   girdle; **pcpl**, posterior centroparapophyseal lamina; **pCV**, posterior cervical vertebrae; **pd**,

196   proximal depth; **pdd**, proximodistal depth; **pDV**, posterior dorsal vertebrae; **Pe**, Pes; **pf**,

197   prefrontal; **phm**, manual phalanx; **php**, pedal phalanx; **pl**, pleurocoel; **plc**, posterolateral

198   crest; **plp**, posterolateral process; **pm**, premaxilla; **pnf**, pneumatic foramina; **po**, postorbital;

199   **pocdf**, postzygapophyseal centrodiapophyseal fossa; **podl**, postzygodiapophyseal lamina;

200   **popr**, paroccipital process; **posl**, postspinal lamina; **poz**, postzygapophysis; **pp**, posterior

201 process; **pp-fp**, distance posterior process to frontoparietal suture; **ppapd**, pubic peduncle
202 anteroposterior depth; **ppf**, posterior pneumatic fossa; **ppfo**, postparietal foramen; **pph**,
203 pneumatopore height; **ppl**, pneumatopore length; **ppw**, pubic peduncle transverse width; **pra**,
204 proatlas; **prap**, preacetabular process; **prapl**, preacetabular process length; **prc**, procoelous;
205 **prcdf**, prezygapophyseal centrodiapophyseal fossa; **prdl**, prezygodiapophyseal lamina; **pre**,
206 pre-epipophysis; **pro**, prootic; **prpl**, prezygoparapophyseal lamina; **prsl**, prespinal lamina;
207 **prz**, prezygapophysis; **ps**, proximal spur; **psr**, parasphenoid rostrum; **pt**, pterygoid; **ptc**,
208 platycoelous; **ptf**, posttemporal fenestra; **pto**, posterior tooth; **ptr**, vertical distance from
209 proximal articular surface to trochanter; **pts**, prezygapophysis transverse sulcus; **ptw**,
210 proximal transverse width; **pu**, pubis; **pua**, pubic articular surface; **pual**, pubic articular
211 surface length; **pup**, pubic peduncle; **pupl**, pubic peduncle length; **pvf**, posteroventral flanges;
212 **pvfo**, posteroventral fossa; **PvG**, pelvic girdle; **pvl**, posteroventral lip; **pvlp**, posterior
213 ventrolateral process; **pw,** posterior width; **q**, quadrate; **qj**, quadratojugal; **qr**, quadrate ramus;
214 **r**, radius; **rt**, tubercle for articulation with radius; **sa**, surangular; **saf**, surangular foramen; **sc**,
215 scapula; **sdf**, spinodiapophyseal fossa; **sh**, shaft height; **snc**, sagittal nuchal crest; **so**,
216 supraoccipital; **SP**, sternal plates; **spdl**, spinodiapophyseal lamina; **spof**,
217 spinopostzygapophyseal fossa; **spol**, spinopostzygapophyseal lamina; **sprl**,
218 spinoprezygapophyseal lamina; **sprl ab**, spinoprezygapophyseal lamina anterior bulge; **sq**,
219 squamosal; **sqr**, squamosal ramus; **SR**, sternal ribs; **stf**, supratemporal fenestra; **SV**, sacral
220 vertebrae; **sw**, shaft width; **sy**, sacricostal yoke; **sym**, symphysis; **T**, teeth; **tb**, tibia; **tc**, tooth
221 crown; **tic**, tibial condyle; **tif**, tibial facet; **tp**, transverse process; **tpol**, interpostzygapophyseal
222 lamina; **tprl**, interprezygapophyseal lamina; **tr**, tooth root; **tub**, tuberculum; **u**, ulna; **ucp**,
223 ulnar condylar processes; **ung**, ungual; **ut**, tubercle for articulation with ulna; **v**, vomer; **vk**,
224 ventral keel; **vlh**, ventral longitudinal hollow; **vlr**, ventrolateral ridge; **vmc**, ventral median
225 constriction; **vsf**, ventral spinal fossa; **wcd**, width condyle; **wct**, width cotyle; **wf**, wear facet;
226 **wpo**, width across postzygapophyses; **wpr**, width across prezygapophyses; **Wn**, width notch.
227 **Other abbreviations**
228 **AmAl**, *Amphicoelias altus*; **AtIm**, *Atlantosaurus immanis*; **AuBo**, *Australodocus bohetii*;
229 **C23-1**, state 1 of character 23; **CeSt**, *Cetiosauriscus stewarti*; **EI**, elongation index; **ew**, equal
230 weighting **HaPr**, *Haplocanthosaurus priscus*; **HOS**, histological ontogenetic stage; **HQ**,
231 Howe Quarry; **HScQ**, Howe-Scott Quarry; **HStQ**, Howe-Stephens Quarry; **iw**, implied
232 weighting; **mdA**, more derived Apatosaurines; **mdD**, more derived Diplodocoidea; **mdE**,

233 more derived Eusauropoda; **MOS**, morphological ontogenetic stage **OTU**, operational

234 taxonomic unit; **PMI**, premaxilla-maxilla index; **RI**, robustness index; **SI**, slenderness index;

235 **SHQ**, Spring Hill Quarry; **SuVi**, *Supersaurus vivianae*; **ToAf**, *Tornieria africana*.

Description of a new diplodocine species

Locality

238 The new specimen described in the following (SMA 0011) was found at the Howe-Scott

239 quarry, one of three major sites on the Howe Ranch, north of Shell, Wyoming. The Howe-

240 Scott quarry is located between the better known Howe Quarry (Brown, 1935; Ayer, 2000;

241 Michelis, 2004; Tschopp and Mateus, 2013b) and the Howe-Stephens quarry (Ayer, 2000;

242 Schwarz et al., 2007c; Christiansen and Tschopp, 2010; Fig. 1). The site was found in 1995 by

243 a team from the Sauriermuseum Aathal, Switzerland, and excavated in three periods (1995,

244 2000, 2002-2003). Stratigraphically, it lies just slightly above the Howe-Stephens quarry, 30

245 meters above the J-5, and 30 meters below the K-1 unconformities, which define the lower

246 and upper limits of the Morrison Formation, respectively (Michelis, 2004; Fig. 2). In addition

247 to SMA 0011, five partial diplodocid specimens (mostly appendicular material), a possible

248 brachiosaur hindlimb, two partly-to-almost complete *Hesperosaurus* (Ornithischia,

249 Stegosauria), some *Othnielosaurus* bones (Ornithischia, Neornithischia), numerous shed

250 theropod teeth, carbonized wood, and various freshwater shells were recovered at the Howe-

251 Scott quarry (Michelis, 2004; ET, pers. obs., 2003). However, none of these specimens has

252 yet been ~~formerly~~formally described or identified.

Material

254 **SMA 0011.** The specimen SMA 0011 consists of an almost complete, disarticulated skull,

255 eleven cervical vertebrae (probably CV 1-6, 8, 9, 11, 12, and 15, see below), the complete

256 dorsal column, including several dorsal and sternal ribs, a partial sacrum, the right scapula and

257 coracoid, both humeri, the left ulna, radius and manus, the right ilium and pubis, a left

258 ischium, femur, tibia, fibula and nearly complete pes. The specimen was found in two parts:

259 1) skull and vertebral column from the atlas to DV 3, and 2) dorsal vertebrae 4 to 10, sacrum,

260 and appendicular elements (Fig. 4). It is interpreted to belong to a single individual due to

261 matching size, no overlap of elements, and an extremely similar pattern of neurocentral

262 closure in cervical and dorsal vertebrae (see below). The specimen SMA 0011 was excavated

263 in 1995 and 2000.

Systematic Paleontology

Dinosauria Owen, 1842

Sauropoda Marsh, 1878

Eusauropoda Upchurch, 1995

Neosauropoda Bonaparte, 1986

Diplodocoidea Marsh, 1884 (see Upchurch, 1995)

Flagellicaudata Harris and Dodson, 2004

Diplodocidae Marsh, 1884

Diplodocinae Marsh, 1884

Galeamopus gen. nov.

Type species. *Galeamopus hayi* (Holland, 1924)

Diagnosis. *Galeamopus* is diagnosed by the following autapomorphies: portion of the parietal contributing to the skull roof is practically inexistent (unique among Flagellicaudata), a foramen in the notch that separates the two basal tubera (unique among Diplodocinae), well-developed anteromedial processes on the atlantal neurapophyses, which are distinct from the posterior wing (unique among Diplodocoidea), the posterior wing of atlantal neurapophyses remains of subequal width along most of its length (unambiguous), and the axial prespinal lamina develops a transversely expanded, knob-like tuberosity at its anterior end (unambiguous).

Etymology. 'Galeam' means helmet, and 'opus' need, necessity in Latin, remembering and honoring the two 'Williams' intimately connected with the genoholotype specimen HMNS 175: William H. Utterback and William J. Holland. The English name 'William' derives from the German name 'Wilhelm', meaning "want helmet, protection". Utterback found HMNS 175 in 1902 and Holland described its braincase in 1906, and named the holotype species *G. hayi* as *Diplodocus hayi* in 1924 – although already stating that the morphological differences between *G. hayi* and *Diplodocus* might prove to allow the erection of a new genus in future. *Galeamopus* is also an allusion to the fact that the fragile braincase is the only described part of the holotype skeleton to date. Last but not least, the referred specimen SMA 0011 was informally called "Max", after the kid's story 'Max and Moritz' from the German writer Wilhelm Busch.

Comments. The holotype specimen SMA 0011 is housed at Sauriermuseum Aathal, Switzerland. This museum is open to the public, and specimens are available for study by researchers ~~director, vice-director, and staff, are allowing and even actively offering their specimens for various research purposes~~ (see Schwarz et al., 2007; Klein and Sander, 2008; Christiansen and Tschopp 2010; Carballido et al. 2012a; Klein et al., 2012; Tschopp and

Mateus, 2013a, 2013b). The excavations are very well documented, and the preparation of the material follows the latest scientific standards. ~~For all his scientific and educational effort with the Sauriermuseum, its founder and present director Hans-Jakob Siber received the honorary doctor title of the University of Zurich (Switzerland) as well as the Amanz-Gressly Award of the Swiss Society of Paleontology in 2010.~~ The museum recognizes the scientific importance of holotype specimens, and takes all efforts to preserve them and provide permanent public access. The policy is publicly stated on their homepage (http://www.sauriermuseum.ch/de/museum/wissenschaft/wissenschaft.html).

The specimen itself is currently being further prepared in order to mount it. In the display mount, particular attention will be pa~~ye~~id to easy access for researchers.

Description of SMA 0011

Terminology. Anatomical terms ~~are used following~~used here follow the traditional use of anterior and posterior instead of cranial and caudal. Vertebral laminae and fossae are described following the nomenclature of Wilson (1999) and Wilson et al. (2011), respectively, with the changes proposed by Tschopp and Mateus (2013b).

Skull (Figs 5-14; Tab. 4)

The skull of *Galeamopus* ███████ SMA 0011 has a typically diplodocid shape. It is elongate, with the external nares retracted and dorsally facing, and slender, peg-like teeth (Figs 5-7). Given the completeness of the skull, a reconstruction was created in cooperation with the Portuguese illustrator Simão Mateus (ML; Fig. 8). When ~~comparing~~compared with recent reconstructions of the skull of *Diplodocus* (Wilson and Sereno, 1998; Whitlock, 2011b), ~~it can be seen that~~ *Galeamopus* has a more triangular skull outline in lateral view, and more sinuous ventral maxillary edges in dorsal view (Fig. 8).

Premaxilla. The premaxillae are completely preserved. They are anteroposteriorly long and transversely narrow elements that contact each other medially and the maxillae laterally. The posterior end of the premaxillae delimits the nasal opening anteriorly. In dorsal view, the elements are narrow in their central part and widen anteriorly and posteriorly. The anterior edge is straight to slightly convex, whereas the posterior margin is deeply concave, such that the two premaxillae together form a triangular process that enters the nasal opening. The medial margin is straight, and the lateral one concave due to the central narrowing of the element. Some nutrient foramina are present on the anterior-most portion of the dorsal surface, as is a groove originating at the premaxillary-maxillary contact, and extending

360　obliquely anteromedially. The groove is faint and relatively short, not reaching either the

361　anterior or the medial margin. Such a groove was usually interpreted as typical for

362　dicraeosaurids (Remes, 2009; Whitlock, 2011a), but is also present in other diplodocids (ET,

363　pers. obs., 2011). However, a fading out of this feature is uncommon in dicraeosaurids, where

364　the groove is distinct (Janensch, 1935; Remes, 2009). Ventrally, the anterior portion of the

365　premaxillae thickens slightly dorsoventrally in order to bear the replacement teeth, but not to

366　the extent seen in USNM 2673 (ET, pers. obs., 2011). Five teeth are mounted, but only four

367　alveoli are present occur in the left element, whereas the right premaxilla appears to show five.

368　The alveoli of the articulated premaxillae do not contact each other medially, such that there

369　would be space for two more teeth in between, or a gap. At the border with the maxilla, where

370　the premaxilla narrows from the broader anterior part to the narrow central part, the two bones

371　form an elongated fossa which bears the subnarial and the anterior maxillary foramen. Both

372　foramina lie on the medial edge of the maxilla, very close together.

373　**Maxilla.** Only the right maxilla is preserved, and it is complete. The broad anterior portion

374　bears a posterior process, which contacts the jugal and quadratojugal, and a posterodorsal

375　process, which contacts the lacrimal, nasal, and possibly the prefrontal. The maxilla forms the

376　dorsal, anterior, and anteroventral margins of the antorbital fenestra, and completely encloses

377　the preantorbital fossa and fenestra. Unlike *Kaatedocus* and *Dicraeosaurus*, the preantorbital

378　fossa is pierced by a large fenestra. The fenestra is dorsally capped by a distinct ridge similar

379　to *Diplodocus*, but unlike *Apatosaurus*. This distinct dorsal edge was previously thought to

380　represent an autapomorphy of *Diplodocus*, but was shown to be present occur in other taxa as

381　well (Tschopp and Mateus, 2013b). The preantorbital fenestra does not fill the entire

382　preantorbital fossa: the anterior-most area remains closed by a thin bony wall. The fossa is

383　anterodorsally accompanied by a short, narrow groove more or less following the curvature of

384　the anterior end of the dorsal rim of the fossa. The posterior end of the fossa is interconnected

385　with the central portion of the antorbital fenestra by a distinct groove that extends

386　posterodorsally to the dorsal corner of the posterior process, which is regarded as an

387　autapomorphy herein (Fig. 9). Remaining parts of the dorsal surface of the maxilla do not bear

388　other distinctive morphological features, with the exception of the anterior-most portion,

389　where a few nutrient foramina can be seen, similar to those present on the premaxilla.

390　**Prefrontal.** Both prefrontals are present and complete. They contact the frontals posteriorly,

391　the nasals medially, the lacrimal laterally, and the maxilla anterolaterally. The prefrontals are

392 short, anteroposteriorly convex elements. Their lateral margin is straight, the medial one with

393 an anterior and a posterior concavity for the attachment of the nasal and the frontal,

394 respectively. A sharply pointed, medially projecting process separates the two concavities.

395 The posterior edge is anterolaterally-posteromedially oriented, forming a hook-like

396 posteromedial process as is typical for Diplodocidae (Wilson, 2002; Whitlock, 2011a). The

397 process almost reaches the frontal midlength, as is the case in diplodocine skulls CM 3452

398 and 11161 (ET, pers. obs., 2011). Anteriorly, the prefrontal tapers to a narrow tip, which is

399 slightly dorsoventrally expanded. The left element bears a small nutrient foramen on the

400 dorsal surface of the anterior part. The ventromedial edge is very distinct.

401 **Frontal.** Both frontals are completely preserved. They contact the prefrontal anterolaterally,

402 the nasal anteromedially, the other frontal medially, the parietal posteromedially, and the

403 postorbital posterolaterally. Ventrally, the frontal makes contact with the braincase,

404 articulating with the orbitosphenoid. The frontals have a smooth dorsal surface, which is

405 slightly convex posterolaterally-anteromedially. Their medial border is generally straight, but

406 curves laterally at its posterior and anterior ends. Both a pineal fenestra (as in dicraeosaurids;

407 width 14 mm) and an anterior notch are thus present (as in *Kaatedocus*; length 18 mm). The

408 anterior notch is rather V-shaped than U-shaped as in *Kaatedocus*, and wider than in

409 *Spinophorosaurus* (Knoll et al., 2012; Tschopp and Mateus, 2013b). The anterior margin of

410 the frontal is strongly convex in order to accommodate the posterior, hook-like process of the

411 prefrontal anterolaterally. From the posterior-most point of the posterior process of the

412 prefrontal, the frontal has a straight edge extending obliquely anterolaterally, before it reaches

413 the lateral edge, with which it includes a very acute angle. The lateral border is distinctly

414 concave in dorsal view, smooth in its anterior part, but becoming highly rugose posteriorly,

415 close to where it articulates with the postorbital. Posteriorly, the lateral and posterior edges

416 form an acute angle. The lateral portion of the posterior margin is slightly displaced

417 anteriorly, compared to the medial portion, resulting in a somewhat sinuous posterior edge.

418 Ventrally, the frontals are marked by a distinct ridge, extending obliquely from the

419 anterolateral corner, below the posterior process of the prefrontal, to an elevated, broad area

420 for the attachment of the braincase.

421 **Postorbital.** Both elements are complete. The postorbital is a triradiate bone with an anterior

422 process articulating with the jugal, a posterior process overlapping the squamosal laterally,

423 and a dorsomedial process covering the frontal posteriorly and connecting to the anterolateral

424 process of the parietal posteromedially, thereby excluding the frontal from the margin of the

425 supratemporal fenestra. Anteromedially, the dorsomedial process abuts the antotic process of

426 the braincase. The anterior process has a subtriangular cross section, long dorsally and

427 ventrally, with a narrow lateral and an even thinner medial margin. The anterior process is

428 dorsally slightly concave. Towards the anterior end, it tapers to a point. The posterior process

429 is short and triangular. At its base, one (on the right postorbital) or two (on the left element)

430 nutrient foramina can be seen. The process is compressed transversely. The dorsomedial

431 process is dorsoventrally concave anteriorly and convex posteriorly. It is relatively high

432 dorsoventrally, but narrow anteroposteriorly. It is anteroposteriorly broader laterally than

433 medially. The anterior face of the dorsomedial process is marked by a horizontal ridge at its

434 base. The ridge supports the posterior edge of the frontal.

435 **Jugal.** Both jugals are preserved and complete. The jugal is a flat, relatively large bone with a

436 posterior process contacting the postorbital, and a dorsal process articulating with the

437 lacrimal. The main portion connects to the quadratojugal ventrally and the maxilla anteriorly.

438 The jugal forms the anteroventral rim of the orbit, the posteroventral border of the antorbital

439 fenestra, as well as the anterodorsal edge of the laterotemporal fenestra. The bases of the

440 dorsal and posterior processes are relatively broad, before they taper dorsally and posteriorly,

441 respectively. The anterior edge of the jugal is slightly concave, as is the anteroventral margin.

442 Therefore, these two edges include an acute angle.

443 **Quadratojugal.** The quadratojugals are both complete. They are transversely thin bones with

444 a posterior dorsal process overlying the quadrate laterally, and a long anterior ramus

445 contacting the jugal dorsally and the maxilla anteriorly. The quadratojugals form the

446 anteroventral margins of the laterotemporal fenestra, and the ventral border of the skull. The

447 anterior ramus of the quadratojugal is narrow at its base but extends dorsoventrally towards its

448 anterior end. The ventral edge is almost straight; it is thus the concave dorsal margin of the

449 anterior ramus that accounts mostly for this dorsoventral expansion. The shape of the anterior

450 margin is not discernible in the mounted skull. The dorsal process is less than half the length

451 of the anterior process. It is inclined posterodorsally, as in all diplodocids (Upchurch, 1998;

452 Wilson, 2002; Whitlock, 2011a). It is anteroposteriorly convex externally, relatively broad at

453 its base, and tapers to a point dorsally, reaching about midlength of the quadrate shaft.

454 **Lacrimal.** Only the dorsal half of the left lacrimal is presentpreserved. It is a narrow element

455 expanding towards its dorsal end, where it contacts the posterodorsal process of the maxilla

456 anteriorly, the prefrontal dorsally, and possibly the nasal medially. Ventrally, the lacrimal

457 would contact the jugal, if preserved. The lacrimal is the element separating the orbit from the

458 antorbital fenestra. It is anteroposteriorly narrow in its ventral half, with a triangular cross

459 section, ~~being~~ flat externally but bearing a distinct dorsoventral ridge internally. The anterior

460 edge develops a short, but dorsoventrally high, anterior process at its dorsal end. The posterior

461 margin is generally straight, with only a weak bulge on its dorsal portion. The dorsal-most end

462 curves backwards, below the prefrontal. The internal ridge becomes slightly higher dorsally,

463 posteriorly enclosing the lacrimal foramen, which is small and shallow in SMA 0011.

464 **Quadrate.** Only the right quadrate is preserved, but it is complete. It has a complex anatomy,

465 with a quadrate shaft articulating with the squamosal and the paroccipital process

466 posterodorsally and posteroventrally, respectively; a pterygoid flange interconnecting the

467 outer skull with the pterygoid medially; and a ventral ramus ~~being~~ overlapped by the

468 quadratojugal externally and bearing the articulating surface with the lower jaw ventrally. The

469 quadrate shaft is elongate posteriorly, and has concave dorsal and lateroventral surfaces. The

470 lateral edge is a thin crest, where it is not capped by the squamosal or the quadratojugal. The

471 posterior surface of the quadrate shaft and the ventral ramus is shallowly concave, forming the

472 quadrate fossa. The pterygoid flange originates on the medial half of the quadrate shaft. It is

473 very thin mediolaterally, but anteroposteriorly long, and curves medially at its dorsal tip. The

474 dorsal edge of the flange is straight and more or less horizontally oriented. The medial side of

475 the pterygoid flange is concave, but does not form such a distinct fossa like that which is

476 present autapomorphically in *Kaatedocus* (Tschopp and Mateus, 2013b). The ventral ramus is

477 subtriangular in cross-section, with concave anterior and posterolateral surfaces. It has a

478 thinner lateral than medial margin. The articular surface is subtriangular, with a concave

479 anterior border, and a pointed posterior corner. The entire ventral ramus of the quadrate of

480 SMA 0011 is posterodorsally inclined, as in all diplodocids (Upchurch, 1998; Wilson, 2002;

481 Whitlock, 2011a).

482 **Squamosal.** Both squamosals are preserved, but lack a part of their anterior process (the right

483 one more so than the left). The squamosals form the posteroventral corner of the skull. They

484 have a complicated morphology, ~~having to accommodate~~accomodating a variety of elements

485 from the braincase and outer skull. The anterior process overlies the posterior end of the

486 quadrate. Dorsally, the squamosal is laterally covered by the posterior process of the

487 postorbital~~,~~ and forms the external margin of the supratemporal fenestra. Posteriorly the

squamosal it contacts the paroccipital processes, and dorsoposteriorly the posterolateral process of the parietal. The squamosal is strongly curved posterolaterally. The anterior process appears to be the longest of all squamosal processes, even though it is not preserved in its entire length. The ventral edge of the squamosal develops a short ventral projection at its posterior end, similar to, but much less distinct than the ventral prong as present in advanced dicraeosaurids (Salgado and Calvo, 1992; Whitlock, 2011a). A concave area appears to be present on the laterodorsal surface, in order to accommodates the posterior process of the postorbital. Other morphological features are difficult to observe in the articulated and reconstructed skull of SMA 0011.
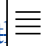
Parietal. Both parietals are complete but slightly distorted. They are tightly sutured with the frontals anteriorly, and develop a short anterolateral process to contact the dorsomedial process of the postorbital, with which they form the anterior margin of the supratemporal fenestra. The posterior face of the parietal contacts the exoccipital and the supraoccipital medioventrally. The posterolateral process of the parietal forms the posterior margin of the supratemporal fenestra and reaches the squamosal laterally. The dorsal portion of the parietal in SMA 0011 is very narrow. The two elements do not touch each other medially, but this appears to be due to postmortem breakage of the extremely thin bone behind the parietal fenestra, which the parietals form together with the frontals. The dorsal portion is flat, and not well separated from the posterior surface by a ridge like that present in *Kaatedocus*. It The parietal widens anteroposteriorly at its lateral end, where it develops a short anterolateral and a long and dorsoventrally deep posteroventral process. The parietal thus contributes most to the margin of the supratemporal fenestra. The posterior surface has an oblique ventromedial border, which has a very sinuous suture together with the supraoccipital. The dorsal margin of the posterolateral process is straight as well, and does not cover the anterior border of the supratemporal fenestra in posterior view. Their ventral edges are excluded from the posttemporal fenestra by the squamosal and a laterally projecting spur of the exoccipital.

Supraoccipital. The supraoccipital is complete, and fused with the parietals and the exoccipital-opisthotic complex. It The supraoccipital is a somewhat hexagonal bone, that which contacts the parietals dorsolaterally, the exoccipital-opisthotic complex ventrolaterally, and borders the foramen magnum ventrally. The supraoccipital is fused with the exoccipital-opisthotic, and the suture is barely visible. The dorsolateral edges of the supraoccipital are slightly concave. The ventrolateral edges are only laterally indicated. More medially, the

520 suture is not traceable up to the foramen magnum, but probably extended below the two

521 distinct tubercles located dorsolaterally to the foramen magnum. These tubercles served for

522 the attachment of the proatlases. The tubercles are ellipsoid, and oriented with their long axes

523 extending dorsomedially-ventrolaterally. The elevation is much more distinct ventrally than

524 dorsally. The dorsal portion of the supraoccipital bears a complex arrangement of ridges and

525 concavities, as if it would lack an additional element topping this structure. No distinct

526 sagittal ridge is present, but if an element is lacking, it could be this element that forms the

527 crest (Fig. 10). However, it has never been reported that the sagittal nuchal crest derives from

528 an additional skull element. This would thus be highly unusual and possibly autapomorphic.

529 The supraoccipital is ~~widest slightly more~~slightly wider ventrally than dorsally. No distinct

530 foramina ~~are present~~occur close to the border with the parietal, unlike in *Kaatedocus*

531 (Tschopp and Mateus, 2013b). The dorsolateral edges of the supraoccipital are straight, not

532 concave as in *Apatosaurus* CM 11162, or MB.R.2388, where it forms a distinct dorsal

533 elevation (Berman and McIntosh, 1978; Remes, 2009).

534 **Exoccipital-opisthotic complex.** This outer portion of the braincase is completely preserved.

535 No sutures can be seen between the exoccipital and the opisthotic. They bear two elongate

536 paroccipital processes that extend lateroventrally to articulate with the squamosal and the

537 posterior end of the quadrate. Ventrally, the exoccipital-opisthotic borders almost the entire

538 the foramen magnum except for a small dorsal contribution of the supraoccipital. The

539 exoccipital contributes the dorsolateral corners to the occipital condyle. As in *Suuwassea* and

540 *Diplodocus* CM 11161, the exoccipital almost excludes the basioccipital from the

541 participation in the dorsal surface of the occipital condyle (Harris, 2006a). The paroccipital

542 processes have slightly convex external surfaces, but do not bear a ridge as in *Kaatedocus*

543 (Tschopp and Mateus, 2013b). The ventral edge is straight, only the dorsal corner of the distal

544 end is expanded dorsally, resulting in a distinctly concave dorsal edge. The lateral margin of

545 the paroccipital process is subtriangular, with a longer, vertically oriented dorsal portion, and

546 a shorter, laterally inclined ventral part. In lateral view, it is straight, unlike the curved ends of

547 the element in *Suuwassea* (Harris, 2006a; ANS 21122, ET, pers. obs., 2011).

548 **Basioccipital and basisphenoid.** The basioccipital forms the main portion of the occipital

549 condyle. It is relatively short and connects the articular surface of the occipital condyle with

550 the basal tubera, which are of about the same width. The articular surface is offset from the

551 condylar neck. Narrow ridges connect the central part of the condylar neck with the

552 posteromedial corner of the basal tubera, and the lateral face with the posterolateral corner.

553 The posterior surface of the basal tubera is therefore concave, as are the lateral surfaces of the

554 basioccipital. The basal tubera are box-like, and separated by a distinct, but relatively narrow

555 notch. The ventral edges of the tubera form a nearly straight line in posterior view, whereas

556 the anterior edges are angled in a wide V-shaped manner in ventral view. Anteriorly, the

557 basipterygoid processes attach to the tubera. In the reconstructed skull, t̲the processes are

558 mounted slightly dorsal to their actual location, above the anteroventral end of the crista

559 prootica. When articulated properly, they would be elongate (5.3 times longer than wide), and

560 straight, and would also includeform a narrower angle than as mounted. This is important

561 asbecause shorter and more widely diverging basipterygoid processes are typical for

562 *Apatosaurus*, whereas narrower angles are presenttypical in *Diplodocus* (Berman and

563 McIntosh, 1978). The processes are not as well connected at their base as is the case in

564 *Kaatedocus* (Tschopp and Mateus, 2013b). The distal ends of the basipterygoid processes are

565 expanded.

566 **Orbitosphenoid.** The orbitosphenoids delimit the endocranial cavity anteriorly, and attach to

567 the frontals and parietals dorsally, the contralateral orbitosphenoidsthemselves medially, and

568 the laterosphenoids lateroventrally. Each orbitosphenoid is relatively wide dorsally and

569 develops an anteroventral process, which is expanded at its end and separates the two

570 openings for cranial nerves II medially (the optic foramen) and III laterally (the trigeminal

571 foramen; Janensch, 1935; Harris, 2006a; Balanoff et al., 2010). Other than in *Suuwassea*

572 (Harris, 2006a), the optic foramen is bridged over by bone medially. Anterodorsally, the two

573 orbitosphenoids form the olfactory fenestra together with the frontals (Janensch, 1935;

574 Balanoff et al., 2010), and posterolaterally, at the junction with the laterosphenoid, the

575 foramen for cranial nerve IV (the trochlear foramen; Balanoff et al., 2010) defines the outline

576 of the orbitosphenoid.

577 **Laterosphenoid.** The laterosphenoid mainly consists of a crest that develops the antotic

578 process posterodorsally and extends anteroventrally to join the crista prootica. It connects to

579 the parietal posteriorly, the orbitosphenoid anterodorsally, and the prootic posteroventrally.

580 As for the orbitosphenoid, also the laterosphenoid outline is defined by various openings: the

581 cranial nerves III and IV anterodorsally at the junction with the orbitosphenoid, the facial

582 foramen posterodorsally (cranial nerve V; Balanoff et al., 2010), as well as the oculomotor

583 foramen and the abducens foramen anteroventrally (Balanoff et al., 2010).

584 **Prootic.** The prootic lies between the laterosphenoid anterodorsally, the parietal and
585 paroccipital processes posterodorsally, and the basisphenoid anteroventrally. ~~It~~The prootic
586 bears the well-developed crista prootica, which extends relatively far laterally, but is very thin
587 dorsoventrally. It does not end in an additional transverse expansion anteriorly, as is typical
588 for dicraeosaurids (Janensch, 1935). Posteriorly, the crista prootica extends to the base of the
589 paroccipital processes, where it separates foramina IX to XI from XII (Janensch, 1935; Harris,
590 2006a).

591 **Pterygoid.** The left pterygoid is ~~preserved, but is~~ only partly prepared (Fig. 11). The
592 pterygoid connects the quadrate posterolaterally with the basipterygoid processes
593 posteromedially, the ectopterygoid and palatine anterolaterally, and the vomer anteromedially.
594 The two elements would join along the midline of the skull. The pterygoid of SMA 0011
595 resembles the same bone in CM 3452 in its dorsoventrally deeper shape compared to
596 *Camarasaurus* and *Giraffatitan* (McIntosh and Berman, 1975). ~~It bears a~~A shallow
597 articulation facet for the basipterygoid processes~~, without a~~ lacks the hook-like process ~~as~~
598 present in dicraeosaurids and *Camarasaurus* (Wilson, 2002; Whitlock, 2011a).

599 **Hyoid.** Only the right hyoid is preserved, but appears to be almost complete (Fig. 12). It is a
600 narrow bone, with a distinct upward curve at midlength. The anterior ramus becomes
601 transversely flattened towards its anterior end, which bears a shallow longitudinal groove on
602 the medial side. The hyoid slightly widens dorsoventrally where it curves upwards and
603 towards the squamosal, as was shown in *Tapuiasaurus* (Zaher et al., 2011). The posterodorsal
604 end is rounded and offset from the shaft by a distinct rim.

605 **Mandible**

606 **Dentary.** Both dentaries are preserved. The dentary is the anterior-most bone of the lower jaw
607 and the only one bearing teeth. Posteriorly, it is followed by the surangular dorsally and the
608 angular ventrally. Internally, it is overlain by the splenial ventrally. The dentary is a thin bone,
609 with a dorsoventrally high dentigerous portion, developing the typical 'chin' of
610 flagellicaudatans (Upchurch, 1998; Whitlock, 2011a). Posterior to the tooth bearing portion,
611 the dentary tapers dorsoventrally, the right one much more so than the left. The symphysis is
612 oblong and strongly anteriorly inclined.

613 **Surangular.** Both surangulars are present. This bone is very flat transversely, curves ventrally
614 at its posterior end and bears a foramen at its highest point, which is also the highest point of
615 the entire lower jaw. The jaw thus does not develop a coronoid eminence.

616 **Angular.** Both angulars are ~~preserved but~~ incomplete anteriorly. They are concave externally,
617 due to the laterally curving ventral edge. They taper relatively continuously anteriorly, but
618 abruptly at their posterior ends, where they expand transversely in order to accommodate the
619 articular, which is not preserved.
620 **?Prearticular.** Both prearticulars appear to be present, but are partly hidden in the mount or
621 only partially prepared (Fig. 13). They are ~~very~~ thin, elongate bones that taper posteriorly. A
622 very shallow groove marks the probable lingual surface, extending anteroposteriorly,
623 following the somewhat sinuous curve of the dorsal edge of the bone. In its anterior half, the
624 bone becomes slightly thicker and curves outwards.
625 **Teeth.** The teeth have the typical diplodocoid, peg-like shape (Fig. 14). They are slightly
626 wrinkled but do not have denticles. Worn teeth usually have ~~one~~a single wear facet at a low
627 angle to the long axis of the tooth, but some teeth also show two facets that are conjoined
628 medially. In these teeth, the lingual facet is more steeply inclined than the labial one. The
629 crown tips are slightly wider than deep, which is especially ~~well~~ visible in replacement and/or
630 unworn teeth, which have a very weakly spatulate upper-most crown. The enamel is
631 distributed evenly on all sides, and no grooves mark the lingual face. In the jaws, the teeth are
632 inclined anteriorly compared to the long axis of the jaw, and set side-by-side without
633 overlapping each other. There are at least eleven, possibly twelve, dentary teeth.
634
635 **Cervical vertebrae (Figs 15-22; Tab. 5)**
636 **Proatlas.** The right proatlas is preserved and complete (Fig. 15). It is strongly curved and
637 tapers distally. The proximal articular surface is ovoid, with the largest width located in the
638 dorsal half. The medial surface is concave, the lateral one convex. The proatlas of SMA 0011
639 is different from the element in *Kaatedocus* due to its much narrower distal tip.
640 **Atlas.** The atlantal centrum is not fused to the neurapophyses (Fig. 16). It has a well-
641 developed anteroventral process as is typical for diplodocids, but convergently present in
642 several other sauropods (Mannion, 2011; Whitlock, 2011a). A large foramen lies between the
643 posterior knobs of the intercentrum. The lateral surface of the centrum is concave and bears a
644 foramen as well. The neurapophyses have a relatively wide base, and turn upwards and
645 backwards to articulate with the prezygapophyses of the axis. A wide medial process develops
646 anteriorly, as in AMNH 969 (Holland, 1906). This process articulates with the proatlas, and is
647 much better developed than in *Diplodocus carnegii* CM 84 or *Kaatedocus* (Hatcher, 1901;

648 Tschopp and Mateus, 2013b). A small but distinct subtriangular process ~~is present~~occurs on

649 the opposite side of the medial process, projecting laterally.

650 **Axis.** The axis of SMA 0011 (Fig. 16A) has a closed but still slightly visible neurocentral

651 synostosis, and separate cervical ribs. The centrum is opisthocoelous. The pleurocoel extends

652 over almost the entire centrum, with short horizontal ridges at its anterior and posterior end.

653 No vertical subdivision of the pleurocoel is present. Anteriorly, the pleurocoel extends onto

654 the parapophysis. The ventral surface of the centrum bears a distinct longitudinal keel in its

655 posterior portion. The parapophysis is rounded, and faces anterolaterally and slightly

656 ventrally. The neural arch is high and weakly posteriorly inclined. The prezygapophyses are

657 not preserved. The only well-defined lamina is the podl. The prsl is slightly expanded

658 transversely at its anterior end, similar to, but not as distinct as in AMNH 969 (ET, pers. obs.,

659 2011). The diapophysis projects somewhat posteriorly, but does not bear a distinct posterior

660 process. In lateral view, the anterior edge of the neural spine is slightly concave at its base,

661 and straight in the upper part. The spine top is rugose, slightly expanded transversely, and

662 entirely restricted anterior to the postzygapophyseal facets. This anterior restriction is unusual

663 for sauropods, but present in *Diplodocus carnegii* CM 84 (Hatcher, 1901), and could thus

664 represent a diplodocine synapomorphy. Other than in CM 84, however, the neural spine

665 summit of SMA 0011 develops a posterior projection, similar to the condition in *Giraffatitan*

666 (Janensch, 1950). The spol is strongly concave, becoming vertical on the upper part. Small

667 epipophyses are present laterally above the postzygapophyses, which do not project

668 backwards. A large rugose area is present on the lateral side of spine, slightly above mid-

669 height. It is ~~of~~ subtriangular ~~shape~~, broader towards the spol, ~~and~~ with a pointed, elongate tip

670 towards the center of the sdf. This rugosity could be homologous to the distal lateral

671 expansion in the axis of *Camarasaurus* or *Suuwassea* (Madsen et al., 1995; Harris, 2006b),

672 just that the neural spine top is much more elevated in SMA 0011. Such a rugosity appears to

673 be absent in the element of *Diplodocus carnegii* (Hatcher, 1901). The postzygapophyses of

674 the axis of SMA 0011 slightly overhang the centrum posteriorly, and bear subtriangular facets

675 with a straight border anteriorly.

676 **Postaxial cervical vertebrae.** Eleven cervical vertebrae are present. They were found in four

677 blocks, with CV 1-6 constituting the first one (Figs 16, 17), CV 8 and 9 the second (Fig. 18),

678 CV 11 and 12 the third set (Fig. 19), and CV 15 (Fig. 20) was recovered articulated with the

679 first three dorsal vertebrae. The interpretation of the gaps is mainly based on the position of

680   the bones in the quarry, and on the fact that diplodocid cervical series are generally

681   considered to comprise 15 vertebrae (Hatcher, 1901; Gilmore, 1936; Upchurch, 1998; Wilson,

682   2002; Whitlock, 2011a). However, since only two nearly complete, and largely articulated

683   diplodocid necks have been reported to date (*Diplodocus carnegii* CM 84, lacking the atlas,

684   Hatcher, 1901; *Apatosaurus louisae* CM 3018, Gilmore, 1936), this count may also have been

685   different in diplodocid genera other than *Apatosaurus* or *Diplodocus*. A more detailed study

686   of the morphological changes within the cervical column will be needed to show if the present

687   assignment is correct, but is out of the scope of this description. For a phylogenetic

688   assessment of the specimen, it is sufficient to order the single vertebrae in anterior, mid-, and

689   posterior cervical vertebrae, which is perfectly possible in the present case.

690   The cervical centra are all opisthocoelous and relatively elongate. As is typical for nearly all

691   sauropods, the most elongated elements are the mid-cervical vertebrae. All cervical centra

692   have well-developed pleurocoels extending over the entire length of the centrum, ~~and~~ also

693   invading the dorsal surfaces of the parapophyses. The internal structure of the pleurocoel

694   varies along the column: the anterior and posterior horizontal ridges described in the axis

695   disappear by CV 4, and a vertical subdivision in anterior and posterior pneumatic fossae

696   becomes visible in CV 3, and is pronounced from CV 5 backwards. The subdividing ridge is

697   oriented anterodorsally-posteroventrally, as in *Kaatedocus* (Tschopp and Mateus, 2013b). The

698   posterior pneumatic fossae of CV 5 and 6 bear a large, slightly ellipsoid foramen at their

699   anterior end~~,~~ and become pointed posteriorly, due to the development of a shallow

700   posteroventral fossa, which diagnoses most Diplodocinae (except *Kaatedocus*; Tschopp and

701   Mateus, 2013b). From CV 6 backwards, the anterior pneumatic fossa becomes subdivided by

702   a horizontal ridge at about mid-height. The ventral portion of the anterior fossa becomes

703   vertically divided in CV 11. The latter is also the first element in the series to show a

704   separation of the posterior-most portion of the posterior pneumatic fossa. In addition, CV 12

705   also has a horizontally subdivided posteroventral fossa. In CV 15, the pleurocoel becomes less

706   complex again.

707   In CV 15, the anterior condyle is damaged, so that it reveals the internal structure. The

708   condyle is composed of large internal cavities, surrounded by 2-4 mm thick, relatively dense

709   bony struts. The arrangement appears symmetric, with a subtriangular cavity dorsomedially,

710   and two subcircular cavities following both medially and laterally.

711   The parapophyses become slightly anteroposteriorly elongate in CV 3 and 4. ~~They~~These

712 | structures project ventrolaterally in all elements~~,~~ and are interconnected with the anterior

713 | condyle through a transversely wide, somewhat rugose area. The fossa on its dorsal surface is

714 | subdivided by a short, oblique ridge from CV 6 ~~backwards~~and posteriorly. In CV 11 and 12,

715 | the parapophysis is subtriangular, ~~being long~~ anteroposteriorly elongated, and wider

716 | posteriorly than anteriorly.

717 | The ventral surface is hourglass-shaped and relatively narrow in anterior and mid-cervical

718 | vertebrae, but becomes relatively wide posteriorly. In anterior cervical vertebrae, ~~it~~the ventral

719 | surface bears a distinct longitudinal keel on its anterior half, with prominent~~well visible~~

720 | pneumatic foramina lateral to it in CV3, but less ~~so~~prominent in more posterior elements. In

721 | CV 3, a shallow ventral ridge ~~is also present on~~also occupies the posterior end, but already in

722 | CV 4 this ridge cannot be seen anymore. The ventral surfaces of CV 5 and more posterior

723 | vertebrae are concave without any traces of ridges or pneumatic foramina. Posteriorly, [≡]y

724 | are bordered by distinct posteroventral flanges, which is a synapomorphy of Diplodocinae,

725 | according to Tschopp and Mateus (2013b). These flanges become rugose ventrally in CV 15.

726 | None of the centra are fused with the corresponding cervical ribs. The neurocentral synostosis

727 | is closed but visible in the anterior and posterior cervical vertebrae, whereas in posterior mid-

728 | cervical vertebrae it is completely open. Where it is closed, the zigzagging neurocentral

729 | synostosis is ~~better~~more visible anteriorly than posteriorly (Fig. 21). In the most anterior and

730 | posterior elements, the synostosis becomes extremely faint to completely obliterated

731 | posteriorly. It lies on top of the centrum, such that the entire pedicels of the neural arches are

732 | detached in the unfused elements. The synostosis line is highest in the anterior half and

733 | descends anteriorly and posteriorly.

734 | [≡] neural arch is high in anterior cervical vertebrae, but becomes lower posteriorly. In all

735 | elements, it appears very fragile and slender, with very thin but distinct lamination. In

736 | posterior cervical vertebrae, the neural arch is somewhat displaced anteriorly, reaching close

737 | to the anterior condyle, but being well distant from the posterior edge of the centrum. The

738 | displacement reaches its maximum in CV 15.

739 | The prezygapophyses project anteriorly and slightly dorsally in most elements. Close to the

740 | cervico-dorsal transition, they become more elevated. They bear suboval facets in CV 3, with

741 | the long axis extending anteroposteriorly. From CV 4 onwards, the facets become

742 | subtriangular, with the tip located medially. The facets are convex as in all diplodocines

743 | (McIntosh, 1990b; Wilson, 2002; Whitlock, 2011a). Only in CV 5 are they concave, but this

744 appears to be due to taphonomic distortion. In CV 8 and 9, the articular facets are elevated on

745 pedestals, but no transverse sulcus is present posteriorly, unlike in *Kaatedocus* (Tschopp and

746 Mateus, 2013b). The prezygapophyses cap the prcdf dorsally, which in CV 5 and 6 is

747 subdivided by a vertical accessory lamina connecting acdl and prdl right at the diapophysis.

748 Anteriorly, the prezygapophyses are ventrally supported by the cprl, which is single in

749 anterior cervical vertebrae. From CV 8 backwards, the cprl is divided, with one distinct and

750 few short, weak accessory lamina in the prcdf. The accessory laminae subdividing the prcdf

751 become stronger in more posterior elements. Weak pre-epipophyses mark the lateral surface

752 anteriorly in CV 4 and more posterior elements. Only in CV 10 do they extend anterior to the

753 prezygapophyseal facet. This is in contrast to *Kaatedocus*, where the majority of mid- and

754 posterior cervical vertebrae bear anteriorly projecting pre-epipophyses (Tschopp and Mateus,

755 2013b). Posteriorly on the prezygapophyseal process, the anterior portion of the sdf develops

756 a deep, but not well defined fossa in CV 3.

757 The sprl is distinct on the prezygapophyseal process, disappears around midlength of the

758 dorsal portion, and becomes visible again on the spine top in anterior cervical vertebrae. In

759 mid-cervical vertebrae, the sprl is weak to almost absent on the prezygapophyseal process, as

760 is typical for Diplodocinae (Tschopp and Mateus, 2013b). In posterior cervical vertebrae, the

761 sprl is again better developed. Due to a backwards curve of the spine top in anterior cervical

762 vertebrae, the sprl has a somewhat sinuous appearance in lateral view in these elements.

763 Below the backwards curve, the sprl extends almost vertically in CV 3 to 5, but becomes

764 posteriorly inclined in more posterior vertebrae. A prsl is present at the base of neural arch in

765 unbifurcated spines, which reach back to CV 8, as in *Barosaurus* (McIntosh, 2005).

766 The diapophysis is entirely located in the anterior half of the vertebra. It is supported by

767 distinct acdl, prdl, podl, and pcdl. The acdl and prdl are separated along their entire length, a

768 feature typical for *Apatosaurus*, and usually absent in diplodocines. The pcdl is almost

769 horizontal, and the podl steeply inclined in CV 3, but in CV 4 and more posterior elements,

770 they approach each other, forming a more acute angle anteriorly. In anterior elements, the

771 podl and pcdl unite before curving laterally, but more posteriorly they remain separate as the

772 acdl and prdl, and the pocdf is therefore extended onto the posterior surface of the

773 diapophysis. They do not form such distinct posterior processes such as those present in

774 *Kaatedocus* (Tschopp and Mateus, 2013b). The pcdl bifurcates anteriorly in the mid-cervical

775 vertebrae, whereas in more posterior elements two parallel pcdl are present. This sheds new

776 light on serial variation of these characters, as they are used to distinguish different species in

777 some cases (e.g. *Apatosaurus parvus* or *Australodocus bohetii*; Upchurch et al., 2004b;

778 Remes, 2007). However, ~~since~~because in the majority of cases (*Apatosaurus parvus* UW

779 15556, or *Barosaurus lentus* AMNH 6341 and YPM 429; Gilmore, 1936; Upchurch et al.,

780 2004b; ET, pers. obs., 2011) only one of these states is present, they are still considered as

781 taxonomically informative. The cdf lies directly ventral to the diapophyseal process. In CV 15

782 of SMA 0011, a short but stout accessory lamina ~~is present in~~occupies the posterior portion of

783 the fossa. In mid- and posterior vertebrae of SMA 0011, an accessory lamina is present

784 between the pcdl and podl, facing posteriorly. In CV 12, there is even a second vertical

785 accessory lamina subdividing the pocdf. Dorsomedial to the accessory lamina, the pocdf is

786 pierced by a large foramen, such that the pocdf is interconnected with the spof. A similar state

787 appears to be present in the anterior cervical vertebrae of *Dicraeosaurus* MB.R.4886 (ET,

788 pers. obs., 2011), a partial mid-cervical vertebra of *Suuwassea* ANS 21122 (Harris, 2006b:

789 fig. 8B), and *Eobrontosaurus* Tate-001, but in these taxa, the borders of the opening seem to

790 be broken (ET, pers. obs.). Fossae at the same location ~~are present~~occur in many taxa,

791 including *Diplodocus* or *Supersaurus* (Hatcher, 1901; ET, pers. obs., 2013), but none of them

792 opens up into a large foramen as in SMA 0011 (Fig. 22).

793 The sdf is of generally simple morphology. In CV 5 and 6, a shallow but dorsally well offset

794 fossa is located close to the spine summit. In CV 6 and 8, the sdf bears a distinct,

795 dorsoventrally elongate fossa posterolateral to the sprl, at about mid-height of the

796 metapophysis. From CV 8 backwards, a vertical accessory lamina follows the sprl posteriorly,

797 as in *Diplodocus carnegii* CM 84 (Hatcher, 1901). No subfossae are present in the sdf of

798 posterior cervical vertebrae, but in CV 15, the sdf becomes clearly delimited dorsally, just

799 below the anteroposterior narrowing of the spine top.

800 The neural spine undergoes distinct changes in development and orientation from anterior to

801 posterior. In anterior cervical vertebrae, it is vertical, and dorsoventrally elongate, reaching

802 well above the postzygapophyses. The axis, as well as CV 3 and 4 have a distinctly

803 posteriorly turning spine summit, as can also be seen in the corresponding elements of

804 *Eobrontosaurus*. There is an abrupt change in height from CV 5 to 6, resulting in a smaller

805 total height of CV 6 compared to CV 5. Such a development has only been described in

806 *Dicraeosaurus* (Janensch, 1929a), but neural spines are often incomplete, where anterior

807 cervical vertebrae have been found (e.g. *Diplodocus carnegii* CM 84, *Apatosaurus louisae*

808   CM 3018; Hatcher, 1901; Gilmore, 1936), which makes a thorough assessment of this

809   character difficult. However, SMA 0011 is clearly different from the state in *Kaatedocus*

810   *siberi* SMA 0004, as well as the indeterminate diplodocines AMNH 7530, 7535, and CM

811   3452, where the anterior cervical neural spines are low, and total vertebral height

812   continuously increases throughout the vertebral column (Tschopp and Mateus, 2013b; ET,

813   pers. obs., 2011). From CV 6 backwards, the cervical neural spines of SMA 0011 decrease in

814   relative length, compared to pedicel height, but remain vertical. Towards the cervico-dorsal

815   transition, neural spine height increases again, such that CV 15 has a highly elevated spine

816   summit. In this vertebra, the spine summit is also strongly anteriorly inclined. The distal-most

817   part of the neural spine of CV 15 is anteroposteriorly short but elongated dorsoventrally.

818   Bifurcation of the spine is present, but only from CV 9 backwards, as is the case in

819   *Barosaurus* AMNH 6341 (McIntosh, 2005). Unbifurcated neural spines slightly expand

820   transversely towards their distal end, similar to the state in *Suuwassea emilieae* (Harris,

821   2006b). Posteriorly, the spol are thin but project far posterodorsally, and connect to each other

822   across the spine summit. Therefore, they enclose a distinct and deep spof. Elements with bifid

823   neural spines have a median tubercle. The lateral surface of the neural spine summits becomes

824   rugose in posterior vertebrae.

825   Following the changing orientation and elevation of the spine, the spol also has a quite

826   variable morphology from anterior to posterior cervical vertebrae: itthe structure is strongly

827   concave in CV 3, and less so in CV 4, due to the more expressed backwards leaning of the

828   spine top in CV 3. The spol is gently curved in CV 5, but forms a 90° angle in CV 6. Due to

829   the low spine top, the spol is almost horizontal in CV 8 to 12. In CV 15, it becomes concave

830   again, but remains almost horizontal posteriorly, where it unites with the epipophysis. The

831   latter is well developed in all cervical vertebrae, often overhanging the postzygapophyses. It

832   constitutes the posterior end of the spol, and is often pointed. The postzygapophyseal facets

833   are suboval to subcircular in the anterior cervical vertebrae, but become subtriangular more

834   posteriorly, with the tip pointing medially. They are concave and thus face both downwards

835   and outwards. They are ventrally supported by a vertical, single cpol.

836   **Dorsal vertebrae (Figs 23-28; Tab. 6)**

837   **Dorsal vertebrae 1 and 2.** The first two dorsal vertebrae are still embedded in matrix, and

838   only the right sides are prepared (Figs 23, 24). The diapophysis is not preserved in either

839   vertebra, and DV 2 also lacks the right metapophysis and postzygapophysis. The anterodorsal

840 part of the right lateral surface of the centrum of DV 2 is reconstructed, including the

841 neurocentral synostosis.

842 The dorsal vertebrae 1 and 2 more closely resemble the cervical vertebrae than more posterior

843 elements of the dorsal sequence. Compared to the last cervical vertebra, DV 1 and 2 have a

844 considerably deeper diapophysis, and less distinct epipophyses. Their centra are

845 opisthocoelous, and have an intermediate elongation compared to the last cervical and DV 3.

846 The lateral surface is marked by elongate pleurocoels that occupy the central and anterior

847 portion of the centrum. In DV 2, the pleurocoel is more restricted towards the anterior than in

848 DV 1, being almost entirely situated above the parapophysis. The parapophysis lies

849 anteroventral to the pleurocoels, which extend onto its dorsal face. Posteroventral flanges are

850 present, but become less distinct in DV 2. The ventral surface is concave and broad, with a

851 shallow longitudinal ridge located anteriorly.

852 The neural arch height is more or less equal to centrum length, not counting the condyle. As

853 in anterior and posterior cervical vertebrae, the neurocentral synostosis is closed, but still

854 visible in its anterior half. The neural spine is divided. The prezygapophysis is broad, and

855 projects slightly anterior to the condyle in both vertebrae, although it is more vertically

856 oriented in DV 2. A weak pre-epipophysis is present, but does not extend beyond the

857 prezygapophyseal facet. The sprl is strongly concave, due to the strong anterior inclination of

858 the spine top. The prdl does not contact the acdl directly, but they are interconnected by a

859 vertical lamina below the diapophysis. The latter is thus slightly elevated above the centrum,

860 and dorsoventrally high. The broken diapophysis of DV 2 reveals large open spaces that are

861 surrounded by narrow laminae of relatively dense bone tissue. Both the acdl and the pcdl are

862 only slightly inclined. The pocdf is subdivided by a strong, laterally facing, almost vertical

863 accessory lamina, forming a posteroventral branch of the podl. This differs from the posterior

864 cervical vertebrae, where the accessory lamina in the pocdf faces posteriorly. Unlike the mid-

865 and posterior cervical vertebrae, DV 1 and 2 do not have any fenestra connecting the pocdf

866 with the spof. The spine summit is anteroposteriorly narrow, and inclined anteriorly, but the

867 inclination decreases in DV 2 and more posterior elements. The lateral surface of the spine is

868 marked by the sdf, which is well delimited dorsally, similar to the state in CV 15. From the

869 top of the sdf, the spine of DV 1 and 2 forms a narrow anterodorsal projection. The medial

870 surface of the spine (visible in DV 2) is slightly convex and smooth, unlike the subtriangular

871 shape present in most apatosaurs (e.g. NSMT-PV 20375; Upchurch et al., 2004b).

Dorsal vertebrae 3 and 4. Both elements are broken and deformed such that it is difficult to understand their morphology in detail (Figs 25, 26). Dorsal vertebra 3 lacks the right diapophysis and neural spine, such that the internal surface of the left spine is visible in the mount. The dorsal portion of the centrum and ventral half of the neural arch are crushed, and various pieces of each became intermingled. Dorsal vertebra 4 preserves a very deformed centrum, mounted in anteroventral view, which is not fused with the neural arch. A part of the neural arch is preserved intermingled with the fractured pieces of DV 3.

The dorsal vertebrae from DV 3 towards the sacrum are considerably shorter than DV 1 and 2, but remain of about the same length (not considering the condyle). DV 3 has a strongly opisthocoelous centrum, whereas DV 4 is only slightly opisthocoelous. A distinct pleurocoel is present on the anterodorsal corner of the lateral side. It is shorter than in DV 1 or 2. The position of the parapophysis is difficult to see, but appears to be still on the centrum, above the pleurocoel in DV 3, whereas the centrum of DV 4 does not show any traces of a parapophysis. The ventral side of DV 3 is well delimited by posterior ridges between the lateral and ventral surfaces. A broad, but relatively distinct midline ridge marks the anterior half of the ventral side of the centrum of DV 3. The articulation surface of the centrum of DV 4 for the neurocentral synchondrosis is broad and curved. The neural canal is narrowest at midlength of the centrum.

The neural arch of DV 3 is higher, but more anteroposteriorly compressed, than in DV 2. The prezygapophysis is relatively short. The sprl is oriented almost vertically, and no strong anterior inclination of the neural spine is present anymore. The medial side of the neural spine of DV 3 is gently convex, and slightly wider anteroposteriorly than in DV 2. Postzygapophyses are not preserved.

Mid- to posterior dorsal vertebrae (DV 5 to 10). Dorsal vertebra 5 ~~is lacking~~lacks its right neural arch, diapophysis, and spine, as well as the distal tip of the left diapophysis (Fig. 27). Dorsal vertebra 6 lacks the anterior part of the centrum, the right diapophysis, parapophysis, and prezygapophysis, and the spine top. In dorsal vertebra 7, the right diapophysis, parapophysis, and the spine top are missing. Dorsal vertebrae 8 and 9 lack the right diapophysis and parapophysis. The last dorsal vertebra lacks the neural spine process, whereas the arch below the postzygapophysis, the diapophysis, and the prezygapophyses are preserved (Fig. 28).

The mid- and posterior dorsal centra are short, and generally amphiplatyan to amphicoelous.

Only DV 5 shows a weak anterior condyle. The pleurocoel is largest in DV 6 to 8, occupies the dorsal half of the centrum, and extends slightly onto the pedicels, below the neurocentral synchondrosis. The ventral surface is convex, and not well separated from the lateral side. The centrum is slightly shorter ventrally than at mid-height. In DV 6 and 7, a zigzagged line marks the neurocentral synostosis at the dorsal edge of the centrum. Dorsal vertebrae 8 to 10 have unfused neurocentral synchondroses. The neural arch is high, with highly elevated postzygapophyses, resulting in longer pedicels than neural spines in at least DV 5 to 8. Pre- and postzygapophyses are on more or less a horizontal line. The pedicels below do not show a strong lamination, but the acpl, pcdl, and cpol can be well distinguished. Dorsal vertebrae 6 to 9 furthermore show a weakly developed pcpl. An accessory lamina can be found in DV 7, connecting the pcdl with the podl, and in DV 8 between the prpl and the prdl. The presence and development of the hyposphene-hypantrum articulation cannot be distinguished due to the articulated state of the vertebrae. The parapophysis lies at mid-height on the pedicels in DV 6, at two thirds in DV 7 and at three fourths in DV 8. More posteriorly, the parapophysis seems to have been attached to the prezygapophysis. The spine is relatively low in DV 5 to 8, and only in DV 9 and probably 10 does it exceed the pedicel height. The spines are situated above the posterior-most portion of the centrum, and are vertically oriented. This differs from the strongly anteriorly inclined posterior dorsal neural spines of *Diplodocus* (Hatcher, 1901; Gilmore, 1932). The sprl is vertical in DV 6, strongly dorsoventrally convex in DV 7 and 8, and slightly convex in DV 9. The spdl is short and only expressed at its ventral end. Dorsally it merges with the spol, which extends onto the lateral surface of the spine. The posl, or possibly medial spol, is straight and vertical. Due to the preservation and mounting, it cannot be distinguished at this point how far back the bifurcation proceeds. The last definitively bifid neural spines are present in DV 5.

Ribs

Cervical ribs. The cervical ribs are thin, fragile elements. The axial cervical rib has almost no tuberculum, and is thus a straight, elongate, and transversely compressed sheet of bone (Fig. 16). Anterior to mid-cervical ribs are longer than their corresponding centra, but they only overlap a small portion of the following vertebra (Figs 16, 17). The anterior process is distinct, but very short in CR 3, and pointed in anterior and mid-cervical ribs. ~~It~~This process becomes very broad and rounded anteriorly in posterior cervical ribs, with a central longitudinal lamina connecting to the capitulum. The tuberculum is posteriorly inclined in

936　anterior cervical ribs, and subtriangular in cross-section at midlength. The rib itself is concave

937　internally, with a lamina connecting the tuberculum with the capitulum internally, producing

938　two separate fossae anteriorly and posteriorly. Cervical rib 6 bears a pneumatic foramen

939　internally on the capitulum.

940　**Dorsal ribs.** Several ribs have been recovered associated with the dorsal series, but the

941　correct position of the single elements cannot be confidently determined at this point. There is

942　some information from the quarry maps that the rib associated with DV 1 (as interpreted

943　herein) looks much like a cervical rib. It is short, with a straight shaft, and has the typical

944　anterior process of cervical ribs. However, the rib is detached from the centrum, as in all

945　presacral vertebrae of SMA 0011. Also, if the vertebra herein described as DV 1 would

946　actually be the last cervical vertebra, the second dorsal vertebra would be considerably shorter

947　than the first. Such an early length decrease in the dorsal column would be unusual, and

948　different from *Diplodocus* or *Barosaurus*, where this happens between DV 2 and 3 (CM 84,

949　or AMNH 6341; Hatcher, 1901; McIntosh, 2005). The cervical-like rib shape of DR 1 is thus

950　interpreted to be due to cervicalization, which appears to be an important evolutionary trend

951　within diplodocids (McIntosh, 2005).

952　More posterior ribs are transversely compressed to slightly subtriangular at midshaft. Some of

953　the elements have anteroposteriorly expanded distal ends (probably the anterior ribs, see

954　Schwarz et al., 2007a), whereas others taper to a point. The capitulum is generally elongate,

955　and the tuberculum low, but distinct. Between them, a relatively thin sheet of bone forms a

956　triangular bony plate, which in at least some of the elements bears a ridge externally, but

957　remains flat internally (contrary to the state in most other diplodocines). None of the ribs bear

958　pneumatic foramina. The longest preserved rib has a length of 1400 mm (measured along the

959　curve).

960　**Sternal ribs.** Several morphotype C elements (sensu Tschopp and Mateus, 2013a) were

961　recovered associated with SMA 0011, but remain unprepared. They are elongate, narrow

962　bones. No additional information can be gleaned to date that would help to confirm or discard

963　the interpretation of Claessens (2004) and Tschopp and Mateus (2013a) that these elements

964　are sternal ribs.

965　**Forelimb (Figs 29-32; Tab. 7)**

966　**Scapula R, external view.** The right scapula lacks the dorsal part of the acromion and of the

967　distal end of the blade (Fig. 29). The acromion and the blade form an acute angle, but the

968 acromial ridge is only very slightly developed. The area anterior to the acromial ridge is

969 concave. The posteroventral edge is mostly straight, and does not bear a triangular process as

970 present in some *Camarasaurus* specimens, or *Dystrophaeus* (Osborn and Mook, 1921;

971 McIntosh, 1997). The distal end of the blade is slightly curving ventrally as in *Apatosaurus*

972 *excelsus* YPM 1980 (Upchurch et al., 2004b). The anterodorsal, or acromial edge of the

973 scapula is much more concave, due to the stronger extensions of both the dorsal portion of the

974 acromion, as well as the indicated widening of the distal shaft, which starts more anteriorly on

975 this edge than on the posteroventral one. No oval rugose tubercle is present on the base of the

976 shaft, unlike in *Apatosaurus excelsus* YPM 1980 (Upchurch et al., 2004b; ET, pers. obs.,

977 2011).

978 **Coracoid R, external view.** The coracoid is somewhat tear-drop shaped (Fig. 29), with a

979 concave anterodorsal edge, and a strongly, continuously convex, narrow dorsal margin, unlike

980 the squared coracoids of apatosaurs (Riggs, 1903; Bakker, 1998). The coracoid foramen is

981 completely enclosed, but the coracoid is not fused with the scapula. The bone is gently convex

982 dorsoventrally. It curves slightly medially at its anterior margin. No distinct notch is present

983 anterior to the glenoid surface. The glenoid is strongly transversely expanded at its center, and

984 tapers dorsally and ventrally. The glenoid surface and the articulation surface with the scapula

985 enclose an angle of about 155°.

986 **Humerus R, anterior view.** The right humerus is complete but slightly compressed

987 anteroposteriorly (Fig. 30A). It is widely expanded at its proximal end, both laterally and

988 medially. The distal end is expanded as well, but less so. The proximal portion is concave

989 transversely, and does not bear a central rugose tubercle as present in the apatosaur AMNH

990 6114 (ET, pers. obs., 2011). The deltopectoral crest does not extend to midshaft. Its distal end

991 is distinct and follows the lateral margin. It is not transversely expanded as would be typical

992 for titanosaurids (Wilson, 2002; Curry Rogers, 2005). The crest is concave laterally, but this

993 depression is probably exaggerated taphonomically. Two ridges mark the distal end

994 anteriorly, indicating the extensions of the medial and lateral condyles. The ridges are

995 relatively well visible and extend proximally. The medial condyle is much more prominent

996 than the lateral one.

997 **Ulna L, anterior view.** The ulna lacks the proximal-most portion of the anterior arm of the

998 condylar processes. The bone is strongly transversely compressed in its proximal half (Fig.

999 30B). It is generally slender, with a triradiate proximal end. The anterior arm is considerably

longer than the lateral one, even though this is enhanced due to compression. The ulna has relatively strongly concave anterolateral and posterolateral surfaces. The lateral arm is somewhat wider than the anterior one. The distal part of the anteromedial surface bears two strong and elevated, longitudinal ridges. They proceed both distally and proximally, but narrower and with a smooth surface. Proximally, the more lateral of the two ridges extends above midlength. Distally, the more medial ridge is more pronounced, reaching the distal articular surface. The distal end is expanded medially and somewhat transversely. The articular surface is subtriangular in outline.

Radius L, anterior view. The radius is complete, but its proximal end is compressed (Fig. 30B). It has thus a narrow, ellipsoid outline, but would probably be subcircular if undeformed. The shaft ~~appears~~is subrectangular in cross-section. As in the ulna, also the distal end of the radius is slightly expanded. The posterolateral surface bears at least one longitudinal ridge on its distal portion for the articulation with the ulna (more is obscured due to the mounting in matrix).

Carpal L. The carpal is a block-like element (Fig. 30B). Only one has been found in the otherwise articulated manus. The entire bone is relatively rugose and articulates with the radius. Comparison with the carpal elements found in other diplodocids (Hatcher, 1902; Gilmore, 1936; Bedell and Trexler, 2005) would suggest that it has been mounted upside down, although it was mounted as found, according to the quarry maps. If the mount is correct, it has a flat proximal, and an irregular, but transversely convex distal surface, contrary to the case in other diplodocids (Hatcher, 1902; Gilmore, 1936; Bedell and Trexler, 2005). It is anteroposteriorly wider at its medial end than laterally. There are no distinct articulation surfaces for the metacarpals, unlike the state in *Camarasaurus* (Tschopp, 2008). The carpal of SMA 0011 is longer proximodistally than the element known from the apatosaurs CM 3018 or UW 15556 (Hatcher, 1902; Gilmore, 1936). The anterior surface is concave transversely. Other than in apatosaurs, where the carpal articulated with both the ulna and the radius, and capped the median three metacarpals proximally (Hatcher, 1902; Gilmore, 1936), the carpal of SMA 0011 appears to overlie metacarpals I, II, and possibly III. This is the same arrangement as found in the articulated manus of WDC-FS001A (Bedell and Trexler, 2005).

Metacarpals L, anterior view. All metacarpals are complete and articulated (Fig. 30B). They are relatively elongate bones, but less than in *Camarasaurus* (Tschopp, 2008). Metacarpal III is the longest, followed by mc II, IV, I, and V (Tab. 7). Metacarpal I and II have

subrectangular proximal articulation surfaces, contrasting with triangular ones in mc III and IV triangular ones.

　　　　Metacarpal I is relatively stout, with distinct anterior, lateral, and medial surfaces. The lateral condyle is much longer proximodistally than the medial one. This results in a strongly inclined distal surface, such that the phalanges project posteromedially in the articulated manus.

　　　　Metacarpal II has very distinct, straight anteromedial and anterolateral edges. The proximal and distal ends are slightly expanded in all directions. The distal surface slightly curves into the anterior surface. Its lateral and medial condyles are only visible in distal and posterior view. The proximal portions of both the medial and lateral surfaces are concave, laterally more than medially.

　　　　Metacarpal III has a very distinct posterior corner of the proximal surface, probably connecting to a median ridge on the posterior surface, as is typical for Sauropoda (Upchurch et al., 2004a). Whereas no distinct transition from the anterior onto the medial surface occurs on mc III, the lateral face is clearly separated. The proximally and distal articular surfaces are slightly twisted. The distal surface is ellipsoid, and does not extend considerably onto the anterior face.

　　　　Metacarpal IV has a triangular proximal articulation surface, with a concave medial edge. As in mc III the shaft of mc IV is twisted, and a distinction of the anterior face is not possible. The distal articular surface is subtriangular as well, with the apex anteriorly, and inclined medial and lateral edges. Two condyles are visible posteriorly. The apex of the distal articular surface curves onto the anterior face.

　　　　Metacarpal V is short and widely expanded transversely at its proximal end. The distal end is lacking, but the preserved parts indicate that it is transversely expanded. This expansion occurs perpendicular to the proximal one.

Manual non-ungual phalanges L, anterior view. The manual non-ungual phalanges are relatively short and stocky (Fig. 30B). They are wider than long, as is typical for the eusauropod manus (Bonnan, 2003). The m

　　　　Manual phalanx I-1 is mounted in posterior view. The proximal surface is concave anteroposteriorly. The phalanx I-1 has a concave posterior surface, with a proximally projecting ventral lip. Its medial surface is shorter than the lateral one, enhancing the outwards twist of the ungual phalanx even more. Well-developed medial and lateral condyles

are present distally. The lateral extension of the posterolateral edge forms a thin, short crest (Fig. 31). Nothing similar is present in the manus of *Camarasaurus* (Osborn, 1904; Tschopp, 2008), but too few articulated proximal manual phalanges are known in diplodocids in order to decide if this might be autapomorphic in SMA 0011 or is instead more widespread within the clade. A phalanx figured by Jensen (1985: fig. 1E) appears to show a similar development of the posterolateral edge, but has not been identified below Sauropod indet. (Jensen, 1985).

~~The m~~Manual phalanx II-1 has a concave proximal surface, which is probably ovoid in outline (only the dorsal portion can be seen as it is currently mounted). It is only minimally wider than the shaft. The medial surface is broader, but shorter than the lateral one. The anterior surface is convex transversely. The distal articular surface is expanded transversely, and the well-developed condyles extend onto the lateral surfaces. ~~The m~~

Manual phalanx II-2 is a vestigial, suboval bony nubbin. A distinct ridge separates the proximal and distal surfaces. The manual phalanges III-1 and IV-1 are very similar, with III-1 being slightly larger. They have concave proximal articular surfaces, transversely more so than anteroposteriorly. The surfaces are suboval in outline, and their anterior margins are pronounced medially. The anterior surfaces are concave proximodistally, but slightly convex transversely. The distal surfaces are without condyles. They have a continuous, rounded surface, which curves proximally at its medial and lateral end, almost reaching the proximal articular surface. The medial and lateral surfaces are thus practically nonexistent. The lack of medial and lateral condyles implies that there were no vestigial terminal phalanges in these digits, unlike in *Camarasaurus* (Tschopp, 2008). The unusual shape of phm III-1 and IV-1 (as mounted) resembles phm V-1 in the camarasaur SMA 0002 (Tschopp, 2008).

Given that no additional phalanx was found to mount with digit V, the elements mounted on the third and fourth digit might actually represent phm IV-1 and V-1. Both of these bones were not found articulated with their corresponding metacarpals, which makes a definitive assignment difficult. However, given that the manus would otherwise be complete, the mount is herein interpreted to be right, and no, or only a vestigial phalanx would have been present in digit V. ~~Comparing~~When compared with the manus of the camarasaur SMA 0002, this would indicate that the peculiar shape without distal condyles of phm III-1, and IV-1 of SMA 0011, or phm V-1 of SMA 0002 represent an intermediate stadium of phalangeal reduction, between the usual phalangeal shape and the nubbin-like vestigial elements found with digits two of both SMA 0011 and SMA 0002 (Tschopp, 2008).

1096 **Manual ungual L, anterior view.** One ungual is present, ~~and~~ situated on the first digit (Fig.
1097 30B). It is a long, high, and transversely compressed element. The proximal surface is tear-
1098 drop shaped, with a laterally curving anterior tip, and a widened posterior portion, where the
1099 articular surface lies. Anterior to the articular surface, the proximal surface projects somewhat
1100 proximally, and is rugose. This rugosity extends as a short ridge posteriorly, into the articular
1101 surface. The medial surface is convex anteroposteriorly. A short groove marks the distal-most
1102 portion, which is slightly elevated (about 1 mm) above the more proximal portion of the claw,
1103 and shows a different surface texture (Fig. 32). The latter might represent fossilized remnants
1104 of the keratinous sheet covering the claw. The lateral surface is almost plane, with a long,
1105 proximodistally extending, straight groove covering the distal half of the surface.
1106
1107 **Hindlimb (Figs 33-35; Tab. 8)**
1108 **Ilium R, external view.** The ilium lacks a large part of its posterior upper portion. The
1109 preacetabular process has a very pointed apex, which is pointing anterolaterally. The anterior
1110 portion is strongly concave, with the ventral margin facing laterally. The ventral preacetabular
1111 border and the pubic process form an angle of 90°, which is uncommon in *Diplodocus*, but
1112 present in the holotype of *Galeamopus hayi* (Hatcher, 1901; HMNS 175, ET, pers. obs.,
1113 2010). A triangular depression is located laterally at the base of the pubic process, with
1114 horizontal and medio- and lateroventrally inclined sides. This is similar to the putative
1115 diplodocid ilium from Spain (CPT-1074; Royo-Torres and Cobos, 2004; ET, pers. obs.,
1116 2012). The pubic peduncle is distinctly concave transversely at its posterior end, but fractures
1117 indicate that the concavity is exaggerated and that the transverse width of the pubic peduncle
1118 would be slightly larger. The ischial tubercle is facing slightly laterally. The acetabular
1119 margin is thinnest just posterior to the pubic peduncle, and extends transversely both
1120 posteriorly and anteroventrally, reaching the articulation surfaces of the ischium and pubis.
1121 **Pubis R, internal view.** The right pubis is almost complete. Its anterodorsal corner is slightly
1122 eroded, and the middle portion of the ischial articulation is missing. The entire bone is
1123 relatively slender (Fig. 33A). The pubic foramen is closed, and located in the proximal third
1124 of the ischial articulation. Even though eroded, the anterodorsal corner does not seem to bear
1125 a very pronounced ambiens process, as seen in *Diplodocus* or *Supersaurus* (Hatcher, 1901;
1126 Lovelace et al., 2007). This corner is laterally expanded, and from here, the pubis slightly
1127 tapers along the acetabular surface. The medial surface of the proximal half of the bone is

1128   proximodistally concave and transversely slightly convex. The latter convexity becomes more

1129   pronounced towards midlength, where the ventral margin curves back from the expanded

1130   ischial articulation to the narrow midshaft. The dorsal edge of the pubis is gently concave. Its

1131   anterior end is expanded both transversely and anteroposteriorly. The narrowest portion of the

1132   shaft lies at about two thirds of the entire length of the pubis.

1133   **Ischium L, internal view.** The ischium lacks the posterior half of the shaft (Fig. 33B). Its

1134   proximal portion is wide and concave. The acetabular surface is inclined, such that the medial

1135   border forms a thin crest. This crest is relatively straight in medial view, but concave and

1136   curved in proximal view. Unlike the state in rebbachisaurids, the acetabular surface does not

1137   expand towards the articulation surfaces for the ilium and the pubis (Calvo and Salgado,

1138   1995; Whitlock, 2011a). The iliac process has thus no distinct neck, and is relatively narrow.

1139   The pubic articulation is much longer, and straight in medial view. It curves slightly medially

1140   towards its ventral end. The shaft is weakly convex at its base, separating the concave

1141   acetabular portion from the again shallowly concave posterior shaft. The dorsal and ventral

1142   margins are parallel, only the posterior-most preserved portion of the dorsal edge indicates a

1143   slight dorsal expansion towards the end, as is typical for diplodocids (McIntosh, 1990a, b;

1144   Upchurch, 1998; Wilson, 2002). No distinct ridges or scars can be seen on the internal

1145   surface. Oblique, minuscule elongated cavities indicate the presence of a now eroded shallow

1146   ridge extending from about midlength of the ventral edge of the shaft proximodorsally onto

1147   the convex base of the shaft and ending on the dorsal margin where it curves into the

1148   acetabular portion.

1149   **Femur L, posterior view.** The greater trochanter and the intercondylar groove are ~~missing~~not

1150   preserved the femur of SMA 0011 (Fig. 34A). The medial edge is gently curved below the

1151   femoral head, not as distinct as in *Dyslocosaurus* (McIntosh et al., 1992). The head is not well

1152   separated from the shaft ventrally. The fourth trochanter terminates slightly above midlength.

1153   It is entirely located on the posterior surface of the shaft, but close to the medial border

1154   proximally. The distal end of the fourth trochanter curves distinctly laterally. The distal

1155   condyles of the femur project far posteriorly. The lateral condyle bears an epicondyle. Both

1156   condyles expand slightly outwards, and the medial one projects further distally than the lateral

1157   one. In posterior view, the two condyles are slightly inclined medially.

1158   **Tibia L, anterior view.** The tibia is complete (Fig. 34B). It is slightly expanded at both ends.

1159   A small convexity marks the distal end of the medial edge, similar, but broader and less

1160 distinct than in *Dyslocosaurus* (AC 663, ET, pers. obs., 2011). The cnemial crest is somewhat

1161 displaced distally, and distally thicker than proximally. The proximal end appears longer

1162 transversely than anteroposteriorly, but not the entire surface is visible. This also precludes

1163 the assessment of the outline of the proximal articular surface, which is subrectangular in

1164 apatosaurines, whereas it is subtriangular in diplodocines (Lovelace et al., 2007), and would

1165 thus yield further information on the correct taxonomic assignment of SMA 0011.

1166 **Fibula L, anterior view.** The fibula is a slender bone, with a strongly expanded proximal

1167 end, and less so distally (Fig. 34B). The proximal end is transversely compressed. The

1168 attachment site for the iliofibularis muscle is situated slightly above midheight, as in

1169 *Diplodocus* (Whitlock, 2011a).

1170 **Astragalus L, anterior view.** The astragalus is wedge-shaped in both anterior and proximal

1171 views (Fig. 35A). The anteromedial corner is reduced. Proximally, the astragalus is marked by

1172 a high ridge connecting to the ascending process, which extends ⊟ckwards to the posterior

1173 end. The high, broad ridge separates the two fossae for the articulation with the tibia medially

1174 and the fibula laterally. The tibial fossa is larger, and subdivided by a more shallow,

1175 anteroposteriorly oriented ridge in a medial and a lateral portion. The fibular fossa is

1176 relatively uniform, with the anterior edge more developed than the posterior one. It is thus

1177 visible in posterior view, a diplodocoid synapomorphy, convergently acquired by *Jobaria*

1178 (Whitlock, 2011a).

1179 **Metatarsals L, anterior view.** All left metatarsals were recovered complete (Fig. 35B). The

1180 metatarsals III and IV are the longest, mt I and II the stoutest elements (Tab. 8).

1181 Metatarsal I is very stocky, and has a D-shaped proximal surface. The anterior surface

1182 is considerably shorter medially than laterally, resulting in angled proximal and distal

1183 surfaces, compared to the long axis of the shaft. The anterior surface bears few nutrient

1184 foramina, as is the case in *Cetiosauriscus* and *Suuwassea*, but not in camarasaurs (Harris,

1185 2007; Tschopp, 2008; NHMUK R3078, ET, pers. obs., 2011). Distally, the lateral condyle

1186 projects much further than the medial, and develops a distinct posterolateral process, as is

1187 typical for diplodocids (McIntosh, 1990a, b). The medial surface is slightly convex, the lateral

1188 one concave for the reception of mt II. The distal articular surface bears a distinct

1189 intercondylar groove visible in anterior view.

1190 Metatarsal II has a more squared proximal surface, and ~~also~~ the anterior surface is less

1191 trapezoidal than in mt I. However, the proximal and distal articular surfaces are still angled to

1192 the long-axis of the shaft. As observed in mt I, ~~also~~ mt II has a strong posterolateral process.

1193 The distal portion of the anterolateral edge bears a distinct rugosity, which does not extend

1194 onto the anterior surface, unlike in *Dyslocosaurus* AC 663 or *Cetiosauriscus* NHMUK R3078

1195 (McIntosh et al., 1992; ET, pers. obs., 2011).

1196 _____Metatarsal II of SMA 0011 has a very distinct anteromedial edge, but a less developed

1197 anterolateral one. No intercondylar groove can be seen between the distal condyles in anterior

1198 view.

1199 _____Metatarsal III is elongate, with a narrow shaft and greatly expanded proximal and

1200 distal ends. The proximal and distal articular surfaces stand perpendicular to the shaft axis.

1201 The proximal articular surface is subrectangular to subtriangular, with the posterior margin

1202 being shorter than the anterior one. It is relatively flat, and does not show distally curving

1203 edges as in mt I and II. A weak, narrow rugosity marks the distal end of the anterolateral edge.

1204 _____Metatarsal IV is similarly elongate as mt III, but the proximal expansion reaches

1205 further down the shaft. The proximal end seems slightly twisted in respect to the long axis. It

1206 is subtriangular in outline, with a concave posterior margin, resembling the shape of mt IV of

1207 the camarasaur SMA 0002, but with a less well-developed concavity (Tschopp, 2008). The

1208 surface is flat, as in mt III. The shaft is smooth, without any distinct rugosities. The distal end

1209 does only have incipient condyles, which are hardly recognizable in both anterior and distal

1210 views. ~~The m~~

1211 _____Metatarsal V has the typical paddle-shaped outline known from almost all sauropods

1212 (Bonnan, 2005). The proximal articulation surface is subtriangular, with the apex pointing

1213 anteriorly. From there, a ridge extends distally, separating the proximal portion of the anterior

1214 surface from the medial one. The ridge disappears in the distal half. The shaft is smooth,

1215 unlike in mt V of the camarasaur SMA 0002 (Tschopp, 2008). The distal surface is a single,

1216 convex facet.

1217 **Pedal non-ungual phalanges L, anterior view.** The left pes of SMA 0011 preserves four

1218 proximal non-ungual phalanges (Fig. 35C). They are relatively short bones with a flat

1219 proximal articular surface, and subsequently less well-developed distal condyles, from php I-1

1220 to php IV-1. ~~The p~~

1221 _____Pedal phalanx I-1 is slightly wedge-shaped, with a considerably shorter lateral than

1222 medial surface. Therefore, the distal condyles face laterodistally, resulting in the typical

1223 lateral deflection of the pedal unguals of eusauropods (Bonnan, 2005). The anterior surface is

1224 transversely narrower than the posterior surface. Due to the semi-emerged mounting method,

1225 which covers the posterior half of the phalanx, the angle between the posterior and the

1226 proximal surface cannot be determined.

1227 Pedal phalanges II-1 and III-1 are similar in general shape. The former is slightly

1228 broader than php III-1, which has subequal widths and lengths (Tab. 8). The medial condyle

1229 of both phalanges is transversely compressed, but projects further distally than the lateral one.

1230 The phalanx mounted as php IV-1 has a similar outline ~~as~~to that of php II-1, but is

1231 about half its size. The surfaces are relatively undefined, and distal condyles are barely

1232 distinguishable. This implies that if a second phalanx was present in the same digit, it was

1233 most probably vestigial. The indistinct shape of this element suggests that it might actually

1234 also represent php III-2 or php V-1. In *Apatosaurus* and *Camarasaurus*, php IV-1 has a

1235 distinct shape in being the only element with a longer lateral than medial surface (Gilmore,

1236 1936; Tschopp, 2008). It usually also shows distinct medial and lateral condyles, at least in

1237 distal view (Hatcher, 1901; Gilmore, 1936; Janensch, 1961; Bonnan, 2005; Tschopp, 2008),

1238 unlike the element mounted as php IV-1 in the pes of SMA 0011.

1239 **Pedal unguals L, anterior view.** Three unguals are present in the left pes of SMA 0011 (Fig.

1240 35C). As mounted, this amounts to a pedal phalangeal formula of 2-2-2-1-0. This, however, is

1241 most probably underestimated, as comparisons with other diplodocid feet~~,~~ and the

1242 questionable assignment of php IV-1 indicate (Hatcher, 1901; Gilmore, 1936; Janensch, 1961;

1243 Bonnan, 2005). The pedal unguals are sickle-shaped~~,~~ and decreas~~ing~~e in length from the first

1244 to the third. They are strongly transversely compressed, but this is possibly slightly

1245 exaggerated due to taphonomy. The anterior edge is strongly curved and narrow. The medial

1246 surfaces are convex, the lateral sides concavoconvex anteroposteriorly. The pedal unguals are

1247 wider transversely in their plantar half, especially at the proximal end, where the wider area

1248 bears the proximal articular surface. ~~The u~~Ungual III is the most stout element, as the

1249 proximal width remains more or less the same from ungual I to III, whereas the length

1250 decreases.

1251 **Ontogeny**

1252 The specimen SMA 0011 shows a variety of features that were previously reported to

1253 indicate a juvenile age ~~of~~for ~~the~~an animal. Cranial ontogeny in diplodocids was extensively

1254 discussed by Whitlock et al. (2010), who proposed the following juvenile features in

1255 *Diplodocus*: a relatively rounded snout, with tooth rows that reach further back, and a large

1256   orbit. Whereas the latter is typical for most amniotes (Varricchio, 1997; Whitlock et al.,

1257   2010), the first two characteristics also occur in subadults ~~to~~and adults of other diplodocines,

1258   showing that at least in *Diplodocus*, ontogeny ~~is recapitulating~~recapitulated phylogeny to

1259   some degree (Tschopp and Mateus, 2013b). The skull of SMA 0011 has an orbit of about the

1260   same relative size as CM 11161, and thus relatively smaller than the juvenile CM 11255

1261   (Whitlock et al., 2010). However, the snout is more rounded, reaching only 72% in the PMI,

1262   compared to more than 80% in CM 11161 (Whitlock, 2011b). Taken together, this indicates a

1263   more basal phylogenetic position of SMA 0011 compared to *Diplodocus* CM 11161. Another

1264   feature in the skull of SMA 0011 deserves special notion: the canal connecting the

1265   preantorbital fossa with the antorbital fenestra. This canal could indicate that the posterior and

1266   dorsal processes of the maxilla ~~start~~started growing out of the main body of the maxilla

1267   independently, and that ~~only late in ontogeny,~~ they fused posteriorly only late in ontogeny.

1268   _____Osteological characteristics of young age in the postcranial skeleton of SMA 0011

1269   include unfused vertebral centra and neural arches, unfused cervical ribs, the ilium, which is

1270   detached from the sacrum, and a separate scapula and coracoid (Gilmore, 1925; Janensch,

1271   1961; McIntosh, 1990b; Wedel and Taylor, 2013). Other characteristics often proposed to be

1272   an indicator for a young age, but absent in SMA 0011, are open coracoid and pubic foramina,

1273   or relatively smooth articular surfaces of the long bones (Hatcher, 1903; McIntosh, 1990b;

1274   Bonnan, 2003; Schwarz et al., 2007c). Furthermore, the ~~lacking~~absence of fusion of sacral

1275   vertebrae was shown to reflect ontogeny (Riggs, 1903; Mook, 1917; Wedel and Taylor,

1276   2013), and the sternal plates are thought to adopt their definitive shape in adult animals only

1277   (Wilhite, 2003, 2005), but neither the sacrum nor any sternal plate are preserved in SMA

1278   0011. Carpenter and McIntosh (1994) furthermore proposed that the longitudinal ridges on the

1279   distal shafts of radius and ulna develop during ontogeny, but this could also be a

1280   taxonomically valid character, given that *Dyslocosaurus* or *Diplodocus* appear to have them

1281   much less developed than *Apatosaurus* (ET, pers. obs., 2011). Wilson (1999), Bonnan (2007),

1282   Schwarz et al. (2007c), and Carballido and Sander (2013) showed that vertebral lamination

1283   and pneumaticity increases during ontogeny, but only the smallest neosauropod specimens

1284   show largely reduced pleurocoels and laminae (equivalent to the MOS 1; Schwarz et al.,

1285   2007c; Carballido and Sander, 2013; CM 566, SMA 0009, ET, pers. obs., 2011). Wedel et al.

1286   (2000) reported an increase in cervical centra elongation of 35-65% in *Apatosaurus*.

1287   However, their calculation was based on juvenile vertebrae from Oklahoma, identified as

1288   *Apatosaurus* by Carpenter and McIntosh (1994), but some of them might actually belong to

1289   *Camarasaurus* (Upchurch et al., 2004b). Increase in centrum elongation was also shown to

1290   happen during ontogeny of *Europasaurus* (Carballido and Sander, 2013). Recently, it has

1291   furthermore been suggested that the bifurcation of the neural spine is ontogenetically

1292   controlled (Woodruff and Fowler, 2012).

1293   Given the presence of both open neurocentral synchondroses as well as closed

1294   synostoses in some cervical and dorsal vertebrae of SMA 0011, the present specimen qualifies

1295   for MOS 3 and 4 of Carballido and Sander (2013), which in *Europasaurus* already show all

1296   phylogenetically significant characters of the species (Carballido and Sander, 2013). The

1297   same was hypothesized for *Suuwassea emilieae* ANS 21122 (Hedrick et al., 2012) and

1298   *Bonitasaura salgadoi* (Gallina, 2011, 2012) and is thus here regarded to be valid as well for

1299   SMA 0011. Contrary to Woodruff and Fowler (2012), the immature state of some vertebrae of

1300   SMA 0011 does thus not appear to be correlated with the posterior onset of neural bifurcation,

1301   which is herein regarded as phylogenetically significant. Furthermore, Woodruff and Fowler

1302   (2012) based their assessment on material that has not yet been identified to genus or species

1303   level, and given that this feature changes among different genera (McIntosh, 2005), their

1304   results remain doubtful.

1305   **Histology.** The histology of the scapula, humerus, and femur of SMA 0011 has been

1306   ~~studied~~described by Klein and Sander (2008). This allows for an accurate comparison of

1307   morphological and histological ontogenetic markers. Both the humerus as well as the femur of

1308   SMA 0011 were classified within HOS stage 9, whereas the scapula showed a varying degree

1309   of remodeling from medial to lateral (Klein and Sander, 2008). This is the same age as

1310   suggested for *Suuwassea* (Hedrick et al., 2012) and *Bonitasaura* (Gallina, 2012), and is

1311   probably the stage~~,~~ where sexual maturity is reached (Klein and Sander, 2008), although the

1312   timing of sexual maturity is still a matter of debate (Hedrick et al., 2012).

1313   **Timing of neurocentral closure.** The pattern of neurocentral closure is variable among

1314   archosaurs (Brochu, 1996; Irmis, 2007; Birkemeier, 2011; Ikejiri, 2012). Even within

1315   Sauropoda, varying patterns have been reported (Harris, 2006b; Irmis, 2007; Gallina, 2011;

1316   Carballido and Sander, 2013). The incomplete nature and rare finds of immature specimens

1317   result in additional difficulties, and ~~only~~ very little information is available from articulated or

1318   associated vertebral columns (Gilmore, 1925; Harris, 2006b; Schwarz et al., 2007c; Gallina,

1319   2011; Carballido et al., 2012a). The current specimen is thus of special importance for the

1320 study of neurocentral closure in sauropods.

1321 SMA 0011 has closed, but visible neurocentral synostoses in anterior and posterior cervical

1322 vertebrae, and in anterior and mid-dorsal vertebrae. Mid-cervical, one mid-dorsal, and all

1323 posterior dorsal vertebrae of SMA 0011 have open neurocentral synchondroses. No cervical

1324 rib is fused to its corresponding centrum. Given that long bone histology revealed that SMA

1325 0011 already reached sexual maturity (Klein and Sander, 2008), it seems that open

1326 synchondroses still occurred in sexually mature sauropods. In *Suuwassea*, the same is the case

1327 for caudal vertebrae, but all preserved presacral vertebrae are fused (Harris, 2006b). However,

1328 only fragmentary mid- and posterior cervical, and no mid- and posterior dorsal vertebrae are

1329 preserved in ANS 21122, which are the only elements still showing unfused centra and neural

1330 arches in SMA 0011. As for SMA 0011, also ANS 21122 also has unfused cervical ribs, a

1331 separate scapula and coracoid, but a closed coracoid foramen and relatively rugose articular

1332 surfaces of the longbones (Harris, 2006b, 2007; Hedrick et al., 2012). The two specimens

1333 therefore seem to be of about the same individual age. The titanosaur *Bonitasaura* MPCA-460

1334 appears to show a slightly different pattern of neurocentral closure, with a completely fused

1335 axis, but open anterior cervical and dorsal vertebrae, and closed posterior elements (Gallina,

1336 2011). However, also MPCA-460 was shown to fit into HOS 9 (Gallina, 2012). These three

1337 specimens therefore indicate that neurocentral closure was delayed and only completed after

1338 sexual maturity in sauropods. They also show that the pattern of closure is not as simple as

1339 previously thought. bBased on comparisons with crocodiles, and on partial finds of

1340 specimens with open synchondroses and closed neurocentral synostoses, a posterior-to-

1341 anterior sequence was postulated (Brochu, 1996; Irmis, 2007; Birkemeier, 2011; Ikejiri, 2012;

1342 Tschopp and Mateus, 2013b). However, SMA 0011 shows that - at least in diplodocids - in

1343 both the cervical and the dorsal column, the middle elements fuse last, and that within one

1344 single vertebra, the fusion starts posteriorly and progresses anteriorly (Fig. 21). Adding the

1345 information from *Suuwassea* ANS 21122, anterior cervical vertebrae appear to fuse first (also

1346 in SMA 0011, these are the ones where the synchondroses are the least visible), followed by

1347 anterior dorsal and posterior cervical vertebrae, posterior dorsal vertebrae, whereas mid-

1348 cervical, mid-dorsal, and anterior to mid-caudal vertebrae fuse last. This varies from

1349 *Bonitasaura*, where a posterior-to-anterior pattern was proposed both within the postaxial

1350 cervical and in the dorsal columns (Gallina, 2011). A general posterior-to-anterior fusion

1351 pattern also appears to be present in at least one *Camarasaurus* (Trujillo et al., 2011), and the

small juvenile, probably basal titanosauriform SMA 0009, which already have closed, but still visible, synchondroses in anterior caudal vertebrae (Schwarz et al., 2007c; Carballido et al., 2012a). Different fusion patterns might thus prove to be a taxonomically valid character, with Macronaria showing a faster neurocentral closure than Diplodocoidea, and following a more strict posterior-to-anterior pattern, at least in the single vertebral regions. However, too few specimens are known to date, where neurocentral closure can be directly compared with histology, in order to evaluate this character statistically. Nonetheless, these finds have further implications for the individual age of the holotype specimen of *Kaatedocus siberi*, SMA 0004 (Tschopp and Mateus, 2013b). The latter does not show any traces of neurocentral synostoses in any cervical vertebra, and also has completely fused cervical ribs (Tschopp and Mateus, 2013b). Being a diplodocine, this implies that Tschopp and Mateus (2013b) were right in identifying SMA 0004 as at least subadult specimen, which retained a relatively small size. Moreover, as Carballido and Sander (2013) showed for *Europasaurus*, sauropod vertebrae already show the majority of the phylogenetically informative characters of their respective species before the completion of the neurocentral closure.

Specimen-based phylogenetic analysis of Diplodocidae

Methods

The phylogenetic analysis is based on Whitlock (2011a), with changes introduced by Mannion et al. (2012) and Tschopp and Mateus (2013b), and combined with the specimen-based analysis of *Apatosaurus* by Upchurch et al. (2004b). The taxon list was extended in order to include all holotypes of putative diplodocid taxa, as well as reasonably complete specimens previously assigned to any diplodocid taxon (Tab. 1). The OTU slots for the diplodocid genera and species used in the previously published analyses were substituted by single specimens. Based on earlier publications or personal observations of the specimens, 243 characters were added to the version published in Tschopp and Mateus (2013b). Changes and character deletions proposed by Tschopp et al. (2013) were applied. Operational taxonomic units were scored based on personal observations where possible, on published descriptions where existing, or on photos from fellow researchers (Tab. S1).

Phylogenetic analysis

The phylogenetic analysis was performed with the software TNT (Goloboff et al., 2008),

using the New Technology Search tool and enabling all options (Sect. Search, Ratchet, Drift, and Tree Fusing). Of the 53 multi-state characters, 23 were treated as ordered (explained in the character descriptions below). The consensus tree was stabilized five times with factor 75.

Main analyses. Several preliminary analyses were run in order to test previous hypotheses that unified several specimens into one individual (see below). By doing so, the data set was reduced from 81 operational taxonomic units to 76, which decreased the percentage of highly incomplete taxa and increased taxon overlap, which would otherwise have been very low (Tab. S2). The final reduced data set was again analyzed with the above stated settings. Additionally, in order to find all possible shortest trees, the TNT script 'bbreak' was used with tree bisection and reconnection (command: bbreak=tbr safe). A reduced consensus tree was produced by using the heuristic method (Trees > Comparison > Agreement subtrees). Specimens not represented in the reduced consensus were added one by one to check their possible phylogenetic positions. Subsequently, pruned trees were generated (Trees > Comparison > Pruned Trees), with the parameters different from the default set as follows: up to 4 taxa, list as text. Since the three taxon combinations proposed by the 'pruned tree analysis' include only six specimens in total, a strict consensus tree was generated excluding all of these six OTUs a posteriori.

Given the low consistency index (CI) and thus high number of homoplasies in the dataset, an additional analysis with the same settings, but under implied weighting was conducted. Implied weighting calculates and adapts the weight of the characters during the analysis, based on the consistency index of the single characters (Goloboff, 1993). ~~As~~Because characters with a high number of homoplasies in a specimen-based analysis are possibly coding for individual variation, and thus not phylogenetically significant, downweighting of these characters would be expected to yield more accurate results. Furthermore, as ontogenetic changes generally occur in a similar way in closely related taxa, and given that the dataset includes several putative juvenile to subadult specimens (YPM 1901, SMA 0009, CM 566, and possibly ANS 21122, SMA 0004, CM 3452, SMA 0011, AMNH 7530, AMNH 7535, SMA O25-8, SMA D16-3), characters describing them are probably more homoplastic than others and thus downweighted as well. Downweighting of the homoplastic characters was preferred over deleting, because certain characters were only homoplastic in one part of the tree. Traits variable within one clade can thus still be diagnostic for another group

Support values. For both analyses, symmetric resampling was preferred over bootstrapping

1415   or jackknifing for quantifying node support (Analyze > Resample; using the default settings).

1416   Symmetric resampling is not affected by differential weighting of the characters, and thus a

1417   more meaningful value for the analysis with implied weights (Goloboff et al., 2003). For

1418   better comparison between the trees of the two methods, the same method was used for both

1419   analyses.

1420   In order to quantify overlap within the single clades recovered, an overlap index was created

1421   together with F. Tschopp (Jona, Switzerland), indicating how many characters of the total 477

1422   are available for analysis between the ingroup species. Overlaps were defined as the number

1423   of specimens for which a character was scorable, minus one, because if only one specimen of

1424   the group preserves a certain bone, no anatomical overlap is present in order to compare with

1425   other specimens of the same group. The index increases when more characters are scored in at

1426   least two specimens, or when the number of specimens scorable for the same character is

1427   enlarged. It thus combines a measure for the completeness of the matrix with the

1428   comparability of single characters within specimens of a single group. Thereby, it gives an

1429   idea of the strength of the matrix to recover certain clades. However, it does not provide a

1430   measure for the significance of the result, as incomplete specimens might still bear

1431   taxonomically highly significant characters, which allow to identify it even to genus or

1432   species level. The overlap index is thus especially useful to evaluate taxa changing their

1433   positions between different trees. By calculating the overlap index for the sister group

1434   arrangements including the questionable taxon, researchers get an idea of how well the

1435   arrangement is supported based on overlapping skeletal material.

Positional terms for vertebrae

1437   Serial variation within the vertebral column is highly developed in sauropods, and of

1438   taxonomical importance (Wilson, 2002, 2012). The high variability requires detailed character

1439   descriptions restricted not only to cervical, dorsal or caudal vertebrae, but even to areas within

1440   the respective portions of the column. It is thus general use in phylogenetic analyses that

1441   characters are restricted to anterior cervical vertebrae, or mid- and posterior caudal vertebrae,

1442   for example (Wilson, 2002; Upchurch et al., 2004a, b; Whitlock, 2011a; Mannion et al., 2012;

1443   Tschopp and Mateus, 2013b). However, a majority of the papers using phylogenetic analyses

1444   do not state how they define these subdivisions. The definitions used in the present analysis

1445   mostly follow the ones proposed by Mannion et al. (2013), and are summarized in table 10.

Material

Ingroup specimens phylogenetic analysis

The following individual, presumed diplodocid, specimens were included in the ingroup of the phylogenetic analysis. All of these are reasonably complete specimens of reputed diplodocid species, or constitute the holotypes of taxa, irrespective of completeness, which have been either referred or associated to Diplodocidae. Previous classifications and assignments, as well as comments on the likelihood that they represent singular individuals, are given below, alphabetically ordered. Outgroups comprise species-, or genus-level taxa from non-neosauropod Eusauropoda, Macronaria, as well as closely related Diplodocoidea. They are not further discussed here.

Amphicoelias altus, **AMNH 5764 and AMNH 5764 ext.** The holotype of *Amphicoelias altus* originally included a tooth, two dorsal vertebrae, a pubis, and a femur (Cope, 1877a). A scapula, coracoid, and an ulna were later provisionally referred to the specimen (Osborn and Mook, 1921). However, the strongly expanded distal end of the scapula, and the relatively deep notch anterior to the glenoid on the coracoid actually resemble more *Camarasaurus* than any diplodocid (ET, pers. obs., 2011). The same accounts for the single tooth stored at AMNH (Osborn and Mook, 1921). The tooth has already been excluded from scores of *A. altus* in recent phylogenetic analyses (Whitlock, 2011a; Mannion et al., 2012), which is followed here. Two different preliminary phylogenetic analyses were performed with a reduced (excluding the scapula and coracoid) and the extended holotype material (including all referred elements). ~~As~~Because both analyses yielded the same position for the specimens, the reduced holotype was preferred in the final analysis. The risk of adding dubious information from potentially wrongly referred material was thus circumvented. More detailed analysis is needed in order to refine these assignments.

'*Amphicoelias***' *latus*, **AMNH 5765.** This is a fragmentary specimen comprising four caudal vertebrae and a right femur from the same site as the holotypes of *Camarasaurus supremus* and *Amphicoelias altus* (Cope, 1877a; Osborn and Mook, 1921; Carpenter, 2006). Both the vertebrae and the femur show greater resemblance with *Camarasaurus* than to *Amphicoelias*, which led Osborn and Mook (1921) to synonymize *A. latus* with *C. supremus*.

Apatosaurus ajax, **YPM 1860.** The holotype of *Apatosaurus ajax* also constitutes the genoholotype of *Apatosaurus*. During collection and shipping it became intermingled with YPM 1840, the holotype of *Atlantosaurus immanis* (McIntosh, 1995). As a result, it is

1478 currently difficult to distinguish the two individuals, even though they come from different

1479 quarries. I follow the suggestions of Berman and McIntosh (1978) and McIntosh (1995), in

1480 deciding which elements of the mingled taxa presently comprise the holotype of *Apatosaurus*

1481 *ajax*. The only material not confidently referable to either specimen is a braincase currently

1482 labeled 'YPM 1860'. In order to investigate the taxonomic implications of the attribution of

1483 this braincase to the types of *Apatosaurus ajax* or *Atlantosaurus immanis*, two supplementary

1484 analyses were performed with scores of the braincase added to YPM 1840 and 1860,

1485 respectively. Adding the information from the braincase to YPM 1840, tree length increases

1486 but positions of the two specimens remain the same. An assignment of the braincase to the

1487 holotype of *Apatosaurus ajax* appears thus more parsimonious, indicating that it was labeled

1488 ~~right~~correctly.

1489 ***Apatosaurus ajax*, AMNH 460.** This specimen was recovered as *Apatosaurus ajax* in the

1490 specimen-based phylogenetic analysis of Upchurch et al. (2004b). Because AMNH 460 is

1491 mounted with reconstructed contribution of other specimens, caution has to be used, in order

1492 to not code characters based on reconstructed bones or elements actually belonging to other

1493 specimens (for a list of bones belonging to AMNH 460, see table S1).

1494 ***Apatosaurus ajax*, NSMT-PV 20375.** Described by Upchurch et al. (2004b), this specimen is

1495 the only fully described skeleton previously referred to *A. ajax*. It is relatively complete,

1496 although abnormal length ratios of the humerus, radius and metacarpal III suggest that

1497 NSMT-PV 20375 might be composed of more than one individual, possibly including bones

1498 of the *Camarasaurus* specimens found intermingled in the quarry (Upchurch et al., 2004b).

1499 These forelimb elements were thus excluded from scores of the OTU in the present analysis.

1500 **'*Apatosaurus*' *grandis*, YPM 1901.** Marsh (1877a) initially assigned this species to

1501 *Apatosaurus*, but subsequently referred it to *Morosaurus* (Marsh, 1878; later synonymized

1502 with *Camarasaurus*: Mook, 1914). There is some confusion about the correct assignment of

1503 several bones to either the holotype YPM 1901 or the referred specimens YPM 1902 or YPM

1504 1905 from the same quarry (see Ostrom and McIntosh, 1966). Herein, scores are included

1505 from all elements potentially belonging to YPM 1901 (according to Ostrom and McIntosh,

1506 1966). ~~As~~Because all three specimens were referred to *Camarasaurus*, this should have no

1507 influence on the ingroup relationships of the current phylogenetic analysis.

1508 ***Apatosaurus laticollis*, YPM 1861.** *Apatosaurus laticollis* is based on a single, fragmentary

1509 cervical vertebra (Marsh, 1879). Subsequent studies proposed that this vertebra actually

belongs to the same individual as the holotype material of *Atlantosaurus immanis* (YPM 1840), which were both found in the Lakes Quarry 1 (McIntosh, 1995). Here, the specimens were kept apart in order to evaluate this hypothesis.

***Apatosaurus louisae*, CM 3018 (holotype) and CM 11162.** The most complete specimen of *Apatosaurus* is CM 3018, a postcranial skeleton that was preliminarily described as new species by Holland (1915a) and followed by a detailed monographic treatment by Gilmore (1936). An obvious diplodocid skull (CM 11162) was found near it, but the historical referral of the latter specimen remained confused for a time (Holland, 1915b, 1924; Berman and McIntosh, 1978). Because *Apatosaurus* was thought to have a more *Camarasaurus*-like skull at the time, Holland's proposal that CM 11162 was the actual skull of CM 3018 (Holland, 1915b, 1924) was largely unaccepted by others (e.g. Gilmore, 1936). Only with the detailed description and study of the specimen by Berman and McIntosh (1978) did CM 11162 become the now widely accepted skull-form of *Apatosaurus*. Given the small distance between skull and postcrania in the quarry, as well as the perfectly fitting size of the cranial occipital condyle and postcranial atlas, the probability that the two belong to the same individual is very high (Holland, 1915b; Berman and McIntosh, 1978). Accordingly, the OTU representing the holotype of *Apatosaurus louisae* in the present analysis comprises scoring from both CM 3018 and 11162.

***Apatosaurus louisae*, CM 3378.** The specimen was identified as *Apatosaurus louisae* in the analysis of Upchurch et al. (2004b). Although never described in detail, CM 3378 yields important information on the number of vertebrae in *Apatosaurus*, as this specimen is the only known with an articulated, uninterrupted vertebral column from the mid-cervical region to the last caudal vertebra (Holland, 1915b; McIntosh, 1981). CM 3378 was found at the Dinosaur National Monument, associated with a diplodocid skull (CM 11161; interpreted as *Diplodocus*), as well as appendicular elements. However, according to McIntosh (1981), these materials cannot be attributed to the same individual as CM 3378 with certainty, and no scores from them were thus included in this OTU.

'*Apatosaurus*' *minimus*, AMNH 675. Initially described as new species of *Apatosaurus* (Mook, 1917), AMNH 675 is now generally considered an indeterminate sauropod, with affinities to Titanosauriformes, based on the shape of the ilia and the six sacral vertebrae (McIntosh, 1990a). In order to test this, *Isisaurus colberti* was added to the analysis. *Isisaurus* has the typical titanosaurian sacrum with six vertebrae and the preacetabular lobe oriented

1542 perpendicular to the vertebral axis (Jain and Bandyopadhyay, 1997), as is the case in AMNH

1543 675. At AMNH, a diplodocid chevron is also accessioned in AMNH 675. However, because

1544 AMNH record indicate it was 'found loose with other Bone Cabin Quarry material', we

1545 excluded scoring it as part of *A. minimus*.

1546 ***Apatosaurus parvus*, UW 15556.** This specimen was found by the Carnegie Museum,

1547 intermingled with the holotype specimen of *Elosaurus parvus*, CM 566 (Hatcher, 1902;

1548 Peterson and Gilmore, 1902). It first bore the specimen number CM 563, but was later

1549 transferred to the University of Wyoming (McIntosh, 1981). Usually identified as *A. excelsus*

1550 (Gilmore, 1936), a specimen-based phylogenetic analysis supported the retention of the

1551 species *parvus* for CM 566 and UW 15556 (Upchurch et al., 2004b).

1552 ***Apatosaurus* sp., FMNH P25112.** Riggs (1903) described this specimen (formerly FMNH

1553 7163) as *A. excelsus*, which led him to two important conclusions: 1) *Brontosaurus* is a junior

1554 synonym of *Apatosaurus*, and 2) during ontogeny, additional vertebrae are added from the

1555 dorsal and caudal series to the sacrum. Later, the specimen-based phylogenetic analysis of

1556 Upchurch et al. (2004b) recovered it on a disparate branch within *Apatosaurus*, suggesting

1557 that FMNH P25112 represents a novel species. The specimen is mounted at FMNH together

1558 with the neck and forelimbs of FMNH P27021 (W. Simpson, pers. comm., 2013).

1559 ***Apatosaurus* sp., ML 418.** This specimen is very badly preserved. One dorsal vertebra has

1560 been prepared and was identified as a possible *Apatosaurus* or *Dinheirosaurus* (Antunes and

1561 Mateus, 2003; Mateus, 2005; Mannion et al., 2012). Additional unprepared material includes

1562 dorsal rib fragments, and a partial tibia. A mid- or posterior cervical vertebra of the same

1563 individual was lost due to the friable preservation, and scores concerning the cervical

1564 vertebrae therefore are based on photographs.

1565 ***Atlantosaurus immanis*, YPM 1840.** This is possibly the same individual as YPM 1861

1566 (*Apatosaurus laticollis*), and it was mingled with YPM 1860 (*Apatosaurus ajax*) during

1567 shipping (see above). McIntosh (1995) tried to separate them based on their color, and on the

1568 sparse field notes. In the YPM collections, the specimens remain tagged as they have been

1569 before McIntosh's study, therefore it is difficult to reproduce his results. Scores for an ischium

1570 of YPM 1840 are based on personal observation, whereas cervical and dorsal vertebral

1571 characters are derived from the literature (Marsh, 1896; Ostrom and McIntosh, 1966;

1572 Upchurch et al., 2004b).

1573 ***Australodocus bohetii*, holotype and paratype.** The holotype and paratype are two

1574   successive mid-cervical vertebrae from the same individual (Remes, 2007). Mannion et al.

1575   (2013) suggested *Australodocus* to be a non-lithostrotian titanosaur. Accordingly,

1576   *Ligabuesaurus leanzai* was added to the taxon list in order to include a possible closely

1577   related derived titanosauriform that has anatomical overlap with *A. bohetii*.

1578   ***Barosaurus affinis*, YPM 419.** The holotype of *B. affinis* consists only of pedal material, and

1579   has no overlap with the holotype of *B. lentus* (Marsh, 1890, 1899). Because they come from

1580   the same quarry, the two species were usually regarded as synonyms (Lull, 1919; McIntosh,

1581   2005). McIntosh (2005) identified the elements as mt I and partial mt II, but the latter is

1582   herein interpreted to represent the proximal portion of mt V instead. The bone is widely

1583   expanded, and has the typical 'paddle'-shape of the metatarsal V in sauropods (ET, pers. obs.,

1584   2011).

1585   ***Barosaurus lentus*, YPM 429.** Although this specimen is the genoholotype of *Barosaurus*

1586   (Marsh, 1890; Lull, 1919), most characterization of *Barosaurus* is based on another, more

1587   complete, and articulated specimen (AMNH 6341, see below). YPM 429 as presently

1588   available has a high degree of reconstruction, especially in some cervical vertebrae.

1589   ***Barosaurus* sp., AMNH 6341.** This specimen is the most complete probable *Barosaurus*

1590   (McIntosh, 2005). It was collected in three parts and subsequently separated by different

1591   institutions (USNM, CM, and UUVP), but later brought together by B. Brown for the AMNH

1592   (Bird, 1985). Some doubts exist concerning the correct attribution of a tibia-fibula pair, which

1593   might also belong to a *Diplodocus* specimen found in the vicinity of AMNH 6341 (McIntosh,

1594   2005).

1595   ***Barosaurus* sp., AMNH 7530.** Both the holotype specimen of *Kaatedocus siberi* (SMA

1596   0004) and AMNH 7530 were found at Howe Quarry (Michelis, 2004; Tschopp and Mateus,

1597   2013b). AMNH 7530 is tagged as *Barosaurus* on display at AMNH, probably based on a

1598   tentative identification made by Brown (1935), but without detailed study. AMNH 7530 is an

1599   important specimen for diplodocid taxonomy because it includes articulated anterior and mid-

1600   cervical vertebrae and a partial skull.

1601   ***Barosaurus* sp., AMNH 7535.** This specimen was recovered with *Kaatedocus siberi* SMA

1602   0004 and AMNH 7530 at Howe Quarry (Michelis, 2004; Tschopp and Mateus, 2013b), and

1603   has been simply cataloged as *Barosaurus* in the collections of the AMNH (likely by B.

1604   Brown; Brown, 1935). AMNH 7535 largely preserves the same elements as SMA 0004 and

1605   AMNH 7530, and appears to be of about the same size. A partial tail is also accessioned under

1606 AMNH 7535, but given the chaotic distribution of specimens in the quarry (Tschopp and

1607 Mateus, 2013a: fig. 1), it is impossible to confidently attribute disparate and disarticulated

1608 portions to any single common individual. A diplodocid quadrate that was initially cataloged

1609 under AMNH 7535 now bears the number AMNH 30070. ~~Since~~Because the original

1610 attribution of this quadrate to AMNH 7535 was probably based on their vicinity in the quarry,

1611 two analyses were performed with and without the information of this bone, yielding the same

1612 phylogenetic position in both iterations. On both instances, information from the caudal series

1613 were omitted from scores of AMNH 7535. Scores on the quadrate were retained in the final

1614 analysis because AMNH 30070 shows some differences with the quadrates known from

1615 *Kaatedocus* (e.g. lack of the small fossa dorsomedially on the quadrate shaft, ET, pers. obs.,

1616 2011), as do also the cervical vertebrae.

1617 ***Barosaurus* sp., CM 11984.** Together with YPM 429 and AMNH 6341, CM 11984

1618 represents a third, relatively complete, likely *Barosaurus* specimen (McIntosh, 2005). Some

1619 of the material of CM 11984 is still unprepared, and further crucial information on

1620 *Barosaurus* can be expected once these are freed from matrix. In addition to the vertebral

1621 column, a pes is accessioned under CM 11984, which McIntosh (2005) considered to have a

1622 dubious association with the remaining material, given the chaotic quarry situation at

1623 Dinosaur National Monument. Therefore, this pes is not considered as part of the scoring of

1624 CM 11984.

1625 ***Brachiosaurus* sp., SMA 0009.** Initially described as a diplodocid (Schwarz et al., 2007c), a

1626 reassessment of the systematic position of SMA 0009 after further preparation of the mid-

1627 cervical vertebrae revealed probable titanosauriform affinities (Carballido et al., 2012a).

1628 Because Carballido et al. (2012a) suggested that SMA 0009 represents an immature

1629 *Brachiosaurus*, *B. altithorax* (Riggs, 1904; Taylor, 2009) was included in the dataset.

1630 ***Brontosaurus amplus*, YPM 1981.** The type of *B. amplus* (Marsh, 1881) is generally

1631 accepted as synonym to *Apatosaurus excelsus* (Gilmore, 1936; McIntosh, 1990a, 1995;

1632 Upchurch et al., 2004b), but has never been described in detail.

1633 ***Brontosaurus excelsus*, YPM 1980.** The holotype of *Brontosaurus excelsus* (now commonly

1634 synonymized with *Apatosaurus*) was the first to be published with a reconstruction of the

1635 entire skeleton (Marsh, 1883)~~,~~ and is still one of the best preserved diplodocid specimens

1636 worldwide. For the mount at YPM it was extensively reconstructed, such that special care has

1637 to be taken when scoring its characters from the original specimen.

1638 ***Cetiosauriscus stewarti*, NHMUK R3078.** The holotype specimen was first described in the

1639 early 1900s (Woodward, 1905) as *Cetiosaurus leedsi*. However, Huene (1927) identified

1640 '*Cetiosaurus*' *leedsi* as a separate genus, *Cetiosauriscus*, and highlighted the then referred

1641 specimen NHMUK R3078 as exemplifying the new genus. NHMUK R3078 was made the

1642 holotype of *Cetiosauriscus stewarti* (Charig, 1980), which later was instated as the type

1643 species of *Cetiosauriscus* (Charig, 1993). It was included in Diplodocidae by McIntosh

1644 (1990b), based on pedal morphology, but subsequent analyses proposed a closer relationship

1645 with the non-neosauropod eusauropods *Mamenchisaurus* or *Omeisaurus*, as well as with

1646 *Tehuelchesaurus* (Heathcote and Upchurch, 2003). *Mamenchisaurus* and *Omeisaurus* were

1647 thus included in the present analysis in order to test these competing hypotheses. A detailed

1648 restudy of the material is in preparation by P. Mannion and P. Upchurch (pers. comm., 2011,

1649 2012), and will doubtlessly reveal more valid characters. ~~Since~~Because personal observation

1650 of the caudal vertebrae of *Spinophorosaurus nigerensis* revealed high similarity with

1651 *Cetiosauriscus*, *S. nigerensis* was added to the matrix, in order to appraise the phylogenetic

1652 ~~role~~significance of their morphological similarities.

1653 ***Dinheirosaurus lourinhanensis*, ML 414.** The holotype of *Dinheirosaurus lourinhanensis*

1654 was originally referred to *Lourinhasaurus alenquerensis* by Dantas et al. (1998), but

1655 Bonaparte and Mateus (1999) realized that ML 414 represents a different genus. Contrary to

1656 the phylogenetic assignment of ~~-~~*L. alenquerensis*, which is now thought to be a basal

1657 macronarian (see below), the diplodocid affinities of *D. lourinhanensis* are well supported by

1658 four phylogenetic analyses (Rauhut et al., 2005; Whitlock, 2011a; Mannion et al., 2012;

1659 Tschopp and Mateus, 2013b).

1660 ***Diplodocus carnegii*, CM 84.** The holotype of *D. carnegii* is one of a few specimens of

1661 *Diplodocus* that includes cervical vertebrae. It is mounted at CM, and completed with bones

1662 from various other specimens: CM 94, 307, 21775, 33985, HMNS 175, USNM 2673, and

1663 AMNH 965 (McIntosh, 1981; Curtice, 1996). Scores of the holotype of *D. carnegii* are based

1664 on this mounted specimen, with effort taken to ensure that only material from CM 84 was

1665 included. *D. carnegii* was erected based on comparisons to AMNH 223, which showed some

1666 differences in caudal neural spine orientation. If compared with the original type material, the

1667 differences are not as clear, and were in fact disputed by Gilmore (1932).

1668 ***Diplodocus carnegii*, CM 94.** This specimen was described as a paratype of *D. carnegii*

1669 (Hatcher, 1901). Both holotype and paratype specimens were found in the same quarry, from

1670 where also material of other genera was recovered (Hatcher, 1901). Oddly, CM 94 includes

1671 two pairs of ischia, which casts some doubt on the true attribution of bones to individual

1672 specimens (McIntosh, 1981; ET, pers. obs., 2011). As both pairs of ischia show the same

1673 characteristics, we included the entire material excluding one pair of ischia from the OTU

1674 representing CM 94 (including some bones mounted with the holotype of *Galeamopus hayi*

1675 HMNS 175, see below). However, further studies are needed in order to definitively assign

1676 the various bones among the at-least two individuals present.

1677 ***Diplodocus* cf. *carnegii*, WDC-FS001A.** This specimen has not been described entirely, but

1678 is the most complete referral to *Diplodocus* that has a manus with associated hindlimb and

1679 axial material (Bedell and Trexler, 2005). The specimen was found in two spatial clusters in

1680 the quarry, but the lack of duplicated bones, the two similarly sized humeri, and osteological

1681 indications of a single ontogenetic stage led Bedell and Trexler (2005) to identify the

1682 materials as belonging to a single individual with affinities to *D. carnegii*.

1683 ***Diplodocus lacustris*, YPM 1922.** The original type material of *D. lacustris* comprises teeth,

1684 a premaxilla, and a maxilla (Marsh, 1884). However, personal observations at YPM reveal

1685 that the cranial bones clearly belong to ***Camarasaurus*** or a morphologically similar taxon,

1686 and that there is no relationship between them and the teeth. Mossbrucker and Bakker (2013)

1687 describe a newly found putative apatosaur maxilla and two premaxillae from the same quarry,

1688 proposing that they might belong to the same individual as the teeth of YPM 1922. However,

1689 given the lacking field notes from the first excavations, such a referral will be difficult to

1690 prove. Therefore, in the present analysis, only the teeth were scored for *D. lacustris*.

1691 ***Diplodocus longus*, YPM 1920.** YPM 1920 constitutes the genoholotype of *Diplodocus*

1692 (Marsh, 1878)~~,~~ and has thus special taxonomic importance. Unfortunately, it is highly

1693 incomplete, with only two nearly complete caudal vertebrae, and few additional fragmentary

1694 anterior to mid-caudal vertebrae identifiable in the YPM collections. A chevron was reported

1695 as belonging to the same individual (Marsh, 1878; McIntosh and Carpenter, 1998), but it

1696 could not ~~have been~~be located at YPM in 2011. Other articulated vertebrae were found in the

1697 field but discarded due to their friable preservation (McIntosh and Carpenter, 1998).

1698 Extraneous materials were once assigned to the same specimen, including a skull, femur,

1699 tibia, fibula, astragalus, and five metatarsals (still accessioned under YPM 1920), as well as

1700 an ulna, radius, and partial manus assigned YPM 1906 (McIntosh and Carpenter, 1998).

1701 However, only the caudal series and the chevron can be ~~surely~~confidently identified as

1702 belonging to the holotypic individual (McIntosh and Carpenter, 1998), as scored in the present

1703 analysis.

1704 ***Diplodocus* sp., AMNH 223.** The specimen was first described as *Diplodocus longus*

1705 (Osborn, 1899). It was the first reasonably articulated specimen of *Diplodocus* and thus

1706 became one of the important specimens on which to base comparisons ~~to~~ (see Hatcher, 1901).

1707 Three partial cervical neural arches, described and figured by Osborn (1899), could not be

1708 located at AMNH (ET, pers. obs., 2010, 2011). Coding of these elements is thus based

1709 entirely on Osborn (1899).

1710 ***Diplodocus* sp., AMNH 969.** This skull and associated atlas and axis were identified as *D.*

1711 *longus*, based on an earlier report of a skull allegedly belonging to the holotype specimen of

1712 *D. longus*, YPM 1920 (Marsh, 1884; Holland, 1906). However, the only reported *Diplodocus*

1713 specimen with an articulated skull and anterior cervical vertebrae is CM 3452, of which only

1714 the skull has been described (Holland, 1924). ~~Since~~Because no anterior cervical vertebrae are

1715 definitely attributable to *D. longus*, the only comparison that can be made is with the *D.*

1716 *carnegii* type specimens, of which only CM 84 preserves the axis. ~~As~~Because the two differ

1717 in morphology (e.g. of the prespinal lamina), AMNH 969 was herein regarded *Diplodocus*

1718 sp., before the analysis (see below).

1719 ***Diplodocus* sp., CM 3452.** On display at CM, this specimen is the only possible *Diplodocus*

1720 with articulated skull and anterior cervical vertebrae (McIntosh and Berman, 1975). However,

1721 the cervical vertebrae have not been described, and no detailed study has been done in order

1722 to identify the species affinity for CM 3452 ~~belongs to~~. Comparison with other specimens

1723 referred to *Diplodocus* is hampered due to very little anatomical overlap.

1724 ***Diplodocus* sp., CM 11161.** This specimen is only a skull. It was described as *Diplodocus*

1725 *longus* by Holland (1924) and McIntosh and Berman (1975), based on comparisons with the

1726 earlier reported putative *Diplodocus* skulls AMNH 969, USNM 2672, and 2673. However,

1727 because all of them were disarticulated and found in quarries that also produced other

1728 diplodocid genera, care must be taken concerning these identifications. Our knowledge of

1729 diplodocid skulls to date suggests that they are extremely similar to each other, and very few

1730 distinguishing characters have yet been proposed (Berman and McIntosh, 1978; McIntosh,

1731 2005; Harris, 2006a; Remes, 2006; Whitlock et al., 2010; Whitlock, 2011b; Tschopp and

1732 Mateus, 2013b; Whitlock and Lamanna, 2012). Thus, ~~it is refrained here~~we refrain from

1733 referring CM 11161 to any species of *Diplodocus* until postcranial diagnostic traits are

1734 robustly linked to cranial morphologies.

1735 ***Diplodocus* sp., DMNS 1494.** This specimen is a relatively complete, articulated find from

1736 the Dinosaur National Monument. The only disarticulated elements are the right

1737 scapulacoracoid and the left hindlimb. These elements were not included in the present

1738 analysis because DMNS 1494 was found intermingled with other skeletons (V. Tidwell, pers.

1739 comm., 2010). DMNS 1494 was collected by the Carnegie Museum, and later transferred to

1740 DMNS for exhibit. A right fibula and astragalus of the same specimen remained at CM

1741 (presently CM 21763; McIntosh, 1981). The specimen has never been formally described, but

1742 is ascribed to *D. longus* (e.g. Gillette, 1991). Together with CM 84, DMNS 1494 is the only

1743 *Diplodocus* specimen included here with articulated, and complete cervical vertebrae.

1744 ***Diplodocus* sp., USNM 2672.** Like AMNH 969, USNM 2672 preserves a partial skull and

1745 atlas. It was the first diplodocid skull to be reported, and was initially included among the

1746 holotype of *D. longus*, YPM 1920 (Marsh, 1884). However, the skull and holotypic caudal

1747 vertebrae were not found in articulation or even close association, therefore this attribution

1748 has to be regarded as questionable (McIntosh and Carpenter, 1998), and the two specimens

1749 were treated as distinct OTUs.

1750 ***Diplodocus* sp., USNM 10865.** Although USNM 10865 is one of the most complete

1751 *Diplodocus* specimens, it has only been preliminarily described and was tentatively referred to

1752 *D. longus* by Gilmore (1932). USNM 10865 was found close to the articulated *Barosaurus*

1753 AMNH 6341 ('#340' in Gilmore, 1932; McIntosh, 2005). According to McIntosh (2005), two

1754 sets of left lower legs of different lengths were found associated with USNM 10865. The

1755 shorter set was mounted by Gilmore (1932), but McIntosh (2005) suggests that this

1756 assignment might have been wrong. For the character relating to the tibia/femur length, the

1757 higher ratio was therefore used, following McIntosh (2005).

1758 ***Dyslocosaurus polyonychius*, AC 663.** The only specimen of this putative diplodocid

1759 sauropod consists solely of ~~solely~~ appendicular elements of dubious origin and association

1760 (McIntosh et al., 1992). No field notes exist, but personal observations of differing color and

1761 preservation led to the conclusion that at least the supposed php III-1 was probably not

1762 collected at the same place as the rest of the holotype specimen. It is therefore excluded from

1763 scores of *Dyslocosaurus* in this phylogenetic analysis. A more detailed reassessment of this

1764 specimen is in progress (Tschopp and Nair, in prep.), and might reveal additional information

1765 on its taxonomic affinities. The phylogenetic position yielded in the present analysis is

1766 regarded as preliminary.

1767 ***Dystrophaeus viaemalae*, USNM 2364.** This specimen is highly fragmentary, but was

1768 identified as possibly diplodocoid by McIntosh (1990b; his 'Diplodocidae' conforms to the

1769 current use of the Diplodocoidea). The type material is only partly prepared, which largely

1770 impedes identifying crucial character states. The type locality was relocated in the mid-1990s,

1771 and more material of the probable holotypic individual was excavated, of which only a

1772 phalanx has been identifiable (Gillette, 1996a, b). However, Gillette (1996a, b) states that

1773 more material is probably present, such that additional information on *Dystrophaeus* might be

1774 forthcoming. Both in the initial description (Cope, 1877b) and a reassessment (Huene, 1904),

1775 several of the bones were misidentified: metacarpal V (according to Huene, 1904) is most

1776 probably a metacarpal I, based on the angled distal articular surface (McIntosh, 1997; ET,

1777 pers. obs., 2011). Cope (1877b) correctly identified a partial scapula (contra Huene, 1904,

1778 who thought it was a pubis), but misidentified a complete ulna and a partial radius as humerus

1779 and ulna, respectively, as already recognized by Huene (1904).

1780 ***Dystylosaurus edwini*, BYU 4503.** The holotype of *Dystylosaurus edwini* is an anterior dorsal

1781 vertebra (Jensen, 1985). There is some doubt concerning its taxonomic affinities: it has been

1782 identified as either brachiosaurid (Paul, 1988; McIntosh, 1990b; Upchurch et al., 2004a;

1783 Chure et al., 2006) or diplodocid, possibly even from the same individual as the *Supersaurus*

1784 *vivianae* holotype scapulacoracoid (Curtice and Stadtman, 2001; Lovelace et al., 2007). It was

1785 included in a preliminary analysis as an OTU independent from *Supersaurus vivianae* BYU

1786 and WDC DMJ-021 in order to clarify its taxonomic status. The results yielded 102 most

1787 parsimonious trees, where *Dystylosaurus* always grouped with the two *Supersaurus* OTUs,

1788 which sometimes include *Dinheirosaurus* ML 414, *Diplodocus hayi* HMNS 175, *Barosaurus*

1789 *affinis* YPM 419, or *Diplodocus lacustris* YPM 1922 within the same branch. In 31 out of 102

1790 most parsimonious trees *Dystylosaurus* and the two *Supersaurus* OTUs formed sister taxa.

1791 This result corroborates the hypothesis of Curtice and Stadtman (2001) and Lovelace et al.

1792 (2007) that the *Dystylosaurus* holotypic vertebra is *Supersaurus*, and most probably from the

1793 same individual as the *Supersaurus* holotype. In the definitive analysis BYU 4503 was thus

1794 included as part of the combined OTU representing the BYU specimens of *Supersaurus*

1795 *vivianae*.

1796 ***Elosaurus parvus*, CM 566.** CM 566 is a small juvenile that is generally referred to

1797 *Apatosaurus excelsus* (McIntosh, 1995), or constitutes the independent species *Apatosaurus*

1798 *parvus* together with an adult specimen (UW 15556; Upchurch et al., 2004b), with which it
1799 was found associated (Peterson and Gilmore, 1902). However, it was initially described as a
1800 unique genus (Peterson and Gilmore, 1902).
1801 ***Eobrontosaurus yahnahpin*, Tate-001.** Initially described as *Apatosaurus yahnahpin* (Filla
1802 and Redman, 1994), a separate genus was erected for the specimen (Bakker, 1998), partly
1803 based on differences in coracoid morphology to *Apatosaurus*. The specimen has been
1804 considered a camarasaurid (Upchurch et al., 2004a), but more recently, Mannion (2010)
1805 suggested diplodocid affinities. The taxon has never been included in any phylogenetic
1806 analysis, but a detailed description of the entire material appears to be in preparation (R.
1807 Bakker, pers. comm., cited in Mannion, 2010).
1808 ***Galeamopus hayi*, HMNS 175.** The holotype specimen was initially housed at CM (as CM
1809 662), prior to residing in Cleveland for a time (formerly CMNH 10670). Holland (1924)
1810 described it as a novel species of *Diplodocus*, based solely on cranial characters. At that time,
1811 *Apatosaurus* was thought to bear a *Camarasaurus*-like skull (see Berman and McIntosh,
1812 1978), which probably influenced researchers to identify any elongate, diplodocid skull as
1813 *Diplodocus*. McIntosh (1990a), amongst others, later suggested that '*D.*' *hayi* might actually
1814 not be a *Diplodocus*, but a unique genus, based on various similarities with *Apatosaurus* in
1815 the cranium, forelimb, and tail. Because the specimen is mounted at HMNS (together with
1816 reconstructions and original bones from CM 94; McIntosh, 1981), it is only of limited
1817 accessibility. Based on the results of the present phylogenetic analysis (see below),
1818 '*Diplodocus*' *hayi* HMNS 175 is herein referred to its own genus *Galeamopus*, of which it
1819 constitutes the genoholotype specimen (see above).
1820 ***Galeamopus* ▮▮▮▮▮▮ SMA 0011.** This specimen is described here for the first time, and
1821 found to form its own species (see above). It has been mentioned by Klein and Sander (2008)
1822 as Diplodocinae indet.
1823 ***Kaatedocus siberi*, SMA 0004.** Before its detailed examination, the holotype of *Kaatedocus*
1824 *siberi* was generally reported as *Diplodocus* (Ayer, 2000) or *Barosaurus* (Michelis, 2004).
1825 Subsequently, a description and phylogenetic reappraisal of SMA 0004 revealed its generic
1826 separation from *Diplodocus* and *Barosaurus* (Tschopp and Mateus, 2013b).
1827 ***Losillasaurus giganteus*, MCNV Lo-1 to 26.** The OTU represents an individual containing
1828 the holotypic caudal vertebra, Lo-5, the paratypes Lo-10 and Lo-23, and several additional
1829 elements. All the bones of MCNV Lo-1 to 26 were found associated and no duplication of

1830 bones occurred (Casanovas et al., 2001). *Turiasaurus* was added as recent phylogenetic

1831 studies proposed them to be sister taxa (Royo-Torres et al., 2006, 2009; Royo-Torres and

1832 Upchurch, 2012).

1833 ***Lourinhasaurus alenquerensis*, lectotype.** The species was first described by Lapparent and

1834 Zbyszewski (1957) as referable to *Apatosaurus*, but later included into *Camarasaurus*

1835 (McIntosh, 1990a). Subsequently, Dantas et al. (1998) erected a new genus for the species,

1836 but only Antunes and Mateus (2003) clearly assigned a specific type specimen to the species.

1837 The genus was usually recovered as basal macronarian in phylogenetic analyses (Upchurch et

1838 al., 2004a; Royo-Torres and Upchurch, 2012; Mocho et al., 2014).

1839 ***Seismosaurus hallorum*, NMMNH 3690.** The holotype of *S. hallorum* was initially described

1840 as *S. halli*, and as one of the largest sauropods ever (Gillette, 1991). However, this was mainly

1841 based on an incorrect assignment of the position of some mid-caudal vertebrae (Curtice, 1996;

1842 Herne and Lucas, 2006). Subsequent reanalysis of the specimen revealed that it is

1843 indistinguishable from *Diplodocus*, and that it probably belongs to the same species as

1844 AMNH 223 and USNM 10865 (Lucas et al., 2006; Lovelace et al., 2007). Gillette himself

1845 (1994) corrected the species name from *halli* to *hallorum*, as he did not apply the right latin

1846 ending for the plural in the initial description (Gillette, 1991, 1994). Because the corrected

1847 name has since been used more widely than the original proposal, it is followed here. Herne

1848 and Lucas (2006) added a femur (NMMNH 25079) from the same quarry to the holotype

1849 individual, which is also used to score the taxon in the analysis herein.

1850 ***Supersaurus vivianae*, BYU (various specimen numbers**⊟*upersaurus vivianae* is based on

1851 a scapulacoracoid (Jensen, 1985; Curtice et al., 1996; Curtice and Stadtman, 2001; Lovelace

1852 et al., 2007). It was found at the Dry Mesa Quarry, intermingled with other large bones of

1853 diplodocid, brachiosaurid, and camarasaurid affinities (Jensen, 1985, 1987, 1988; Curtice and

1854 Stadtman, 2001). Jensen (1985) described three new taxa based on this material: *Supersaurus*

1855 *vivianae*, *Dystylosaurus edwini*, and *Ultrasauros macintoshi*. Subsequent study of the Dry

1856 Mesa specimens indicates that the holotypic dorsal vertebra of *Dystylosaurus*, as well as a

1857 dorsal vertebra referred to *Ultrasauros* by (Jensen, 1985, 1987) probably belonged to the

1858 same individual as the holotypic scapulacoracoid of *Supersaurus vivianae* (Curtice and

1859 Stadtman, 2001). Lovelace et al. (2007) revised this referral based on a new find from

1860 Wyoming, agreeing in large parts with Curtice and Stadtman (2001). Since a preliminary

1861 analysis of the phylogenetic affinities of *Dystylosaurus* (see above) further corroborated this

1862 referral, a combined OTU was used for the final analysis.

1863 ***Supersaurus vivianae*, WDC DMJ-021.** WDC DMJ-021 is a reasonably articulated skeleton

1864 and represents the most complete specimen of *S. vivianae* (Lovelace et al., 2007). It is not

1865 directly comparable with the holotype, because no scapulacoracoid was found. Nevertheless,

1866 based on the overlap with additional material attributed to the holotypic individual (see above;

1867 Lovelace et al., 2007), the identification of WDC DMJ-021 as *S. vivianae* has been widely

1868 accepted.

1869 ***Suuwassea emilieae*, ANS 21122.** *Suuwassea* was initially identified as flagellicaudatan with

1870 uncertain affinities to Diplodocidae or Dicraeosauridae (Harris and Dodson, 2004). Further

1871 analyses pointed to a closer relationship with the Dicraeosauridae (Whitlock and Harris, 2010;

1872 Whitlock, 2011a), which would mean that *Suuwassea* is the only North American

1873 representative of this taxon.

1874 ***Tornieria africana*, holotyp[=]** The holotype specimen was found at the locality A at

1875 Tendaguru, Tanzania (Fraas, 1908; Remes, 2006). *Tornieria* was initially described as

1876 *Gigantosaurus africanus* Fraas, 1908, but Sternfeld (1911) noted that this generic name was

1877 preoccupied, proposing the combination *Tornieria africana* as replacement. Janensch (1922)

1878 suggested synonymy of *Tornieria* and *Barosaurus*, resulting in the combination *Barosaurus*

1879 *africanus*, and later referred much more material from various quarries to the same genus

1880 (Janensch, 1935, 1961). However, in a reassessment of the entire material, which also

1881 resurrected the name *Tornieria africana*, only two or three individuals were positively

1882 identified as belonging to *Tornieria* (Remes, 2006). Remes (2006) identified additional

1883 material from the same quarry, and most probably from the same individual as the holotype. I

1884 therefore follow Remes (2006) by including all the *Tornieria* material found at locality A in

1885 the holotypic OTU.

1886 ***Tornieria africana*, skeleton k.** A second specimen of *T. africana* comes from the k-quarry at

1887 Tendaguru and was the only individual found at that site (Heinrich, 1999; Remes, 2006).

1888 Initially relatively complete with semi-articulated vertebral column and numerous

1889 appendicular elements, much of it has been lost or was destroyed during World War II

1890 (Remes, 2006). For these elements, descriptions and figures in Janensch (1929b) were used to

1891 complement the scoring.

Character list

Skull

Premaxillary anterior margin, shape: without step (0); with marked but short step (1); with marked and long step (2) (Upchurch, 1998; Wilson and Sereno, 1998; modified by Carballido et al., 2012b; Fig. 36).

Comments. The character describes the presence and development of a horizontal portion of the premaxilla, which lies anterior to the nasal process. The step, when present, is best visible in lateral view. It was initially proposed by Upchurch (1998), who scored the Diplodocoidea as unknown or inapplicable, due to a supposed absence of the ascending process. However, some diplodocoids, (e.g. *Suuwassea*) clearly show a distinction between the anterior main body and the posterior ascending process in dorsal view, where they show an abrupt narrowing (Harris, 2006a; ANS 21122, ET, pers. obs., 2011). Diplodocoidea should therefore be scored as '0'. A third state was added in order to distinguish Brachiosauridae from other macronarian sauropods (Carballido et al., 2012b). The character is treated as ordered, due to the gradual change in morphology.

C2: Premaxilla, external surface: without anteroventrally orientated vascular grooves originating from an opening in the maxillary contact (0); vascular grooves present (1) (Wilson, 2002; Sereno et al., 2007; Fig. 37).

Comments. The presence of these grooves was previously found as a synapomorphy of Dicraeosauridae (Whitlock, 2011a; Mannion et al., 2012). However, faint grooves originating at the premaxillary-maxillary contact are also visible in *Nigersaurus* (Sereno et al., 2007) and in some diplodocid specimens. In the latter, they fade anteriorly, shortly after the suture (e.g. in CM 11161, 11162, SMA 0011, USNM 2672). In the present analysis, all of these specimens are scored as apomorphic.

C3: Premaxilla, shape in dorsal view: main body massive, with proportionally short ascending process distinct (0); single elongate unit, distinction between body and process nearly absent (1) (Upchurch, 1998; wording modified; Fig. 37).

Comments. Upchurch (1998) formulated this character differently, based on his interpretation that the ascending process of the premaxilla was absent in Diplodocoidea. As stated above, this is not the case. The wording of the derived state was thus changed accordingly.

1924 C4: Premaxilla, angle between lateral and medial margins of premaxilla as seen in dorsal

1925 view: > 40° (0); 17°-40° (1); < 17° (2) (Upchurch, 1999; modified; Tab. S3).

1926 **Comments.** Upchurch (1999) was the first to note significant differences in these angles

1927 between diplodocoids (around 10°), nemegtosaurids (18°), and remaining taxa (e.g.

1928 *Giraffatitan*, 30°; Upchurch, 1999: fig. 7). He used this character (with two states) as one of

1929 several that supported the inclusion of Nemegtosauridae within Diplodocoidea (Upchurch,

1930 1999), a view now falsified by nearly complete finds of new nemegtosaurids that show them

1931 to be deeply nested within titanosaurians, but with convergences with Diplodocoidea

1932 (Wilson, 2002; Curry Rogers, 2005; Zaher et al., 2011). The OTUs included in this dataset

1933 were rescored for this character based on figures or on original material. Because the lateral

1934 margin is concave to sinuous in most taxa, a straight line was drawn from the anterior-most

1935 point of the premaxillary-maxillary contact to the point where the lateral edge curves

1936 medially, at the base of the ascending process. The results (Tab. S3) indicate that the

1937 distribution of the character scores is not as straightforward as previously thought:

1938 *Shunosaurus*, as well as some specimens of *Camarasaurus* appear to show similarly narrow

1939 angles as *Dicraeosaurus* and *Suuwassea*. A third state was thus added, such that diplodocid

1940 and rebbachisaurid OTUs now score in the narrow-most range, and *Mamenchisaurus* and

1941 *Jobaria* are classed as significantly wide-angled taxa. Because the plesiomorphic state is state

1942 one, the character was left unordered.

1943 C5: Premaxilla, posteroventral edge of ascending process in lateral view: concave (0); straight

1944 and dorsally oriented (1); straight, and directed posterodorsally (2) (Whitlock, 2011a; wording

1945 modified; Fig. 36).

1946 **Comments.** Whitlock (2011a: p.35) described the character as follows: 'Ascending process of

1947 the premaxilla, shape in lateral view: convex (0); concave, with a large dorsal projection (0);

1948 sub-rectilinear and directed posterodorsally (1)'. This formulation is misleading, and the states

1949 overlap with those of character 1, which describes the premaxillary 'step'. Varying

1950 morphologies of the ascending process, following the states of Whitlock (2011a), were

1951 observed among the included taxa regarding the posteroventral edge of the ascending process

1952 – the margin that delimits the nasal opening anteriorly. The description of the character was

1953 adapted, reducing the character to only encompass the orientation of the posteroventral edge,

1954 thereby avoiding overlap with character 1. The directional terms in the states are meant in

1955 relation to a horizontally oriented ventral edge of the maxilla. SinceBecause no state is

1956 obviously intermediate relative to the other two, the character is left unordered.

1957 C6: Premaxilla, posterolateral process and the lateral process of the maxillary, shape: without

1958 midline contact (0); with midline contact forming a marked narial depression, subnarial

1959 foramen not visible laterally (1) (Wilson, 2002; Fig. 38).

1960 **Comments.** Whitlock (2011a) reversed the polarity of this character, due to a more limited

1961 outgroup sampling. With the inclusion of *Shunosaurus* (Mannion et al., 2012), the most basal

1962 OTU again lacks the midline contact, as is the case in Diplodocoidea. The original phrasing of

1963 Wilson (2002) is therefore preferred.

1964 C7: Premaxilla, dorsoventral depth of anterior portion: remains the same as posteriorly, or

1965 widens gradually (0); widens considerably, and abruptly (1) (Harris, 2006a; Fig. 39).

1966 **Comments.** Harris (2006a) stated this difference as useful to distinguish *Suuwassea* (which

1967 retains the same depth) from *Diplodocus* (which widens). A similar, narrow premaxilla is

1968 furthermore present in *Kaatedocus* (Tschopp and Mateus, 2013b). The character is difficult to

1969 observe in articulated skulls, but single elements do show a significant difference.

1970 C8: Subnarial foramen and anterior maxillary foramen, position: well distanced from one

1971 another (0); separated by narrow bony isthmus (1) (Wilson, 2002; Fig. 40).

1972 C9: Maxilla, large foramen anterior to the preantorbital fossa, separated by a narrow bony

1973 bridge: absent (0); present (1) (Zaher et al., 2011; wording modified; Fig. 38).

1974 **Comments.** Generally, sauropod maxillae are pierced by a number of small foramina

1975 anteriorly, probably for innervation and/ blood supply of the replacement teeth. The

1976 foramen described by Zaher et al. (2011) in *Tapuiasaurus*, however, is relatively large, and

1977 closely attached to the preantorbital fossa. The same is the case in *Dicraeosaurus hansemanni*

1978 MB.R.2336 (Janensch, 1935), but not in diplodocids.

1979 C10: Maxilla, large foramen posterior to anterior maxillary foramen, dorsal to preantorbital

1980 fossa: absent (0); present (1) (New; Fig. 38).

1981 **Comments.** Few diplodocid specimens show a large foramen posterior to the anterior

1982 maxillary foramen (e.g. *Kaatedocus* SMA 0004). This foramen cannot be the same as the one

1983 described in character 9, given that both are present in *Dicraeosaurus*.

1984 C11: Anterior maxillary foramen, location: detached from maxillary-premaxillary boundary,

1985 facing dorsally (0); lies on medial edge of maxilla, opening medially into the premaxillary-

1986 maxillary boundary (1) (New; Fig. 38).

1987 **Comments.** Usually, diplodocids have the subnarial and the anterior maxillary foramina

1988 enclosed within a single, elongated fossa at the maxillary-premaxillary boundary (Wilson and

1989 Sereno, 1998; Whitlock, 2011b). However, in *Kaatedocus*, the anterior maxillary foramen is

1990 detached and laterally positioned, within a unique, small fossa. It thus resembles the

1991 plesiomorphic state present in *Jobaria* or *Camarasaurus* (Wilson and Sereno, 1998; Sereno et

1992 al., 1999), although it is still much closer to the subnarial foramen. Primitive outgroup taxa

1993 (those normally basal to *Jobaria*) were coded as unknown, as it is unclear if the intermaxillary

1994 foramen that is present in these taxa (e.g. He et al., 1988; Ouyang and Ye, 2002) is

1995 homologous to the anterior maxillary foramen or the subnarial foramen.

1996 C12: Maxilla, canal connecting the antorbital fenestra and the preantorbital fossa: absent (0);

1997 present (1) (New; Fig. 38).

1998 **Comments.** Such a canal is only present in SMA 0011, and is thus interpreted as

1999 autapomorphy of *Galeamopus* ▮▮▮▮▮▮ Taxa without a preantorbital fossa were scored as

2000 unknown in order to avoid absence coding.

2001 C13: Maxilla, dorsal process, posterior extent: anterior to or even with posterior process (0);

2002 extending posterior to posterior process (1) (Whitlock, 2011a; Fig. 36).

2003 **Comments.** The character is applied to skulls in lateral view, with the ventral edge of the

2004 maxillary oriented horizontally.

2005 C14: Maxilla-quadratojugal contact: absent or small (0); broad (1) (Yu, 1993; Fig. 36).

2006 **Comments.** Upchurch (1998) reported some difficulties in scoring some taxa tofor his

2007 version of this character, which was defined as a simple absence-presence feature. Reduced,

2008 small contacts are present in *Camarasaurus*, but only diplodocids are known to have

2009 developed a broad area where the maxilla contacts the quadratojugal (Upchurch, 1998;

2010 Wilson and Sereno, 1998). Therefore, Whitlock (2011a) redefined the states, such that the

2011 apomorphic state now describes a synapomorphy of at least Diplodocidae (it is unknown in

2012 Dicraeosauridae and Rebbachisauridae). The derived state appears to be a convergence in

2013 some nemegtosaurids (Upchurch, 1998; Wilson, 2005).

2014 C15: Preantorbital fossa: absent (0); present (1) (Tschopp and Mateus, 2013b; Fig. 36).

2015 **Comments.** Although some flagellicaudatan taxa have reduced to entirely closed

2016 preantorbital fenestrae, all show a distinct fossa, which is otherwise only present in some

2017 nemegtosaurids (Wilson, 2005).

2018 C16: Preantorbital fossa, if present: with relatively indistinct borders (0); dorsally capped by a

2019 thin, distinct crest (1) (Wilson, 2002; modified; Fig. 38).

2020 **Comments.** Wilson (2002) originally proposed the presence of a dorsally capped

2021 preantorbital fenestra as autapomorphy of *Diplodocus*. A broader survey of this character

2022 shows that within Flagellicaudata, the absence of this dorsal crest is instead only known from

2023 a single apatosaur skull (CM 11162), and thus might represent an autapomorphy of

2024 *Apatosaurus louisae*.

2025 C17: Preantorbital fenestra: reduced to absent (0); present, occupying at least 50% of the

2026 preantorbital fossa (1) (Berman and McIntosh, 1978; Fig. 39).

2027 **Comments.** Upchurch (1995) was the first to use this feature in a phylogenetic analysis.

2028 Tschopp and Mateus (2013b) modified the character, and included the dorsal crest as well.

2029 However, ~~since~~because these two features are not correlated (*Kaatedocus* has a dorsal crest

2030 but a reduced to absent fenestra), the states were adjusted, and a ratio is given to distinguish

2031 the small opening in *Dicraeosaurus* from the large ones in *Galeamopus*, for example. Large

2032 preantorbital fenestrae are convergently present in nemegtosaurids (Wilson, 2005; Zaher et

2033 al., 2011).

2034 C18: Antorbital fenestra, maximum diameter: much shorter than orbital maximum diameter,

2035 less than 90% of orbit (0); subequal to orbital maximum diameter, greater than 90% orbit (1)

2036 (Yu, 1993; modified; Tab. S4).

2037 **Comments.** Wilson (2002) proposed the character without any clear state boundaries, which

2038 were later added by Whitlock (2011a), and changed herein from 85% to 90% in order to have

2039 *Mamenchisaurus* within the plesiomorphic state.

2040 C19: Antorbital fenestra, anterior extension: is restricted posterior to preantorbital fossa (0);

2041 reaches above preantorbital fossa (1) (New; Fig. 36).

2042 **Comments.** The character has to be scored with the ventral border of the maxilla oriented

2043 horizontally. Within flagellicaudatans, the derived state is most developed in *Kaatedocus*

2044 SMA 0004, but nemegtosaurids like *Rapetosaurus* have extremely elongated antorbital

2045 fenestrae that even reach anterior to the entire preantorbital fossa (Curry Rogers and Forster,

2046 2004).

2047 C20: Antorbital fenestra, shape of dorsal margin: straight or convex (0); concave (1)

2048 (Whitlock, 2011a; Fig. 36).

2049 **Comments.** The diplodocine skull AMNH 969 appears to have a convex dorsal margin at first

2050 glance. However, the presence of a lateral projection in the upper half of this edge indicates

2051 that the convex shape might be due to deformation. The lateral projection in AMNH 969 is at

the same location, and has the same shape as the osteological feature producing the concave

dorsal edge of the antorbital fenestra in CM 11161. AMNH 969 is thus interpreted to be

derived and ~~thus~~ to share the flagellicaudatan synapomorphy.

C21: External nares, position: retracted to level of orbit, facing laterally (0); retracted to

position between orbits, facing dorsally or dorsolaterally (1) (McIntosh, 1989; Upchurch,

1995; modified by Whitlock, 2011a; Fig. 36).

Comments. Upchurch (1995) was the first to include this character in a phylogenetic analysis,

based on observations made by McIntosh (1989). Whitlock (2011a) adjusted the state

description, since the reduced taxon sampling made a third state redundant (anterior to orbit,

the plesiomorphic state in Sauropoda; Upchurch, 1995).

C22: External nares, maximum diameter: shorter than orbital maximum diameter (0); longer

than orbital maximum diameter (1) (Upchurch, 1995; modified by Wilson and Sereno, 1998).

Comments. Upchurch (1995) initially defined the character states in relation to skull length,

but later, Wilson and Sereno (1998) changed them to relate with orbital diameter. The latter

has since been widely used and is thus retained here.

C23: Prefrontal, medial margin, shape: without distinct anteromedial projection (0); curving

distinctly medially anteriorly to embrace the anterolateral corner of the frontal (1) (New; Fig.

41).

Comments. In some basal sauropods, the prefrontal is located entirely anterior to the frontal.

These cases are scored as plesiomorphic.

C24: Prefrontal, posterior process size: small, not projecting far posterior of frontal-nasal

suture (0); elongate, approaching parietal (1) (Wilson, 2002; Fig. 42).

Comments. This character is not as straight-forward as it seems. Care has to be taken that one

observes the frontal and prefrontal in exactly perpendicular view. In some reconstructed

dorsal views of the skull of *Diplodocus* (Wilson and Sereno, 1998; Whitlock, 2011b), the

posterior extension of the prefrontal is remarkable, but this is due to the view~,~ in which the

reconstruction is drawn. The frontal slants posteriorly, and more posterior distances therefore

appear shorter. In direct dorsal view, differences in distance between taxa diminish. However,

the character remains informative: in diplodocids like *Apatosaurus* or *Diplodocus*, the

posterior process of the prefrontal almost reaches or surpasses the midlength of the frontal,

whereas in Rebbachisauridae or in *Kaatedocus* and *Tornieria*, it remains restricted to about

the anterior third (Fig. 42).

2084 C25: Prefrontal, posterior process shape: straight (0); hooked (1) (Wilson, 2002; modified;
2085 Fig. 42).

2086 **Comments.** As the posterior elongation of the prefrontal, ~~also~~ this character was initially
2087 defined in a somewhat ambiguous way (flat/hooked). *Nigersaurus* does have a posteriorly
2088 facing, pointed prefrontal. The description 'flat' therefore does not fit very well, and it is
2089 replaced by 'straight'. Hooked is herein interpreted to describe a medially curving posterior
2090 process, such that its posterior end forms the medial-most extension of the prefrontal.

2091 C26: Frontals, midline contact (symphysis): patent suture (0); fused in adult individuals (1)
2092 (Salgado and Calvo, 1992; Yu, 1993; Fig. 40).

2093 **Comments.** Fusion of skull bones is usually considered an ontogenetic feature (Varricchio,
2094 1997; Whitlock et al., 2010). However, the ontogenetic stages~~,~~ when fusion begins~~,~~ might still
2095 be different between taxa and thus phylogenetically significant. This appears to be the case
2096 here, where the braincases of *Dicraeosaurus* and *Amargasaurus* have completely obliterated
2097 sutures between the frontals, whereas large-sized diplodocid skulls do not (e.g. CM 11161).
2098 Nonetheless, it remains possible that non-dicraeosaurid sauropods fuse their frontals at an old
2099 age. In future, it might be helpful to constrict the character to a specific age-range (possibly
2100 subadult or early adult), but to date, the exact individual age of the specimens showing the
2101 fused frontals remains unknown.

2102 C27: Frontal, anteroposterior length: long, > 1.4 times minimum transverse width (0); short,
2103 1.4 or less times minimum transverse width (1) (Gauthier, 1986; modified; Tab. S5).

2104 **Comments.** This character was widely used in phylogenetic analyses of sauropod dinosaurs
2105 (Upchurch, 1998; Wilson, 2002; Whitlock, 2011a; Mannion et al., 2012; Tschopp and
2106 Mateus, 2013b), with varying definitions of the state boundaries. In addition, it was often
2107 unclear if minimum or maximum transverse width was intended (e.g. Whitlock, 2011a;
2108 Tschopp and Mateus, 2013b). As shown in table S5, there are significant differences in the
2109 ratios, with more distinct changes when comparing frontal length and minimum transverse
2110 width. Therefore, state boundaries were herein defined numerically, which also led to some
2111 differential scorings compared to Tschopp and Mateus (2013b). *Kaatedocus*, for example, is
2112 now well within the ratios for the apomorphic state.

2113 C28: Frontal-nasal suture, shape: flat or slightly bowed anteriorly (0); v-shaped, pointing
2114 posteriorly (1) (Whitlock, 2011a; Fig. 41).

2115 **Comments.** The frontals of *Galeamopus hayi* might have a posteriorly pointing nasal contact

2116 as well (Holland, 1906). However, the nasals are not preserved in this specimen, and it seems
2117 thus more appropriate to code HMNS 175 as unknown.
2118 C29: Frontals, distinct anterior notch medially between the two elements: absent (0); present
2119 (1) (Tschopp and Mateus, 2013b; modified; Fig. 40).
2120 **Comments.** The shape description of the notch was excluded from the character in order to
2121 include also *Spinophorosaurus,* and SMA 0011 in the apomorphic state. The frontal usually
2122 becomes extremely thin in this part, and it is thus easily broken. ~~Since~~Because the notch still
2123 appears genuine in these three taxa/specimens, ~~the notch still appears genuine,~~ the character
2124 was retained. Tschopp and Mateus (2013b) mentioned this feature as an autapomorphy of
2125 *Kaatedocus*. Given that a similar notch is present in SMA 0011, this character might actually
2126 be more widespread within Diplodocidae. In fact, many specimens (e.g. *Apatosaurus* CM
2127 11162) show broken anteromedial edges in the frontal, which makes it difficult to evaluate
2128 this character. ~~Additional, n~~New finds of diplodocid frontals might shed some more light on
2129 the distribution of this character.
2130 C30: Frontals, dorsal surface: without paired grooves facing anterodorsally (0); grooves
2131 present, extend on to nasal (1) (Whitlock, 2011a; Fig. 40).
2132 **Comments.** Grooves appear to be present on the frontals of the dicraeosaurid *Amargasaurus*
2133 *cazaui* (Salgado and Calvo, 1992: fig. 2B), but these extend onto the prefrontals and not the
2134 nasals, and do not extend as far posteriorly as in *Limaysaurus*. *Amargasaurus* is thus scored
2135 as plesiomorphic, following Whitlock (2011a).
2136 C31: Frontal, lateral edge in dorsal view: relatively straight (0); deeply concave (1) (New;
2137 Fig. 42).
2138 **Comments.** This character has a somewhat ambiguous distribution. There is some difference
2139 in the shapes taken together in the plesiomorphic state as well: Rebbachisauridae, in contrast
2140 with most other taxa, have a weakly convex lateral frontal edge. Diplodocids exhibit varying
2141 shapes: *Apatosaurus* and *Diplodocus* have concave edges, whereas *Kaatedocus* or *Tornieria*
2142 have straight margins.
2143 C32: Frontal, contribution to dorsal margin of orbit: less than 1.5 times the contribution of
2144 prefrontal (0); at least 1.5 times the contribution of prefrontal (1) (Whitlock, 2011a; modified
2145 by Mannion et al., 2012; Tab. S6).
2146 **Comments.** The lengths of the frontal and prefrontal are measured in a straight line in lateral
2147 view, from the mid-point of the frontal-prefrontal articulation to the anterior-most (prefrontal)

2148 or posterior-most (frontal) point. Whitlock (2011a) proposed the character leaving a gap

2149 between plesiomorphic and apomorphic states (subequal, or twice), which was changed by

2150 Mannion et al. (2012). A comparative analysis of the included specimens confirms the utility

2151 of the boundary proposed by Mannion et al. (2012).

2152 C33: Frontal, free lateral margin: rugose (0); smooth (1) (Tschopp and Mateus, 2013b; Fig.

2153 42).

2154 **Comments.** Rugosities are present around the dorsal margin of almost all sauropods, but in

2155 some cases, they are shifted onto the prefrontal or the postorbital. Tschopp and Mateus

2156 (2013b) hypothesized that the rugosities served for an attachment of a palpebral element.

2157 C34: Frontal, contribution to margin of supratemporal fenestra/fossa: present (0); absent,

2158 frontal excluded from anterior margin of fenestra/fossa (1) (Wilson and Sereno, 1998; Fig.

2159 40).

2160 **Comments.** In the derived state, the frontal is excluded from a contribution to the margin of

2161 the supratemporal fenestra by a contact between the medial process of the postorbital and the

2162 anterolateral process of the parietal.

2163 C35: Frontal-parietal suture, position of medial portion: closer to anterior extension of

2164 supratemporal fenestra (0); closer to posterior extension (1) (Tschopp and Mateus, 2013b;

2165 modified; Fig. 40).

2166 **Comments.** Tschopp and Mateus (2013b) formulated the character inspired by Remes (2006),

2167 who mentioned the position of the fronto-parietal suture as a feature to distinguish *Tornieria*

2168 from *Diplodocus*. They used a ~~three~~tri-partite character, with an intermediate state as close~~r~~

2169 the the central portion of the supratemporal fenestra (Tschopp and Mateus, 2013b). The

2170 position of the suture is difficult to assess in some diplodocid specimens, because it describes

2171 a strongly sinuous curve (e.g. CM 11161, Fig. 42). The character is thus restricted to the

2172 medial portion of the suture herein. By doing so, it becomes clear that the majority of

2173 *Diplodocus* skulls shifted the suture backwards, whereas all other specimens have it anteriorly

2174 located. The posterior dislocation might thus prove to be an autapomorphy of *Diplodocus*.

2175 The intermediate state becomes redundant, and is not included here.

2176 C36: Pineal (parietal) foramen between frontals and parietals: present (0); absent (1) (Yu,

2177 1993; modified; Fig. 40).

2178 **Comments.** This character was proposed ~~combined~~in combination with the presence of a

2179 postparietal foramen (Yu, 1993). The two are herein separated in two characters, because

2180 *Kaatedocus* SMA 0004 has a postparietal but no pineal foramen (Tschopp and Mateus,

2181 2013b). The presence of a pineal foramen is often difficult to assess due to breakage of the

2182 area around the fronto-parietal suture (McIntosh, 1990b; Upchurch et al., 2004a; Harris,

2183 2006a). However, in some specimens, the presence or absence of this feature is genuine, and

2184 it thus appears appropriate to include this character. Specimens, where the presence of the

2185 foramen has been doubted previously are scored as unknown. At the current state of

2186 knowledge, the presence seems to be a retained plesiomorphy characterizing the

2187 Dicraeosauridae, but in many diplodocid specimens its presence cannot be dismissed yet.

2188 C37: Orbit, anterior-most point: anterior to the anterior extremity of lateral temporal fenestra

2189 (0); roughly even with or posterior to anterior extent of lateral temporal fenestra (1) (Gauthier,

2190 1986; Upchurch, 1995; modified by Whitlock, 2011a; Fig. 36).

2191 **Comments.** The original character was a multistate character (Upchurch, 1995). Given the

2192 limited taxon sampling of Whitlock (2011a) and the herein presented analysis, the third state

2193 becomes redundant (infratemporal fenestra restricted posterior to orbit).

2194 C38: Orbital ventral margin, anteroposterior length: broad, with subcircular orbital margin

2195 (0); reduced, with acute orbital margin (1) (Wilson and Sereno, 1998; Fig. 36).

2196 **Comments.** The derived state results in a teardrop-shape of the orbit. With the ventral margin

2197 of the maxilla held horizontally, the 'ventral margin' would be better described with

2198 'anteroventral corner'.

2199 C39: Postorbital, posterior process: present (0); absent (1) (Wilson, 2002; Fig. 36).

2200 **Comments.** The postorbital is usually a triradiate bone, with a relatively short posterior

2201 process that overlaps the squamosal. The latter is absent in rebbachisaurids (Wilson, 2002;

2202 Whitlock, 2011a).

2203 C40: Jugal, contribution to antorbital fenestra: very reduced or absent (0); large, bordering

2204 approximately one-third of its perimeter (1) (Berman and McIntosh, 1978; Upchurch, 1995;

2205 modified by Whitlock, 2011a; Fig. 43).

2206 **Comments.** Recognized as distinctive feature of Diplodocoidea by Berman and McIntosh

2207 (1978), the contribution of the jugal to the antorbital fenestra was first used as phylogenetic

2208 character by Upchurch (1995). Whitlock (2011a) defined the state boundaries quantitatively.

2209 C41: Jugal, contact with ectopterygoid: present (0); absent (1) (Upchurch, 1995; Fig. 44).

2210 **Comments.** The development of this character is barely known in sauropods. ~~If~~When

2211 preserved, the osteology of the palatal complex is often left obscured by matrix ~~due to~~for

2212 stability of the specimenreasons. At the current state of knowledge, the ectopterygoid

2213 becomes anteriorly dislocated in Neosauropoda, and contacts the maxilla instead of the jugal.

2214 Future CT scanning of additional skulls will yield more detailed results.

2215 C42: Jugal, posteroventral process: short and broad (0); narrow and elongate (1) (New; Fig.

2216 43).

2217 **Comments.** This character shows varying shapes in the skulls traditionally identified as

2218 *Diplodocus* (CM 11161 has a short process, whereas in all other skulls they are elongated).

2219 However, too few diplodocid jugals are preserved entirely in order to evaluate the distribution

2220 of this character to date.

2221 C43: Jugal, dorsal process: present (0); absent (1) (Yu, 1993; polarity inverted; Fig. 43).

2222 **Comments.** Yu (1993) proposed the dorsal process as a synapomorphy for Diplodocidae.

2223 However, no jugal is known from dicraeosaurids, and such a process is also present in

2224 *Shunosaurus*, *Omeisaurus*, and *Mamenchisaurus* (Janensch, 1935; He et al., 1988; Salgado

2225 and Calvo, 1992; Chatterjee and Zheng, 2002; Ouyang and Ye, 2002). SinceBecause the latter

2226 basal taxa show dorsal processes of the jugal, the character polarity was inverted relative to

2227 the original version (Yu, 1993). Although they are scored for the plesiomorphic state,

2228 Diplodocidae are still distinguishable from *Shunosaurus* and the other taxa by the strong

2229 development of the dorsal process, and its anterior displacement. In *Omeisaurus*, e.g., the

2230 dorsal process is short and located at midlength of the jugal-lacrimal suture (He et al., 1988).

2231 C44: Jugal, anterior spur dorsally, which projects into antorbital fenestra: absent (0); present

2232 (1) (New; Fig. 43).

2233 **Comments.** Such a spur is present in many diplodocid specimens, although in USNM 2672, it

2234 only occurs on the left side (ET, pers. obs., 2011). However, the possibility to develop such a

2235 spur still appears to be restricted to Diplodocidae, and the character is thus used in the

2236 analysis. USNM 2672 is scored as 'present'.

2237 C45: Quadratojugal, position of anterior terminus: anterior margin of orbit or posteriorly

2238 restricted (0); beyond anterior margin of orbit (1) (Whitlock, 2011a; modified; Fig. 36).

2239 **Comments.** The character is coded with the ventral margin of the maxilla held horizontally.

2240 State boundaries by Whitlock (2011a: posterior to middle of orbit, anterior margin or beyond)

2241 were adjusted because all diplodocoids show strongly elongated anterior processes that end

2242 significantly anterior to the orbit. On the other hand, in *Mamenchisaurus* or *Brachiosaurus*,

2243 y reach the anterior margin of the orbit (Janensch, 1935; Ouyang and Ye, 2002), which

2244 would ~~request~~require a coding as apomorphic when following the description of Whitlock

2245 (2011a).

2246 C46: Quadratojugal, angle between anterior and dorsal processes: less than or equal to 90°, so

2247 that the quadrate shaft is directed dorsally (0); greater than 90°, approaching 130°, so that the

2248 quadrate shaft slants posterodorsally (1) (Gauthier, 1986; Upchurch, 1995; Fig. 36).

2249 **Comments.** The angle between the quadratojugal processes reach~~es~~ ~~their~~its maximum in the

2250 large skulls CM 11161 and 11162. In smaller skulls (of both ontogenetically younger as well

2251 as phylogenetically more basal specimens), the angle is of approximately 110° (e.g.

2252 *Kaatedocus* SMA 0004; Tschopp and Mateus, 2013b), but still clearly in the derived state.

2253 C47: Lacrimal, anterior process: absent (0); present (1) (Wilson, 2002; polarity reversed by

2254 Mannion et al., 2013; Fig. 36).

2255 **Comments.** Wilson (2002) initially proposed the character with inverted polarity. This was

2256 changed by Mannion et al. (2013), and herein in order to have the chosen outgroups showing

2257 the plesiomorphic state. An anterior process is usually interpreted to be absent in

2258 diplodocoids. However, *Galeamopus* ▮▮▮▮▮ SMA 0011 and *Dicraeosaurus* do have one.

2259 On the other hand, it is possible that the feature is more widespread among Diplodocoidea,

2260 but that the anterior process is obscured by the posterodorsal process of the maxilla. The latter

2261 partly overlaps the anterior process of the lacrimal in SMA 0011. The presence of an anterior

2262 process of the lacrimal would otherwise be one of the distinguishing characteristics between

2263 diplodocoids and nemegtosaurids (Wilson, 2005).

2264 C48: Lacrimal, dorsal portion of lateral edge: flat (0); bears dorsoventrally elongate, shallow

2265 ridge (1); bears a dorsoventrally short laterally projecting spur (2) (Tschopp and Mateus,

2266 2013b; Fig. 38).

2267 **Comments.** There is some evidence that this character is ontogenetically controlled (Tschopp

2268 and Mateus, 2013b): only small skulls show the laterally projecting spur. The character is

2269 retained here in order to test its validity. The character is treated as ordered due to

2270 intermediate morphologies.

2271 C49: Quadrate, articular surface shape: quadrangular in ventral view, orientated transversely

2272 (0); roughly triangular in shape (1); thin, crescent-shaped surface with anteriorly directed

2273 medial process (2) (Whitlock, 2011a; Fig. 45).

2274 **Comments.** The character is treated as ordered ~~as~~because state '1' is intermediate in

2275 morphology. ▤

2276 C50: Quadrate, short transverse ridge medially on posterior side of ventral ramus, close to the

2277 articular surface with the lower jaw: absent (0); present (1) (New; Fig. 46).

2278 **Comments.** This ridge is a ~~small~~ detail which appears to be synapomorphic for Diplodocidae.

2279 Most of the diplodocid quadrates could ~~not have been~~be investigated in the original material

2280 for this character. Therefore a more detailed evaluation of this character has to be undertaken

2281 in order to corroborate the presence or absence of such a ridge, and its taxonomic utility.

2282 C51: Quadrate fossa, depth: shallow (0); deeply invaginated (1) (Russell and Zheng, 1993;

2283 Fig. 46).

2284 C52: Quadrate, shallow, second fossa medial to pterygoid flange on quadrate shaft (not the

2285 quadrate fossa): absent (0); present, becoming deeper towards its anterior end (1) (Tschopp

2286 and Mateus, 2013b; wording modified; Fig. 47).

2287 **Comments.** The medial surface of the pterygoid flange is nearly always concave, but concave

2288 dorsoventrally. In SMA 0004, as well as some other diplodocid specimens, the second fossa is

2289 transversely concave, lies anteriorly on the posterior shaft, medial to where the pterygoid

2290 flange originates. There is a chance that the character might be ontogenetic, given that no

2291 large-sized skull has yet been identified to bear this second fossa. The character was slightly

2292 reworded from its original version (Tschopp and Mateus, 2013b) in order to describe the

2293 location of the fossa better.

2294 C53: Quadrate, dorsal margin: concave, such that pterygoid flange is distinct from quadrate

2295 shaft (0); straight, without clear distinction of posterior extension of pterygoid flange (1)

2296 (New; Fig. 47).

2297 C54: Quadrate, posterior end (posterior to posterior-most extension of pterygoid ramus): short

2298 and stocky (0); elongate and slender (1) (New; Fig. 47).

2299 C55: Squamosal, anterior extent: restricted to postorbital region (0); extends well past

2300 posterior margin of orbit (1); extends beyond anterior margin of orbit (2) (Whitlock, 2011a;

2301 Fig. 36).

2302 **Comments.** The anterior extent of the squamosal is measured with the ventral border of the

2303 maxilla oriented horizontally. The character is treated as ordered.

2304 C56: Squamosal-quadratojugal contact: present (0); absent (1) (Upchurch, 1995; Fig. 48).

2305 **Comments.** In diplodocids, where no contact is present, the distance between the squamosal

2306 and the quadratojugal varies (Whitlock et al., 2010; Whitlock and Lamanna, 2012). However,

2307 most of the diplodocid specimens do not preserve the entire anterior ramus of the squamosal

2308 (ET, pers. obs., 2011), and it seems thus premature to include the distance as a phylogenetic

2309 character.

2310 C57: Squamosal, posteroventral margin: smooth, or with short and blunt ventral projection

2311 (0); with prominent, ventrally directed 'prong' (1) (Whitlock, 2011a; modified; Fig. 48).

2312 **Comments.** The original character description of Whitlock (2011a) was modified, and an

2313 additional binary character was added (see below) in order to describe better the state in

2314 *Kaatedocus*, where a short ventral projection of the squamosal is present.

2315 C58: Squamosal, posteroventral margin: smooth, without ventral projection (0); ventral

2316 projection present (1) (Whitlock, 2011a; modified; Fig. 48).

2317 **Comments.** A short projection is present in almost all preserved flagellicaudatan skulls. On

2318 the contrary, most non-flagellicaudatan sauropods do have smooth posteroventral margins of

2319 the squamosal.

2320 C59: Parietal, contribution to posttemporal fenestra: present (0); absent (1) (Wilson, 2002;

2321 Fig. 49).

2322 **Comments.** The absence of parietal contribution to the posttemporal fenestra is sometimes

2323 difficult to observe due to imperfectly preserved or distorted skulls. All diplodocid skulls have

2324 exoccipitals that bear a dorsolateral spur, which forms the dorsomedial end of the

2325 posttemporal fenestra (the 'posttemporal process' of Harris, 2006a). Additionally, most of

2326 ~~them~~specimens have dorsally extended distal ends of the paroccipital processes, which curve

2327 back towards the exoccipital spur. These two prominences are interconnected by the

2328 squamosal in complete diplodocid skulls (CM 11161, ET, pers. obs., 2011).

2329 C60: Parietal, portion contributing to skull roof, anteroposterior length/transverse width: wide,

2330 > 50% (0); narrow, 7-50% (1); practically nonexistent, < 7% (2) (New; Tab. S7).

2331 **Comments.** In some taxa, the posterior-most point of the fronto-parietal suture is located

2332 posterior to the supratemporal fenestra. The minimum values are compared in this ratio. The

2333 character was treated as ordered in the present analysis.

2334 C61: Parietal, distance separating supratemporal fenestrae: less than 1.5 times the width of the

2335 long axis of the supratemporal fenestra (0); at least 1.5 times the length of the long axis of the

2336 supratemporal fenestra (1) (Wilson, 2002; modified by Mannion et al., 2012; Tab. S8).

2337 **Comments.** The original character states of Wilson (2002) left a gap (subequal, or double).

2338 The distance between the supratemporal fenestrae in many diplodocid specimens does not

2339 reach two times the maximum diameter of the fenestra, which led Mannion et al. (2012) to

2340 adjust the state boundaries. Specimens were remeasured where possible (Tab. S8), for others

2341 scorings of Wilson (2002) or Mannion et al. (2012) were used. The new measurements show

2342 that the ratios are often overestimated, and that there seem to be three clusters of taxa (less

2343 than one: *Brachiosaurus*, and probably *Mamenchisaurus*, *Omeisaurus*, *Jobaria*, *Turiasaurus*;

2344 between one and 1.6 times: *Spinophorosaurus*, *Camarasaurus*, *Kaatedocus*, CM 11161 and

2345 11162; more than 1.6 times, *Suuwassea*, *Galeamopus*, CM 3452, and probably

2346 Rebbachisauridae and Dicraeosauridae). However, a more inclusive study of this character

2347 should be performed in order to recognize the most useful state boundaries for phylogenetic

2348 analyses. At the moment it seems wisest to ~~stay with~~retain the proposed version of Mannion

2349 et al. (2012).

2350 C62: Parietal, posterolateral process, dorsal edge in posterior view: straight, and

2351 ventrolaterally oriented, so that the supratemporal fenestra is slightly facing posteriorly as

2352 well (0); convex, so that the postorbital and thus the supratemporal fenestra are not visible (1)

2353 (Tschopp and Mateus, 2013b; Fig. 49).

2354 **Comments.** The posterior view of the skull corresponds to the view parallel to the long axis

2355 of the occipital condylar neck, which was found to be oriented parallel to the lateral

2356 semicircular canal, thus indicating the neutral head position (Schmitt, 2012).

2357 C63: Parietal, occipital process, dorsoventral height: low, subequal to less than the diameter

2358 of the foramen magnum (0); high, nearly twice the diameter of the foramen magnum (1)

2359 (Wilson, 2002; modified; Tab. S9).

2360 **Comments.** Measurements are taken in strict posterior view (see above). Height is measured

2361 vertically between the dorsal-most and ventral-most extension of the occipital process, and the

2362 foramen magnum. In case of the occipital process, the dorsal- and ventral-most points are

2363 usually transversely shifted against each other. The measurement are therefore taken between

2364 horizontal lines intersecting the extremes. The state boundaries are tentatively set at 1.5, but

2365 more inclusive analyses would have to be undertaken in order to score this character

2366 adequately.

2367 C64: Parietal, occipital process, distal end: ventrolaterally oriented, such that dorsolateral

2368 edge is straight or convex (0); curving laterally, such that dorsolateral edge becomes concave

2369 distally (1) (New; Fig. 49).

2370 **Comments.** The distal end of the posterolateral process of the parietal of non-diplodocine

2371 flagellicaudatans curves outwards to meet the squamosal. This is not the case in the

2372   diplodocine skulls examined for this analysis.

2373   C65: Parietal, distinct horizontal ridge separating dorsal from posterior portion: absent,

2374   transition more or less confluent (0); present, creating a distinct nuchal fossae below the ridge

2375   (1) (Tschopp and Mateus, 2013b; wording modified; Fig. 50).

2376   **Comments.** This character is best ~~observable~~observed in oblique posterolateral view, if one

2377   does not have the specimens at hand. In the derived state, the transverse ridge caps the nuchal

2378   fossa dorsally, creating a distinct concavity below it. Given that small skulls appear to have

2379   this feature most expressed (AMNH 7530, CM 3452, SMA 0004), there is some possibility

2380   that the nuchal fossae become shallower during ontogeny.

2381   C66: Postparietal foramen: absent (0); present (1) (Upchurch, 1995; Fig. 40).

2382   **Comments.** Postparietal foramina have been interpreted to be a dicraeosaurid synapomorphy

2383   (Whitlock, 2011a), but were recently shown to be present as well in Diplodocidae (Tschopp

2384   and Mateus, 2013b). The opening is located at the posteromedial corner of the two parietals,

2385   where they meet the supraoccipital. It might be associated with a vertical groove internally on

2386   the supraoccipital (Remes, 2006; see below), but additional CT studies would have to be

2387   performed in order to check for the presence or absence of this groove in specimens without

2388   the postparietal foramen. Many diplodocid specimens are damaged in this region of the skull,

2389   which makes it difficult to verify the presence of the foramen~~,~~ and impedes an evaluation of

2390   its distribution among flagellicaudatans. The definitive presence in *Kaatedocus*, and the

2391   unknown state in the two apatosaur skulls CM 11162 and YPM 1860 (due to crushing; ET,

2392   pers. obs., 2011), indicates that it might be plesiomorphic for Flagellicaudata, subsequently

2393   lost in *Tornieria* and *Diplodocus*.

2394   C67: Paroccipital process (popr), posterior face: smooth/flat (0); with longitudinal ridge along

2395   popr body extending from dorsomedial to ventrolateral corners (1) (Tschopp and Mateus,

2396   2013b; Fig. 51).

2397   **Comments.** Most of the specimens examined have a slightly convex posterior face of the

2398   paroccipital processes. However, few have such a distinct ridge as is present in *Kaatedocus*.

2399   In the latter, this ridge is accompanied by a rugose area at its dorsomedial origin. None of

2400   these structures are present in CM 11161, for example.

2401   C68: Paroccipital process distal terminus: expanded vertically (0); not expanded (dorsal and

2402   ventral edges are subparallel) (1) (Upchurch, 1998; modified; Fig. 49).

2403   **Comments.** Upchurch (1998) included two morphologies in one character: the dorsoventral

2404 expansion, and the rounded or straight distal edge. The shape of the distal edge is difficult to

2405 assess qualitatively, ~~as~~because many specimens have slightly convex~~,~~ or somewhat triangular

2406 lateral ends of the paroccipital process (e.g. *Suuwassea* ANS 21122, or *Kaatedocus* SMA

2407 0004, Fig. 49). Therefore, the character description was limited to the distal expansion.

2408 C69: Paroccipital process, distal end in lateral view: straight (0); curved (1) (New; Fig. 52).

2409 **Comments.** Due to the slight posterior orientation of the paroccipital processes in many

2410 sauropod taxa, a strict lateral view of the skull does often not allow for an accurate coding of

2411 this character. Also, on pictures of articulated skulls it is often difficult to see the distal end of

2412 the paroccipital process well enough, because it is partly obscured by the squamosal. In most

2413 cases, a posterolateral instead of lateral view would thus be more helpful.

2414 C70: Supratemporal fenestra: present, relatively large (anteroposterior diameter is at least 5%

2415 of occiput width) (0); absent, or greatly reduced (so that anteroposterior diameter is less than

2416 5% of occipital width) (1) (Wilson, 2002; modified by Mannion et al., 2012).

2417 **Comments.** Wilson (2002) proposed this feature as present/absent character, but Mannion et

2418 al. (2012) showed that one of Wilson's (2002) derived taxa (*Limaysaurus*) actually has a

2419 supratemporal fenestra, although an extremely reduced one. ~~Since~~Because this is a derived

2420 state of Rebbachisauridae, and because all diplodocid skulls show large openings, no

2421 additional measuring was done for this analysis.

2422 C71: Supratemporal fenestra, maximum diameter: more than 1.2 times greatest diameter of

2423 foramen magnum (0); less than 1.2 times the greatest length of foramen magnum (1) (Yu,

2424 1993; modified by Mannion et al., 2012).

2425 **Comments.** Mannion et al. (2012) introduced the quantitative state boundaries to the original

2426 description (Yu, 1993). Basically, this character is an extension of the previous one, with the

2427 exception that *Nigersaurus* is impossible to score due to the complete absence of the

2428 supratemporal fenestra in this taxon. In addition to *Limaysaurus*, the quantitative boundaries

2429 of Mannion et al. (2012) also include the dicraeosaurids *Dicraeosaurus* and *Amargasaurus*,

2430 which have reduced supratemporal fenestra as well, but not to the extent shown by

2431 Rebbachisauridae. As stated above, the difference in relative size of the supratemporal

2432 fenestrae between the mentioned taxa and Diplodocidae is large, and thus no additional

2433 measurements were taken in order to test the boundaries proposed by Mannion et al. (2012).

2434 C72: Supraoccipital, anterodorsal margin: internally concave, associated with a channel

2435 extending ventrally on the internal face (0); straight (1) (Remes, 2006; Fig. 53).

2436 **Comments.** The channel was proposed by Remes (2006) as a distinguishing character
2437 between *Tornieria* and Dicraeosauridae, where the presence of the canal is coupled with the
2438 presence of a postparietal fenestra. However, as shown in *Kaatedocus*, these two features are
2439 not necessarily correlated. A separate coding for the two characters is thus justifiable. This is
2440 the first analysis to include this character.

2441 C73: Supraoccipital, dorsal extension: high and vaulted, such that the dorsolateral edges are
2442 strongly sinuous (0); low, with the dorsolateral edges straight (1) (Remes, 2006; Fig. 49).

2443 **Comments.** Remes (2006) used this character in order to distinguish *Tornieria* from
2444 *Apatosaurus*, but did not include it in his phylogenetic analysis. The present analysis is thus
2445 the first one to do so.

2446 C74: Supraoccipital: sagittal nuchal crest: broad, weakly developed (0); narrow, sharp, and
2447 distinct (1) (Whitlock, 2011a; Fig. 54).

2448 **Comments.** The nuchal crest lies on the midline of the supraoccipital, extending
2449 dorsoventrally. A narrow, sharp crest was previously thought to be a synapomorphy for
2450 Dicraeosauridae, but Tschopp and Mateus (2013b) showed that it also occurs in certain
2451 diplodocids.

2452 C75: Supraoccipital, foramen close to contact with parietal: absent (0); present (1) (Tschopp
2453 and Mateus, 2013b; Fig. 54).

2454 **Comments.** This foramen is called external occipital foramen by Balanoff et al. (2010), and is
2455 sometimes located entirely on the supraoccipital (*Dicraeosaurus hansemanni* MB.R.2379,
2456 Janensch, 1935), and in other cases on the suture with the parietal (*Kaatedocus siberi* SMA
2457 0004, ET, pers. obs., 2010). Only taxa with well visible foramina are coded as apomorpic.

2458 C76: Crista prootica, size: rudimentary (0); expanded laterally into dorsolateral process (1)
2459 (Salgado and Calvo, 1992; Upchurch, 1995; Fig. 55).

2460 **Comments.** Although diplodocids have a laterally protruding crista prootica (e.g. SMA
2461 0011), only dicraeosaurids develop distinct lateral processes at the anteroventral ends of the
2462 crista prootica.

2463 C77: Occipital condyle, articular surface: well offset from condylar neck (0); continuously
2464 grading into condylar neck (1) (New; Fig. 56).

2465 **Comments.** Whereas in more basal sauropods the articular surface of the occipital condyle is
2466 usually well delimited, and offset from the condylar neck by a distinct ridge, diplodocids
2467 generally do not have such a clear distinction. The character states are most easily

2468 distinguished in dorsal view.

2469 C78: Basioccipital, contribution to dorsal side of occipital condylar neck: present and broad,

2470 around 1/3 of entire dorsal side (0); reduced to absent (1) (Harris and Dodson, 2004; Fig. 49).

2471 **Comments.** Harris and Dodson (2004) proposed the narrow contribution of the basioccipital

2472 to the dorsal face of the occipital condyle as characteristic for *Suuwassea*. A wider survey of

2473 the distribution of this character showed that the contribution of the basioccipital to the dorsal

2474 side of the occipital condylar neck is reduced in some diplodocid specimens as well.

2475 C79: Basioccipital, distance from base of occipital condyle to base of basal tubera (best

2476 visible in lateral view): short, such that area is gently U-shaped in lateral view (0); elongate,

2477 with a flat portion between occipital condyle and basal tubera (1) (Tschopp and Mateus,

2478 2013b; wording modified; Fig. 52).

2479 **Comments.** The distance is taken relative to the height of the basal tuber, creating a narrow

2480 U-shape or a shallow, wide concavity in lateral view (Fig. 52).

2481 C80: Basioccipital depression between foramen magnum and basal tubera: absent (0); present

2482 (1) (Wilson, 2002; Fig. 57).

2483 **Comments.** The depression is a concave area on the posterolateral sides of the basioccipital,

2484 which is different from the concavity on the posterior face of the basal tubera described in

2485 character 85.

2486 C81: Basioccipital, pit between occipital condyle and basal tubera: absent (0); present (1)

2487 (New; Fig. 58).

2488 **Comments.** Various pits can be present in the area around the basal tubera: YPM 1860 bears

2489 one within the notch between the tubera (see below), and a second one on the basioccipital

2490 posterior to the tubera (which is the one described here). ~~Also t~~The basipterygoid recess is

2491 also located close by, but anterior to the basal tubera on the basisphenoid, instead of the

2492 basioccipital.

2493 C82: Basal tubera: globular (0); box-like (1) (Whitlock et al., 2010; Fig. 59).

2494 **Comments.** Whitlock et al. (2010) used this character as one of the features distinguishing the

2495 juvenile diplodocid skull CM 11255 from *Apatosaurus*. It is herein used for the first time as a

2496 phylogenetic character.

2497 C83: Basal tubera, breadth: <1.3 times (0); 1.3-1.85 times (1); >1.85 times occipital condyle

2498 width (2) (Wilson, 2002; modified; Tab. S10).

2499 **Comments.** The character was initially defined without clear state borders, and only with two

2500 states (Wilson, 2002). Mannion (2011) suggested ~~to further subdivide~~further subdivision of

2501 the character, based on a wider survey of this ratio among sauropods. Mannion's (2011) table

2502 was here extended and the character state boundaries were modified following higher-level

2503 taxonomy and gaps in the distribution of the values.

2504 C84: Basal tubera: distinct from basipterygoid (0); reduced to slight swelling on ventral

2505 surface of basipterygoid (1) (Whitlock, 2011a; Fig. 60).

2506 **Comments.** The use of this character and its coding overlaps with an additional character

2507 proposed by Wilson (2002): 'Basal tubera, anteroposterior depth: approximately 33%, or

2508 more, of dorsoventral height (0); sheetlike, less than 33% (normally around 20%)

2509 dorsoventral height (1)'. Whitlock's (2011a) character is herein preferred as the directional

2510 terms used in Wilson (2002) are sometimes confusing due to varying orientations of the basal

2511 tubera of Diplodocoidea and non-diplodocoid sauropods.

2512 C85: Basal tubera, shape of posterior face: convex (0); flat (1); slightly concave (2)

2513 (Whitlock, 2011a; modified by Tschopp and Mateus, 2013b; Fig. 60).

2514 **Comments.** The 'posterior face' of the basal tubera is herein intended to be the side facing the

2515 occipital condyle. The concavity described herein is different from the concavity sometimes

2516 present on the lateral side of the basioccipital (see above).

2517 C86: Basal tubera, posteroventral face: continuous (0); marked by a distinct transverse ridge

2518 (1) (New; Fig. 60).

2519 **Comments.** The surface of the basal tubera is usually regularly rugose, and without distinct

2520 structuring. SMA 0004, however, bears a distinct transverse ridge on the posteroventral face

2521 of its basal tubera.

2522 C87: Basal tubera, longest axes: parallel (0); in an angle to each other, pointing towards the

2523 occipital condyle (1) (New; Fig. 61).

2524 **Comments.** The character is to be coded based on a view perpendicular to the orientation of

2525 the basipterygoid processes. It is inspired by the character of Tschopp and Mateus (2013b)

2526 describing the anterior margin of the tubera as V- or U-shaped, which included two differing

2527 morphologies in the same character (orientation of the tubera and shape of the anterior

2528 margin). The two morphologies are here treated as different characters (see below). In some

2529 cases (e.g. CM 11162), the outline of the tubera is subtriangular, with a more or less right

2530 angle pointing posterolaterally. These cases were treated as apomorphic, because the longest

2531 distance follows the obliquely oriented hypotenuse of the triangle.

2532 C88: Basal tubera, anterior edge: straight or convex (0); concave (1) (Tschopp and Mateus,

2533 2013b; Fig. 61).

2534 **Comments.** The second of the two characters inspired by Tschopp and Mateus' (2013b)

2535 character about the anterior margin of the basal tubera. The anterior edge is the one facing

2536 towards the basipterygoid processes, which in non-diplodocoid sauropods is oriented rather

2537 anteroventrally. In specimens with angled basal tubera (see above), the anterior margin is

2538 oriented obliquely.

2539 C89: Basal tubera in posterior view: facing ventrolaterally (0); facing straight ventrally,

2540 forming a horizontal line (1) (Tschopp and Mateus, 2013b; wording modified; Fig. 59).

2541 **Comments.** Some specimens (in particular non-flagellicaudatans) have rounded basal tubera,

2542 which extend onto the lateral surface of the basioccipital. These are treated as plesiomorphic,

2543 because the line projecting through the medial- and lateral-most points of the tubera is oblique

2544 in these cases.

2545 C90: Basal tubera, foramen in notch that separates the two tubera: absent (0); present (1)

2546 (Tschopp and Mateus, 2013b; Fig. 58).

2547 **Comments.** This foramen is one of three openings that can ~~be present~~occur in this area (see

2548 above and below). However, the pit described in this character cannot be homologous to the

2549 other ones because it ~~is present~~occurs together with the basipterygoid recess in HMNS 175

2550 (Holland, 1906)~~,~~ and together with the basioccipital pit in YPM 1860 (ET, pers. obs., 2011).

2551 C91: Basisphenoid/basipterygoid recess: absent (0); present (1) (Wilson, 2002; polarity

2552 reversed; Fig. 58)

2553 **Comments.** The basipterygoid recess is a pit located anterior~~ly~~ to the basal tubera, on the

2554 basisphenoid. Its absence was considered autapomorphic for *Apatosaurus*, representing a

2555 reversal to the plesiomorphic state in Sauropoda (Wilson, 2002). However, in ~~the~~his

2556 phylogenetic analysis, Wilson (2002) scored *Apatosaurus* as having a recess, sharing this state

2557 with basal sauropods like *Shunosaurus*. The character was organized as a presence/absence

2558 character, with the presence being plesiomorphic (Wilson, 2002). Assuming that the

2559 discussion of the autapomorphies is right, polarity of the character states was inverted herein.

2560 The basipterygoid recess might be confused with the pits located in the notch between the

2561 tubera or the one posterior to them (see above), so it is important to state that it lies anterior to

2562 the tubera, between the bases of the basipterygoid processes.

2563 C92: Basipterygoid processes: widely diverging (> 60°) (0); intermediate, 31°-60° (1);

2564 narrowly diverging (< 31°) (2) (Yu, 1993; modified; Fig. 55; Tab. S11).

2565 **Comments.** There are several modes to measure the angle between the processes, and no

2566 previous analysis defines how this angle should be measured. Here, divergence is measured

2567 between lines drawn from the basisphenoid center, where the bases of the basipterygoid

2568 processes meet, to the anteromedial-most point of the processes. This is preferably done in

2569 posterior or posteroventral view, perpendicular to the longitudinal axis of the processes. The

2570 present measuring technique yields slightly different results compared to earlier studies, but

2571 general trends are similar.

2572 C93: Basipterygoid processes, orientation: directed more than 75° to skull roof (normally

2573 perpendicular) (0); angled less than 75° to skull roof (normally approximately 45°) (1)

2574 (McIntosh, 1990b; modified; Tab. S12).

2575 **Comments.** New numeric state boundaries were established, because a survey of diplodocoid

2576 braincases showed that there is more variety than previously recognized (Tab. S12). However,

2577 the difference was already recognized as taxonomically important by McIntosh (1990b). The

2578 angle is measured between the skull roof and a line through the center of the proximal and

2579 distal ends. This is important, ~~as~~ especially because macronarian basipterygoid processes tend

2580 to curve backwards at their distal ends, thereby increasing the angle as measured here.

2581 ~~There is some possibility~~It is possible that this character is correlated with the large angle

2582 between the anterior and dorsal quadratojugal processes and the backwards inclination of the

2583 ventral ramus of the quadrate. This entire region is interconnected by the pterygoid, and the

2584 anterior shifting of the basisphenoid-pterygoid articulation due to the changed orientation of

2585 the basipterygoid processes might have been caused by, or the reason for the more anteriorly

2586 orientated ventral ramus of the quadrate, and therefore also the widening of the angle between

2587 the quadratojugal processes⊟owever, ~~since~~because there is no evidence of correlation and

2588 ~~few to~~ no skulls are known of basal diplodocoid taxa~~, which~~ that might show intermediate

2589 states, if they were present, the separate characters are retained ~~separate here, lacking~~

2590 ~~definitive evidence of correlation~~.

2591 Furthermore, there is some indication that the character could be ontogenetically controlled:

2592 the two relatively small diplodocine skulls CM 3452 and SMA 0004 ~~have~~ both have

2593 somewhat larger angles compared to larger specimens (Tab. S12), and lower angles in the

2594 quadratojugal. However, further studies are needed to decide if this is really ontogenetic, or if

2595 it could be taxonomically significant.

2596 C94: Basipterygoid processes, ratio of length:basal transverse diameter: < 4 (0); = or > 4.0 (1)

2597 (Wilson, 2002; modified; Fig. 55; Tab. S13).

2598 **Comments.** The character was initially defined as ratio of length to maximum basal diameter

2599 (Wilson, 2002). However, maximum basal diameter is often oriented dorsoventrally (at least

2600 in diplodocids), which means that one cannot take the measurements in a picture of the

2601 processes in ventral view only. Also, dorsoventral height changes considerably, and

2602 continuously, towards the base of the processes in some specimens (e.g. *Dicraeosaurus*

2603 *hansemanni* MB.R.2379; Janensch, 1935; Fig. 55). I, and in lateral view, it is sometimes

2604 difficult to decide where exactly the base of the process is situated. Therefore, and because

2605 ventral views are obtainable more frequently than lateral views, the ratio length/basal

2606 transverse diameter is preferred herein. The dimensions should be measured perpendicular to

2607 each other. Wilson (2002) initially left a gap in the definition of the states (2 or less, 4 or

2608 more), which was corrected for by Mannion et al. (2012). However, as a more rigorous

2609 assessment of these ratios shows (Tab. S13), the state boundary should rather be set to four,

2610 the derived, elongate state resulting as a shared synapomorphy for Diplodocinae and

2611 Dicraeosauridae.

2612 Measuring the basipterygoid processes in such a way leads to much higher elongation ratios

2613 for the holotype of *Kaatedocus siberi* (SMA 0004) than reported in its initial description

2614 (Tschopp and Mateus, 2013b). The low ratio also served as local autapomorphy for the genus

2615 (Tschopp and Mateus, 2013b). Following the results presented herein, this is most probably

2616 an artifact based on differing measurement protocols, asbecause Tschopp and Mateus (2013b)

2617 compared length with dorsoventral height, which is the maximum basal diameter in SMA

2618 0004 (Tschopp and Mateus, 2013b). The current measurements show that *Kaatedocus* is

2619 actually well in the range of Diplodocinae, which can easily be distinguished from

2620 *Apatosaurus louisae* CM 11162 (Tab. S13).

2621 C95: Basipterygoid, area between the basipterygoid processes and parasphenoid rostrum: is a

2622 mildly concave subtriangular region (0); forms a deep slot-like cavity that passes posteriorly

2623 between the bases of the basipterygoid processes (1) (Upchurch, 1995, 1998; Fig. 55).

2624 C96: Basipterygoid processes, orientation of proximal-most portions: same as central portion

2625 of shaft (0); parallel to each other, outwards curve of shaft happens only more anteriorly (1)

2626 (New; Fig. 62).

2627 **Comments.** The development of this character is best seen in ventral view. In the derived

2628 state, the parallel portion of the basipterygoid processes are often interconnected

2629 dorsomedially by a thin sheet of bone. On the other hand, a similar sheet can also be present if

2630 the processes are entirely straight.

2631 C97: Basipterygoid processes, distal end: straight (0); curving outwards (1) (New; Fig. 57).

2632 **Comments.** This character compares the distal end of the basipterygoid process with the

2633 central portion. It is thus different from the feature described in character 96.

2634 C98: Basipterygoid processes, distal lateral expansion: absent (0); present (1) (New; Fig. 57).

2635 **Comments.** Only abrupt distal expansions are coded as apomorphic. Gradually extending

2636 processes are treated as plesiomorphic.

2637 C99: Parasphenoid rostrum, groove on dorsal edge: absent (0); present (1) (Upchurch, 1995,

2638 1998; modified; Fig. 55).

2639 **Comments.** Upchurch (1995, 1998) proposed the character combining the presence of a

2640 dorsal groove with the lateral shape of the rostrum, thereby implying that the dorsoventrally

2641 thin parasphenoid of diplodocoids would not bear dorsal grooves. However, a more detailed

2642 study of diplodocoids shows that the groove is actually present in most of them.

2643 C100: Optic foramen: paired (0); unpaired (1) (Berman and McIntosh, 1978; Sander et al.,

2644 2006; Fig. 63).

2645 **Comments.** The optic foramen ~~is lying~~lies close to the midline, within the orbitosphenoid in

2646 most sauropod taxa. Generally, ~~they~~the foramina are separated medially by a narrow bony

2647 bridge, which is absent in some diplodocoid specimens (e.g. *Suuwassea*, Harris, 2006a).

2648 Sander et al. (2006) were the first to include the character in~~to~~ a phylogenetic analysis.

2649 C101: Palatobasal contact, shape: pterygoid with small facet (0); dorsomedially orientated

2650 hook (1) (Wilson, 2002; modified by Tschopp and Mateus, 2013b; Fig. 64).

2651 **Comments.** Tschopp and Mateus (2013b) deleted a third state ~~present~~from ~~in~~ the original

2652 character, which describes the specific rocker-like morphology of this region in

2653 nemegtosaurid sauropods (Wilson, 2002). ~~Since~~Because no taxon of this clade is included, the

2654 additional state is redundant here.

2655 C102: Pterygoid, transverse flange (i.e. ectopterygoid process) position: between orbit and

2656 antorbital fenestra (0); anterior to antorbital fenestra (1) (Upchurch, 1995; Fig. 44).

2657 **Comments.** The transverse flange of the pterygoid connects to the maxilla through the

2658 ectopterygoid (Upchurch et al., 2004a).

2659 C103: Vomer, anterior articulation: maxilla (0); premaxilla (1) (Wilson, 2002; polarity

2660 reversed; Fig. 44).

2661 **Comments.** Polarity was reversed compared to Wilson's (2002) character due to the limited

2662 taxon sampling.

2663 C104: Dentary, anteroventral margin shape: gently rounded (0); sharply projecting triangular

2664 process or 'chin' (1) (Upchurch, 1998; Fig. 65).

2665 **Comments.** Usually considered a flagellicaudatan synapomorphy, ~~also~~ some specimens of

2666 *Camarasaurus* <u>also</u> show a weak ventral expansion at the anterior extreme of the lower jaw.

2667 However, this never reaches the chin-like state ~~as~~ present in *Diplodocus*, and *Camarasaurus*

2668 is thus included in the plesiomorphic state here.

2669 C105: Dentary, cross-sectional shape of symphysis: oblong or rectangular (0); subtriangular,

2670 tapering sharply towards ventral extreme (1); subcircular (2) (Whitlock, 2011a; Fig. 65).

2671 **Comments.** Diplodocids have ventrally tapering symphyses, but they do not taper to a point

2672 as in dicraeosaurids (Whitlock and Harris, 2010) and have thus still to be scored as

2673 plesiomorphic.

2674 C106: Dentary, tuberosity on labial surface near symphysis: absent (0); present (1) (Whitlock

2675 and Harris, 2010; reworded by Whitlock, 2011a; Fig. 66).

2676 **Comments.** This character was originally proposed by Whitlock and Harris (2010) to unite

2677 *Suuwassea* and *Dicraeosaurus*.

2678 C107: Dentary, anterolateral corner: not expanded laterally beyond mandibular ramus (0);

2679 expanded beyond lateral mandibular ramus (1) (Whitlock, 2011a; Fig. 66).

2680 **Comments.** The derived state of this character describes the extreme case of character 112.

2681 To date, it is only known in the rebbachisaurid *Nigersaurus* (Sereno et al., 2007).

2682 C108: Mandible, coronoid eminence: strongly expressed, clearly rising above plane of

2683 dentigerous portion (0); absent (1) (Whitlock, 2011a; Fig. 65).

2684 **Comments.** Some diplodocids have dorsally expanded coronoid areas, but they do not reach

2685 above the plane of the dentigerous portion.

2686 C109: Surangular foramen: absent (0); present (1) (New; Fig. 67).

2687 **Comments.** The location of the surangular foramen can vary in different taxa. Usually, it is

2688 situated in the anterior, horizontally oriented portion, but in some cases it is shifted

2689 posteriorly.

2690 C110: External mandibular fenestra: present (0); absent (1) (McIntosh, 1990b; Russell and

2691 Zheng, 1993; Fig. 67).

2692 **Comments.** The presence is a retained plesiomorphy, shared with early sauropodomorphs

2693 (Wilson, 2002).

2694 C111: Snout shape in dorsal view: premaxilla-maxilla index (PMI; Whitlock et al., 2010) <

2695 67% (0); 67-85% (1); > 85% (2) (Upchurch, 1998; Whitlock, 2011a; modified; Tab. S14).

2696 **Comments.** In order to avoid gaps, an intermediate state was added to Whitlock's (2011a)

2697 version. The state boundaries were chosen following high-level phylogenetic differences.

2698 Measurements taken on photos from slightly different angles of the skulls CM 3452, 11161,

2699 11162, and SMA 0011 show that the orientation of the skull has a relatively high influence on

2700 the measured PMI (Tab. S14). In order to avoid this, the same measurements were taken in

2701 more than one picture of the same skulls, where possible. In future, one should check and

2702 remeasure this ratio in all diplodocid skulls, making sure that they are always taken in exactly

2703 the same orientation. Best results are to be expected with the ventral maxillary edge oriented

2704 horizontally.

2705 Whitlock et al. (2010) reported that the snout becomes more squared during ontogeny in

2706 diplodocids. It might thus be possible that more juvenile specimens become artificially

2707 grouped closer to more basal taxa when including this character. The character was treated as

2708 ordered.

2709 **Teeth**

2710 C112: Shape of tooth row in occlusal view: follows curvature of dentary (0); anterolateral

2711 corner of tooth row displaced labially (1) (Whitlock and Harris, 2010; Fig. 66).

2712 **Comments.** In dicraeosaurids, it seems to be the tooth row, which is mostly responsible for

2713 the squared appearance of the lower jaw ⊟ he ventral portions of the dentary would be much

2714 more rounded (Whitlock and Harris, 2010). The diplodocid AMNH 969 has a similar

2715 development as *Suuwassea*.

2716 C113: Tooth rows, length: restricted anterior to orbit (0); restricted anterior to antorbital

2717 fenestra (1); restricted anterior to subnarial foramen (2) (Gauthier, 1986; modified by

2718 Whitlock, 2011a; Fig. 36).

2719 **Comments.** In order to score this character, the skull should be ~~ho~~eld with the ventral margin

2720 of the maxilla oriented horizontally. The tooth row is usually more anteriorly restricted in the

2721 lower jaw than in the maxilla. Here, the maxillary tooth row is used as a reference. As for the

2722 snout shape, ~~also~~ the anterior restriction of the tooth row also was interpreted as juvenile

2723 feature (Whitlock et al., 2010). The character is treated as ordered.

2724 C114: Dentary teeth, number: greater than 17 (0); 10-17 (1); 9 or fewer (2) (Wilson and

2725 Sereno, 1998; modified by Carballido et al., 2012b; Tab. S15).

2726 **Comments.** Carballido et al. (2012b) added a third state to distinguish *Demandasaurus* and

2727 *Suuwassea* from other sauropod specimens. ~~Since~~Because the reduction of the number of

2728 dentary teeth was ~~accomplished and~~ apparently reversed several times⊟~~is not entirely clear~~

2729 ~~how evolution worked in this case. T~~the character was therefore left unordered.

2730 C115: Replacement teeth per alveolus, number: three or fewer (0); four or more (1) (Wilson,

2731 2002).

2732 **Comments.** The number of replacement teeth ~~appears to change~~varies between the tooth-

2733 bearing bones of the same individual (D. Schwarz-Wings, pers. comm., 2012). However,

2734 maximum number of replacement teeth is still informative, and therefore the character was

2735 retained.

2736 C116: Teeth, crown-to-crown occlusion: present (0); absent (1) (Wilson and Sereno, 1998;

2737 polarity reversed by Whitlock, 2011a).

2738 C117: Teeth, wear facets shape: v-shaped (0); planar (1) (Wilson and Sereno, 1998; modified;

2739 Fig. 68).

2740 **Comments.** The initial character (Wilson and Sereno, 1998) was first adapted by Sereno et al.

2741 (2007), in order to include the paired planar facets of *Nigersaurus*. Here, the shape and

2742 number of wear facets are considered independent characters (see character 118).⊟

2743 C118: Teeth, occlusal pattern: paired wear facets (0); single facet (1) (Wilson and Sereno,

2744 1998; modified; Fig. 69).

2745 **Comments.** See character 117.

2746 C119: Teeth, SI values for tooth crowns: < 3.4 (0); 3.4 or greater (1) (McIntosh, 1989;

2747 Upchurch, 1998; modified; Tab. S16).

2748 **Comments.** The SI value describes the slenderness of the teeth. It was defined as crown

2749 length/mesiodistal width (Upchurch, 1998). The state borders were changed, following large

2750 gaps apparently corresponding to higher-level taxonomy (Tab. S16).

2751 C120: Tooth crowns, orientation: aligned slightly anterolingually, tooth crowns overlap (0);

2752 aligned along jaw axis, crowns do not overlap (1) (Wilson and Sereno, 1998; polarity reversed

2753 by Whitlock, 2011a; Fig. 67).

2754 C121: Tooth crowns, cross-sectional shape at midcrown: D-shaped (0); cylindrical (1)

2755 (Russell and Zheng, 1993; modified by Wilson and Sereno, 1998; Fig. 70).

2756 **Comments.** Unworn diplodocoid teeth often have ellipsoid cross-sections. However, this is

2757 different from the spatulate non-diplodocoid teeth as e.g. typical for *Camarasaurus*. Teeth of

2758 the latter genus have a slightly concave lingual face, unlike the convex surface of

2759 diplodocoids. In the absence of nemegtosaurid titanosaurs, which show similarly shaped teeth

2760 (Upchurch, 1999; Wilson, 2005), the derived state results as unambiguous synapomorphy of

2761 Diplodocoidea.

2762 C122: Teeth, orientation relative to long axis of jaw: perpendicular (0); oriented anteriorly

2763 (procumbent) (1) (Upchurch, 1998; Fig. 67).

2764 **Comments.** Tooth orientation is best recognized in the posterior-most teeth in the maxilla and

2765 dentary.

2766 C123: Teeth, longitudinal grooves on lingual aspect: absent (0); present (1) (Wilson, 2002;

2767 Fig. 68).

2768 **Comments.** Wilson (2002) initially scored only rebbachisaurids with the derived state.

2769 However, several non-diplodocoid taxa with spatulate teeth actually have a midline ridge on

2770 the lingual face of their teeth, creating two grooves mesially and distally to it (e.g. Osborn and

2771 Mook, 1921; Ouyang and Ye, 2002). Consequently, these taxa are scored as derived here as

2772 well.

2773 C124: Teeth, thickness of enamel asymmetric labiolingually: absent (0); present (1)

2774 (Whitlock, 2011a; Fig. 70).

2775 **Comments.** This feature can be observed easily in wear facets or cross-sections.

2776 C125: Teeth, marginal denticles: present (0); absent (1) (McIntosh, 1990b; Fig. 68).

2777 **Comments.** There is some morphological variation in the location of the denticles (Carballido

2778 et al., 2012b), but ~~as~~because no diplodocid shows denticles, this simplified version of the

2779 character is used herein.

2780 **Cervical vertebrae**

2781 C126: Presacral neural spines, bifurcation: absent (0); present (1) (McIntosh, 1989; Wilson,

2782 2002; modified; Tab. S17).

2783 **Comments.** Wilson (2002) divided this character into the different regions, where the

2784 bifurcation can be present. ~~However, like this~~As a result, taxa with unbifurcated neural spines

2785 are coded several times for the same state. In the present analysis, presence of bifurcation and

2786 the first bifid element are treated as two different characters (see character 140).

2787 C127: Number of cervical vertebrae: < 13 (0); 14-15 (1); 16 or more (2) (McIntosh, 1990b;

2788   modified; Tab. S18).

2789   **Comments.** The character is used in various versions in different phylogenetic analyses

2790   (Upchurch, 1998; Wilson, 2002; Whitlock, 2011a), depending on their specific focus. Herein,

2791   the states are adjusted to fit the included taxa, excluding redundancy. Only one diplodocid

2792   specimen preserves a complete neck (*Apatosaurus louisae* CM 3018), and even here, the

2793   possibility of ~~lacking~~missing elements cannot be ruled out entirely, due to gaps between

2794   certain cervical vertebrae as they were found (McIntosh, 2005). A second specimen

2795   (*Diplodocus carnegii* CM 84) lacks the atlas, and seems otherwise complete, although the

2796   same concerns ~~account as in~~exist as for CM 3018 (McIntosh, 2005). However, as the more

2797   anterior and posterior elements in these cases fit well together, we followed McIntosh (2005)

2798   in assuming that no vertebra was lost at the position of these gaps in CM 84 and 3018.

2799   McIntosh (2005) suggested that *Barosaurus* had 16 cervical vertebrae, instead of 15 as

2800   *Apatosaurus* and *Diplodocus*. The assumption was primarily based on the fact that AMNH

2801   6341 only has nine dorsal vertebrae, and that the neosauropod presacral column generally

2802   consists of 25 elements (McIntosh, 2005). ~~Since~~Because none of the *Barosaurus* specimens

2803   preserves an entire neck, none of the *Barosaurus* OTUs can be coded for this character. The

2804   inability to code incomplete specimens might be circumvented by using additive binary

2805   characters (Upchurch, 1998). However, this would imply that the corresponding multistate

2806   character is continuous (Wilson, 2002), which means that the number of cervical vertebrae

2807   could not increase directly by more than one element during speciation. Given that the

2808   contrary is shown to be possible in dorsal and sacral vertebrae of mice (Wellik and Capecchi,

2809   2003), it seems reasonable to argue that the same accounts for sauropod cervical vertebrae.

2810   The character is thus treated as unordered herein. This also indicates that 'analysis 1' of

2811   Mannion et al. (2012), where these characters are treated as unordered, should be preferred

2812   over 'analysis 2'.

2813   C128: Cervical vertebrae width to height ratio: less than 0.5 (0); 0.5-1.5 (1); more than 1.5 (2)

2814   (Upchurch et al., 2004b; modified; Tab. S19).

2815   **Comments.** Upchurch et al. (2004b: p. 105) defined the ratio as follows: "~~,~~Height is

2816   measured from the top of the neural spine to the ventral surface of the centrum. Width is

2817   defined as the distance between the distal tips of the diapophyses." A third state was added

2818   (less than 0.5) ~~as~~because derived dicraeosaurids have a distinctly lower ratio compared to

2819   other flagellicaudatans. Given that evolution appears to have worked in both directions

2820   character is left unordered.

2821   C129: Cervical pneumatopores (pleurocoels): absent (0); present (1) (McIntosh, 1990b;

2822   Upchurch, 1995; Fig. 71).

2823   **Comments.** McIntosh (1990b) already used this character to distinguish advanced sauropods

2824   from the most basal forms, but Upchurch (1995) was the first to include it into a phylogenetic

2825   analysis.

2826   C130: Cervical centra, internal pneumaticity: absent (0); present with single and wide cavities

2827   (1); present, with several small and complex internal cavities (2) (Upchurch, 1998; Wilson

2828   and Sereno, 1998; modified by Carballido et al., 2012b; Fig. 72).

2829   **Comments.** Introduced as character by Upchurch (1998) and Wilson and Sereno (1998), only

2830   Wedel et al. (2000) and Wedel (2003) analyzed the distribution of this feature in detail.

2831   Carballido et al. (2012b) divided the original character, which did not discriminate between

2832   cervical and dorsal vertebrae (Upchurch, 1998; Wilson and Sereno, 1998).

2833   C131: Cervical vertebrae, small fossa on posteroventral corner: absent (0); shallow,

2834   anteroposteriorly elongate fossa present, posteroventral to pleurocoel (1) (Whitlock, 2011a;

2835   Fig. 71).

2836   **Comments.** *Kaatedocus siberi* SMA 0004, AMNH 7530, and the apatosaurines YPM 1980

2837   and AMNH 460 have shallow depressions at the same place, but they do not create distinct

2838   fossae as in *Barosaurus* or *Diplodocus* (see Hatcher, 1901; McIntosh, 2005), and are thus

2839   coded as plesiomorphic.

2840   C132: Cervical centra, midline keels on ventral surface: prominent and plate-like (0); reduced

2841   to low ridges (1) (Upchurch, 1998; Upchurch et al., 2004a; modified; Fig. 73).

2842   **Comments.** ~~Since~~Because the presence or absence is already coded ~~for~~ in

2843   ~~following~~subsequent characters, the complete absence is here excluded from the original

2844   character description (Upchurch, 1998; Upchurch et al., 2004a), and taxa without ventral

2845   ridges are scored as unknown.

2846   C133: Cervical vertebrae, longitudinal sulcus on ventral surface: absent (0); present (1)

2847   (Upchurch, 1995, 1998; Fig. 73).

2848   **Comments.** Due to the lateroventral projecting cervical parapophyses of *Apatosaurus*,

2849   cervical vertebrae of this genus have a concave anterior portion of the ventral surface.

2850   However, this is the case in almost all sauropod taxa, and therefore only specimens with

2851   transversely concave ventral surfaces throughout the entire length of the centrum are herein

2852 scored as apomorphic.

2853 C134: Cervical vertebra, posterior projection on transverse processes: present (0); absent (1)

2854 (Remes et al., 2009; polarity reversed; Fig. 74).

2855 **Comments.** A distinct, triangular posterior projection marks the transverse process of

2856 *Spinophorosaurus* and many diplodocines. Posteriorly convex transverse processes are not

2857 considered projections. Due to reduced taxon sampling, the character polarity of the original

2858 version (Remes et al., 2009) was inverted here.

2859 C135: Cervical vertebrae, posterior extension of posterior centrodiapophyseal lamina: is

2860 anteriorly restricted (0); reaches below posterior end of neural canal (1) (New; Figs 71, 75).

2861 **Comments.** *Apatosaurus* specimens appear to have a consistently more developed pcdl

2862 compared to Diplodocinae. The only apatosaur specimen with an anteriorly restricted pcdl is

2863 the juvenile holotype of *Elosaurus parvus*, CM 566. The development of vertebral laminae

2864 has previously been linked with ontogeny (Carballido and Sander, 2013; Schwarz et al.,

2865 2007b).

2866 C136: Cervical vertebrae, short second posterior centrodiapophyseal lamina ventral to the one

2867 uniting with the dorsal shelf of the diapophysis: absent (0); present (1) (New; Fig. 76).

2868 **Comments.** ~~The presence of a~~A short accessory pcdl appears to be linked with the

2869 bifurcation of the pcdl in more posterior elements in *Galeamopus* (see above). However,

2870 bifurcated pcdl also occur in some apatosaur specimens which do not have an additional pcdl

2871 in more anterior elements (e.g. UW 15556; Gilmore, 1936), and therefore, these morphologies

2872 are treated as independent characters.

2873 C137: Cervical vertebrae, foramen on dorsal side of postzygodiapophyseal lamina, just

2874 anterior to base of neural spine process: absent (0); present (1) (Remes, 2007; Fig. 76).

2875 **Comments.** Distinct foramina in the sdf are usually considered typical for brachiosaurids, and

2876 their presence in *Australodocus* was therefore one of the reasons why Whitlock (2011c)

2877 reinterpreted *Australodocus bohetii* as a titanosauriform, instead of a diplodocine as initially

2878 proposed (Remes, 2007). However, ~~also~~ *Barosaurus* sometimes shows small foramina in

2879 similar positions (YPM 429, ET, pers. obs., 2011), but they are usually less prominent. The

2880 putative juvenile *Brachiosaurus* specimen SMA 0009 does not have such foramina, but

2881 ~~since~~because the development of pneumatic structures appears to be ontogenetically

2882 controlled (Carballido and Sander, 2013; Schwarz et al., 2007c), this might be explained ~~like~~

2883 ~~that~~as such.

2884　C138: Cervical vertebrae, epipophysis: reduced ~~to~~or absent (0); pronounced, forming a

2885　distinct projection above the postzygapophysis (1) (Remes et al., 2009; modified; Fig. 76).

2886　C139: Cervical vertebrae, pneumatized epipophyses: absent (0); present (1) (New; Fig. 77).

2887　**Comments.** The pneumatic foramen can be situated anteriorly as in *Diplodocus carnegii* (CM

2888　84, 94, ET, pers. obs., 2011), or posteriorly as in *Barosaurus lentus* YPM 429 (ET, pers. obs.,

2889　2011).

2890　C140: Cervical neural spines, first bifid element, if present: CV 3 (0); first mCV (1); posterior

2891　mCV (2); restricted to pCV (3) (Wilson, 2002; modified; Tab. S17).

2892　**Comments.** Taxa with unbifurcated neural spines are scored as unknown. The subdivision

2893　into anterior, mid-, and posterior cervical vertebrae depends on the number of elements in the

2894　column (Tab. 10). Absolute numbers other than CV 3, which is the first postaxial cervical

2895　element, would thus be misleading and are avoided here. The character is treated as ordered.

2896　C141: Cervical vertebrae, unbifurcated neural spines in anterior/posterior view: with parallel

2897　lateral edges or converging (0); distal end expanded laterally (1) (New; Fig. 78).

2898　**Comments.** The real distribution of this character within Diplodocidae is difficult to assess to

2899　date, ~~as~~because there are only a few specimens reported that preserve complete neural spines

2900　of anterior, unbifurcated neural spines.

2901　C142: Cervical vertebrae, summits of bifid neural spines: are laterally compressed (0); are

2902　rounded (1) (Upchurch et al., 2004b; Fig. 74).

2903　**Comments.** The derived state of this character is shared by some apatosaur specimens and

2904　*Suuwassea*. The spine summits in most other taxa with bifurcated spines are generally

2905　anteroposteriorly elongate~~,~~ and transversely compressed, resulting in narrow sheets of bone.

2906　In *Suuwassea* as well as in some apatosaur specimens, the lateral edge of the spine summit is

2907　distinctly convex, producing a semi-circular outline. Some other taxa (e.g. *Kaatedocus*;

2908　Tschopp and Mateus, 2013b) have medial ridges connecting the summit with the base, but

2909　these are always relatively shallow, and do not form rounded outlines.

2910　C143: Proatlas, distal end: broadly rounded (0); narrow and elongate, almost pointed (1)

2911　(New; Fig. 79).

2912　C144: Atlantal intercentrum, anteroventral lip: absent, anterior edge of intercentrum straight

2913　in lateral view (0); present, anterior edge of intercentrum concave (1) (Wilson, 2002;

2914　modified; Fig. 80).

2915　**Comments.** Initially regarded as flagellicaudatan synapomorphy (Wilson, 2002), ~~the presence~~

of an anteroventral lip is now known to ~~be present~~occur in *Mongolosaurus* as well (Mannion, 2011). Following the original description of the character states (Wilson, 2002: intercentrum shape in lateral view: rectangular or ventrally longer than dorsally), ~~also~~ *Camarasaurus* and other non-flagellicaudatan taxa also would have to be scored as apomorphic. However, they do not show a distinct anteroventral lip, resulting in a strongly concave anterior edge of the intercentrum, when seen in lateral view.

C145: Atlantal intercentrum, foramen between posterior ventrolateral processes: absent (0); present (1) (New; Fig. 80).

C146: Atlantal neurapophyses, anteromedial process: weakly developed (0); well-developed and distinct from posterior wing (1) (New; Fig. 81).

Comments. The anteromedial process corresponds to the prezygapophyses of more posterior elements. It articulates with the posterior end of the proatlas. In *Kaatedocus*, this process is relatively short transversely, and curves gradually into the posterior process, whereas in SMA 0011 and AMNH 969, the anteromedial process is distinct and at least as wide transversely as long anteroposteriorly.

C147: Atlantal neural arch, small subtriangular, laterally projecting spur at base: absent (0); present (1) (New; Fig. 81).

Comments. When present, this spur is located at the base of the neurapophysis, opposite ~~to~~ the ~~position of the~~ anteromedial process, and much smaller. It is also present in some, but not all, *Camarasaurus* specimens (Ikejiri, 2004).

C148: Atlantal neurapophyses, posterior wing: gradually tapering along its length (0); of subequal width along most of its length (1) (New; Fig. 81).

Comments. The posterior wing of the neurapophysis articulates with the prezygapophysis of the axis.

C149: Atlantal neural arch: without foramen (0); with foramen (1) (Wilson, 2002; Whitlock, 2011a; Fig. 81).

Comments. Wilson (2002) proposed the presence of such a foramen as an autapomorphy of *Apatosaurus*, and it was included as character in the phylogenetic analysis of Whitlock (2011a). Due to the small number of preserved atlantal neurapophyses, only one specimen can currently be positively assigned to the apomorphic state (*Apatosaurus louisae* CM 3018). It could thus also represent a species autapomorphy, instead of being valid for the entire genus.

C150: Axial centrum, pneumatic fossae on ventrolateral edges, right posterior to

2948 parapophyses: absent (0); present (1) (New; Fig. 82).

2949 **Comments.** Many specimens have a well-developed median keel on their ventral surfaces. In

2950 lateral view, this sometimes appears ~~like~~as a bifurcation of the ventrolateral edge, although

2951 this is not the case. The apomorphic state of the character proposed herein only includes

2952 fossae bordered by ridges that originate at the parapophysis anteriorly.

2953 C151: Axis, prespinal lamina: of constant width (0); developing a transversely expanded,

2954 knob-like tuberosity at its anterior end (1) (New; Fig. 83).

2955 C152: Axis, postspinal lamina: absent (0); present (1) (Harris and Dodson, 2004; Fig: 82).

2956 C153: Axis neural spine: projects beyond posterior border of centrum (0); terminates in front

2957 of or at posterior border of centrum (1); is restricted anterior to postzygapophyseal facets (2)

2958 (New; Fig. 83).

2959 **Comments.** Due to intermediate morphologies, this character is treated as ordered.

2960 C154: Anterior cervical vertebrae, total height/centrum length ratio: < 0.9 (0); 0.9-1.2 (1); >

2961 1.2 (usually around 1.5) (1) (Whitlock, 2011a; modified; Tab. S20).

2962 **Comments.** Total height is herein measured between the ventral-most expansion of the

2963 centrum (usually the parapophysis or posterior cotyle). A third state was added in order to

2964 distinguish apatosaurs from *Diplodocus*. Given the high amount of changes in ratios during

2965 evolution, as indicated by the analysis, the character is left unordered.

2966 C155: Cervical vertebrae 2 and 3, centrum length: moderate length increase, CV3 < 1.3 x CV

2967 2 (0); length increases considerably CV 3 at least 1.3 x CV 2 (1) (Russell and Zheng, 1993;

2968 Tab. S21).

2969 **Comments.** Even though this does not seem to follow higher-level taxonomy, there are two

2970 groups with ratios well separated from each other (Tab. S21). The state boundaries are

2971 therefore set in order to distinguish between these two groups.

2972 C156: Anterior cervical vertebrae, posterior edge of anterior condyle: anteriorly inclined (0);

2973 posteriorly inclined (1) (New; Fig. 84).

2974 **Comments.** This character is strictly applicable to anterior cervical vertebrae. In SMA 0011,

2975 which has apomorphic anterior vertebrae, CV 6 and more posterior elements show the usual

2976 anteriorly inclined edge.

2977 C157: Anterior cervical centra, pleurocoels: single (0); subdivided (1) (New; Fig. 84).

2978 **Comments.** The subdivision of the pleurocentral cavity is sometimes regarded as

2979 ontogenetically controlled (Carballido and Sander, 2013; Schwarz et al., 2007b). However,

2980 given that the completely mature anterior cervical vertebrae (sensu Carballido and Sander,

2981 2013) of the *Kaatedocus siberi* holotype SMA 0004 have undivided pleurocoels, in contrast to

2982 the still immature vertebrae of other specimens like SMA 0011 (see above), at least some

2983 taxonomic differences ~~appear to be present~~are likely.

2984 C158: Anterior cervical vertebrae, pleurocoel extending onto dorsal surface of parapophysis:

2985 absent (0); present (1) (Upchurch, 1998; modified by Whitlock, 2011a; polarity reversed; Fig.

2986 84).

2987 **Comments.** Upchurch (1998) distinguished between continuous extensions or fossae that are

2988 separated from the main anterior pneumatic fossa or pleurocoel by a transverse ridge. The

2989 latter distinction was abandoned by Whitlock (2011a), who instead divided the character into

2990 the different regions (anterior and mid- and posterior cervical vertebrae, see below). Character

2991 polarity was herein reversed ~~as~~because basal outgroups used in the present analysis do have

2992 expanded pleurocoels.

2993 C159: Anterior cervical vertebrae, longitudinal ridge on ventral surface: present (0); absent

2994 (1) (Upchurch, 1998; modified).

2995 **Comments.** The ventral ridge (if present) can have various morphologies in diplodocid

2996 specimens, which is accounted for in other characters of this analysis. In addition to the

2997 original version of Upchurch (1998; character 132 herein), a strict presence-absence character

2998 was included for both anterior and mid- and posterior cervical vertebrae in the present

2999 analysis. The subdivision is necessary as in some specimens, where ~~the presence of~~ a ventral

3000 keel is restricted to anterior elements only (*Suuwassea* ANS 21122, *Eobrontosaurus* Tate-001,

3001 *Galeamopus* ███████ SMA 0011). This indicates that incomplete necks without ventral

3002 keels on posterior cervical vertebrae might still bear midline ridges anteriorly. For the various

3003 developments of the keels see figure 73, which shows mid- and posterior cervical vertebrae,

3004 but the morphology is the same in anterior elements.

3005 C160: Anterior cervical vertebrae, paired pneumatic fossae on ventral surface: absent (0);

3006 present (1) (Whitlock, 2011a).

3007 **Comments.** Like the ventral keel, ~~also~~ the paired pneumatic foramina are sometimes

3008 restricted to the anterior cervical vertebrae (e.g. in SMA 0011, see above). Whereas the

3009 presence of paired pneumatic foramina imply the presence of a ventral keel as well, this does

3010 not apply the other way around, as shown by the anterior cervical vertebrae of *Kaatedocus*

3011 SMA 0004 (Tschopp and Mateus, 2013b). The characters are therefore retained as

3012 independent. The morphology of the foramina is equal in anterior and mid- and posterior

3013 cervical vertebrae, where present (see Fig. 73).

3014 C161: Anterior cervical vertebrae, prespinal lamina: absent (0); present (1) (Carballido et al.,

3015 2012b; Figs 78, 84).

3016 **Comments.** In some diplodocid specimens, it appears that the prespinal lamina in undivided

3017 vertebrae gives rise to the median tubercle in divided, more posterior elements. However,

3018 given the presence of a prespinal lamina in *Camarasaurus* (Madsen et al., 1995), which does

3019 not have a median tubercle between bifurcated neural spines, these two characters should be

3020 treated as independent.

3021 C162: Anterior and mid-cervical centra, pleurocoel pierced by one or two large, rounded

3022 foramina around centrum midlength: absent (0); present (1) (New; Fig. 85).

3023 **Comments.** Such a foramen is ~~not present~~absent in the anterior-most elements, but very

3024 distinct in CV 5 or 6 of SMA 0011, whereas it disappears again by CV 8 or 9. In SMA 0011,

3025 these foramina are situated at the anterior end of the posterior pneumatic fossa. Taxa where

3026 CV 5 to 7 or 8 are not preserved, and other elements do not show such a development, are

3027 scored as unknown. Similarly distinct, rounded foramina are only present in *Supersaurus*

3028 (Lovelace et al., 2007), and *Australodocus* (Remes, 2007; Whitlock, 2011c).

3029 C163: Anterior and mid-cervical vertebrae, spinoprezygapophyseal lamina: continuous as a

3030 lamina (0); reduced to ridge or totally interrupted in the middle (at base of prezygapophysis)

3031 (1) (Tschopp and Mateus, 2013b; Fig. 86).

3032 C164: Anterior and mid-cervical neural spines height: high (project well above the level of

3033 postzygapophyses) (0); low (terminates level with postzygapophyses) (1) (Upchurch et al.,

3034 2004b; modified; Fig. 76).

3035 **Comments.** This character is similar to character 168. It was added because it includes

3036 anterior cervical vertebrae, which are different in height among diplodocids and within

3037 Diplodocinae, and because it would have differing state boundaries, if it would be treated

3038 numerically.

3039 C165: Anterior and mid-cervical neural spines, dorsoventrally elongate coel on lateral

3040 surface: absent (0); present (1) (Mannion et al., 2012; modified; Fig. 85).

3041 **Comments.** The presence of a dorsoventrally elongate fossa in the spinodiapophyseal fossa is

3042 usually used as derived character for posterior cervical vertebrae only (Mannion et al., 2012).

3043 However, there are differences in anterior and mid-cervical neural arches as well, which

3044   appear to be phylogenetically significant.

3045   C166: Mid-cervical centra, anteroposterior length/height of posterior face: 2.5-3.2 (0); 3.3-4.4

3046   (1); 4.5+ (2) (Upchurch, 1995; modified; Tab. S22).

3047   **Comments.** Elongation index as used herein is measured following the protocol of Wilson

3048   and Sereno (1998: total centrum length/height posterior cotyle). The mean elongation index is

3049   used for this metric. *Tornieria* specimen k is scored '2' ~~as~~because the centrum length to width

3050   ratio is very high (5.4; Remes, 2006), and thus a high EI as used herein can be expected with

3051   confidence.

3052   C167: Mid-cervical pre-epipophyses anterior extreme: about the same as prezygapophyseal

3053   facet (0); projects considerably anterior to articular facet, forming a distinct spur (1) (Sereno

3054   et al., 1999; Fig. 86).

3055   **Comments.** A distinct anterior extension of the pre-epipophysis was used as an

3056   autapomorphy for *Australodocus bohetii* within Diplodocidae (Remes, 2007). However, it has

3057   been shown to be present in *Kaatedocus*, as well~~, as also~~ as in some non-diplodocid sauropods

3058   (Sereno et al., 1999; Ksepka and Norell, 2006; Tschopp and Mateus, 2013b). Taxa without

3059   pre-epipophyses are scored as unknown.

3060   C168: Mid-cervical neural spine height: considerably shorter than height of neural arch, <0.45

3061   (0); subequal to height of neural arch, 0.45-1.6 (1); considerably higher than neural arch, >1.6

3062   (2) (Rauhut et al., 2005; modified; Tab. S23).

3063   **Comments.** Neural arch height is measured in a vertical line from the centrum to the dorsal

3064   edge of the postzygapophyses, and neural spine height from dorsal edge of the

3065   postzygapophyses to the spine summit. The centrum is oriented such that the ventral floor of

3066   the neural canal is horizontal. The majority of the ratios were measured from photos or figures

3067   in lateral view. As exemplified by CV 6 of *Suuwassea* ANS 21122, this approach can yield

3068   major differences depending on slight changes in perspective (or left and right lateral views;

3069   CV 6 of ANS 21122 has ratios ranging from 0.91-1.27; Tab. S23). Although such differences

3070   are partly avoided by using mean ratios, it would be unwise to use closely spaced numerical

3071   state boundaries in this case. Therefore, only two steps were regarded as sufficiently objective

3072   and phylogenetically significant~~, and objective enough~~. The character was left unordered due

3073   to diverging evolutionary trends.

3074   C169: Mid-cervical neural spines, orientation: vertical (0); anteriorly inclined (1) (Rauhut et

3075   al., 2005; Fig. 87).

3076 **Comments.** The neural spine is interpreted to be anteriorly inclined, when the anterior end of

3077 the summit reaches further anterior than the posterior-most point of the sprl.

3078 C170: Mid-cervical vertebrae, angle between postzygodiapophyseal and

3079 spinopostzygapophyseal laminae: acute (0); right angle (1) (Rauhut et al., 2005; Fig. 85).

3080 **Comments.** Angles are measured between lines connecting the posterior-most point of podl

3081 and spol (often the epipophyses) with their opposing ends.

3082 C171: Mid- and posterior cervical centra, pleurocoels: single without division (0) divided by a

3083 bone septum, resulting in an anterior and a posterior lateral excavation (1); divided in three or

3084 more lateral excavations, resulting in a complex morphology (2) (Carballido et al., 2012b;

3085 modified; Fig. 71).

3086 **Comments.** The original character (Carballido et al., 2012b) includes a fourth character state,

3087 which describes the shallow posterior pneumatic fossa. As such, it overlaps with character

3088 172, introduced by Whitlock (2011a). Furthermore, subdivision of the pleurocoel is not

3089 correlated with the depth of the single pneumatic fossae in diplodocids. Therefore, the fourth

3090 state was omitted here.

3091 C172: Mid- and posterior cervical vertebrae, pneumatization of lateral surface of centra: large,

3092 divided pleurocoel over approximately half of centrum (0); reduced, large fossa but sharp-

3093 bordered coel, if present, restricted to area above parapophysis (1) (Whitlock, 2011a; Fig. 75).

3094 **Comments.** Taxa with single pleurocoels are scored as unknown.

3095 C173: Mid- and posterior cervical vertebrae, pleurocoel extending onto dorsal surface of

3096 parapophysis: present (0); absent (1) (Upchurch, 1998; modified by Mannion et al., 2012;

3097 based on Whitlock, 2011a; Fig. 71).

3098 C174: Mid- and posterior cervical vertebrae, longitudinal ridge on ventral surface: present (0);

3099 absent (1) (New).

3100 C175: Mid- and posterior cervical vertebrae, ventral keel: single (0); bifid, connects

3101 posterolaterally to the ventrolateral edges of the centrum (1) (New; Fig. 73).

3102 **Comments.** Taxa without ventral keels are scored as unknown.

3103 C176: Mid- and posterior cervical vertebrae, paired pneumatic fossae on ventral surface,

3104 separated by ventral midline keel: absent (0); present (1) (New; Figs 73, 88).

3105 **Comments.** Usually, these fossae are situated anteriorly between the parapophyses, separated

3106 by a ventral keel. Some apatosaur specimens (e.g. YPM 1861, ET, pers. obs., 2011) show

3107 paired pneumatic fossae located posterior to the parapophyses, facing ventrolaterally, and not

3108   separated by a keel. This morphology is considered different, and accounted for in character

3109   177.

3110   C177: Mid- and posterior cervical vertebrae, lateral edge posterior to parapophysis:

3111   continuous (0); marked by a deep groove extending anteroposteriorly along the edge (1)

3112   (New; Fig. 88).

3113   **Comments.** Such a groove was proposed as autapomorphic for *Dinheirosaurus* (Mannion et

3114   al., 2012). However, ~~it~~a groove ~~is also present~~also occurs in *Supersaurus vivianae* WDC

3115   DMJ-021, *Apatosaurus laticollis* YPM 1861, and *Dicraeosaurus hansemanni* MB.R.4886. As

3116   in most of these specimens, such a groove appears together with more centrally placed ventral

3117   pneumatic foramina (see character 176), so two different characters are used.

3118   C178: Mid- and posterior cervical vertebrae, rugose tuberosity on anterodorsal corner of

3119   lateral side: absent (0); present (1) (Tschopp and Mateus, 2013b; modified; Fig. 87).

3120   **Comments.** The character description was extended to mid-cervical vertebrae in order to

3121   include *Suuwassea emilieae*. In the latter, the distinct rugose tubercles appear in mid-cervical

3122   vertebrae, whereas in *Kaatedocus siberi*, mid-cervical vertebrae only have very shallow

3123   tubercles. An additional character for serial variation is avoided ~~as~~because it could only be

3124   scored for these two taxa~~,~~ and would thus not be phylogenetically significant.

3125   C179: Mid- and posterior cervical centra with longitudinal flanges in the lateroventral edge on

3126   the posterior part of the centrum: absent (0); present (1) (Tschopp and Mateus, 2013b; Fig.

3127   73).

3128   **Comments.** These flanges are mainly responsible for the posterior portion of the ventral

3129   sulcus typical for diplodocines. However, ~~also~~ some apatosaur specimens also have weak

3130   flanges, but no continuous ventral sulcus marking the ventral surface ☰

3131   C180: Mid- and posterior cervical prezygapophyses, articular surfaces flat (0); articular

3132   surfaces strongly convex transversely (1) (Upchurch, 1995, 1998; Fig. 89).

3133   C181: Mid- and posterior cervical vertebrae, pre-epipophysis: absent (0); present (1) (Remes,

3134   2007; Figs 75, 86).

3135   **Comments.** The pre-epipophysis is herein defined as a rugose, horizontal ridge laterally

3136   below the prezygapophyseal facet, which connects with the prdl anteriorly.

3137   C182: Mid- and posterior cervical vertebrae, spinoprezygapophyseal lamina, anterior end:

3138   remains vertical, with the free edge facing dorsally (0); is strongly inclined laterally

3139   (sometimes roofing a lateral fossa in the prezygapophyseal process (1) (Tschopp and Mateus,

3140 2013b; modified; Fig. 90).

3141 **Comments.** At a first glance, it appears possible that this character is correlated with the

3142 occurrence of transversely convex prezygapophyseal facets. However, this is not the case, as

3143 can be seen in the several varying scores for these two characters.

3144 C183: Mid- and posterior cervical neural arches, lateral fossae on the prezygapophysis

3145 process: absent (0); present (1) (Harris, 2006b; Tschopp and Mateus, 2013b; Figs 86, 90).

3146 **Comments.** Where such a lateral fossa is present, it is dorsally roofed by a laterally tilted

3147 anterior end of the sprl. However, not all specimens with a laterally tilted lamina also bear

3148 these fossae, which justifies the use of two independent characters. The character was first

3149 used in a phylogenetic analysis by Tschopp and Mateus (2013b).

3150 C184: Mid- and posterior cervical vertebrae, prezygapophyseal centrodiapophyseal fossa:

3151 single cavity (0); subdivided into two cavities by a ridge (1); several accessory laminae

3152 subdivide the fossa into various smaller partitions (2) (Gilmore, 1936; Upchurch et al., 2004b;

3153 modified; Figs 73, 75).

3154 **Comments.** A third state was added in order to be able to accurately code the holotype

3155 specimen of *Barosaurus lentus* (YPM 429), as well as a few other specimens. The character is

3156 treated as ordered, ~~as~~because an increase in lamination is thought to happen step-wise. Two

3157 specimens coded as '0' actually only preserve mid-cervical vertebrae (AMNH 7535, CM 3452,

3158 ET, pers. obs., 2011). It would thus be possible that more posterior elements of these cervical

3159 columns had subdivided prcdf.

3160 C185: Mid- and posterior cervical neural arches, centroprezygapophyseal lamina: single (0);

3161 dorsally divided, resulting in a lateral and medial lamina, the medial lamina being linked with

3162 the interprezygapophyseal lamina and not with the prezygapophysis (1); divided, resulting in

3163 the presence of a "true" divided centroprezygapophyseal lamina, which is dorsally connected

3164 to the prezygapophysis (2) (Upchurch, 1995; modified by Carballido et al., 2012b; Fig. 89).

3165 **Comments.** Usually, taxa with "true" divided cprl also have a lamina connecting from the

3166 base of the cprl to the tprl.

3167 C186: Mid- and posterior cervical transverse processes: posterior centrodiapophyseal lamina

3168 (pcdl) and postzygodiapophyseal laminae (podl) meet at base of transverse process (0); pcdl

3169 and podl do not meet anteriorly, postzygapophyseal centrodiapophyseal fossa extends onto

3170 posterior face of transverse process (1) (New; Fig. 91).

3171 C187: Mid- and posterior cervical vertebrae, accessory horizontal lamina in center of

3172 spinodiapophyseal fossa, not connected with any surrounding laminae: absent (0); present (1)

3173 (New; Fig. 92).

3174 **Comments.** This accessory lamina could be a vestigial version of the epipophyseal-

3175 prezygapophyseal lamina (sensu Wilson, 2012) or the accessory lamina connecting the podl

3176 with the sprl (as used herein, following Carballido et al., 2012b). However, ~~as~~because no

3177 connection exists ~~to~~with any surrounding lamina, this cannot be definitely confirmed in the

3178 cases included here. The use of an independent character is thus preferred. The lamina is

3179 generally situated in the center of the sdf.

3180 C188: Mid- and posterior cervical vertebrae, posterior centrodiapophyseal lamina: is single

3181 (0); bifurcates towards its anterior end (1) (Upchurch et al., 2004b; wording modified; Fig.

3182 92).

3183 **Comments.** Evidence from SMA 0011 shows that the presence of anteriorly bifurcated pcdl

3184 sometimes are a precursor of entirely double pcdl (see above). However, ~~as~~because in various

3185 specimens only bifurcated~~,~~ and no~~t~~ entirely double pcdl exist ▤ ᵉ character was retained as

3186 independent from the one describing the single or double pcdl (see character 136).

3187 C189: Mid- and posterior cervical vertebrae, centropostzygapophyseal lamina (cpol): single

3188 (0); divided, with the medial part contacting the interpostzygapophyseal lamina (1)

3189 (Carballido et al., 2012b; Fig. 91).

3190 C190: Mid- and posterior cervical neural arches, interpostzygapophyseal lamina projects

3191 beyond the posterior margin of the neural arch (including the centropostzygapophyseal

3192 lamina), forming a prominent subrectangular projection in lateral view: absent (0); present (1)

3193 (D'Emic, 2012; modified by Mannion et al., 2013; Fig. 75).

3194 **Comments.** A reduced subrectangular projection is present in mid-cervical vertebrae of

3195 *Supersaurus* WDC DMJ-021. Generally, the development of this feature increases in more

3196 posterior elements (e.g. in *Diplodocus carnegii* CM 84; Hatcher, 1901). *Supersaurus* WDC

3197 DMJ-021 was thus scored as apomorphic, although it is not prominent in the preserved

3198 vertebrae. On the other hand, *Apatosaurus louisae* CM 3018, where only CV 13-15 bear weak

3199 projections, was coded as plesiomorphic.

3200 C191: Mid- and posterior cervical vertebrae, postzygapophyseal centrodiapophyseal fossa and

3201 spinopostzygapophyseal fossa: entirely separated (0); connected by a large foramen (1) (New;

3202 Fig. 71).

3203 **Comments.** The laminae in this area are very thin and might ~~brake~~break easily. In fact, many

3204 specimens do show an opening here, but most of them also show broken margins around this

3205 opening, making it impossible to decide if the feature is genuine or not. Often, possible

3206 foramina are also closed with plaster or similar material during preparation, probably ~~due~~

3207 ~~to~~for stability reasons, and because the presence of such foramina has never been reported

3208 before. In fact, only SMA 0011 can be confidently scored as apomorphic to date.

3209 C192: Posterior cervical vertebrae, Elongation Index (cervical centrum length, excluding

3210 condyle, divided by posterior centrum height): less than 2.0 (0); 2.0 - 2.6 (1); higher than 2.6

3211 (2) (Gauthier, 1986; Mannion et al., 2012; modified; Tab. S24).

3212 **Comments.** In vertebrae with inclined posterior edges of the anterior condyle, a vertical line

3213 is drawn through the posterior-most point of the posterior edge, and the horizontal distance

3214 from this vertical line to a second vertical line through the posterior-most extension of the

3215 centrum is measured and taken as centrum length in this case. In some cases, only

3216 measurements of the complete centrum length were available, and the EI for the centrum

3217 length without anterior ball was calculated based on the mean difference between EI with and

3218 without condyle. Singular ratios given in table S24 have to be taken with care, as they differ

3219 considerably within posterior cervical centra (decreasing towards posterior). Ratios

3220 ~~basing~~based only on anterior posterior cervical vertebrae ~~have thus~~thus have to be corrected to

3221 a lower ratio (e.g. in UW 15556, Tab. S24).

3222 C193: Posterior cervical vertebrae, ventral keel: anteriorly placed (0); restricted to posterior

3223 portion of centrum (1) (New; Fig. 88).

3224 **Comments.** Taxa without ventral ridges are scored as unknown.

3225 C194: Posterior cervical prezygapophyses: terminate with or in front of articular ball of

3226 centrum (0); terminate well behind articular ball (1) (Upchurch et al., 2004b; modified; Fig.

3227 75).

3228 **Comments.** The neural canal should be held horizontally, in order to accurately assess the

3229 expansion of the prezygapophysis.

3230 C195: Posterior cervical vertebrae, prezygapophysis articular facet posterior margin:

3231 confluent with prezygapophyseal process (0); bordered posteriorly by conspicuous transverse

3232 sulcus (1) (Tschopp and Mateus, 2013b; Figs 74, 90).

3233 **Comments.** The distribution of this character is dubious, ~~as~~because it is difficult to observe in

3234 photos and drawings. To date, only the holotype specimen of *Kaatedocus siberi* (SMA 0004)

3235 was reported to bear such a sulcus. The character in its present state thus does not contribute

3236 to the resolution of the tree. It was retained because more work on actual specimens has to be

3237 performed in order to confirm or discard this character as an unambiguous autapomorphy of

3238 *K. siberi*.

3239 C196: Posterior cervical vertebrae, spinoprezygapophyseal lamina: continuous (0);

3240 developing an anterior projection (just beneath but independent from the spine summit) (1)

3241 (Tschopp and Mateus, 2013b; Fig. 74).

3242 **Comments.** Sometimes the spine summit projects anteriorly which is not what this character

3243 describes. Diplodocines often have an anterior projection below the summit, which forms the

3244 most anterior point of the spine.

3245 C197: Posterior cervical vertebrae, accessory lateral lamina connecting postzygodiapophyseal

3246 and spinoprezygapophyseal laminae: absent (0); present (1) (Gallina and Apesteguía, 2005;

3247 Fig. 71).

3248 **Comments.** This lamina was termed epipophyseal-prezygapophyseal lamina by Wilson and

3249 Upchurch (2009), but there are different ways of how to unite the epipophysis with the

3250 prezygapophysis (Carballido et al., 2012b; Wilson, 2012). Therefore, the description of

3251 Carballido et al. (2012b) was preferred herein.

3252 C198: Posterior cervical vertebrae, accessory, subvertical lamina in the postzygapophyseal

3253 centrodiapophyseal fossa, with free edge facing laterally: absent (0); present (1) (New; Fig.

3254 91).

3255 **Comments.** T~~here are t~~wo types of accessory laminae are present in the pocdf of certain

3256 sauropod taxa: 1) laterally facing, relatively broad laminae, which are mostly located

3257 posteriorly, marking the lateral wall of the neural canal, and 2) more distinct, posteriorly

3258 facing laminae connecting the pcdl and podl anteriorly, at the base of the transverse process.

3259 The present character describes the presence of the first type, and the second type is

3260 accounted for in ~~the~~ character 199.

3261 C199: Posterior cervical vertebrae, accessory, subvertical lamina in the postzygapophyseal

3262 centrodiapophyseal fossa, with free edge facing posteriorly: absent (0); present (1) (Gilmore,

3263 1936; Upchurch et al., 2004b; modified; Fig. 71).

3264 **Comments.** Rarely, these accessory laminae ~~can~~ appear as a parallel pair as in SMA 0011

3265 (Fig. 71). *Jobaria* has posteriorly facing laminae in the posterior portion of the pocdf,

3266 connecting to the postzygapophyses. They are herein interpreted as lateral cpol, which are

3267 somewhat anteriorly shifted. *Jobaria* is thus scored as plesiomorphic in this character.

3268 C200: Posterior cervical postzygapophyses: terminate at or beyond posterior edge of centrum

3269 (0); terminate in front of posterior edge (1) (Upchurch et al., 2004b; modified by Tschopp and

3270 Mateus, 2013b; Fig. 92).

3271 C201: Posterior cervical neural arch, interpostzygapophyseal lamina (tpol): connects directly

3272 with roof of neural canal (0); vertical lamina connects tpol with neural canal roof (1) (New;

3273 Fig. 91).

3274 **Comments.** Carballido and Sander (2013) termed this vertical lamina 'single

3275 intrapostzygapophyseal lamina' (stpol).

3276 C202: Posterior cervical neural arches, epipophyses: transversely compressed (0);

3277 dorsoventrally compressed (1) (New; Fig. 77).

3278 **Comments.** Two different morphologies of the epipophyses ~~are present~~occur in diplodocids:

3279 1) dorsoventrally compressed, usually forming a horizontal, rugose ridge above the

3280 postzygapophyseal facet, on the lateral side of the spol, and 2) transversely compressed, such

3281 that it is formed by a dorsal expansion of the posterior end of the spol, in some cases (e.g.

3282 *Diplodocus carnegii* CM 84) forming a rugose, vertical plate above the zygapophyseal facet,

3283 but never accompanied by a horizontal ridge. Taxa without epipophyses are scored as

3284 unknown.

3285 C203: Posterior cervical neural arches, accessory spinal lamina: absent (0); present, running

3286 vertically just posterior to spinoprezygapophyseal lamina (1) (Whitlock, 2011a; Fig. 75).

3287 **Comments.** This lamina could represent a reduced spdl. The presence of a distinct lamina is

3288 restricted to advanced diplodocines, but a reduced lamina is present in *Spinophorosaurus* as

3289 well (NMB-1699-R, ET, pers. obs., 2011).

3290 C204: Posterior cervical neural spines, dorsoventrally elongate coel on lateral surface: absent

3291 (0); present (1) (Mannion et al., 2012; Fig. 88).

3292 C205: Posterior cervical neural spine, horizontal, rugose ridge right below spine summit on

3293 lateral surface: absent (0); present, serves as distinct dorsal edge of the spinodiapophyseal

3294 fossa (1) (Tschopp and Mateus, 2013b; Fig. 77).

3295 **Comments.** The ridge ~~can be~~are slightly curved in some taxa ☰ hen absent (plesiomorphic

3296 state), the sdf fades dorsally.

3297 C206: Posterior bifid, cervical neural spines, medial surface: marked by distinct, dorsoventral

3298 ridge from base to spine summit (0); smooth (1) (New; Fig. 93).

3299 C207: Posterior cervical neural and/or anterior-most dorsal neural spines: vertical (0);

3300   anteriorly inclined (1) (Rauhut et al., 2005).

3301   **Comments.** See comments in character 169 for definition of inclined.

3302   C208: Posterior cervical and anterior dorsal vertebrae, roughened lateral aspect of

3303   prezygodiapophyseal lamina: absent (0); present (1) (Whitlock, 2011a; Fig. 94).

3304   **Comments.** The rugose area in the derived taxa lies ventrolateral to the pre-epipophysis,

3305   ~~where~~when present.

3306   C209: Posterior cervical and anterior dorsal vertebrae, prespinal lamina: absent (0), present

3307   (1) (Salgado et al., 1997; Fig. 95).

3308   **Comments.** The presence of a prespinal lamina does not imply the presence of a median

3309   tubercle or vice versa. However, a dorsally expanded prespinal lamina can form a median

3310   tubercle (see below). In anterior dorsal vertebrae of *Diplodocus carnegii* CM 94, the median

3311   tubercle leans anteriorly, but no lamina connects~~is present connecting~~ it with the base of the

3312   notch between the metapophyses (ET, pers. obs., 2011).

3313   C210: Posterior cervical and anterior dorsal bifid neural spines, median tubercle: absent (0);

3314   present (1) (McIntosh, 1990b; Upchurch, 1995; Fig. 74).

3315   **Comments.** The median tubercle can be either an independent structure in the trough between

3316   the metapophyses, or a dorsal projection of the prespinal lamina.

3317   C211: Posterior cervical and anterior dorsal bifid neural spines, orientation: diverging (0);

3318   parallel to converging (1) (Rauhut et al., 2005; modified; Fig. 95).

3319   **Comments.** Some taxa have diverging neural spines, with only their summits approaching an

3320   almost parallel orientation (e.g. CM 11984 or USNM 10865). They are scored as

3321   plesiomorphic herein. The character was initially proposed including the rate of divergence

3322   (Rauhut et al., 2005). The character was divided ~~as~~because orientation and distance between

3323   the metapophyses are not regarded to be dependent characters.

3324   C212: Posterior cervical and anterior dorsal bifid neural spines, divergence: wide (0); narrow,

3325   distance between spine summits subequal to neural canal width (1) (Rauhut et al., 2005;

3326   modified; Fig. 95).

3327   **Comments.** This is the second part of the character proposed by (Rauhut et al., 2005; see

3328   character 211).

3329   C213: Posterior cervical, and anterior and mid-dorsal vertebrae, anterior projection of

3330   diapophysis right lateral to prezygapophysis: absent (0); present (1) (New; Fig. 93).

3331   **Comments.** The projection described herein is not to be confused with the projection

3332 sometimes formed by the pre-epipophysis, which is posteriorly accompanied by a horizontal,

3333 rugose ridge.

3334 C214: Cervical ribs, length: long, reaching posterior to posterior end of centrum (0); short, not

3335 reaching posterior end of centrum (1) (Russell and Zheng, 1993; modified; Fig. 86).

3336 **Comments.** An additive binary version describing cervical rib length is preferred herein over

3337 the multistate character of Whitlock (2011a).

3338 C215: Cervical ribs, length: overlapping several centra posterior (0); overlapping no more

3339 than the next cervical vertebra in sequence (1) (Russell and Zheng, 1993; modified; Fig. 76).

3340 C216: Cervical ribs, position relative to centrum: not projecting far beneath centrum (0);

3341 projecting well beneath centrum, such that length of posterior process is subequal in length to

3342 fused diapophysis/tuberculum (1) (Wilson, 2002; Whitlock, 2011a; modified; Fig. 75).

3343 **Comments.** Whitlock (2011a) included two characters describing the length of the ventral

3344 projection (from Wilson, 2002) and comparing the length of the posterior process with the

3345 length of the fused diapophysis/tuberculum. However, the length of the fused diapophysis and

3346 tuberculum depends on how far the cervical ribs project ventrally, and the length of the

3347 posterior process is accounted for in the characters defining cervical rib length. Wilson (2002)

3348 defined the ventral projection as strong when it leads to a vertebral height that exceeds its

3349 length. Such a ratio is also present in dicraeosaurids, but because of their highly elevated

3350 neural spines. The ventral projection of the cervical rib of dicraeosaurids is minimal as in all

3351 taxa other than apatosaurs. Therefore, the two characters of Wilson (2002) and Whitlock

3352 (2011a) are herein combined, in order to define ventral projection compared to the length of

3353 the posterior process of the cervical rib.

3354 C217: Cervical ribs, posteriorly projecting spur on dorsolateral edge of posterior shaft: absent

3355 (0); present (1) (New; Fig. 84).

3356 **Comments.** The spur was proposed as autapomorphic for *Turiasaurus* (Royo-Torres et al.,

3357 2006), but it is also present in some apatosaurs and *Dicraeosaurus* (ET, pers. obs., 2011,

3358 2012).

3359 C218: Anterior and mid-cervical ribs, tuberculum in lateral view: is directed nearly vertically

3360 (0); is directed upwards and backwards (1) (Upchurch et al., 2004b; modified; Fig. 85).

3361 **Comments.** The orientation of the tuberculum tends to become more vertical in more

3362 posterior elements. Some apatosaurs scored as plesiomorphic here actually do not have any

3363 anterior cervical vertebrae preserved, which means that they could still have inclined

tubercula in the anterior elements. However, ~~as~~because others have distinctly inclined tubercula in mid-cervical ribs as well, a differential coding is still justifiable. Taxa that do not preserve cervical ribs were coded based on the relative positions of diapophysis and parapophysis.

C219: Posterior cervical ribs, anterior process: present (0); absent (1) (Upchurch et al., 2004b; modified; Fig. 75).

C220: Posterior cervical ribs, anterior process: distinct, much longer anteroposteriorly than high dorsoventrally (0); reduced to a short bump-like process or absent (1) (New; Fig. 96).

Comments. The last two characters serve as additive binary characters describing the reduction of the anterior process in apatosaurs in general and its complete absence in some apatosaur specimens (e.g. CM 3018; Gilmore, 1936; Wedel and Sanders, 2002).

C221: Posterior cervical ribs, anterior process: ~~is~~ rounded in lateral view (0); has an acute pointed tip in lateral view (1) (Upchurch et al., 2004b; modified; Fig. 96).

Comments. The anterior processes of cervical ribs can be rounded in dorsal view, but dorsoventrally compressed (as in SMA 0011, see above). Therefore, they are still pointed in lateral view.

C222: Posterior cervical ribs, rounded sub-triangular process in lateral view, immediately below tuberculum: absent (0); present (1) (Wedel and Sanders, 2002; Upchurch et al., 2004b; modified; Fig. 96).

Comments. Upchurch et al. (2004b) scored the holotypic cervical vertebra of *Apatosaurus laticollis* YPM 1861 as plesiomorphic. However, as Wedel and Sanders (2002) showed, a process is clearly present in this specimen.

C223: Posterior cervical rib shafts: nearly straight and directed backward and a little upwards (0); initially directed in same direction but turn to run a little downwards toward distal tip (1) (Upchurch et al., 2004b; Fig. 96).

Dorsal vertebrae

C224: Number of dorsal vertebrae: 13 or more (0); 12 (1); 10 (2); 9 (3) (McIntosh, 1990b; Russell and Zheng, 1993; modified; Tab. S25).

Comments. *Amargasaurus* was initially described to have 9 dorsal vertebrae (Salgado and Bonaparte, 1991), but the putative first dorsal has the parapophysis positioned dorsally to the pleurocoel, which is highly unusual in sauropods (Carballido et al., 2012a). Generally, this position marks the second or third dorsal vertebrae, which means that there would be at least

3396 ten dorsal elements, which was the coding used by Mannion et al. (2012). Herein, a coding as

3397 unknown is preferred, following Carballido et al. (2012b).

3398 C225: Dorsal centrum length (excluding articular 'ball'), remains approximately the same

3399 along the sequence (0); shortens from anterior to posterior dorsal vertebrae (1) (Mannion et

3400 al., 2012; Tab. S26).

3401 **Comments.** The exclusion of the articular ball for measuring centrum length for this character

3402 is crucial, ~~as~~because anterior dorsal vertebrae often have considerably larger anterior condyles

3403 than posterior elements. In taxa lacking measurements or good figures to compare between

3404 anterior and posterior elements, scores of Mannion et al. (2012) were used (e.g. *Omeisaurus*).

3405 C226: Dorsal vertebrae, opisthocoely (including a prominent anterior articular 'ball')

3406 disappears: between D2 and D3 (0); between D3 and D4 or more posteriorly (1) (Holland,

3407 1915a; Gilmore, 1936; Upchurch et al., 2004b; Tab. S27).

3408 **Comments.** The definition of 'prominent anterior ball' is somewhat ambiguous. However, a

3409 new definition is not given here, ~~as~~because the character is interpreted to describe a

3410 significant change within the same vertebral column. These changes can be of different

3411 absolute size if one compares between specimens, but are relatively obvious within the same

3412 individual. The decrease is thus relative to its development in more anterior elements, but can

3413 be low in an absolute sense.

3414 C227: Dorsal pneumatopores (pleurocoels): present (0); absent (1) (Gauthier, 1986; McIntosh,

3415 1990b; Upchurch, 1995; polarity reversed; Fig. 97).

3416 **Comments.** The dorsal centra of all included sauropod taxa have pleurocoel-like depressions

3417 on their lateral side, but in some taxa they do not bear a foramen.

3418 C228: Dorsal centra, pneumatic structures: absent, dorsal centra with solid internal structure

3419 (0); present, dorsal centra with simple and big air spaces (1); present, dorsal centra with small

3420 and complex air spaces (2) (Carballido et al., 2011; modified by Carballido et al., 2012b; Fig.

3421 72).

3422 C229: Dorsal neural arches, paired, subdivided pneumatic chambers dorsolateral to neural

3423 canal: absent (0), present (1) (Sereno et al., 1999; Whitlock, 2011a; Fig. 98).

3424 **Comments.** Paired pneumatic foramina are present in some diplodocids (e.g. UW 15556,

3425 YPM 1840), but they are not subdivided and are far less deep than in *Nigersaurus* or

3426 *Demandasaurus*. The latter are thus the only taxa with the apomorphic state.

3427 C230: Dorsal transverse processes, orientation: horizontal or only slightly inclined dorsally

3428 (0); more than 30° inclined dorsally from the horizontal (1) (Yu, 1993; modified by

3429 Upchurch, 1998; Fig. 98).

3430 **Comments.** The angle of the transverse processes is easily affected by diagenetic distortion,

3431 as can be seen in dorsal vertebra 3 of *Suuwassea* ANS 21122, which most probably would

3432 actually have horizontal transverse processes.

3433 C231: Dorsal vertebrae, single (not bifid) neural spines, spinoprezygapophyseal laminae:

3434 separate along entire length (0); joined distally, forming single prespinal lamina (1)

3435 (Upchurch, 1995; modified by Whitlock, 2011a; Fig. 99).

3436 **Comments.** In some taxa (e.g. *Losillasaurus* or *Camarasaurus*), the sprl unite dorsally with

3437 the prsl, but remain separate up to that point. Here, only taxa, where the prsl is formed by the

3438 junction of the two sprl, are scored as apomorphic.

3439 C232: Dorsal vertebrae, spinodiapophyseal webbing: laminae follow curvature of neural spine

3440 and diapophysis in anterior view (0); laminae 'festooned' from spine, dorsal margin does not

3441 closely follow shape of neural spine and diapophysis (1) (Sereno et al., 2007; Fig. 100).

3442 C233: Dorsal vertebrae with single neural spines, middle single fossa projected through

3443 midline of neural spine: present (0); absent (1) (Carballido et al., 2012b; Fig. 99).

3444 **Comments.** The fossa described herein is a distinctly confined area within the sprf, restricted

3445 to the anterior edge of the neural spine process.

3446 C234: Dorsal (single) neural spines, postspinal lamina, dorsal end: flat to convex transversely

3447 (0); concave transversely (1) (New; Fig. 101).

3448 C235: Dorsal vertebrae, transition from bifid to single neural spines: gradual (0); abrupt (1)

3449 (New).

3450 **Comments.** Gradual transitions go from deeply bifid, to shallowly bifid, to notched, to

3451 unsplit, as defined by Wedel and Taylor (2013). If one of the intermediate states is lacking,

3452 the taxon is scored as derived. Obviously, only specimens with articulated dorsal vertebrae

3453 can be scored for this character. Taxa without spine bifurcation are scored as unknown.

3454 C236: Dorsal neural arches, hyposphene-hypantrum articulations: present (0); absent (1)

3455 (Gauthier, 1986; Salgado et al., 1997; Tab. S28).

3456 C237: Dorsal vertebrae, hyposphene first appears: on D3 (0); on D4 or more posteriorly (1)

3457 (Upchurch et al., 2004b; modified; Tab. S28).

3458 **Comments.** Both in *Apatosaurus* and *Camarasaurus* there are differences in the appearance

3459 of the hyposphene (Ikejiri, 2004; Upchurch et al., 2004b). ~~Since~~Because the genotype species,

3460 *C. supremus*, appears to show the plesiomorphic state, the genus was scored as such as well.

3461 Ikejiri (2004) suggests that the development of the hyposphene might depend on ontogeny,

3462 based on observations in the juvenile specimen CM 11338. However, the latter specimen is

3463 articulated, and the region with the hyposphene is obliterated, such that its presence or

3464 absence is difficult to assess (McIntosh et al., 1996a).

3465 C238: Dorsal vertebrae, single vertical lamina supporting the hyposphene from below: absent

3466 (0); present (1) (Gilmore, 1936; Upchurch et al., 2004b; modified; Fig. 98).

3467 **Comments.** The original character description (Upchurch et al., 2004b) interfered with the

3468 character proposed by Wilson (2002) distinguishing between single and double cpol in mid-

3469 and posterior dorsal vertebrae (see character 261). The character of Upchurch et al. (2004b)

3470 was thus simplified, and polarity was reversed due to the differential taxon sampling. The

3471 lamina described herein corresponds to the stpol (Carballido and Sander, 2013). Taxa without

3472 hyposphene are scored as unknown.

3473 C239: Dorsal vertebrae 1 and 2, centrum length: DV 1 > DV 2 (0); DV 2 > DV 1 (1)

3474 (Upchurch et al., 2004b; modified; Tab. S29).

3475 **Comments.** The character was originally defined implying that either DV 1 or 2 were the

3476 longest in the series (Upchurch et al., 2004b), which is not always the case (see Tab. S29).

3477 C240: First dorsal vertebrae, pleurocoel location: occupy the anterior and middle part of the

3478 centrum (0); occupy the posterior part of the centrum (1) (Holland, 1915a; Gilmore, 1936;

3479 Upchurch et al., 2004b; modified; Fig. 94).

3480 **Comments.** The character was restricted to the first dorsal, as also in *Apatosaurus louisae*, for

3481 which this character was proposed as a species autapomorphy (Holland, 1915a; Gilmore,

3482 1936; Upchurch et al., 2004b). In this taxon, DV 2 and 3 already have a centrally placed

3483 pleurocoel (CM 3018, ET, pers. obs., 2011).

3484 C241: Anterior dorsal vertebrae, pleurocoels in first few centra: become larger along the

3485 series (0); become smaller (1) (Gilmore, 1936; Upchurch et al., 2004b; wording modified;

3486 Tab. S30).

3487 **Comments.** Taxa without dorsal pleurocoels are scored as unknown.

3488 C242: Anterior dorsal vertebrae, ventral keel: absent (0); present (1) (Mannion et al., 2012;

3489 Fig. 102).

3490 C243: Anterior dorsal transverse process position: high, considerably above dorsal edge of

3491 posterior cotyle (0); low, ventral edge about level to dorsal edge of posterior cotyle (1)

(Gilmore, 1936; Fig. 103).

Comments. The differing dorsoventral extension of the transverse processes in the anterior-most dorsal vertebrae was proposed as character to distinguish *Apatosaurus louisae* CM 3018 from the supposed *Apatosaurus excelsus* UW 15556 (Gilmore, 1936). It is here applied for the first time in a phylogenetic analysis. In most taxa, position of the transverse process rises considerably dorsally in the first few dorsal vertebrae. Therefore, this description applies best for the first element in the series.

C244: Anterior, bifid dorsal vertebrae, base of notch between metapophyses: wide and rounded (0); narrow, V-shaped (1) (Gilmore, 1936; Fig. 103).

Comments. As observed in *Apatosaurus*, also *Camarasaurus* also appears to show intrageneric variation: *C. lewisi* has narrow troughs throughout its bifurcated presacral vertebrae, whereas other *Camarasaurus* species have wide bases (Jensen, 1988; McIntosh et al., 1996b). Herein, *Camarasaurus* was scored as plesiomorphic, because new evidence from material at SMA suggests that *C. lewisi*, which was initially described as a new genus (*Cathetosaurus*), was actually erroneously referred to *Camarasaurus* (Mateus and Tschopp, 2013).

C245: Anterior dorsal, bifid neural spines, medial surface: gently rounded transversely (0); subtriangular (1) (New; Fig. 95).

Comments. Some diplodocid specimens bear a dorsoventral ridge on the medial surface of the anterior dorsal neural spines, similar to the ridge present in some diplodocid posterior cervical neural spines. The ridge results in a subtriangular shape of the medial surface.

C246: Dorsal vertebra 3, parapophysis: lies at the top of the centrum (0); lies mid-way between the top of the centrum and the level of the prezygapophyses (1) (Gilmore, 1936; Upchurch et al., 2004b; modified; Fig. 97).

C247: Anterior and mid-dorsal centra, pleurocoels: situated entirely on centrum (0); invade neural arch pedicels (1) (Holland, 1915a; Fig. 104).

Comments. Holland (1915a) proposed this morphology as diagnostic for *Apatosaurus louisae*. It is included in a phylogenetic analysis for the first time. Taxa without dorsal pleurocoels are scored as unknown.

C248: Anterior and mid-dorsal neural arch, hyposphene shape: rhomboid (0); laminar (1) (New; Tab. S28).

Comments. Hyposphene shape can change considerably from front to back, as is seen in

specimens of *Camarasaurus* (Osborn and Mook, 1921; McIntosh et al., 1996b). In the present analysis, two different characters ~~are thus used to~~thus code for the anterior and mid-dorsal vertebrae, as well as for the posterior elements, which are often less developed (see character 276). See figure 98 for an example of a laminar hyposphene.

C249: Mid-dorsal neural arches, height above postzygapophyses (neural spine) to height below (pedicel): 2.1 or greater (0); < 2.1 (1) (Whitlock, 2011a; modified; Tab. S31).

Comments. Pedicel height is measured from the neural canal floor to the ventral-most point of the postzygapophyseal facets, neural spine height from there to the spine top. Both measurements are taken vertically, ignoring spine inclination. The ratio changes considerably between mid- and posterior dorsal vertebrae, therefore the original character of Whitlock (2011a) was divided in two (see character 272). Furthermore, a numerical boundary was introduced.

C250: Mid-dorsal neural spines, form: single, bifid form (if present) does not extend past second or third dorsal (0); bifid, inclusive of at least fifth dorsal vertebrae (1) (Whitlock, 2011a; Tab. S32).

Comments. Notched and unsplit neural spines (sensu Wedel and Taylor, 2013) are counted as single;~~,~~ shallowly and deeply bifurcated spines as bifid. An additional character is used to account for the notched spines. The taxon scores are thus slightly different from the ones in Whitlock (2011a).

C251: Mid-dorsal neural spines, oblique accessory lamina connecting postspinal lamina with spinopostzygapophyseal lamina: absent (0); present (1) (New; Fig. 104).

Comments. In *Supersaurus* and *Dinheirosaurus*, this accessory lamina extends posterodorsally-anteroventrally from near the dorsal end of the posl to the junction of the spol with the spdl.

C252: Mid- and posterior dorsal vertebrae, lateral pleurocoels present in centra: absent (0); present (1) (Gauthier, 1986; McIntosh, 1990b; Upchurch, 1995; modified by Whitlock, 2011a).

C253: Mid- and posterior dorsal vertebrae, vertically oriented rod-like struts divide the lateral pneumatic foramina: absent (0); present (1) (Mannion et al., 2012; Fig. 104).

Comments. Mannion et al. (2012) proposed the presence of such a strut as synapomorphy for the clade uniting *Supersaurus* and *Dinheirosaurus*. However, similar struts ~~are present~~occur as well in some apatosaurs. The pleurocoel is often not completely liberated from matrix

3556 during preparation, potentially obscuring the presence or absence of this structure.

3557 C254: Mid- and posterior dorsal vertebrae, height of neural arch below postzygapophyses

3558 (pedicel) divided by posterior cotyle height: <0.8 (0); 0.8 or greater (1) (Gallina and

3559 Apesteguía, 2005; modified; Tab. S33).

3560 **Comments.** Neural arch height is measured from the neural canal floor to where the

3561 postzygapophyseal facets meet medially, above the hyposphene, where present.

3562 C255: Mid- and posterior dorsal neural arches, prezygoparapophyseal lamina: present (0);

3563 absent (1) (Wilson, 2002; Fig. 105).

3564 C256: Mid- and posterior dorsal parapophyses, location: above centrum, posterior to anterior

3565 edge of centrum (0); straight above anterior edge of centrum, or anteriorly displaced (1)

3566 (New; Figs 104, 105).

3567 **Comments.** The anterior edge of the centrum corresponds to the rim of the anterior condyle

3568 in opisthocoelous elements. In some taxa, the position of the parapophysis changes from front

3569 to back. ,tThese taxa are scored for the majority of the elements in the series (e.g.,

3570 *Haplocanthosaurus*, where DV 10 has a posteriorly placed parapophysis, but the majority of

3571 the mid- and posterior dorsal vertebrae have anteriorly displaced parapophyses; Hatcher,

3572 1903).

3573 C257: Mid- and posterior dorsal neural arches, anterior centroparapophyseal lamina: absent

3574 (0); present (1) (Upchurch et al., 2004a; Fig. 105).

3575 C258: Mid- and posterior dorsal neural arches, posterior centroparapophyseal lamina: absent

3576 (0); present as single lamina (1); present, double (2) (Salgado et al., 1997; modified after

3577 Mannion et al., 2013; Figs 105, 106).

3578 **Comments.** In taxa, where the pcpl is double, the more dorsal branch often connects to the

3579 pcdl. Mannion et al. (2013) defined the third state as 'two parallel laminae', but in certain

3580 specimens (e.g. *Diplodocus carnegii* CM 84), the dorsal branch becomes more horizontal

3581 (Hatcher, 1901). The character is treated as ordered, as it codes for both presence/absence and

3582 morphology.

3583 C259: Mid- and posterior dorsal vertebrae, accessory laminae in region between posterior

3584 centrodiapophyseal lamina and posterior centroparapophyseal lamina: absent (0); present (1)

3585 (Mannion et al., 2012; Fig. 106).

3586 **Comments.** This character is somewhat ambiguous. Some of these accessory laminae might

3587 actually represent dorsal branches of the pcpl (see character 258) or dislocated ppdl. Here,

3588 only laminae not directly connecting to any specifying landmark (see Wilson, 1999) are

3589 considered accessory. More studies are needed to see if these are homologous to the above

3590 mentioned laminae.

3591 C260: Mid- and posterior dorsal vertebrae, accessory lamina linking hyposphene with base of

3592 posterior centrodiapophyseal lamina: absent (0); present (1) (New; Figs 104, 106).

3593 **Comments.** The presence of such an accessory lamina was proposed as autapomorphic for

3594 *Dinheirosaurus* (Mannion et al., 2012), but is herein interpreted to ~~be present~~occur in other

3595 diplodocids as well. The accessory lamina can easily be confused with the lateral branch of

3596 the cpol, but the latter connects directly with the postzygapophyseal facet~~,~~ and not with the

3597 hyposphene. The accessory lamina described herein is thus situated between the two branches

3598 of the cpol.

3599 C261: Mid- and posterior dorsal neural arches, centropostzygapophyseal lamina: single (0);

3600 divided, lateral branch connecting to posterior centrodiapophyseal lamina (1) (Wilson, 2002;

3601 wording modified; Fig. 105).

3602 **Comments.** The lateral branch is often only visible in lateral view.

3603 C262: Mid- and posterior dorsal neural arches, infradiapophyseal pneumatopore between

3604 anterior and posterior centrodiapophyseal laminae: absent (0); present (1) (Wilson, 2002; Fig.

3605 106).

3606 **Comments.** Even though the development of pneumatic structures has been shown to depend

3607 on the ontogenetic stage (Wedel, 2003; Schwarz et al., 2007c), the early juvenile brachiosaur

3608 SMA 0009 already has this pneumatopore.

3609 C263: Mid- and posterior dorsal transverse processes, length: short (0); long (projecting < 1.3

3610 times posterior cotyle width) (1) (Carballido et al., 2012b; modified; Tab. S34).

3611 **Comments.** The length of a single transverse process is compared to the maximum width of

3612 the posterior cotyle. Transverse process length is measured in a horizontal plane.

3613 Measurements taken from figures in posterior view generally underestimate the ratio, which

3614 has to be accounted for when scoring the taxa. In the case of *Brachiosaurus altithorax* FMNH

3615 P25107, true ratios based on the measurements by Riggs (1904) are about 120% of the ratios

3616 taken from published figures (Taylor, 2009), whereas in *Apatosaurus* NSMT-PV 20375 or

3617 *Diplodocus* CM 84, they are only 103% higher. This percentage depends on the relative

3618 position of the transverse processes above the centrum. Ratios generally decrease from

3619 anterior to posterior dorsal vertebrae. Taxa or specimens that preserve only posterior elements

3620 (e.g. *Amphicoelias altus* AMNH 5764) should thus have higher actual ratios than shown in

3621 Tab. S34.

3622 C264: Mid- and posterior dorsal transverse processes, dorsal edge: straight, or curving

3623 downwards at distal end (0); developing a distinct dorsal bump or spur (1) (New; Fig. 98).

3624 **Comments.** Spurs are usually situated at the distal tip, whereas bumps are located more

3625 medially.

3626 C265: Mid- and posterior dorsal neural spines, anteroposterior width: approximately constant

3627 along height of spine, with subparallel anterior and posterior margins (0); narrows dorsally to

3628 form triangular shape in lateral view, with base being approximately twice the width of dorsal

3629 tip (1) (New; Fig. 106).

3630 C266: Middle and posterior dorsal neural spines, breadth at summit: much narrower (0); equal

3631 to or broader (1) transversely than anteroposteriorly (Wilson, 2002; modified).

3632 **Comments.** Neural spine width can change considerably from the spine bottom to the top.

3633 The original character was thus divided in two (see character 265).

3634 C267: Mid- and posterior dorsal neural spines, triangular aliform processes: absent (0);

3635 present but do not project far laterally (not as far as postzygapophyses) (1); present, project at

3636 least as far laterally as postzygapophyses (2) (Carballido et al., 2012b; Figs 98, 99).

3637 **Comments.** The character is treated as ordered.

3638 C268: Posterior dorsal centra, total length/height of posterior articular surface: 1.0 or greater

3639 (0); short, < 1.0 (1) (New; Tab. S35).

3640 C269: Posterior dorsal centra: subequal width and height, or higher than wide (0); wider than

3641 high (1) (Gilmore, 1936; Tab. S35).

3642 **Comments.** Width and height are measured at the posterior cotyle. The boundary is set

3643 between 1.0 and 1.1 in the present study, because it was suggested by Gilmore (1936) to

3644 distinguish *Apatosaurus louisae* from *A. ajax* and *A. excelsus*.

3645 C270: Posterior dorsal centra, articular face shape: amphicoelous (0); slightly opisthocoelous

3646 (1); strongly opisthocoelous (2) (Yu, 1993; wording modified by Carballido et al., 2012b; Fig.

3647 105).

3648 **Comments.** Slightly opisthocoelous means that the condyle is either ventrally or dorsally

3649 restricted, but still visible in lateral view. Strongly opisthocoelous vertebrae have anterior

3650 balls that reach from the dorsal to the ventral edge of the centrum. In *Apatosaurus ajax* YPM

3651 1860, no anterior articulation surface of a posterior dorsal vertebrae is observable, but the

3652 posterior articulation surface of a posterior element has a small, but distinct fossa marking its

3653 upper half. This indicates a slightly opisthocoelous centrum in the following element.

3654 C271: Posterior dorsal vertebrae, pleurocoel shape: oval to circular (0); subtriangular with

3655 apex dorsally (1) (New; Fig. 106).

3656 **Comments.** Taxa without dorsal pleurocoels are scored as unknown.

3657 C272: Posterior dorsal neural arches, height above postzygapophyses (neural spine) to height

3658 below (pedicel): < 3.1 (0); 3.1 or greater (1) (Whitlock, 2011a; modified; Tab. S31).

3659 **Comments.** See character 249.

3660 C273: Posterior dorsal neural arches, parapophyseal centrodiapophyseal fossa: ventrally open,

3661 relatively shallow (0); deep, triangular (1) (Gallina and Apesteguía, 2005; Fig. 106).

3662 **Comments.** The apomorphic state is applied to specimens with the pcpl connecting to the

3663 pcdl or acdl, thus creating a ventrally closed, triangular fossa between them and the ppdl or

3664 prdl. In plesiomorphic taxa, the pcpl fades out posteroventrally or connects to the centrum

3665 anterior to the ventral end of the pcdl.

3666 C274: Posterior dorsal vertebrae, spinoprezygapophyseal lamina: absent or greatly reduced

3667 (0); present (1) (Upchurch et al., 2007; modified; Fig. 107).

3668 **Comments.** Reduced sprl fade out anteroventrally and/or join the prsl at a very ventral level.

3669 C275: Posterior dorsal postzygapophyses: almost horizontal, such that the two articular facets

3670 include a wide angle (0); articular facets oblique, including an almost 90° angle (1) (New;

3671 Fig. 101).

3672 **Comments.** Some diplodocine taxa have curved facets. These are interpreted as horizontal

3673 C276: Posterior dorsal vertebrae, hyposphene-hypantrum system: well developed, rhomboid

3674 shape up to last element (0); weakly developed, mainly as a laminar articulation (1)

3675 (Carballido et al., 2012b; modified; Fig. 98; Tab. S28).

3676 **Comments.** Taxa without hyposphenes are scored as unknown.

3677 C277: Posterior dorsal neural arches, spinopostzygapophyseal laminae: single (0); divided

3678 near postzygapophyses (1) (Wilson, 2002; Fig. 98).

3679 **Comments.** The spol can bifurcate in two ways in different taxa: rebbachisaurids have

3680 ventrally forked laminae, whereas in some diplodocids the spol bifurcates dorsally, creating a

3681 medial and a lateral branch. The presence of a medial spol is accounted for in character 278,

3682 the present one describes the ventral bifurcation.

3683 C278: Posterior dorsal vertebrae, medial spinopostzygapophyseal lamina: absent (0); present

3684 and forms part of median posterior lamina (1) (Carballido et al., 2012b; Fig. 101).

3685 **Comments.** The mspol can either be connected with the lspol ventrally or they can remain

3686 separated.

3687 C279: Posterior dorsal vertebrae, base of neural spines just above transverse processes: longer

3688 than wide (0); subequal in width and length (1) (New).

3689 **Comments.** This is the second character about spine width to length, inspired by a character

3690 from Wilson (2002) (see character 266).

3691 C280: Posterior dorsal neural spines, orientation at its base: vertical (0); anteriorly inclined (1)

3692 (New; Fig. 105).

3693 **Comments.** Anterior inclination can be restricted to the very base of the neural spine, as is the

3694 case in *Apatosaurus louisae* CM 3018 (Fig. 105A). The best indication for the inclination is

3695 the prsl in lateral view.

3696 C281: Posterior dorsal neural spines, midline cleft along the dorsal surface: absent (0); present

3697 (1) (Mannion et al., 2012; modified; Fig. 100; Tab. S32).

3698 **Comments.** The midline cleft described herein corresponds to the notched spines of Wedel

3699 and Taylor (2013). Not all posterior dorsal spines have to be notched in order to be scored as

3700 apomorphic.

3701 C282: Posterior dorsal and/or sacral neural spines (not including arch), height: less than 2

3702 times centrum length (0); 2 to 3 times centrum length (1); more than 3 times centrum length

3703 (2) (Mannion et al., 2012; modified; Tab. S36).

3704 **Comments.** Neural spine height is measured from the top of the postzygapophyses to the

3705 highest point of the spine, vertically. Centrum length does not include the anterior ball. The

3706 original version (Mannion et al., 2012) was restricted here to posterior dorsal and sacral

3707 vertebrae only, ~~as~~because mid-dorsal elements of diplodocids considerably lower the mean

3708 ratio in some cases (Tab. S36). Also, state boundaries are adapted. The character is treated as

3709 ordered.

3710 C283: Dorsal ribs, rib head: area between capitulum and tuberculum flat (0); oblique ridge

3711 present that connects medial and lateral edge at the base of the rib head (1) (New; Fig. 108).

3712 **Comments.** The ridge marks the posterior surface of the rib head of advanced diplodocines.

3713 C284: Dorsal ribs, proximal pneumatopores: absent (0); present (1) (Wilson, 2002; Fig. 108).

3714 **Comments.** In some taxa, only one rib of the entire series bears a pneumatopore. However,

3715 the ability to develop pneumatized ribs appears to be restricted to certain diplodocid groups,

3716 therefore the character was included in this analysis.

3717 C285: Mid-dorsal ribs, orientation of tuberculum: spreading outside from rib shaft (0);

3718 following straight direction of rib shaft (1); following medial bend of rib shaft (2) (Gallina

3719 and Apesteguía, 2005; Fig. 108).

3720 **Sacral vertebrae**

3721 C286: Sacral vertebrae, number: 4 (0); 5 (1); 6 (2) (Salgado et al., 1997; modified; Tab. S37).

3722 **Comments.** Some *Camarasaurus* specimens appear to have six sacral vertebrae, which is

3723 usually considered a synapomorphy of advanced titanosauriforms (Tidwell et al., 2005). The

3724 addition of a sacral vertebra was suggested to be a sign of very old age (Tidwell et al., 2005).

3725 The unusual six sacral vertebrae in the holotype of '*Apatosaurus*' *minimus* AMNH 675 (Mook,

3726 1917) might thus also be ontogenetic.

3727 C287: Sacral vertebral centra, pleurocoels: absent (0); present (1) (Upchurch et al., 2004a;

3728 wording modified).

3729 C288: Sacral rib III, ventral surface: smooth (0); with oblique ridge (1) (Mook, 1917; Fig.

3730 109).

3731 **Comments.** The presence of an oblique ridge was proposed as synapomorphy of *Apatosaurus*

3732 by Mook (1917), but later regarded as ambiguous and thus of little use to diagnose the genus

3733 (McIntosh, 1995). The presence of this ridge is herein used for the first time as a phylogenetic

3734 character, in order to test its utility. According to Mook (1917), the ridge marks the ventral

3735 face of sacral rib II. However, as shown in the holotype specimen ifof *Brontosaurus amplus*

3736 YPM 1981 (Ostrom and McIntosh, 1966), among others, the ridge actually lies on sacral rib

3737 III. Some *Camarasaurus* specimens bear oblique ridges on their sacral ribs (e.g. AMNH 690;

3738 Osborn, 1904), but not the genotype specimen AMNH 5761. In the present analysis,

3739 *Camarasaurus* was thus scored as plesiomorphic.

3740 C289: Sacral neural spines, lateral side, towards summit: flat, with only spinodiapophyseal

3741 lamina (spdl) well-developed (0); with distinct horizontal accessory laminae that connect spdl

3742 to pre- and/or postspinal lamina (1) (New; Fig. 110).

3743 C290: Sacral neural spines, lateral view, spinodiapophyseal lamina: reduced to absent, does

3744 not connect summit and diapophysis (0); present and distinct, connects spine summit with

3745 diapophysis (1) (New; Fig. 110).

3746 C291: Sacral neural spines, lateral view, spinodiapophyseal laminae (spdl): remain vertical

3747 and thus parallel to each other (0); spdl of neighboring spines converge (1) (New; Fig. 110).

3748 **Comments.** Diplodocinae develop a very distinct dorsal widening of the sacral spdl. Together

3749 with the inclination of the spines towards the central portion of the sacrum, this often leads to

3750 a fusion of these anteroposteriorly widened dorsal ends of the spdl.

3751 **Caudal vertebrae**

3752 C292: Caudal neural spines, elliptical depression between lateral spinal lamina and postspinal

3753 lamina on dorsolateral surface: absent (0); present (1) (Sereno et al., 2007; modified; Fig.

3754 111).

3755 **Comments.** Sereno et al. (2007) initially defined the character as follows: 'elliptical

3756 depression between spinodiapophyseal lamina and postspinal lamina on lateral neural spine'.

3757 However, the spinal lamina they were most probably referring to (herein called lateral spinal

3758 lamina) is usually the united spol and sprl (at least in diplodocids). The character description

3759 has thus been reworded in order to clarify this. Sereno et al. (2007) recovered the presence of

3760 such a depression as a synapomorphy of Nigersaurinae, but actually it is present in any taxon

3761 with transversely widened posl, and spol that either fuse with the spdl or the posl. Anterior

3762 caudal vertebrae of *Diplodocus* are a good example for this, although they were scored as

3763 plesiomorphic by Sereno et al. (2007). Taxa without spdl or posl are scored as unknown.

3764 C293: Caudal neural spines with triangular lateral processes: absent (0); present (1) (Sereno et

3765 al., 2007; Fig. 112).

3766 **Comments.** These processes correspond to the triangular lateral processes of dorsal neural

3767 spines, but do not appear to be correlated.

3768 C294: Posterior dorsal, sacral and anterior caudal neural spines, shape in anterior/posterior

3769 view: rectangular through most of length (0); 'petal' shaped, expanding transversely through

3770 75% of its length and then tapering (1) (Calvo and Salgado, 1995; Upchurch, 1998; Fig. 112).

3771 **Comments.** Plesiomorphic caudal neural spines can still be transversely expanded at their

3772 ends. Also, taxa with gradually expanding neural spines that do not taper dorsally are herein

3773 scored as plesiomorphic, ~~as~~because without the tapering, the spines do not develop the 'petal'

3774 shape typical for rebbachisaurs and dicraeosaurs.

3775 C295: First caudal centrum, articular face shape: flat (0); procoelous (1); opisthocoelous (2)

3776 (Wilson, 2002; modified).

3777 **Comments.** The fourth state (biconvex) of Wilson (2002) was deleted ~~as~~because no ~~used~~

3778 OTU in this analysis has a biconvex first caudal vertebra. The probable brachiosaurid SMA

3779 0009 and *Demandasaurus* have platycoel first caudal vertebrae (Torcida Fernández-Baldor et

3780   al., 2011; Carballido et al., 2012a), and are herein scored as opisthocoelous rather than flat.

3781   C296: Anterior-most caudal centra, transverse cross-section: sub-circular with rounded

3782   ventral margin (0); 'heart'-shaped with an acute ventral ridge (1) (Gilmore, 1936; Upchurch et

3783   al., 2004b; wording modified; Fig. 113).

3784   **Comments.** Taxa with ventral hollows in their anterior caudal centra are scored as

3785   plesiomorphic, because the presence of the ventral ridge is regarded as the crucial trait for

3786   which this character codes for.

3787   C297: Anterior-most caudal centra, pneumatic fossae: reduced to absent (0); large pleurocoels

3788   (1) (New; Fig. 111).

3789   **Comments.** Some apatosaur specimens and *Supersaurus* have distinct pleurocoels in their

3790   anterior-most caudal centra, whereas in anterior centra (as defined in table 10), pleurocoels

3791   are reduced to foramina in these taxa (see e.g. Riggs, 1903). The current character is thus

3792   added to the usual one coding for pleurocoels in anterior caudal vertebrae in general.

3793   C298: Anterior-most caudal vertebrae, additional pneumatic fossa on posterodorsal corner of

3794   centrum: absent (0); present (1) (New; Fig. 111).

3795   **Comments.** In lateral views, these additional pneumatic foramina are often obscured by the

3796   transverse process.

3797   C299: Anterior-most caudal transverse processes, shape: triangular, tapering distally (0);

3798   wing-like (1) (McIntosh, 1990b; Yu, 1993; modified; Fig. 112).

3799   **Comments.** A transverse process is herein interpreted as wing-like if it has a distinct

3800   shoulder, i.e., an angled bump on its dorsolateral edge.

3801   C300: Anterior-most caudal vertebrae, transition from 'fan'-shaped to ' normal' caudal ribs:

3802   between Cd 1 and 2 (0); Cd4 and Cd5 (1); Cd5 and Cd6 (2); Cd6 and Cd7 (3); Cd7 and Cd8

3803   or more posteriorly (4) (Upchurch et al., 2004b; modified; Tab. S38).

3804   C301: Anterior-most caudal neural arches, accessory lamina connecting pre- and

3805   postzygapophyses: absent (0); present (1) (New; Fig. 111).

3806   **Comments.** This accessory lamina usually connects the postzygapophysis with the sprl.

3807   C302: Anterior-most caudal neural spine (not including arch), height: less than 1.5 times

3808   centrum height (0); 1.5 times centrum height or more (1) (Yu, 1993; modified after Upchurch

3809   and Mannion, 2009; Tab. S39).

3810   **Comments.** Neural spine height is measured from the dorsal edge of the postzygapophyses to

3811   the spine top, vertically. Centrum height is measured at the posterior articular surface. Yu

3812 (1993) used the entire neural arch height for the ratio, and formulated it as a multistate

3813 character, restricted to the first two caudal vertebrae. The ratio is herein adapted following

3814 Upchurch and Mannion (2009), but keeping the restriction to the anterior-most elements,

3815 instead of including all anterior caudal vertebrae as implemented by Upchurch and Mannion

3816 (2009).

3817 C303: Anterior-most caudal neural spines, lateral spinal lamina: has the same anteroposterior

3818 width ventrally and dorsally (0); expands anteroposteriorly towards its distal end, and

3819 becomes rugose (1) (Upchurch et al., 2004a; wording modified; Fig. 111).

3820 **Comments.** Apatosaurs usually have a more dorsally restricted anteroposterior expansion of

3821 the lateral spinal lamina, compared to diplodocines. SMA 0087 appears to show the

3822 plesiomorphic state, which could be an autapomorphic reversal. However, due to the bad

3823 preservation of the bones, the true morphology of the lateral spinal lamina is difficult to

3824 assess, and it might actually turn out to be widened as well, once all of the material is

3825 prepared.

3826 C304: Anterior caudal centra (excluding the first), articular surface shape: amphiplatyan or

3827 amphicoelous (0); procoelous/distoplatyan (1); slightly procoelous (2); procoelous (3)

3828 (McIntosh, 1990b; Russell and Zheng, 1993; modified after González Riga et al., 2009; Tab.

3829 S38).

3830 **Comments.** Slightly procoelous is herein defined as the slightly opisthocoelous posterior

3831 dorsal centra (see character 270). In diplodocids, the centra change their shape in anterior to

3832 middle caudal vertebrae from slightly procoelous to procoelous/distoplatyan to

3833 amphicoelous/amphiplatyan. This change occurs more posteriorly in *Diplodocus* than in

3834 *Apatosaurus*, for example. T, therefore specimens of the former genus have to be scored as

3835 slightly procoelous for this character, whereas *Apatosaurus* specimens are scored as

3836 procoelous/distoplatyan. However, more detailed studies about this transition is needed in

3837 order to score this character appropriately, asbecause the specimens used herein generally

3838 show some correlation (within Flagellicaudata) of the development of procoely and the

3839 presence of wing-like transverse processes, which also mark more caudal vertebrae in

3840 *Diplodocus* than in less derived Flagellicaudata.

3841 C305: Anterior caudal centra, ventral surface: without irregularly placed foramina (0);

3842 irregular foramina present on some anterior caudal vertebrae (1) (Whitlock, 2011a; Fig. 113).

3843 **Comments.** Foramina can also be present in anterior caudal vertebrae without concave

3844 ventral surfaces (see *Suuwassea emilieae* ANS 21122; Harris, 2006b).

3845 C306: Anterior caudal centra, pneumatopores (pleurocoels): absent (0); present (1) (McIntosh,

3846 1990b; Yu, 1993; modified).

3847 **Comments.** Small pneumatopores also mark the lateral surfaces of the centra in non-

3848 diplodocine sauropods (e.g. *Lourinhasaurus alenquerensis* MIGM specimen, ET, pers. obs.,

3849 2012). The development of the pneumatopores as foramina or deep coels is described in

3850 character 307.

3851 C307: Anterior caudal centra, pneumatopores: restricted to foramina (0); large coels present

3852 (1) (Tschopp and Mateus, 2013b; modified; Fig. 114).

3853 **Comments.** This character only codes for the anterior caudal vertebrae, excluding the

3854 anterior-most elements with wing-like transverse processes. The presence of a large coel in

3855 the latter is coded for in character 297. Taxa without pneumatopores are scored as unknown.

3856 C308: Anterior caudal centra, pneumatopores: disappear by caudal 15 (0); present until caudal

3857 16 or more (1) (McIntosh, 2005; Tab. S38).

3858 **Comments.** McIntosh (2005) recognized this as ~~distinguishing~~ character distinguishing

3859 between *Diplodocus* and *Barosaurus*, but it is applied for the first time as a phylogenetic

3860 character.

3861 C309: Anterior caudal centra, length: subequal amongst first 20 (0); more or less doubling

3862 over first 20 (1) (Upchurch, 1998; modified; Tab. S40).

3863 **Comments.** Lengths were compared between the shortest element among the first three, and

3864 the longest preserved vertebrae within Cd 17 and 22 (or if this part of the tail is lacking, the

3865 longest element preserved). Taxa with a ratio of 1.5 or more are scored as derived.

3866 C310: Anterior caudal vertebrae, concavo-convex zygapophyseal articulation: absent (0);

3867 present (1) (Wilson, 2002; Whitlock, 2011a; Fig. 112).

3868 **Comments.** This character is similar to the one for cervical vertebrae, which describes the flat

3869 versus convex prezygapophyses of diplodocine cervical vertebrae. Wilson (2002) suggested

3870 that convex prezygapophyses and concave postzygapophyses are diagnostic for *Diplodocus*,

3871 but Whitlock (2011a) showed that ~~also~~ *Barosaurus* also showed the derived state. During the

3872 current study, ~~also~~ some apatosaur specimens o were observed to have the apomorphic

3873 condition.

3874 C311: Anterior caudal prezygapophyses, pre-epipophysis laterally below articular facet:

3875 absent (0); present (1) (New; Fig. 111).

Comments. A rugose horizontal ridge marks the lateral surface of the prezygapophysis of *Diplodocus* and very few other taxa, below the articular facet. The position corresponds to where the pre-epipophysis of cervical vertebrae is located and is thus termed equally here.

C312: Anterior caudal vertebrae, transverse processes: ventral surface directed laterally or slightly ventrally (0); directed dorsally (1) (Whitlock, 2011a; Fig. 112).

Comments. This character describes the orientation of the ventral edge of the transverse process in anterior or posterior view.

C313: Anterior caudal transverse processes, anterior diapophyseal laminae (acdl, prdl): reduced or absent (0); present, well defined (1) (Wilson, 2002; modified; see Fig. 114 for equivalent in posterior diapophyseal laminae).

Comments. The original character (Wilson, 2002) was split in two, ~~as~~because the development of the posterior centrodiapophyseal and the postzygodiapophyseal laminae differs between *Apatosaurus* and *Diplodocus*.

C314: Anterior caudal transverse processes, anterior centrodiapophyseal lamina, shape: single (0); divided (1) (Wilson, 2002; Fig. 111).

Comments. In contrast to dicraeosaurids or more basal diplodocoids, diplodocids have wing-like transverse processes, which are anteriorly supported by two independent laminae, which both originate on the centrum and thus classify as acdl (and the latter thus as divided or double). In advanced diplodocines, the lower of the two acdl is furthermore branching in two towards the transverse process.

C315: Anterior caudal transverse processes, posterior diapophyseal laminae (pcdl, podl): reduced or absent (0); present, well defined (1) (Wilson, 2002; modified; Fig. 114).

C316: Anterior caudal transverse processes, anteroposteriorly expanded lateral extremities: absent (0); present (1) (New; Fig. 113).

Comments. Backwards curving transverse processes are not necessarily anteroposteriorly expanded.

C317: Anterior caudal neural spines, maximum mediolateral width to anteroposterior length ratio: < 1.0 (0); 1.0 or greater (1) (Upchurch, 1998; modified by Mannion et al., 2013; Tab. S39).

Comments. The anteroposterior length of the spine is measured at the same level as the maximum mediolateral width, perpendicular to the inclination of the neural spine. The unusual plesiomorphic state of SMA 0087 within the apatosaur specimens might be due to

3908 diagenetic transverse compression.

3909 C318: Anterior caudal neural spines, spinoprezygapophyseal lamina: absent, or present as

3910 small short ridges that rapidly fade out into the anterolateral margin of the spine (0); present,

3911 extending onto lateral aspect of neural spine (1) (Wilson, 2002), modified by (Mannion et al.,

3912 2012; Fig. 111).

3913 C319: Anterior caudal neural spines, spinopre- and spinopostzygapophyseal laminae contact:

3914 absent (0); present (1) (Wilson, 2002; Fig. 111).

3915 C320: Anterior caudal neural arches, prespinal lamina: absent (0); present (1) (Upchurch,

3916 1995; Fig. 111).

3917 **Comments.** Sauropod anterior caudal neural spines are generally rugose anteriorly and

3918 posteriorly, but only derived eusauropods develop distinct ridges or laminae.

3919 C321: Anterior caudal neural spines, thickened anterior rim of prespinal lamina: absent (0);

3920 present (1) (Gallina and Apesteguía, 2005; Fig. 111).

3921 **Comments.** Specimens without prespinal lamina are scored as unknown.

3922 C322: Anterior caudal neural spines, prespinal lamina or rugosity: terminate at or beneath

3923 dorsal margin of neural spine (0); project dorsally above neural spine (1) (Whitlock, 2011a;

3924 modified; see Fig. 114 for equivalent in postspinal lamina).

3925 **Comments.** The original character (Whitlock, 2011a) was split in two, because in the anterior

3926 caudal vertebrae of *Cetiosauriscus stewarti* NHMUK R.3078 only the postspinal rugosity

3927 expands dorsally above the spine summit (Woodward, 1905). The character description was

3928 slightly changed in order to include taxa without distinct prsl.

3929 C323: Anterior caudal neural arches, postspinal lamina: absent (0); present (1) (Upchurch,

3930 1995; Fig. 111).

3931 **Comments.** See character 320. The two characters coding for the presence of pre- or

3932 postspinal laminae, are scored equally in the present analysis, as also in Wilson (2002), and

3933 might thus prove correlated in future. They were both retained herein as they distinguish

3934 between basal and derived non-neosauropod eusauropods and should thus have no influence

3935 on the relationships between ingroup diplodocids.

3936 C324: Anterior caudal neural spines, postspinal lamina or rugosity: terminate at or beneath

3937 dorsal margin of neural spine (0); project dorsally above neural spine (1) (Whitlock, 2011a;

3938 modified; Fig. 114).

3939 **Comments.** See character 322.

3940 C325: Anterior caudal neural arches; hyposphenal ridge on posterior face of neural arch;

3941 present (0); absent (1) (Mannion et al., 2012; Fig. 115).

3942 C326: Anterior caudal neural spines, shape: single (0); slightly bifurcate anteriorly (1)

3943 (Whitlock, 2011a; Fig. 112).

3944 **Comments.** Anterior caudal neural spines can be bifid in two ways: anteroposteriorly and

3945 transversely. The former is coded for in characters 322 and 324, whereas the latter is

3946 described in the present character.

3947 C327: Anterior caudal neural spines, maximum mediolateral width to minimum mediolateral

3948 width ratio: < 2.0 (0); 2.0 or greater (1) (Canudo et al., 2008; Taylor, 2009; modified by

3949 Mannion et al., 2013; Tab. S39).

3950 C328: Anterior caudal neural spines, lateral expansion at distal end: gradual, expanding

3951 through the last third of the neural spine (0); abrupt, restricted to distal fourth of neural spine

3952 (1) (New; Fig. 112).

3953 C329: Anterior and mid-caudal vertebrae, ventrolateral ridges: absent (0); present (1)

3954 (Upchurch et al., 2004a; Fig. 116).

3955 **Comments.** ~~There are t~~Two horizontal ridges ~~marking~~mark some diplodocid caudal centra:

3956 ~~the~~a lateral ridge and ~~the~~a ventrolateral ridge. Usually, only one of the two is present, which is

3957 interpreted as the lateral ridge ☰ he ventrolateral ridge as used herein does not describe the

3958 borders of the ventral longitudinal hollow of advanced diplodocines.

3959 C330: Anterior and mid-caudal centra, ventral longitudinal hollow: absent (0); present (1)

3960 (McIntosh, 1990b; Yu, 1993; Fig. 113).

3961 **Comments.** A ventral hollow is herein interpreted to be longitudinal concavity occupying the

3962 entire ventral surface. Various taxa have very distinct posterior chevron facets~~,~~ with distinct

3963 ridges leading to them, thus creating a posteriorly concave ventral surface. However, these

3964 ridges often fade anteriorly. In some anterior diplodocine caudal centra, <u>longitudinal struts</u>

3965 <u>subdivide</u> the ventral hollow ~~is subdivided by longitudinal struts~~ (e.g. *Tornieria africana*

3966 SMNS 12141a; Remes, 2006).

3967 C331: Anterior- and mid-caudal vertebrae, ventral hollow depth: shallow, 10mm or less (0);

3968 deep, >10mm (1) (Curtice, 1996; Tab. S40).

3969 **Comments.** Ventral hollow depth is used as ~~distinguishing~~ a character <u>distinguishing</u> between

3970 *Diplodocus* and *Barosaurus* (Curtice, 1996; McIntosh, 2005). Curtice (1996) showed that a

3971 caudal centra with a ventral hollow depth of more than 10 mm can be confidently identified as

3972 *Diplodocus*, whereas shallower centra are typical for less derived diplodocines. Only very

3973 limited measurements were available, and the scoring was mainly based on descriptions and

3974 thus the subjective opinion of the respective authors. An interesting case is present in

3975 *Tornieria*, where the only preserved caudal vertebra of the holotype specimen (SMNS

3976 12141a, Cd 2) has a deep ventral hollow, whereas the medial caudal vertebra of skeleton k

3977 (MB.R.2913) is only shallowly excavated (Remes, 2006). More detailed research is needed in

3978 order to sort this out.

3979 C332: Mid-caudal vertebrae, ratio of centrum length to posterior height: < 1,7 (0); 1,7 or

3980 greater (1) (Yu, 1993; modified; Tab. S40).

3981 **Comments.** Usually, this character is included in analyses with its state boundary set at 2. In

3982 the present analysis, it was regarded more useful to put the boundary at 1.7, ~~as~~because some

3983 diplodocine taxa have ratios between 1.7 and 2. Generally, the ratio increases in more

3984 posterior elements, therefore specimens with only anterior mid-caudal vertebrae preserved

3985 (e.g. *Diplodocus longus* YPM 1920, see McIntosh and Carpenter, 1998) most probably would

3986 have higher ratios than indicated in the table.

3987 C333: Mid-caudal vertebrae, lateral surface of centra: without longitudinal ridge at midheight

3988 (0); longitudinal ridge present, centra hexagonal in anterior/posterior view (1) (Upchurch and

3989 Martin, 2002; Fig. 116).

3990 **Comments.** This ridge is not the same as the ventrolateral ridge described above, which is

3991 located below midheight.

3992 C334: Mid-caudal centra, articular surface shape: cylindrical (0); quadrangular (1);

3993 trapezoidal (2); with flat ventral margin but rounded lateral edges (3) (Wilson, 2002; Gallina

3994 and Apesteguía, 2005; modified after Carballido et al., 2012b; Fig. 117).

3995 **Comments.** The character was modified in order to be able to code for the various

3996 intermediate states between cylindrical, quadrangular, and triangular as described by earlier

3997 workers.

3998 C335: Mid-caudal centra ventral surface in lateral view: gently curved (0); greater portion

3999 straight, with expansions on both ends to form the chevron facets restricted to about last

4000 fourth of centrum length (1) (New; Fig. 116).

4001 **Comments.** This description applies especially for anterior mid-caudal elements, more

4002 posterior vertebrae of derived specimens tend to develop a more gentle curvature. This can

4003 create problems in taxa preserving only posterior mid-caudal vertebrae~~, as e.g.~~. For instance,

Tornieria specimen k~, which~ is herein scored as plesiomorphic for this character. Caudal vertebrae from trench dd, however, indicate that *Tornieria* actually might show the derived state, but these have not been found in articulation, and because anatomical overlap with the referred specimens included herein is minimal, their attribution to the species should be regarded as doubtful.

C336: Mid-caudal posterior articular surface: concave (0); flat (1); convex (2) (New; Tab. S38).

C337: Mid-caudal neural arches: over the midpoint of the centrum with approximately subequal amounts of the centrum exposed at either end (0); on the anterior half of the centrum (1) (Huene, 1929; Salgado et al., 1997; Fig. 116).

Comments. For this character, the distance between pre- and postzygapophyses and their location above the vertebral centrum is regarded as reference. The pedicels can still be dislocated anteriorly in plesiomorphic taxa. ~It~This character is generally used as a titanosauriform synapomorphy (Salgado et al., 1997; Wilson, 2002), but also is convergently present in some *Diplodocus* specimens (e.g. AMNH 223, or USNM 10865).

C338: Mid-caudal prezygapophyses: free (0); posteriorly interconnected by a transverse ridge, creating a triangular fossa together with the spinoprezygapophyseal laminae (1) (New; Fig. 118).

Comments. This transverse lamina marks the caudal vertebrae of *Diplodocus longus* YPM 1920~,~ and might prove a valid autapomorphy for the species in the future.

C339: Mid-caudal prezygapophyses position: terminate at or behind anterior edge of centrum (0); project considerably beyond anterior edge of centrum (1) (New).

Comments. Only taxa where the prezygapophyses clearly overhang the centrum (i.e. recognizable without any need of measuring) are scored as derived.

C340: Mid-caudal neural spines, orientation: directed posteriorly (0); vertical (1) (McIntosh, 1990a; Salgado et al., 1997; modified after Carballido et al., 2012b; Fig. 116).

C341: Mid-caudal neural arch, anterior extreme of spine summit: smooth (0); developing a short anterior or anterodorsal projection, such that anterior edge of spine becomes slightly concave (1) (New; Fig. 119).

Comments. Such a spur might also be interpreted as pathologic or ontogenetic. However, its presence in the juvenile to subadult *Apatosaurus* (= *Camarasaurus*) *grandis* YPM 1901 suggests that ontogeny can probably be excluded as a cause. More studies are needed in order

4036 to confirm or ~~refuse~~refute patholog~~yical reasons,~~; in the meanwhile the character is kept in the

4037 analysis.

4038 C342: Mid- and posterior caudal vertebral centra, articular surfaces: subequal in width and

4039 height or higher than wide (0); considerably wider than high (1) (Salgado et al., 1997;

4040 modified; Tab. S40).

4041 **Comments.** A ratio of 1.2 or greater is regarded as considerably wider than high.

4042 C343: Mid- and posterior caudal neural spines: spine summit overhangs postzygapophyses

4043 considerably posteriorly (0); posterior end of spine summit more or less straight above

4044 postzygapophyses (1) (New; Fig. 116).

4045 C344: Mid- and posterior caudal spines: elongate and strongly caudally directed, extending

4046 over more than 50% of length of succeeding vertebral centrum (0); short, not extending far

4047 beyond caudal articular facet of centrum (1) (Remes et al., 2009; polarity reversed; Fig. 119).

4048 C345: Posterior caudal prezygapophyses position: terminate at or behind anterior edge of

4049 centrum (0); project beyond anterior edge of centrum (1) (New).

4050 C346: Distal-most caudal centra, articular face shape: platycoelous (0); biconvex (1) (Wilson

4051 et al., 1999; Tab. S38).

4052 **Comments.** Taxa without distal caudal vertebrae are scored as unknown.

4053 C347: Distal-most caudal centra, length-to-height ratio: < 4.0 (0); 4.0-6.5 (1); > 6.5 (2)

4054 (Upchurch, 1998), modified after (Wilson et al., 1999; Tab. S40).

4055 C348: Distal-most caudal centra, number: ten or fewer (0); more than 30 (1) (Wilson, 2002;

4056 modified).

4057 **Comments.** The character was modified such that it was not restricted to distal-most

4058 'biconvex' caudal centra as in Wilson (2002).

4059 C349: Caudal ribs, last occurs on: Cd 12 or more anteriorly (0); Cd 13 (1); Cd 14 (2); Cd 15-

4060 17 (3); Cd 18 or more posteriorly (4) (Holland, 1915a; Gilmore, 1936; Upchurch et al., 2004b;

4061 modified; Tab. S38).

4062 **Comments.** Upchurch et al. (2004b), who were the first to include this positional character

4063 in~~to~~ a phylogenetic analysis, only distinguished between two states: Cd 14 and/or Cd 12.

4064 However, enlarging the taxon list, a ~~higher~~greater variety becomes evident (Tab. S38). The

4065 state description was thus adapted accordingly. The character is left unordered ~~as~~because no

4066 obvious step-like evolution is recognizable.

4067 C350: Anterior, 'fan'-shaped caudal ribs, foramen: present (0); absent (1) (Gilmore, 1936;

4068 Upchurch et al., 2004b; polarity reversed; Fig. 112).

4069 **Comments.** Polarity was reversed herein given the different taxon sampling compared to

4070 Upchurch et al. (2004b).

4071 **Chevrons**

4072 C351: Chevrons, 'crus' bridging haemal canal: absent in some (0); present in all (1) (Yu, 1993;

4073 modified after Mannion et al., 2012).

4074 **Comments.** Additive binary coding is preferred here in order to be able to code incomplete

4075 tails (following Mannion et al., 2012).

4076 C352: Chevrons, 'crus' bridging haemal canal: present in some (0); absent in all (1) (Yu, 1993;

4077 modified after Mannion et al., 2012; Fig. 120).

4078 **Comments.** See character 351.

4079 C353: Chevrons with anterior and posterior projections: present (0); absent (1) (McIntosh,

4080 1989; Russell and Zheng, 1993; modified; Fig. 121).

4081 **Comments.** This character describes the oft-termed~~en called~~ 'forked chevrons' that inspired

4082 Marsh (1878) to name the specimen YPM 1920 *Diplodocus* (= double beam).

4083 C354: Anterior chevrons, longitudinal median ridge on anterior surface: absent (0); present

4084 (1) (New; Fig. 120).

4085 **Comments.** The ridge extends proximodistally.

4086 C355: Anterior chevrons, posterior edge of distal blade in lateral view: continuous (0);

4087 posteriorly expanded in a step-like fashion (1) (New; Fig. 120).

4088 C356: Anterior mid-chevrons, lateral surface: smooth (0); marked by a horizontal ridge right

4089 below articulation surfaces (1) (New; Fig. 121).

4090 **Comments.** The ridge can be quite broad, but it is always rugose. Anterior mid-chevrons are

4091 meant to be the first elements with anterior projections on the distal blade.

4092 C357: Middle chevrons, distinct fossae on medial surfaces of proximal branches: absent (0);

4093 present (1) (New; Fig. 121).

4094 C358: Forked chevrons, anteroposterior length: short, about 50% of relative vertebral centrum

4095 length (0); elongate, approaching corresponding vertebral centrum length (1) (McIntosh,

4096 1995).

4097 **Comments.** The increased relative length of the chevron compared to its corresponding

4098 caudal vertebra was proposed as a useful character to distinguish *Diplodocus* from

4099 *Apatosaurus* by McIntosh (1995), and is herein used for the first time in a phylogenetic

4100 analysis.

4101 **Pectoral girdle**

4102 C359: Scapular length/minimum blade breadth: > 5.5 (0); 5.5 or less (1) (Carballido et al.,
4103 2012b; polarity reversed; Tab. S41).

4104 **Comments.** Measurements are taken from figures in lateral view, ignoring the proximodistal
4105 curve of the scapula. Greatest length follows the long axis of the scapula, such that orientation
4106 within the articulated skeleton is not taken into account, ~~as~~because this is still debated (see
4107 Schwarz et al., 2007a; Remes, 2008; Hohn, 2011). Minimum blade breadth is measured
4108 perpendicular to the long axis.

4109 C360: Scapular acromion length/scapular length: > 0.54 (0); 0.46-0.54 (1); < 0.46 (2) (Gallina
4110 and Apesteguía, 2005; modified; Tab. S41).

4111 **Comments.** Measurements were taken from figures in lateral view. Acromion length is
4112 measured perpendicular to scapular length, between horizontal lines extending through the
4113 ventral- and dorsal-most points of the acromion, with the distal blade oriented horizontally.
4114 The character is treated as ordered.

4115 C361: Scapula, orientation of scapular, angle with coracoid articulation: > 80° (0); 80° or less
4116 (1) (Wilson, 2002; modified; Tab. S41).

4117 **Comments.** The angle is measured from figures or photos in lateral view.

4118 C362: Scapula, angle between acromial ridge and distal blade: < 70° (0); 70°-81° (1); > 81°
4119 (2) (Riggs, 1903; Carpenter and McIntosh, 1994; Upchurch et al., 2004b; modified; Tab.
4120 S41).

4121 **Comments.** The angle to be measured lies between the dorsal half of the acromial ridge~,~ and
4122 the long axis of the scapular blade. An additional state was added to the original version
4123 (Upchurch et al., 2004b), in order to be able to score specimens with intermediate ratios. The
4124 character is left unordered as no obvious evolutionary trend is observable.

4125 C363: Scapular acromion process, dorsal part of posterior margin: convex or straight (0); U-
4126 shaped concavity (1) (Wilson, 2002; modified by Whitlock, 2011a; Fig. 122).

4127 C364: Scapular, acromion process position: lies near the glenoid level (0); lies nearly at
4128 midpoint of scapular body (1) (Carballido et al., 2012b; Fig. 122).

4129 **Comments.** The position of the acromion process relative to the glenoid has to be checked
4130 with the long axis of the distal blade oriented horizontally.

4131 C365: Scapula, area posterior to acromial ridge and distal blade: is excavated (0); is flat or

4132 slightly convex (1) (Upchurch et al., 2004b; Fig. 123).

4133 **Comments.** This character describes the area posterior to the acromial ridge, and dorsal to the

4134 distal blade, where the two meet.

4135 C366: Scapular glenoid, orientation: relatively flat or laterally facing (0); strongly beveled

4136 medially (1) (Wilson and Sereno, 1998).

4137 **Comments.** The medially beveled glenoid surface was proposed as autapomorphyic for

4138 *Apatosaurus* (Wilson, 2002), but Upchurch et al. (2004b) showed that the orientation was

4139 actually variable within *Apatosaurus* specimens, which is confirmed herein.

4140 C367: Scapular blade, acromial edge: straight (0); rounded expansion at distal end (1);

4141 racquet-shaped (2) (Wilson, 2002; wording modified; Fig. 122).

4142 C368: Scapular blade, ventral edge in lateral view: is straight (0); curves ventrally towards its

4143 distal end (1) (Upchurch et al., 2004b; wording modified; Fig. 122).

4144 **Comments.** Whereas the original character (Upchurch et al., 2004b) described the entire

4145 blade, the derived ventral curving is here restricted to the ventral edge of the blade.

4146 C369: Scapula: without semi-ovate, flat muscle scar just distal to glenoid on scapular shaft

4147 (0); scar present (1) (Whitlock, 2011a; Fig. 123).

4148 **Comments.** The scar described herein lies on the lateral side of the blade.

4149 C370: Scapular blade, subtriangular projection on anterior portion of ventral edge: absent (0);

4150 present (1) (Gallina and Apesteguía, 2005; Fig. 122).

4151 **Comments.** In *Diplodocus* sp. AMNH 223, there are two eminences ≡ se to each other (ET,

4152 pers. obs., 2011).

4153 C371: Scapular blade, expansion of distal end: wide (at least 2 times narrowest width of shaft

4154 in lateral view) (0); narrow (< 2 times narrowest width of shaft) (1) (Yu, 1993; modified; Tab.

4155 S41).

4156 **Comments.** Measurements are taken perpendicular to the long axis of the blade.

4157 C372: Coracoid, anteroventral margin shape: rounded (0); rectangular (1) (Bakker, 1998;

4158 Wilson, 2002; Fig. 124).

4159 C373: Coracoid, infraglenoid groove: reduced to absent (0); present and distinct (1)

4160 (Carballido et al., 2012b; modified; Fig. 124).

4161 C374: Sternal plates, shape: subcircular or oval (0); subtriangular with widened posterior

4162 border (1); elliptical to crescentic, with concave lateral margin (2) (Calvo and Salgado, 1995;

4163 modified; Fig. 125).

Comments. The subtriangular shape was added to the original version of Calvo and Salgado (1995) in order to better describe the difference between typical basal neosauropod or macronarian, and diplodocid shape. The character is treated as unordered, because none of the states can convincingly be interpreted as intermediate.

C375: Sternal plate, ridge on the ventral surface: absent (0); broad and shallow, or elongate and prominent (1) (Upchurch et al., 2004a; wording modified; Fig. 125).

C376: Sternal plate, anterior end: expanded dorsoventrally (0); flat, not expanded (1) (Tschopp and Mateus, 2012; modified; Fig. 125).

C377: Sternal plate, posterior border: convex (0); straight (1) (González Riga, 2002; modified; Fig. 125).

Comments. The true shape of the posterior border can sometimes be obscured due to the presence of fused sternal ribs (Tschopp and Mateus, 2012).

Forelimb

C378: Forelimb: hindlimb length ratio: 0.76 or greater (0); less than 0.76 (1) (Upchurch, 1995, 1998; modified; Tab. S42).

Comments. Forelimb length is the sum of the lengths of the humerus, radius, and metacarpal III.; hindlimb length the sum of the lengths of femur, tibia, and metatarsal III.

C379: Humerus-to-femur ratio: < 0.7 (0); 0.7-0.76 (1); 0.77-0.89 (2); = or > 0.90 (3) (McIntosh, 1990a; modified; Tab. S43).

Comments. State boundaries are chosen such that the generally accepted genera *Apatosaurus* and *Diplodocus* can be distinguished from *Tornieria* and *Barosaurus*. The character is treated as ordered.

C380: Humerus, RI (sensu Wilson and Upchurch, 2003): gracile (less than 0.27) (0); medium (0.28-0.32) (1); robust (more than 0.33) (2) (Carballido et al., 2012b; Tab. S44).

Comments. The humerus RI was defined as the mean between proximal, distal, and midshaft transverse widths, divided by humerus length (Wilson and Upchurch, 2003). Scores for taxa where no measurements were available were taken from Carballido et al. (2012b). The character is herein treated as ordered.

C381: Humerus, shaft twist: minor to absent (0); high, distal articular surface twisted by at least 30° compared to proximal articular surface (1) (Gilmore, 1932; Tab. S44).

Comments. This angle is difficult to measure due to lacking references. It was proposed as a distinguishing feature of *Diplodocus* (Gilmore, 1932) and is here included into a phylogenetic

4196   analysis for the first time.

4197   C382: Humerus, midshaft cross-section, shape: circular, transverse diameter: anteroposterior

4198   diameter ratio is 1.5 or lower (usually close to 1.3) (0); elliptical, transverse diameter:

4199   anteroposterior diameter ratio is greater than 1.5 (usually close to 1.8) (1) (Wilson, 2002;

4200   modified by Mannion et al., 2012; Tab. S44).

4201   C383: Humerus, pronounced proximolateral corner: absent (0); present (1) (Upchurch, 1998;

4202   Fig. 126).

4203   **Comments.** A pronounced proximolateral corner forms a weak hump in anterior or posterior

4204   view.

4205   C384: Humerus, proximal expansion: more or less symmetrical (0); asymmetrical,

4206   proximomedial corner much more pronounced than proximolateral one (1) (Wilhite, 2005;

4207   Fig. 126).

4208   **Comments.** The differing expansions were found to be taxonomically significant (Wilhite,

4209   2005), but have not been previously included in any phylogenetic analysis. This character

4210   forms an additive binary character together with character 385.

4211   C385: Humerus, proximal end expanded laterally in anterior/proximal view: expanded, lateral

4212   margin concave in anterior/posterior view (0); not expanded (1) (Curry Rogers, 2005; polarity

4213   reversed; Fig. 126).

4214   **Comments.** Polarity was reversed compared to the original description (Curry Rogers, 2005),

4215   due to the differing taxon sampling.

4216   C386: Humerus, shallow, but distinct rugose tubercle at the center of the concave proximal

4217   portion of the anterior surface: absent (0); present (1) (New; Fig. 126).

4218   C387: Ulna to humerus length: < 0.65 (0); 0.66-0.76 (1); > 0.76 (2) (Janensch, 1929b; Tab.

4219   S45).

4220   **Comments.** The states were defined in order to include the majority of diplodocids in the

4221   same state. The character is treated as ordered.

4222   C388: Ulna, proximal condylar processes: subequal in length (0); anterior arm longer (1)

4223   (Wilson, 2002; Tab. S46).

4224   **Comments.** The state boundary is here set at 1.1, as this follows best higher-level taxonomy.

4225   C389: Ulna, proximal articular surface, angle between anterior and lateral branch: 90° (0);

4226   acute (1) (New; Tab. S46).

4227   **Comments.** Taxa with angles greater than 83° were scored as plesiomorphic.

4228 C390: Ulna, distal transverse expansion: slight, < 1.3 times minimum shaft width (min sw)

4229 (0); wide, 1.3 times min sw or greater (1) (New; Tab. S46).

4230 **Comments.** Some width measurements published do not state explicitly if they are taken

4231 transversely or anteroposteriorly; they just report maximum distal width. Anteroposterior

4232 width is often much greater than transverse width in distal surfaces of the sauropod ulnae.

4233 This leads to exaggerated ratios, if erroneously included here. Also, ~~especially~~particularly

4234 disarticulated ulnae, where both proximal processes are equally long, are difficult to orient

4235 properly. Nonetheless, the differences in these ratios still appear significant.

4236 C391: Radius, maximum diameter of the proximal end divided by greatest length: < 0.3 (0);

4237 0.3 or greater (1) (McIntosh, 1990a; modified by Mannion et al., 2013; Tab. S47).

4238 **Comments.** Maximum diameter can be width or depth.

4239 C392: Radius, distal articular surface for ulna: reduced and relatively smooth (0); well

4240 developed with one or two distinct longitudinal ridges (1) (New; Fig. 127).

4241 C393: Radius, distal condyle orientation in anterior view: perpendicular or beveled less than

4242 15° to long axis of shaft (0); beveled at least 15° to long axis of shaft (1) (Curry Rogers and

4243 Forster, 2001; Wilson, 2002; modified; Tab. S47).

4244 **Comments.** As stated by Mannion et al. (2013), the beveling of the distal surface often only

4245 affects the lateral half of the distal end. Given the different scope of the phylogenetic analysis,

4246 character state boundaries are different herein compared to Mannion et al. (2013).

4247 C394: Radius, distal breadth: <1.8 times larger than midshaft breadth (0); at least 1.8 times

4248 midshaft breadth (1) (Wilson, 2002; modified).

4249 **Comments.** Breadth is measured mediolaterally.

4250 C395: Carpus, number of carpal bones: 3 or more (0); 2 (1); 1 or less (2) (McIntosh, 1990b;

4251 Upchurch, 1998; modified).

4252 **Comments.** The character was initially proposed with only two character states (three or

4253 more, two or less; Upchurch, 1998). A third state was added here in order to distinguish

4254 *Apatosaurus* from the remaining taxa (Bonnan, 2003). Even though SMA 0011 was found

4255 with only one carpal preserved, its articulated position directly below the radius, and

4256 ~~articulating~~articulation with the first two to three metacarpals suggest that a second element

4257 was present. Such a presence is also indicated by the proximodistal width of the preserved

4258 element, which in articulation would create a large gap between the ulna and the lateral

4259 metacarpals. A similar case can be seen in the putative *Diplodocus* manus described by Bedell

and Trexler (2005). The opposite can be seen in apatosaurs, where the only carpal lies above mc II to IV, is proximodistally flattened, and metacarpals I and V are proximally dislocated in respect to the inner elements (CM 3018, UW 15556; Hatcher, 1902; Gilmore, 1936; Bonnan, 2003). Due to the probable gradual decrease in the number of carpal bones the character is treated as ordered.

C396: Carpals: block-like (0); proximodistally compressed discs (1) (New; Fig. 128).

C397: Metacarpus, shape: spreading (0); bound, with subparallel shafts and articular surfaces that extend half their length (1) (Wilson, 2002).

C398: Metacarpals, shape of proximal surface in articulation: gently curving, forming a 90° arc (0); U-shaped, subtending a 270° arc (1) (Wilson, 2002).

C399: Metacarpus, ratio of longest metacarpal to radius: < 0.40 (0); 0.40 or greater (1) (Calvo and Salgado, 1995; modified by Mannion et al., 2013; Tab. S48).

Comments. The longest metacarpal is usually mc II or mc III.

C400: Metacarpal I, length: shorter than IV (0); longer than IV (1) (Wilson and Sereno, 1998; Tab. S48).

Comments. The state boundary applied herein lies at 1.0.

C401: Metacarpal I, proximal end dorsoventral height to mediolateral width ratio: < 1.8 (0); 1.8 or greater (1) (Apesteguía, 2005; Mannion and Calvo, 2011; Mannion et al., 2013; Tab. S48).

Comments. Mannion et al. (2013) were the first to include this ratio in a phylogenetic analysis.

C402: Metacarpal III, robustness (length/distal transverse width): robust, <2.9 (0); intermediate, 2.9-3.5 (1); slender, > 3.5 (2) (Bedell and Trexler, 2005; Tab. S48).

Comments. Suggested as a distinguishing character between *Diplodocus* and *Apatosaurus*, and especially between WDC-FS001A and *Galeamopus hayi* HMNS 175 (Bedell and Trexler, 2005), which are both probably not *Diplodocus* (see below), metacarpal robustness is herein used for the first time as a character in a phylogenetic analysis. The character is treated as ordered.

C403: Metacarpal V, proximal articular surface: subequal to smaller than (0); or significantly larger than proximal articular surface of mc III and IV (1) (Janensch, 1929b; Fig. 129).

Comments. An enlarged proximal articular surface of mc V can be seen in *Apatosaurus louisae* CM 3018 (Gilmore, 1936). However, this does not seem to be the case in another

4292 apatosaur specimen (NSMT-PV 20375; Upchurch et al., 2004b), such that the derived state

4293 might prove an autapomorphy of the species *A. louisae*. A similar development can be seen in

4294 the manus of *Janenschia robusta* (Janensch, 1922).

4295 C404: Manual phalanx I-1, flange-like sheet of bone projecting from the proximoventral

4296 margin: absent (0); present (1) (Hatcher, 1902; Gilmore, 1936; Upchurch et al., 2004b; Fig.

4297 130).

4298 **Pelvic girdle**

4299 C405: Ilium, ratio of blade height above pubic peduncle to anteroposterior length: <0.40 (0);

4300 0.40 or more (1) (New; Tab. S49).

4301 **Comments.** Blade height is measured vertically above the base of the pubic pedicel, with the

4302 ischiadic tubercle and the anteroventral-most point of the preacetabular process oriented on a

4303 horizontal line.

4304 C406: Iliac preacetabular process, shape: sharply pointed (0); blunt to semicircular anterior

4305 margin (1) (Salgado et al., 1997; Fig. 131).

4306 **Comments.** A strict lateral view of the ilium is often misleading, given the anterolateral to

4307 lateral orientation of the preacetabular lobe.

4308 C407: Ilium, preacetabular process orientation: anterolateral to body axis (0); perpendicular to

4309 body axis (1) (Salgado et al., 1997).

4310 **Comments.** The perpendicular orientation of the preacetabular process is generally

4311 considered synapomorphic for derived titanosauriforms (Salgado et al., 1997; Wilson, 2002),

4312 but they also occur in the holotype of '*Apatosaurus*' *minimus* AMNH 675 (Mook, 1917).

4313 C408: Ilium, angle between the ventral edge of anterior iliac lobe and the anterior surface of

4314 the pubis process: is ~90° (0); is acute (1) (Gilmore, 1936; Upchurch et al., 2004b).

4315 C409: Ilium, dorsal margin shape: flat to slightly convex (0); semicircular (1) (Wilson, 2002;

4316 modified; Fig. 131).

4317 **Comments.** ~~Derived t~~Taxa with the derived state have uniformly convex dorsal margins,

4318 whereas taxa with the apomorphic ~~ones~~state generally have a large straight portion.

4319 C410: Ilium, highest point on dorsal margin: lies posterior to base of pubic process (0); lies

4320 anterior to base of pubic process (1) (Upchurch et al., 2004a; Fig. 131).

4321 **Comments.** The position of the highest point in respect to the pubic peduncle is assessed with

4322 the ischiadic tubercle and the anteroventral-most point of the preacetabular process lying on a

4323 horizontal line.

4324 C411: Ilium, pubic peduncle (measured at the articular surface), anteroposterior to
4325 mediolateral width ratio: > 0.80 (0); 0.80 or less (1) (Taylor, 2009; Mannion et al., 2013;
4326 modified; Tab. S49).

4327 **Comments.** Mannion et al. (2013) was the first to include this character in a phylogenetic
4328 analysis, based on observations made by Taylor (2009). State boundaries are adapted herein
4329 from 0.5 to 0.8, given the different scope and thus taxon sampling of the present analysis.

4330 C412: Ilium, triangular fossa laterally at base of pubic peduncle: absent (0); present (1) (New;
4331 Fig. 131).

4332 **Comments.** The apex of this fossa ~~is pointing~~points ventrally.

4333 C413: Ilium, distinct tubercle in the postacetabular region: absent (0); present (1) (Carballido
4334 et al., 2012a; Fig. 131).

4335 **Comments.** The herein described tubercle is not the transverse widening of the dorsal edge
4336 towards its posterior end, but a second rugose area laterally on the blade (see Schwarz et al.,
4337 2007c; Carballido et al., 2012a).

4338 C414: Pubis, ambiens process development: small, confluent, not differentiated from anterior
4339 border of the pubis (0); evident, but not especially developed (1); prominent, hook-like (2)
4340 (McIntosh, 1990b; Yu, 1993; wording modified; Fig. 132).

4341 **Comments.** The hook-like ambiens process is interpreted to represent an increased
4342 development of the incipient shape. The character is thus treated as ordered.

4343 C415: Pubis, length of puboischial contact: less than 0.41 total length of pubis (0); 0.41 or
4344 more of total length of pubis (1) (Salgado et al., 1997; modified; Tab. S50).

4345 **Comments.** Mannion et al. (2012) used a ratio of 0.45 as state boundary, but as shown in
4346 table S50, ~~for the present set of taxa,~~ 0.41 appears more appropriate for the present set of taxa.

4347 C416: Pubis, participation in acetabulum: subequal to larger, compared to ischium (0);
4348 significantly smaller (1) (Janensch, 1961; Tab. S51).

4349 **Comments.** A state boundary of 0.8 was used herein ~~as~~because the ~~used~~included OTUs show
4350 a large step from ratios below 0.75 to ratios greater than 0.83. The character was proposed as
4351 potentially useful to distinguish taxa by Janensch (1961). It is included in a phylogenetic
4352 analysis for the first time.

4353 C417: Ischium, acetabular articular surface: maintains approximately the same transverse
4354 width throughout its length (0); is transversely narrower in its central portion and strongly
4355 expanded as it approaches the iliac and pubic articulations (1) (Mannion et al., 2012).

Comments. The narrow acetabular surface is only present in some rebbachisaurids (Mannion et al., 2012).

C418: Ischium, acetabular margin, in lateral view: flat or mildly concave (0); strongly concave, pubic articular surface forms an anterodorsal projection (1) (D'Emic, 2012; modified by Mannion et al., 2013; Fig. 133).

Comments. In some diplodocids (e.g. *Apatosaurus excelsus* YPM 1980, see Fig. 133), the lateroventral edge of the acetabular surface is strongly concave, whereas the mediodorsal margin forms a bony sheet extending straight from the iliac to the pubic articular surfaces. In lateral view, this configuration appears straight and was thus scored as plesiomorphic herein.

C419: Ischium, iliac peduncle: iliac peduncle straight or widening in smooth curve distally (0); narrow, with distinct 'neck' (1) (Sereno et al., 2007; Fig. 133).

C420: Ischia pubic articulation/anteroposterior length of pubic pedicel: < 1.5 (0); 1.5 or greater (1) (Salgado et al., 1997; modified; Tab. S52).

Comments. Anteroposterior length of the pubic pedicel is measured perpendicular to the articular surface, from its ventral-most point, to the point where it intersects with a line following the ventral edge of the distal shaft. A numerical state boundary was added to the original version of Salgado et al. (1997), which separates Macronaria from basal Eusauropoda, and most diplodocines from most apatosaurs (Tab. S52).

C421: Ischium, elongate muscle scar on proximal end: absent (0); present (1) (Sereno et al., 2007; Fig. 133).

Comments. We follow Mannion et al. (2012), in that the presence of a distinct ridge on the dorsolateral edge qualifies for the apomorphic state.

C422: Ischium, lateral fossa at base of shaft: absent (0); present (1) (Wilson, 2002; Fig. 133).

Comments. The fossa is longitudinally oriented, and marks the dorsolateral edge.

C423: Ischial distal shaft, shape: blade-like, medial and lateral depths subequal (0); triangular, depth of ischial shaft increases medially (1) (Wilson, 2002; Fig. 133).

C424: Ischial distal shafts, cross-sectional shape: V-shaped, forming an angle of nearly 50° with each other (0); flat, nearly coplanar (1) (Upchurch, 1998; Wilson and Sereno, 1998; Fig. 133).

C425: Ischial shaft, transverse distal expansion: absent (0); present (1) (Whitlock, 2011a; Fig. 133).

Comments. Due to the V-shaped distal end of the ischia, 'transverse' and 'posterodorsal' do

4388   not apply very well to the ingroup specimens. However, given the twist of the ischial shaft in

4389   the taxa with coplanar distal shafts, which results in almost horizontally oriented distal ends,

4390   the main expansion of diplodocid ischia should be regarded as transverse, even though in

4391   lateral view it would appear rather dorsoventral.

4392   C426: Ischium, posterodorsal expansion of distal end: absent (0); present (1) (Lovelace et al.,

4393   2007; Fig. 133).

4394   **Comments.** See comment on transverse expansion in character 425.

4395   **Hindlimb**

4396   C427: Femur, robustness index (sensu Wilson and Upchurch, 2003): gracile, <0.22 (0);

4397   intermediate, 0.22-0.25 (1); robust, > 0.25 (2) (Janensch, 1961; Tab. S53).

4398   **Comments.** Due to the gradual increase in the ratio across sauropods, this character is treated

4399   as ordered.

4400   C428: Femur, lateral bulge (marked by the lateral expansion and a dorsomedial orientation of

4401   the laterodorsal margin of the femur, which starts below the femur head ventral margin):

4402   absent (0); present (1) (Salgado et al., 1997; modified; Fig. 134).

4403   **Comments.** The definition of this character changed in different phylogenetic analyses (e.g.

4404   Salgado et al., 1997; Mannion et al., 2012). Here, we follow Mannion et al. (2012) in that we

4405   also score incipient lateral bulges as apomorphic.

4406   C429: Femoral shaft, lateral margin shape: straight (0); proximal one-third deflected medially

4407   (1) (Wilson, 2002; Fig. 134).

4408   **Comments.** The fact that the probable brachiosaurid juvenile SMA 0009 (in contrast to other

4409   brachisaurids) does not show any medial deflection might indicate that this character changes

4410   during ontogeny. This might be correlated with the weak development of the articular surface

4411   in juvenile specimens (Ikejiri et al., 2005; Schwarz et al., 2007c).

4412   C430: Femur, cross-sectional shape: subequal to anteroposterior diameter (0); 125-150%

4413   anteroposterior diameter (1); at least 185% anteroposterior diameter (2) (Wilson and Smith,

4414   1996; Tab. S53).

4415   **Comments.** The character was added in order to distinguish between titanosauriforms, but it

4416   is also useful for the distinction of *Amphicoelias altus* AMNH 5764. Taxa scored but without

4417   entries in table S53 are taken from Carballido et al. (2012b). The character is treated as

4418   ordered.

4419   C431: Femoral head, position of highest point in anterior view: above point of maximum

4420 curvature of ventral edge of femoral head (0); laterally shifted, above main portion of shaft (1)

4421 (New; Fig. 134).

4422 C432: Femur, ventral surface of head: confluent with shaft (0); stepped (1) (New; Fig. 134).

4423 C433: Femur, greatest anteroposterior thickness of shaft: less than or approximately equal to

4424 half anteroposterior depth of distal articular condyles (0); much greater than half

4425 anteroposterior depth of distal articular condyles (1) (Whitlock, 2011a; Tab. S53).

4426 **Comments.** The state boundary used herein is 0.6. Taxa scored for this character, but not

4427 having any values in table S53, are taken from Whitlock (2011a).

4428 C434: Femur, large nutrient foramen opening midshaft anteriorly on femur: absent (0);

4429 present (1) (Wilson, 2002; Fig. 134).

4430 C435: Femur, pronounced ridge on posterior surface between greater trochanter and head:

4431 absent (0); present (1) (Sereno et al., 2007).

4432 **Comments.** The derived state is a synapomorphy for Nigersaurinae, convergently present in

4433 *Rapetosaurus* (Sereno et al., 2007; Curry Rogers, 2009).

4434 C436: Femur, fourth trochanter: not visible in anterior view (0); prominent, visible in anterior

4435 view (1) (Gallina and Apesteguía, 2005; modified by Whitlock, 2011a; Fig. 134).

4436 **Comments.** In certain taxa, a small bulge is visible on the medial edge in anterior view,

4437 which represents the medially positioned, and prominent fourth trochanter.

4438 C437: Femoral fourth trochanter, present as low rounded ridge (0); greatly reduced so that it

4439 is virtually absent (1) (Mannion et al., 2012).

4440 **Comments.** A reduced fourth trochanter is synapomorphic for rebbachisaurs and some

4441 titanosauriforms (Torcida Fernández-Baldor et al., 2011; Mannion et al., 2012). The reduced

4442 fourth trochanter of the juvenile *Elosaurus parvus* CM 566 implies that the development of

4443 this structure happens during ontogeny.

4444 C438: Femur, fourth trochanter, position: distally displaced (0); on proximal half of shaft (1)

4445 (Schwarz-Wings and Böhm, 2012; Tab. S53).

4446 **Comments.** Distance between femoral head and fourth trochanter is measured to the distal

4447 end of the trochanter. Taxa with ratios of 0.4 are scored as apomorphic.

4448 C439: Femur, shape of distal condyles: articular surface restricted to distal portion of femur

4449 (0); expanded onto anterior portion of femoral shaft (1) (Wilson and Carrano, 1999; Wilson,

4450 2002; Fig. 134).

4451 C440: Tibia to femur length: < 0.68 (0); 0.68 or greater (1) (New; Tab. S54).

4452   C441: Tibia, proximal articulation surface, shape: subcircular to transversely compressed (0);

4453   anteroposteriorly compressed (1) (Wilson, 2002; modified; Fig. 135).

4454   **Comments.** Character descriptions was slightly changed such that ~~the~~ subcircular surfaces are

4455   now scored together with the transversely compressed instead of the anteroposteriorly

4456   compressed as in (Wilson, 2002).

4457   C442: Tibia, proximal articular surface, shape: subrectangular (0); subtriangular (1) (Harris

4458   and Dodson, 2004; Fig. 135).

4459   **Comments.** Rhomboid or suboval outlines are scored as plesiomorphic.

4460   C443: Tibia, short transverse ridge on anteromedial surface of distal end: absent (0); present

4461   (1) (New; Fig. 136).

4462   C444: Tibia, cnemial crest in anterior view: widely rounded (0); subtriangular (1) (New; Fig.

4463   137).

4464   C445: Tibia, posterior surface of cnemial crest: smooth (0); bears a distinct fibular trochanter

4465   (1) (Harris, 2007; Fig. 138).

4466   **Comments.** A distinct fibular trochanter marks the posterior face of the cnemial crest of

4467   *Suuwassea* (Harris, 2007). The character is herein included in a phylogenetic analysis for the

4468   first time.

4469   C446: Tibia, lateral edge of proximal end forms a pinched out projection, posterior to cnemial

4470   crest (the 'second cnemial crest' of Bonaparte et al., 2000): present (0); absent (1) (Mannion et

4471   al., 2013; Fig. 135).

4472   C447: Fibula, proximal end with anteromedially directed crest extending into a notch behind

4473   the cnemial crest of the tibia: absent (0); present (1) (Wilson and Upchurch, 2009; D'Emic,

4474   2012; modified by Mannion et al., 2013).

4475   **Comments.** Most sauropods have ellipsoid proximal articular surfaces of the fibula.

4476   However, some diplodocid specimens (as well as some titanosauriforms; Wilson and

4477   Upchurch, 2009; D'Emic, 2012; Mannion et al., 2013) develop a distinct, narrow,

4478   anteromedial crest.

4479   C448: Fibula, insertion of the M. iliofibularis: located approximately at mid-shaft (0);

4480   proximal, located above midshaft (1) (Whitlock, 2011a; Tab. S55).

4481   **Comments.** Distance from the proximal articular surface to the center of the tubercle was

4482   measured and compared to greatest length. Values of 0.4 or lower were scored as derived.

4483   C449: Astragalus, morphology in anterior view: rectangular (0); wedge-shaped, narrowing

4484 medially (1) (Upchurch, 1995, 1998; modified by Nair and Salisbury, 2012; Fig. 139).

4485 C450: Astragalus, anteroposterior dimension as seen in dorsal view: widens medially or does

4486 not change in width (0); narrows medially (1) (Cooper, 1984; Upchurch, 1998; Fig. 139).

4487 **Comments.** The taxonomic significance of this character was recognized by Cooper (1984),

4488 but included into a phylogenetic analysis for the first time by Upchurch (1998).

4489 C451: Astragalus, proximodistal length/transverse breadth: < 0.55 (0); 0.55 or greater (1)

4490 (McIntosh et al., 1992; Tab. S56).

4491 **Comments.** This ratio was used by McIntosh et al. (1992) to distinguish *Dyslocosaurus* from

4492 *Diplodocus*, but is here included in a phylogenetic analysis for the first time.

4493 C452: Astragalus, mediolateral width to maximum anteroposterior length ratio: 1.6 or greater

4494 (0); < 1.6 (1) (Sander et al., 2006; modified; Tab. S56).

4495 C453: Astragalus, ascending process length: limited to anterior two-thirds of astragalus

4496 anteroposterior width (0); extends beyond two-thirds of astragalus anteroposterior width

4497 (normally to posterior margin of astragalus) (1) (Wilson and Sereno, 1998; Wilson, 2002;

4498 modified by Mannion et al., 2012; Fig. 139).

4499 C454: Astragalus, fibular facet: faces laterally (0); faces posterolaterally, anterior margin

4500 visible in posterior view (1) (Whitlock, 2011a; Fig. 139).

4501 C455: Astragalus, laterally directed ventral shelf underlies distal end of fibula: present (0);

4502 absent (1) (Mannion et al., 2013; based on Wilson and Upchurch, 2009; Fig. 139).

4503 **Comments.** The ventral shelf only underlies a part of the fibula.

4504 C456: Astragalus, anteromedial corner in posterior view: short and blunt (0); elongate and

4505 narrow (1) (New; Fig. 139).

4506 **Comments.** The short and blunt shape is a somewhat intermediate state between triangular

4507 and rectangular outlines, as described in character 449.

4508 C457: Calcaneum: proximodistally compressed (0); globular (1) (Harris and Dodson, 2004).

4509 **Comments.** *Suuwassea* has a globular calcaneum, whereas most other sauropods that

4510 preserve calcanea have dorsoventrally compressed elements. These bones are very rarely

4511 preserved, and were even proposed to be absent in diplodocids (McIntosh, 1990b; Upchurch,

4512 1998). However, Bonnan (2000) reported a probable calcaneum from *Diplodocus*, and also an

4513 apatosaur specimen from Como Bluff, Wyoming (NHMUK R.3215) appears to show such an

4514 element (ET, pers. obs., 2011).

4515 C458: Metatarsals, metatarsal I to metatarsal V proximodistal length ratio: 1.0 or greater (0);

4516   < 1.0 (1) (Mannion et al., 2013; polarity reversed; Tab. S57).

4517   **Comments.** Length is measured between parallel lines through the proximal- and distal-most

4518   points of the metatarsals.

4519   C459: Metatarsal I, dorsal/anterior surface: without foramina (0); several foramina present (1)

4520   (New; Fig. 140).

4521   C460: Metatarsal I proximal articular surface, transverse axis orientation: angled

4522   ventromedially approximately 15º to (0); perpendicular to axis of shaft (1) (Wilson, 2002;

4523   modified by Carballido et al., 2012b; polarity reversed; Fig. 140).

4524   **Comments.** The original character (Wilson, 2002) was split into two by Carballido et al.

4525   (2012b), because some specimens have one of the two articular surfaces in an angle to the

4526   long axis of the shaft, and the other one perpendicular. Herein, polarity was reversed due to

4527   the different taxon sampling.

4528   C461: Metatarsal I, robustness (proximal transverse width/greatest length): relatively gracile,

4529   < 0.8 (0); robust, 0.8 or more (1) (Upchurch et al., 2004a; modified; Tab. S58).

4530   C462: Metatarsal I distal articular surface, transverse axis orientation: angled dorsomedially

4531   to (0); perpendicular to axis of shaft (1) (Wilson, 2002; modified by Carballido et al., 2012b;

4532   polarity reversed; Fig. 140).

4533   C463: Metatarsal I distal condyle, posterolateral projection: absent (0); present (1) (Berman

4534   and McIntosh, 1978; see Fig. 140).

4535   **Comments.** All taxa where the posterolateral corner of the distal articular surface can be seen

4536   in anterior view are scored as apomorphic.

4537   C464: Metatarsal I, distolateral projection, if present: small and blunt, not projecting

4538   considerably lateral to dorsal edge of distal articular surface (0); prominent and pointed,

4539   reaching significantly more laterally than dorsal edge of distal articular surface (1) (McIntosh,

4540   1990b; Fig. 140).

4541   **Comments.** Usually, a prominent posterolateral or distolateral projection exceeds the lateral

4542   expansion of the proximal articular surface in anterior view.

4543   C465: Metatarsals I-III, rugosities on dorsolateral margins near distal ends: absent (0); present

4544   (1) (Upchurch, 1995).

4545   **Comments.** A second character (C468) accounts for the strength of the rugosity on mt II (see

4546   Fig. 141).

4547   C466: Metatarsal II, robustness (mean proximal and distal transverse breadth /maximum

4548 length): slender, <0.53 (0); intermediate, 0.53-0.65 (1); robust, >0.65 (2) (McIntosh et al.,
4549 1992; Tab. S58).

4550 **Comments.** The robustness of metatarsal II was used by McIntosh et al. (1992) to distinguish
4551 between diplodocids, but has never been included in a phylogenetic analysis. The character is
4552 treated as ordered.

4553 C467: Metatarsal II, lateral margin in proximal view: concave (0); straight (1) (Mannion et al.,
4554 2013; Fig. 142).

4555 **Comments.** The medial margin is usually concave. With the lateral margin being concave as
4556 well, the outline of the proximal articular surface of mt II becomes somewhat hourglass-
4557 shaped.

4558 C468: Metatarsal II, rugosity on dorsolateral margin near distal end (if present): shallow (0);
4559 well-developed, extending to center of shaft (1) (New; Fig. 141).

4560 **Comments.** The development of the rugosities in mt I to III differs within the pes (mt II
4561 bearing the most prominent ridge), but more so between taxa. This is exemplified by the well-
4562 developed, rugose ridge of the metatarsal in *Dyslocosaurus polyonychius* AC 663, which
4563 extends almost to the center of the shaft. Taxa without any rugosities are scored as unknown.

4564 C469: Metatarsal II distal condyle, posterolateral projection: absent (0); present (1) (New;
4565 Fig. 141).

4566 **Comments.** The distribution of the posterolateral projection in mt II was discussed by Nair
4567 and Salisbury (2012).

4568 C470: Metatarsal IV, proximal articular surface, outline: L- to V-shaped, with distinctly
4569 concave posterolateral edge (0); subtriangular (1) (New; Fig. 143).

4570 C471: Metatarsal V, proximal articular surface, shape: triangular (0); rhomboid (1) (New; Fig.
4571 144).

4572 C472: Metatarsal V proximal end to distal end maximum mediolateral width ratio: 1.6 or
4573 greater (0); < 1.6 (Mannion et al., 2013; Tab. S58).

4574 **Comments.** Transverse width was measured between parallel vertical lines through the
4575 medial- and lateral-most points of the articular surfaces.

4576 C473: Pes, phalanx I-1: proximal and ventral surfaces meet at approximately 90° (0);
4577 proximoventral corner drawn out into thin plate underlying metatarsal I (1) (McIntosh et al.,
4578 1992; Fig. 145).

4579 C474: Pes, phalanx I-1, distal articular surface shape: wide, maximum transverse width > 1.1

4580 times anteroposterior height (0); narrow, maximum transverse width 1.1 times anteroposterior

4581 height or less (1) (New; Tab. S59).

4582 C475: Pes, phalanx II-2: well developed and subrectangular in dorsal view (0); reduced, with

4583 an irregular D-shaped outline and proximal and distal articular surfaces that meet virtually

4584 along dorsal and plantar margins (1) (McIntosh et al., 1992).

4585 C476: Pes, phalanges III-1 and IV-1: equal to longer than wide (0); wider than long (1)

4586 (McIntosh et al., 1992; Tab. S59).

4587 **Comments.** The greatly elongate php IV-1 of the early juvenile SMA 0009 indicates that

4588 phalanges grow allometrically during early ontogeny.

4589 C477: Pedal unguals, groove on lateral surface: follows curvature of claw (0); straight

4590 horizontally (1) (New; Fig. 146).

4591

Results

4593 The first iteration of the analysis yielded 184 most parsimonious trees with a score of 1,897

4594 steps. The second iteration using the command bbreak increased this number to 41,000 (more

4595 was not possible due to computer limitations). Overall CI and RI were calculated in WinClada

4596 (version 1.00.08, www.cladistics.com), and are equal to 27, and 58, respectively. The strict

4597 consensus tree had twelve nodes, which are exclusively located outside Diplodocidae,

4598 meaning that all ingroup specimens formed one big polytomy (Fig. 147). Deleting the six

4599 most unstable taxa ☰ osteriori, the higher-level clades within Flagellicaudata can be observed

4600 (Dicraeosauridae, Apatosaurinae, and Diplodocinae; Fig. 148). The equally weighted reduced

4601 consensus tree includes 51 from the originally 76 taxa. The classical diplodocid genera as

4602 used in earlier phylogenetic analyses (Whitlock, 2011a; Mannion et al., 2012; Tschopp and

4603 Mateus, 2013b) are all visible (Fig. 149).

4604 Diplodocoidea forms the sister-taxon to Titanosauriformes, with *Camarasaurus* and

4605 Turiasauria forming a more basal clade. This result contradicts most of the recent analyses on

4606 sauropods, and in particular studies on early macronarian phylogenetic relationships

4607 (Carballido et al., 2012b; D'Emic, 2012; Mannion et al., 2013), and appears to corroborate

4608 preliminary results from Upchurch (2009) and Mateus et al. (2011), which recovered

4609 Macronaria as polyphyletic. However, many important taxa and characters usually defining

4610 Macronaria are missing in the present tree, due to the focus on Diplodocoidea. ~~Since~~Because

4611 diplodocoid synapomorphies are often shared with derived titanosauriforms, these characters

4612 probably pulled the entire clade into a closer relationship with Diplodocoidea.

4613 Within Diplodocoidea, Rebbachisauridae forms the most basal clade, followed by

4614 Dicraeosauridae (including *Suuwassea emilieae*), and the Diplodocidae. Diplodocidae are

4615 divided into Apatosaurinae and Diplodocinae. The newly described genera *Kaatedocus* and

4616 *Galeamopus* are deeply nested within Diplodocinae. Taxonomically important specimens not

4617 represented in the equally weighted reduced consensus tree are YPM 1920 (genoholotype of

4618 *Diplodocus*), YPM 1980 (genoholotype of *Brontosaurus*), and CM 566 (genoholotype of

4619 *Elosaurus*).

4620 The single most unstable taxon as recovered by the pruned trees approach was *Diplodocus*

4621 *lacustris* YPM 1922. By excluding this taxon from the strict consensus tree, twelve more

4622 nodes were resolved (*Australodocus* in a trichotomy with *Brachiosaurus* and *Giraffatitan*, a

4623 polytomous Dicraeosauridae including *Dyslocosaurus* and *Suuwassea, Dinheirosaurus* +

4624 *Supersaurus*, an apatosaur clade comprising the new sister arrangement *Elosaurus parvus* CM

4625 566 + UW 15556, and a diplodocine clade including a branch with CM 3452, *Barosaurus*,

4626 and *Kaatedocus*). *Diplodocus lacustris* YPM 1922 was shown to group with a large number

4627 of OTUs, mostly within Flagellicaudata, as exemplified by the large polytomy of the reduced

4628 consensus tree including the specimen. As YPM 1922 is a teeth-only specimen, the result

4629 mentioned above indicates that flagellicaudatan teeth cannot be distinguished at the present

4630 state of knowledge.

4631 The analysis done under implied weighting yielded 202 most parsimonious trees of a length

4632 of 187.97214, but the number was increased by the second iteration of tree branch swapping

4633 to 41,000, as in the first analysis with equal weighting. However, the strict consensus tree

4634 preserved 24 nodes, ~~the~~ double ~~of~~that for the first version (Fig. 150). The pruned tree analysis

4635 with implied weights confirmed that the *Diplodocus lacustris* holotype specimen (YPM 1922)

4636 is the least stable. Deletion of YPM 1922 results in 29 gained nodes, compared to the strict

4637 consensus tree. Omission of the least stable quartet (*D. lacustris* YPM 1922, the diplodocine

4638 skulls CM 11161 and USNM 2672, and the braincase SMA O25-8) resulted in a pruned

4639 consensus tree with 36 nodes more than the complete strict consensus tree, and 17 nodes more

4640 than the pruned tree with equal weighting, where six specimens were deleted a posteriori (Fig.

4641 151). The reduced consensus tree with implied weights includes 66 taxa, 15 more than the

4642 equally weighted reduced consensus tree (Fig. 152).

4643 Implied weighting leads to an exclusion of *Cetiosauriscus stewarti* and *Barosaurus affinis*

from Diplodocoidea, and even Neosauropoda. 'Apatosaurus' minimus is recovered within Somphospondyli. Inside Diplodocinae, *Dinheirosaurus* is separated from *Supersaurus*, which groups with *Australodocus* instead. The clade *Eobrontosaurus + Amphicoelias* is split here, with the latter resolved as most basal diplodocid. Finally, an apatosaurine clade including the genoholotypes of *Brontosaurus*, *Dystrophaeus* and *Elosaurus* is found.

Symmetric resampling did not find much support for ingroup clades (Tab. S60), most probably due to the littleminimal anatomical overlap. However, it found support for three clades that were not recovered in any of the six main trees: the grouping of the two diplodocine skulls USNM 2672 and CM 11161 (resampling value of 12), a dichotomy of holotype and paratype of *Diplodocus carnegii* (CM 84 and 94, resampling value 8), and a clade including the holotypes of *Apatosaurus louisae* and *A. laticollis*, as well as the specimen CM 3378 (resampling value of 15). The latter two clades are actually found in trees excluding *D. longus* YPM 1920 or *Brontosaurus amplus* YPM 1981, respectively. The grouping of the two skulls CM 11161 and USNM 2672 indicates that they are more similar to each other than to any other diplodocine skull. ▤

Discussion

The phylogenetic history of Diplodocidae

Most Eearlier phylogenetic studies of sauropods mostly just included the three genera *Apatosaurus*, *Diplodocus*, and *Barosaurus* (e.g. Upchurch, 1998; Wilson, 2002; Upchurch et al., 2004a). More recent analyses with a narrower focus on diplodocoid intrarelationships included more diplodocid species (Upchurch et al., 2004b; Rauhut et al., 2005; Remes, 2006; Lovelace et al., 2007; Sereno et al., 2007; Whitlock, 2011a; Carballido et al., 2012b; Mannion et al., 2012; Tschopp and Mateus, 2013b). However, other than Upchurch et al. (2004b), all of them included the genera *Apatosaurus* and *Diplodocus* as OTU, rather than their component species, and no analysis was ever done with all proposed diplodocid species (Fig. 153). Basic relationships between diplodocid taxa generally remained the same among the studies, which is probably a consequence of the fact that most were based on Wilson (2002), with only minor changes (Rauhut et al., 2005; Remes, 2006; Lovelace et al., 2007; Sereno et al., 2007). The greatest changes between these four phylogenetic analyses occur in the position of *Suuwassea*, which is recovered within Apatosaurinae (Lovelace et al., 2007), in a polytomy with *Apatosaurus* and Diplodocinae (Remes, 2006), just outside Apatosaurinae + Diplodocinae (Rauhut et al., 2005), or in a trichotomy with Diplodocidae and Dicraeosauridae

4676 (Sereno et al., 2007). Of the remaining diplodocid taxa other than *Apatosaurus*, *Diplodocus*,

4677 or *Barosaurus*, only *Tornieria* was included in more than one of these four analyses, and

4678 found within Diplodocinae (Rauhut et al., 2005; Remes, 2006).

4679 Given the strong focus on interspecific relationships of *Apatosaurus*, Upchurch et al. (2004b)

4680 had a very reduced dataset, with only 16 taxa and 32 characters. The character list was

4681 assembled based on earlier descriptions and diagnoses of the different species (mostly Riggs,

4682 1903; Holland, 1915a; Gilmore, 1936), with some original characters added (Upchurch et al.,

4683 2004b). Whitlock (2011a), although ~~basing~~based in part on Wilson (2002), can be considered

4684 a new analysis as well, given the large number of modifications and added characters, and the

4685 largely increased number of taxa in order to be able to resolve diplodocoid intrarelationships.

4686 Subsequently published analyses (Mannion et al., 2012; Tschopp and Mateus, 2013b) thus

4687 were ~~consequently~~ based on Whitlock (2011a).

4688 The present analysis further increases both taxon and character lists of Whitlock (2011a) by

4689 almost 300% and 250%, respectively (76 versus 26 OTUs, 477 versus 189 characters), and

4690 can thus be considered largely independent as well. Nonetheless, most of the positions of the

4691 common genera included in the analyses remained the same. The analyses thus generally

4692 corroborate each other.

4693 **Difficulties and possibilities of a specimen-based analysis**

4694 **Anatomical overlap.** A specimen-based phylogenetic analysis has both drawbacks and

4695 advantages. One of the major problems is the ~~lacking~~lack of anatomical overlap, most

4696 importantly between incomplete historic holotype specimens. In particular ~~in~~for diplodocid

4697 sauropods, the majority of the type specimens ~~was~~were described by Marsh and Cope during

4698 the so-called "Bone Wars" (Cope, 1877a, b; Marsh, 1877a, 1878, 1879, 1881, 1884, 1890,

4699 1899). New species were rushed into press without detailed description, sometimes even

4700 lacking illustrations (e.g. Marsh, 1881, 1899). In certain cases, subsequent studies revealed

4701 that different species were erected based on different bones of possibly the same skeleton

4702 ('*Atlantosaurus*' *immanis* YPM 1840 and *Apatosaurus laticollis* YPM 1861; Marsh, 1877a,

4703 1879; McIntosh, 1995). More complete skeletons were later recovered, but many of these still

4704 lack a description, and were identified as a particular genus or species without any detailed

4705 study (e.g. '*Diplodocus longus*' DMNS 1494). Lately, more and more nearly complete

4706 specimens are becoming available for study (e.g. Harris and Dodson, 2004; Upchurch et al.,

4707 2004b; Tschopp and Mateus, 2013b; Barrett et al., 2011). Complete, articulated specimens, or

4708 parts of skeletons preserving portions underrepresented in earlier finds (e.g. skulls attached to
4709 their necks, transitions from cervical to dorsal vertebrae, articulated manus or pedes), are
4710 crucial for a specimen-based phylogenetic analysis. They provide the anchorage with which
4711 fragmentary specimens can be compared, thereby allowing for indirect comparisons. Care has
4712 to be taken to include articulated specimens and exclude information from portions of the
4713 skeleton for which an unambiguous association with the specimen to be studied cannot be
4714 ascertained. The most valuable documents to assure genuine association of skeletal parts to
4715 one individual are detailed quarry maps and field notes, but these are often lacking in historic
4716 type specimens. However, efforts were made lately to unravel excavation stories and bone
4717 associations of the most important holotype specimens (e.g. McIntosh, 1990a, 1995; McIntosh
4718 and Carpenter, 1998). The present study heavily relies on these earlier studies to confirm or
4719 discard bone associations. However, certain specimens would still need such a detailed
4720 overhaul, and their phylogenetic positions has still to be regarded provisional (see below).
4721 **Deformation.** An additional problem, for quantitative characters in particular, ~~are~~is specimen
4722 deformation ~~deformed specimens~~. Whereas brittle deformation can be readily identified due
4723 to the introduced cracks, plastic deformation results in unfractured, but distorted fossils
4724 (Tschopp et al., 2013). If plastic deformation happens symmetrically, it is almost impossible
4725 to identify, and least of all to quantify. Retrodeformation can yield some information on how
4726 bones were deformed, but only in bilaterally symmetrical elements (Arbour and Currie, 2012;
4727 Tschopp et al., 2013). For species- or genus-level phylogenetic analyses, mean ratios can be
4728 taken from different individuals of the same taxon, thereby approaching more closely the
4729 ratios generally typical for that taxon. In specimen-based analyses, such an approach is not
4730 possible. However, if a specimen is deformed in such a way that it would be scored
4731 differently from closely related species, or specimens from the same species, it increases
4732 homoplasy of this single character, and decreases its consistency index. By using implied
4733 weighting, as was done in the second analysis herein, this can be partly accounted for.
4734 **Morphological details.** During the study of single specimens, one usually records and
4735 describes morphological details unique to the animal, which might or might not be
4736 taxonomically significant. If the phylogenetic analysis accompanying the description recovers
4737 the new specimen on a separate branch and thus as new taxon, these traits are generally
4738 interpreted as autapomorphic for the new taxon. The confirmation of such an interpretation
4739 can only be made with the discovery of additional specimens of the same species, preserving

4740 the same portions of the skeleton. Before that, variation due to any pre- or post-mortem

4741 processes (ontogeny, individual variation, sexual dimorphism, or taphonomic deformation)

4742 cannot be excluded with certainty as a cause for the morphological disparity found in the

4743 fossil. Specimen-based phylogenetic analyses are the only way to test for such variation. As

4744 mentioned above, highly homoplastic characters ~~are describing~~describe the most variation, in

4745 the case of a specimen-based analysis between individuals. They are thus the most

4746 ~~probable~~liekly to code for individual variation, and should thus either be deleted or

4747 downweighted compared to the less variable characters▦is done by implied weighting

4748 (Goloboff, 1993). Because it cannot be excluded that characters describing individual

4749 variation in some groups actually code for taxonomically significant differences in other taxa,

4750 downweighting the characters in question appears more accurate than deleting them entirely.

4751 Finally, by scoring single specimens of a species, and thereby detecting individual variation in

4752 some characters, researchers create a firmer base for how to score species- or even genus-

4753 level OTUs.

4754 **Validity of recovered diplodocoid subclades**

4755 The following discussion includes only the clades recovered within Diplodocoidea, ~~as~~because

4756 the present analysis was designed for the study of diplodocid intrarelationships, and is thus

4757 not suitable for inferring phylogenetic positions and definitions for clades recovered outside

4758 Diplodocoidea. The systematic affinities of ~~single~~individual specimens included in the

4759 analysis~~, which~~ that are recovered outside of Diplodocoidea~~,~~ are discussed below. Definitions

4760 of the clade names follow Taylor and Naish (2005) and Whitlock (2011a).

4761 One of the problems raised in a specimen-based phylogenetic analysis is where to draw the

4762 line between individual variation, and differences on species or genus level. The decision for

4763 specific versus generic separation is somewhat arbitrary, in particular in paleontology, where

4764 no tests exist for the biological species concept (Carpenter, 2010). If qualitatively assessing

4765 the validity and significance of single characters, subjectivity of the interpretation as separate

4766 species or genus is even more increased. In order to avoid subjectivity at least in part~~s~~, a

4767 quantitative approach was developed. With a numerical approach, personal influence can be

4768 minimized, and the process of generic separation can be rendered more repeatable and thus

4769 scientifically sound. The herein proposed approach ~~bases~~is based on the number and quality

4770 of 'synapomorphies' and 'autapomorphies', as found by the software TNT. Because the

4771 analysis is specimen-based, one has to keep in mind that these do not conform to real species

or genus autapomorphies or synapomorphies, but described unique or shared morphological features of specimens or groups of specimens. In the following, these 'false' apomorphies found by TNT are thus mentioned in quotation marks. The qualitative assessment of the apomorphies, as outlined below, counts for both real and 'false' apomorphies, however. Synapomorphies are separated into four, qualitatively different categories. Unambiguous synapomorphies are shared by all ingroup members of the respective clade, and only by them. Exclusive synapomorphies only mark ingroup members, but not all of them. Shared synapomorphies are present in all ingroup members, but also occasionally occur in taxa outside the clade in question. Ambiguous synapomorphies are neither exclusive, nor shared by all ingroup members, but are still recovered as synapomorphies by at least one analysis with equal and one with implied weighting. Ambiguous synapomorphies recovered by only one type of analysis (equal or implied weighting) are not considered reliable. Specimen 'autapomorphies' are divided into unambiguous, or ambiguous (shared with other taxa). Autapomorphies found by only reduced consensus trees, but no pruned tree are considered invalid, or at least dubious, asbecause more specimens potentially bearing the same morphology are excluded from reduced trees compared to pruned trees. Also, autapomorphies of apatosaurine specimens, which are shared with other apatosaurine specimens or clades (or diplodocine with diplodocine) are interpreted as inappropriate for species diagnosis.

'Synapomorphies' of diplodocid genera and species generally considered valid were then counted and summed between sister taxa (specimens or clades, in this case). A minimum number of synapomorphies was defined for justifying specific or generic separation. The minimum number of needed differences for generic separation was chosen based on the count obtained from the well-established sister genera *Dinheirosaurus* and *Supersaurus*, which are also geographically separated (Portugal, and USA, respectively). The ten differences obtained here were compared with the sum of changes between two species of *Apatosaurus* (*A. ajax* and *A. louisae*) or *Diplodocus* (*D. carnegii* and *D. hallorum*), which were both found to be lower (8 and 9, respectively). Both species were are well established in the literature, and recovered as sister taxa in the presentour analysis. A third count of changes was made between specimens from the same species (*D. carnegii* CM 84 and CM 94, and *A. louisae* CM 3018 and CM 3378). As for the chosen species, also the used specimens were generally considered the same species in the past, and recovered as such in the present analysis. The

4804 sum of changes between these specimens amounts to one. A minimum of ten differences is
4805 thus considered enough for genus-level separation, whereas for species, a margin of five
4806 changes is given in order to account for individual variation (which is already accounted for
4807 by the evaluation of the validity of the autapomorphies, but a wider margin is preferred herein
4808 in order to be more cautious). The precise numbers established here (5 and 10 changes)
4809 cannot be applied to any other analysis, even of the same clade, ~~as~~because the recovery of
4810 'autapomorphies' and 'synapomorphies' depends on the number of characters included in the
4811 analysis~~,~~ and also on the software used. However, the general approach can be used in other
4812 analyses as well.

4813 The discussion of the various clades recovered is done following a bottom-up approach,
4814 starting with dichotomies between single specimens. This is preferred over a top-down
4815 approach, because it is the specimens that define the taxa, not the taxa that determine the
4816 affiliation of the specimen. Based on the validity of the recovered dichotomies between single
4817 specimens, species and finally genera and higher-level taxa can be evaluated more accurately.

4818 *Barosaurus lentus* **YPM 429 + AMNH 6341.** These two specimens were recovered as sister
4819 taxa in all pruned and reduced trees. It has a relatively high resampling value and is supported
4820 by four shared 'synapomorphies' (Tabs S60, S61). All four 'synapomorphies' were
4821 ~~resulting~~recovered as such by every analysis recovering this clade. Whereas the two
4822 'synapomorphies' are only shared with taxa outside Diplodocoidea (with the possible
4823 exception of *Australodocus bohetii*, see below), the other two are also shared with various
4824 specimens within Diplodocidae, or even Diplodocinae. The two specimens are separated by
4825 one change only, indicating that they belong to the same species.

4826 **CM 11984 + (*Barosaurus lentus* YPM 429 + AMNH 6341).** All four trees show this
4827 grouping~~,~~ and found one shared and an ambiguous 'synapomorphy' defining it (Tabs S60,
4828 S62). The ambiguous 'synapomorphy' (prezygapophyseal centrodiapophyseal fossa of mid-
4829 and posterior cervical vertebrae subdivided into various smaller partitions by several
4830 accessory laminae; C184-2) is not present in a mid-cervical vertebra in storage at AMNH, but
4831 the determination of presence or absence of accessory laminae was not possible for posterior
4832 cervical vertebrae on public display. Further studies are needed to clarify this. Both of these
4833 'synapomorphies' are shared with other diplodocine specimens, and ~~do~~ therefore do not
4834 classify as species autapomorphies. No valid 'autapomorphy' separates CM 11984 from the
4835 other two specimens, which are thus interpreted to belong to the same species.

AMNH 7535 + (CM 11984 + (*Barosaurus lentus* YPM 429 + AMNH 6341)). As for the two clades discussed above, ~~also~~ the present arrangement also was recovered by all four trees. Statistical support for it is lower, and only one shared 'synapomorphy' is found (Tabs S60, S63). This 'synapomorphy' (very elongate mid-cervical vertebrae) is the best known and most widely used trait to distinguish *Barosaurus* from *Diplodocus* (e.g. McIntosh, 2005). The lack of other synapomorphies is probably due to the very restricted overlap in the four specimens of this clade, but also with restricted overlap with the closest sister group (*Kaatedocus siberi* SMA 0004 + (SMA D16-3 + AMNH 7530)), which is only known from neck and skull material. Neither delayed nor accelerated transition (DELTRAN and ACCTRAN, respectively) approaches are thus able to find more 'synapomorphies' for either clade, but more probably ~~more~~ will be recovered when it will be possible to add more specimens preserving overlapping material. The number of changes does not allow the erection of different species. ~~Since~~Because the entire clade only includes the holotype specimen of *Barosaurus lentus* (YPM 429), all specimens are herein referred to that species.

SMA D16-3 + AMNH 7530. This clade is not supported by any 'synapomorphy', but is recovered in all four trees. The latter is mainly due to the fact that SMA 0004 (the sister specimen of the current clade) has some morphological features in common with more basal diplodocine specimens, which are ~~not present~~absent in SMA D16-3 or AMNH 7530. ~~Given that~~Because both specimens of this group do not show any specimen 'autapomorphies', a referral to the same species can be regarded as well-supported.

***Kaatedocus siberi* SMA 0004 + (SMA D16-3 + AMNH 7530).** The current triplet constitutes the sister group to the *Barosaurus lentus* clade discussed above. It is found in all four trees~~,~~ and supported by a resampling value of 14, one higher than the clade CM 11984 + (YPM 429 + AMNH 6341) (Tab. S60). Nine shared 'synapomorphies' are recovered (Tab. S64). One additional unambiguous autapomorphy of the genus was proposed by Tschopp and Mateus (2013b), but not recovered as such by the present analyses: a transverse sulcus bordering the prezygapophyseal facets of posterior cervical vertebrae posteriorly. This feature was impossible to code ~~for~~in the other two specimens of *Kaatedocus siberi*, which was probably the reason why it was not found as a synapomorphy or autapomorphy herein. However, SMA 0004 is the only specimen positively scored for its presence in the current analysis, indicating that one more synapomorphy, possibly unambiguous for this clade, might be present. Not counting this, the nine shared 'synapomorphies' of *K. siberi* plus the single 'synapomorphy' of

the sister clade *Barosaurus lentus* sum to ten, which is deemed enough for generic separation (see above). Within *Kaatedocus*, one change separates SMA 0004 from the other two specimens, which are thus referred to the type species *K. siberi*.

Kaatedocus + Barosaurus. The sister arrangement of *Barosaurus* and *Kaatedocus* is herein recovered by both analyses, supported by three shared synapomorphies (Tab. S65). These traits are somewhat problematical, as they concern anterior and mid-cervical vertebrae. Many specimens within Diplodocidae are not represented by anterior cervical vertebrae, and within *Barosaurus*, AMNH 7535 is the only specimen preserving them. Furthermore, overlap between *Kaatedocus* and *Barosaurus* is low. However, differences in the heights of anterior neural spines are very pronounced when comparing *Kaatedocus* SMA 0004 with *Diplodocus* CM 84 or *Galeamopus* SMA 0011, the two genera most closely related to *Kaatedocus + Barosaurus* within Diplodocidae. Dorsoventrally elongate coels on the lateral side of the neural spines are typical for posterior cervical vertebrae of *Diplodocus*, among others, but in this genus, these coels are not present in anterior elements. In *Kaatedocus* and *Barosaurus* AMNH 7535, the serial pattern is inverted, and the coels only mark anterior elements. Additional synapomorphies, in particular from appendicular bones, might be found once a more complete specimen of *Kaatedocus siberi* is described.

CM 3452 + (Kaatedocus + Barosaurus). Before the description of *Kaatedocus siberi* SMA 0004, the specimen CM 3452 was the only diplodocid preserving an almost complete skull in articulation with the most anterior, postaxial cervical vertebrae. Although generally identified as *Diplodocus* (Holland, 1924; McIntosh and Berman, 1975; Whitlock et al., 2010), CM 3452 is recovered as sister taxon to *Barosaurus + Kaatedocus* in all four trees found here. The affiliation of CM 3452 with this group is supported by one unambiguous, nine shared, and one ambiguous synapomorphies. None of these are present in any specimen recovered within the *Diplodocus* clade (Tab. S66). The lateral lacrimal spur recovered as unambiguous synapomorphy for this clade was proposed as an autapomorphy of *Kaatedocus* (Tschopp and Mateus, 2013b), and is actually not unambiguous among sauropods: Tschopp and Mateus (2013b) reported a specimen of *Camarasaurus* (SMA 0002), which shows a similar trait, as do some other camarasaur lacrimals (Madsen et al., 1995). However, within Diplodocidae, of the few skulls known, only CM 3452, SMA 0004, and CM 11255 bear such a spur (Tschopp and Mateus, 2013b). If the feature gets confirmed to diagnose this group, also CM 11255 would have to be referred to it, instead of being identified as *Diplodocus* (Whitlock et al.,

4900 2010). Although tree topologies suggests that CM 3452 constitutes its own genus, the low

4901 number of four changes between the specimen and the *Kaatedocus + Barosaurus* clade does

4902 not support an erection of a new genus nor a species.

4903 **DMNS 1494 + USNM 10865.** These two specimens traditionally referred to *Diplodocus*

4904 (Gilmore, 1932; McIntosh, 2005) are recovered as sister taxa in both trees obtained with

4905 implied weighting, as well as the reduced consensus with equal weighting. The equally

4906 weighted pruned consensus tree shows a polytomy formed by all putative *Diplodocus*

4907 specimens and the clade CM 3452 + mdD. This is probably a consequence of the

4908 incompleteness of important specimens like *D. longus* YPM 1920, or the skulls CM 11161

4909 and USNM 2672. The clade DMNS 1494 + USNM 10865 is supported by a resampling value

4910 of nine (Tab. S60), and one shared 'synapomorphy' (Tab. S67), which is a single instead of

4911 two parallel pcpl in mid- and posterior dorsal neural arches, as present in other *Diplodocus*

4912 specimens. As only one change separates DMNS 1494 from USNM 10865, the two

4913 specimens are referred to the same species.

4914 *Seismosaurus hallorum* **NMMNH 3690 + (DMNS 1494 + USNM 10865).** The current

4915 triplet is found in the equally weighted reduced consensus tree, as well as in both pruned and

4916 reduced consensus trees when applying implied weights. It has a resampling value of six

4917 (Tab. S60), and is supported by one shared 'synapomorphy' (Tab. S68). The four changes

4918 separating *S. hallorum* from the clade DMNS 1494 + USNM 10865 are not enough to justify

4919 the erection of two different species, therefore the entire triplet is referred to the same species.

4920 **AMNH 223 + (*Seismosaurus hallorum* NMMNH 3690 + (DMNS 1494 + USNM 10865)).**

4921 As for the two more exclusive clades discussed above, the present quartet of specimens is

4922 recovered in all trees but the equally weighted pruned tree. It has a resampling value of six

4923 (Tab. S60), and one unambiguous and five shared 'synapomorphies', which distinguish it from

4924 the other *Diplodocus* specimens (Tab. S69). One of these 'synapomorphies' (a subtriangular

4925 process on the scapular blade) also occurs in other diplodocines. Three changes are recovered

4926 between AMNH 223 and the remaining triplet, indicating that they belong to the same

4927 species, as was already suggested by McIntosh (2005).

4928 Sister specimens recovered as such are *D. longus* YPM 1920 in the reduced consensus using

4929 implied weighting, and *D. carnegii* CM 84 + CM 94 in the equally weighted reduced

4930 consensus tree with CM 94 added. Nine changes lie between the *D. carnegii* pair and the

4931 clade discussed herein, whereas only six changes are recovered between the current clade and

4932 *D. longus.* ~~As~~Because both of these remain below the ten changes set as sufficient for genus-

4933 level separation, *Seismosaurus* is here considered a synonym of *Diplodocus*, but as its own

4934 species *D. hallorum*, including the specimens AMNH 223, DMNS 1494, NMMNH 3690, and

4935 USNM 10865.

4936 ***Diplodocus longus*** **YPM 1920 +** ***Diplodocus hallorum*.** Of the four main trees, only the

4937 reduced consensus tree with implied weighting recovered this arrangement~~, but~~. However, by

4938 substituting *D. carnegii* CM 84 by *D. longus* YPM 1920 in the equally weighted reduced

4939 consensus tree, the same result is obtained. Such a grouping, where *D. longus* + *D. hallorum*

4940 form the sister clade to *D. carnegii* CM 84 + CM 94 is not supported by any 'synapomorphy'.

4941 In fact, when adding either the holotype or the paratype specimen of *D. carnegii*, a polytomy

4942 is recovered between CM 84, CM 94, YPM 1920 and *Diplodocus hallorum*, as can be seen in

4943 the pruned consensus tree using implied weighting.

4944 ***Diplodocus carnegii*** **CM 84 + CM 94.** Although not recovered in the four main trees

4945 discussed here, symmetric resampling yielded a value of eight for this clade (Tab. S60)~~, and i~~.

4946 Indeed, when deleting YPM 1920 and adding CM 84 and CM 94 to the reduced consensus

4947 trees, the clade discussed here forms the sister group to *D. hallorum* as discussed above. The

4948 clade is supported by three shared 'synapomorphies', which are all absent in any specimen

4949 referred to *D. hallorum* above (Tab. S70). Together with the six synapomorphies of the *D.*

4950 *hallorum* clade, this amounts to nine changes, which allows erection of different species but

4951 not genera, following the guidelines established above. The recovery of this clade in the

4952 extended reduced consensus trees confirms Hatcher's (1901) assignment of CM 94 as

4953 paratype of the species *D. carnegii*. Both specimens were found in the same stratigraphic

4954 level of the same quarry (Hatcher, 1901).

4955 ***Diplodocus carnegii*** **+** ***Diplodocus hallorum*.** The grouping of these two species within the

4956 genus *Diplodocus* occurs in all trees excluding the skull specimens CM 11161 and USNM

4957 2672. When including *D. longus* YPM 1920 as well, the grouping of CM 84 and 94 is split,

4958 and a polytomy is formed as explained above. All of these specimens are united by six shared

4959 and one unambiguous 'synapomorphies' (Tab. S71). One of these 'synapomorphies' is shared

4960 with ~~one~~a single specimen of *Barosaurus lentus* (anteroposterior width of mid- and posterior

4961 dorsal neural spines remains approximately constant along the height of the spine; C265-0,

4962 shared with YPM 429), and an additional one is shared with a specimen of *Galeamopus*, the

4963 genus forming the sister taxon to *Diplodocus* + mdD (anterior end of the sprl of mid- and

posterior cervical vertebrae remains vertical; 182-0, with SMA 0011). ~~As~~Because all trees recovered also include *D. longus* YPM 1920 within this clade, and because *D. longus* is currently regarded the type species of the genus *Diplodocus* (but see below for a more detailed assessment of YPM 1920), the specimens included in the clade are herein referred to that genus. It is separated from its sister clade CM 3452 + mdD by 18 changes, and both groups are diagnosed with an unambiguous synapomorphy. Seven synapomorphies of the clade CM 3452 + mdD are based on cranial material, none of which is definitely attributable to the *Diplodocus* clade (2-0, 10-1, 19-1, 48-2, 52-1, 65-1, 67-1). All of these traits are different from the two included skulls CM 11161 and USNM 2672, which probably belong to the genus *Diplodocus* (see below for a discussion of their taxonomic affinities). The synapomorphies are thus tentatively retained in the count for the changes between the clades, and the 17 changes between *Diplodocus* and CM 3452 + mdD (excluding the one shared with YPM 429) still confidently justify generic separation.

***Diplodocus* + mdD.** *Diplodocus* is recovered as sister taxon to the clade with *Kaatedocus* and *Barosaurus* in all four principal trees discussed here. It is diagnosed by 13 synapomorphies, of which one is unambiguous, ten are shared, and two are ambiguous (Tab. S72). Four of the shared synapomorphies are unique within Diplodocidae (69-0, 80-0, 154-0, 440-1), and five more within Diplodocinae (196-1, 269-1, 367-0, 381-1, 405-1).

Galeamopus ▮▮▮▮ **SMA 0011 + *Galeamopus hayi* HMNS 175.** All four principal trees show this clade, which is supported by one shared 'synapomorphy' (if strictly following the qualitative assignment of synapomorphies mentioned above; Tab. S73). However, all three trees recovering this synapomorphy exclude the skulls CM 11161, SMA O25-8, and USNM 2672, which all share the same position of the frontal-parietal suture as the *Galeamopus* specimens. When added to the reduced consensus trees, these skulls form polytomies with specimens from *Diplodocus* (CM 11161 and USNM 2672), or *Barosaurus* (SMA O25-8). ~~As~~Because ~~also~~ the skull CM 3452 shows the same morphology, an interpretation of this synapomorphy as diagnosing the clade *Galeamopus* ▮▮▮▮ SMA 0011 + *Galeamopus hayi* HMNS 175 is highly questionable. The clade is thus not diagnosable by any synapomorphy. The two specimens are separated from each other by nine changes, including one unambiguous autapomorphy diagnosing *Galeamopus* ▮▮▮▮ SMA 0011. The high number of differences allows the erection of two species, as suggested in the descriptive part of the thesis: *Galeamopus hayi* as the type species, and *G.* ▮▮▮▮

AMNH 969 + (*Galeamopus hayi* + *G.* ████████ The triplet is recovered in all main trees, and shows a resampling value of two (Tab. S60). It is supported by two unambiguous and two shared 'synapomorphies', which all describe morphological features of the skull, or the atlas-axis complex (Tab. S74). Due to the rare finds of atlantes and axes, these synapomorphies are somewhat dubious, and will have to be assessed in more detail once more complete specimens become available for study. However, the continuous recovery of the same triplet in the same position of all four trees, as well as its higher resampling value compared with most other clades indicates that this grouping forms its own genus. Two changes lie between AMNH 969 and the clade with *G. hayi* + *G.* ████████ therefore not allowing the erection of a third species. The affinities of AMNH 969 will be discussed in more detail below.

***Galeamopus* + mdD.** All four trees show the new genus *Galeamopus* as sister taxon to the clade with *Diplodocus*, *Kaatedocus*, and *Barosaurus*. Two unambiguous, six shared, and two ambiguous synapomorphies diagnose this group (Tab. S75). Only one of the shared synapomorphies is present in other diplodocines as well (posterior dorsal postzygapophyses almost horizontal; C275-0, in ML 418 and *Supersaurus vivianae*), whereas one ambiguous synapomorphy is unique within the sampled Neosauropoda (an accessory spinal lamina in posterior cervical neural arches running vertically just posterior to sprl; C203-1), but *Kaatedocus* autapomorphically bears the reversed state. Between *Galeamopus* and its sister clade *Diplodocus* + mdD, 16 differences are present. One is shared between *Galeamopus* and *Kaatedocus* (47-1), one between *Galeamopus* and the putative *Barosaurus* SMA O25-8 (80-0), a third is present in both SMA 0011 and AMNH 6341 (269-0), and a fourth is shared with CM 94 (367-0). Deleting them from the 16 changes, the remaining twelve are still sufficient for a generic separation.

***Dinheirosaurus* + mdD.** Although *Dinheirosaurus* is recovered in the same relative position in both analyses with equal and implied weighting, the first major difference between the trees of these two analyses is encountered here. Whereas the equally weighted trees show a sister ~~genera~~taxon arrangement of *Dinheirosaurus* and *Supersaurus*, the analyses using implied weighting results in a more basal position of *Supersaurus*. In this paragraph, only the clade excluding *Supersaurus* will be discussed, recovered by applying implied weights. The more parsimonious position of *Supersaurus* will be assessed below. Only one shared 'synapomorphy' supports such an arrangement to the exclusion of *Supersaurus* (Tab. S76). The equally weighted analysis recovers this feature as synapomorphic for the entire

5028 Diplodocidae (in the pruned consensus tree), with a reversal in *Tornieria*. The state is

5029 unknown in *Supersaurus*, due to insufficient information in descriptions, and lacking figures

5030 in anterior view. Future ~~personal~~direct observations of the BYU specimen might clarify its

5031 morphology. The present arrangement yields ten changes between *Dinheirosaurus* and its

5032 sister clade *Galeamopus* + mdD, four more synapomorphies of *Galeamopus* + mdD are not

5033 preserved in the known material from *Dinheirosaurus*.

5034 ***Tornieria africana* holotype + skeleton k.** The earlier referral of these two specimens to

5035 *Tornieria* (Remes, 2006, 2009) is confirmed by both analyses performed herein. They show a

5036 resampling value of four (Tab. S60), and five shared synapomorphies, which all describe

5037 appendicular morphology (Tab. S77). The apparent lack of vertebral characters is due to the

5038 destruction of most putative *Tornieria* vertebrae during World War II (Remes, 2006;

5039 Whitlock, 2011a). A series of caudal vertebrae from trench dd from Tendaguru (MB.R.2956),

5040 referred to *Tornieria* by Remes (2006) was not included into the analysis ~~as~~because concerns

5041 of their attribution to the same individual were raised by Remes (2006). No valid

5042 autapomorphies are recovered for either *Tornieria* specimen, confirming the referral of

5043 skeleton k to the species *T. africana*.

5044 ***Tornieria* + mdD.** A clade with *Tornieria* and more derived Diplodocoidea to the exclusion

5045 of other diplodocine specimens was only recovered in the analysis using implied weighting,

5046 and including all specimens. With equal weights, or by excluding *Australodocus bohetii* from

5047 the analysis with implied weighting a priori, *Tornieria* + mdD corresponds to Diplodocinae.

5048 In the following, the find of the main trees by using implied weights is discussed. One

5049 unambiguous, one exclusive, and one shared synapomorphy are found for this clade (Tab.

5050 S78). Given the more basal position of *Supersaurus* in the implied weight trees, these features

5051 are absent in that genus. Two of the synapomorphies proposed for *Tornieria* + mdD by the

5052 analysis using implied weighting (131-1, 307-1) are also recovered by the equally weighted

5053 trees (for the clade Diplodocinae), with the difference that the unambiguous synapomorphy

5054 becomes exclusive. The same happens when excluding *Australodocus bohetii* from the

5055 implied weights analysis a priori. In the main trees from the analysis with implied weighting,

5056 seven changes separate *Tornieria* from the clade *Dinheirosaurus* + mdD, nine changes are

5057 between *Tornieria* and *Dinheirosaurus*, when adding the autapomorphies of *Dinheirosaurus*

5058 comparable with their states in *Tornieria*. In the equally weighted trees, where the clade

5059 *Tornieria* + mdD corresponds to Diplodocinae, six changes are recovered between *Tornieria*

5060 and *Supersaurus* + mdD. This would not allow the erection of a different genus for *Tornieria*,
5061 but see below for a more detailed taxonomic assessment.
5062 ***Supersaurus vivianae* BYU + WDC DMJ-021.** The unity of the two *Supersaurus* specimens
5063 included in the present analysis is well supported. All four trees show this arrangement, and
5064 resampling yielded a value of 36, which is the highest value reported within Diplodocidae
5065 (Tab. S60). Seven shared 'synapomorphies' define the clade (Tab. S79). Recovery of these
5066 'synapomorphies' highly depends on tree topology, and thus the type of analysis performed. In
5067 the main trees obtained through implied weighting, where *Supersaurus* lies outside *Tornieria* +
5068 mdD, only one 'synapomorphy' (a deep groove extending anteroposteriorly within the lateral
5069 edge posterior to the parapophysis of mid- and posterior cervical vertebrae, C177-1) was
5070 found to unite the two specimens. The split ventrolateral edge is shared with *Dinheirosaurus*,
5071 with which *Supersaurus* groups in all other trees, including the one obtained by implied
5072 weighting, and excluding *Australodocus bohetii* a priori. On the other hand, from the other six
5073 'synapomorphies', three are shared with *Australodocus bohetii* (131-0, 136-1, 172-1), and two
5074 of them result as synapomorphies of this clade as recovered by the main implied weights trees
5075 (see below). In any case, attribution of the two specimens to *Supersaurus* appears well-
5076 supported, and the absence of any valid differences between the specimens confirms the
5077 referral of WDC DMJ-021 to the type species *S. vivianae*, and in turn also corroborates the
5078 assignment of the single bones in the BYU collection to the same individual, as suggested by
5079 Lovelace et al. (2007).
5080 ***Dinheirosaurus* + *Supersaurus*.** A sister taxon relationship of these two taxa to the exclusion
5081 of others is only recovered by using equal weights, or by pruning *Australodocus bohetii* from
5082 the implied weights analysis a priori. In the latter analysis, *Dinheirosaurus* + *Supersaurus* is
5083 the sister clade to the specimen ML 418, with which it forms the sister group to *Galeamopus* +
5084 mdD. Where *Dinheirosaurus* and *Supersaurus* form a clade, they are located within
5085 Diplodocinae, in a position more derived than *Tornieria*. *Dinheirosaurus* + *Supersaurus* is
5086 supported by a resampling value of three (Tab. S60), as well as six shared and one
5087 unambiguous synapomorphies (Tab. S80). One of the shared synapomorphies (a high ratio of
5088 neural spine to pedicel height; C272-1) is present as well in ML 418. *Dinheirosaurus* is
5089 separated from *Supersaurus* by ten changes, and was the main pair of genera on which the
5090 numerical approach of specific and generic distinction was based, given the geographical
5091 distance between the two genera.

5092 ***Australodocus bohetii* type + *Supersaurus*.** Such a group was only recovered in the main

5093 trees of the analysis with implied weighting. There, it is located basal to *Tornieria*, within

5094 Diplodocinae, and thus contrasts with the position of *Supersaurus* when associated with

5095 *Dinheirosaurus*. The more basal position of the clade *Australodocus* + *Supersaurus* is

5096 probably due to the several traits *Australodocus* shares with titanosauriform sauropods.

5097 Resampling does not support the current clade (Tab. S60), which is specified by four shared

5098 synapomorphies (Tab. S81). Two of them are shared with brachiosaurid titanosauriforms

5099 (172-1, 183-1), and actually diagnose the brachiosaurid clade including *Australodocus* in the

5100 pruned tree with equal weighting. The other two synapomorphies recovered for an

5101 *Australodocus* + *Supersaurus* clade (136-1 and 162-1) are not shared with any included taxon

5102 outside Diplodocidae. The two genera are only separated by six changes, which would not

5103 allow generic separation. However, this would only apply if *Australodocus* really would

5104 represent the sister taxon to *Supersaurus*, which is highly questionable, as will be discussed in

5105 more detail below.

5106 ***Supersaurus* + mdD.** Depending on the analysis, this clade includes *Tornieria* or represents

5107 its sister group. ~~Therefore~~Thus, ~~also~~ the combination of synapomorphies changes in the

5108 different trees. Whereas none can be considered valid (based on the guidelines established

5109 above) for the main trees recovered with implied weighting – thus including *Tornieria* – one

5110 shared synapomorphy describes *Supersaurus* + mdD excluding *Tornieria* in the equally

5111 weighted trees (Tab. S82). This synapomorphy is not found in the agreement subtree of the

5112 analysis with implied weights excluding *Australodocus bohetii* a priori, where the position of

5113 *Supersaurus* + mdD is the same as in the equally weighted trees, but furthermore includes ML

5114 418. In this tree, another shared synapomorphy unites the clade: ratio of the pubic articulation

5115 length of the ischium to the anteroposterior length of the pubic pedicel is less than 1.5 (420-

5116 0). However, measurements were only obtainable for four specimens within *Supersaurus* +

5117 mdD, and the validity of this synapomorphy will have to be addressed in more detail in future.

5118 In any case, the only probably valid synapomorphies are found in the trees excluding

5119 *Tornieria* from *Supersaurus* + mdD. In the equally weighted trees, *Dinheirosaurus* +

5120 *Supersaurus* are separated from *Galeamopus* + mdD by 16 changes. *Australodocus* +

5121 *Supersaurus* distinguish only seven changes from their sister clade *Tornieria* + mdD.

5122 **Diplodocinae.** The composition of Diplodocinae is almost equal in all main trees. The only

5123 taxon changing between diplodocine, and non-diplodocine affinities is *Australodocus bohetii*,

as already mentioned above. Due to the incompleteness of ML 418, which was recovered as the most basal diplodocine in the main trees by using implied weights, the number of synapomorphies for the entire clade is much reduced compared to the main equally weighted trees, where ML 418 was excluded from both the pruned and reduced consensus trees. Applying the guidelines for assessing the significance of synapomorphies, two exclusive and eight shared synapomorphies are found by the two analyses (Tab. S83). Three of these synapomorphies are shared with certain apatosaurine specimens (218-1, 283-1, 330-1). Upwards and backwards directed tubercula of anterior and mid-cervical ribs (218-1) are not present in *Australodocus*, such that in the improbable case of diplodocine affinities of this taxon, this character state would become an ambiguous synapomorphy of Diplodocinae, instead of shared. In the trees, where ML 418 represents the most basal diplodocine taxon, ML 418 is separated from the more derived group by just two changes, which does not allow the erection of a new species. This is supported by the fact that ML 418 was among the six most unstable taxa in the equally weighted analysis, and that it switches to a position within the clade *Dinheirosaurus + Supersaurus* when excluding *Australodocus* a priori from the analysis applying implied weighting.

Apatosaurus louisae **CM 3018 + CM 3378.** A clade only including these two specimens is recovered in both reduced consensus trees, and supported by a relatively high resampling value of 23 (Tab. S60). The pruned consensus tree of the analysis using implied weighting shows a polytomy with these two specimens and the holotype specimens of *Apatosaurus laticollis* (YPM 1861) and *Brontosaurus amplus* (YPM 1981). When adding these two specimens to the reduced consensus tree of the equally weighted analysis, *A. laticollis* forms a trichotomy with the *A. louisae* specimens, whereas *B. amplus* is recovered more basally within Apatosaurinae. Two shared 'synapomorphies' are considered reliable (Tab. S84). One of these 'synapomorphies' (the presence of a ridge on the dorsal rib head; C283-1) is otherwise typical for diplodocines. One change lies between the two specimens, confirming the previous referrals to the same species (e.g. McIntosh, 1981; Upchurch et al., 2004b).

Brontosaurus amplus **YPM 1981 + mdA.** This clade is only recovered by the reduced consensus tree obtained applying implied weighting. Adding *A. laticollis* YPM 1861 to the tree, a polytomy is created between *B. amplus*, *A. laticollis*, *A. louisae*, and CM 3378, as visible in the pruned consensus tree with implied weights. In the analysis with implied weights excluding *Australodocus* a priori, *B. amplus* groups with *Apatosaurus ajax* YPM

1860 to form the sister clade to the two *A. louisae* specimens. When excluding *A. laticollis*, only one shared 'synapomorphy' is found (Tab. S85). If *A. laticollis* is added, one unambiguous and three shared synapomorphies are added (Tab. S85). However, it was not possible to score *B. amplus* for any these additional 'synapomorphies'. They thus mostly describe the grouping of *A. laticollis* with the two *A. louisae* specimens. Four changes lie between *B. amplus* YPM 1981 and the two *A. louisae* specimens, two changes separate *A. laticollis* YPM 1861 from the *A. louisae* holotype, and a single change from CM 3378. This would indicate that all four specimens belong to the same species, but see below for a more detailed assessment of the affinities of YPM 1861 and 1981.

***Apatosaurus ajax* YPM 1860 + '*Atlantosaurus*' *immanis* YPM 1840.** The unity of these two specimens is only shown in the equally weighted trees. In the tree obtained with implied weighting, the holotype specimen of '*Atlantosaurus*' *immanis* groups together with NSMT-PV 20375, which was described as belonging to *Apatosaurus ajax* (Upchurch et al. 2004b), but does not group with the holotype YPM 1860 in any of the trees recovered here. Four shared 'synapomorphies' support the clade *Apatosaurus ajax* + '*Atlantosaurus*' *immanis* (Tab. S86). All four 'synapomorphies' are shared with other specimens within Apatosaurinae. Two are shared with the putative *Apatosaurus ajax* specimen NSMT-PV 20375 (168-0, 426-1), and one with the holotype of *Apatosaurus laticollis*, YPM 1861 (198-1). Considering the low overlap index of 13%, and the inability to recover this group by resampling, support for this clade is very low. Six changes lie between the two specimens, which indicate that they are different species, but not different genera.

***Apatosaurus ajax* + mdA.** Such a clade is found with both methods. It is present in the reduced consensus tree from the equally weighted analysis, and both main trees obtained with implied weighting. The only difference lies in the position of '*Atlantosaurus*' *immanis* YPM 1840, which is included in the equally weighted reduced consensus tree, but excluded in the trees with implied weights. This appears to have an influence on the number of 'synapomorphies' found in the different trees, with the equally weighted reduced consensus tree showing less than half of the 'synapomorphies' recovered by implied weighting. In total, eight shared 'synapomorphies' were found (Tab. S87). Only one of these characters is preserved in YPM 1840 as well (208), but the latter specimen does not show the plesiomorphic state. Consequently, this 'synapomorphy' was only found by the trees obtained with implied weights, and excluding YPM 1840 from the clade *Apatosaurus ajax* + mdA.

5188   Three 'synapomorphies' are shared with NSMT-PV 20375 (271-0, 293-0, 365-1), an

5189   additional one with UW 15556 (208-0). Three 'synapomorphies' are not present in any other

5190   apatosaur specimen (253-1, 328-0, 368-0). In the equally weighted reduced tree, *Apatosaurus*

5191   *ajax* YPM 1860 + '*Atlantosaurus*' *immanis* YPM 1840 is separated from the sister clade

5192   *Apatosaurus louisae* CM 3018 + CM 3378 by six changes, whereas *Apatosaurus ajax* YPM

5193   1860 and *Brontosaurus amplus* + mdA are distinguished by a sum of eleven apomorphies.

5194   The difference mainly lies in the high number of 'autapomorphies' found for YPM 1860,

5195   which contrasts with the low number of 'synapomorphies' of the clade YPM 1860 + YPM

5196   1840. Two of the 'autapomorphies' are from the braincase included in YPM 1860, which

5197   cannot definitively be attributed to the same specimen (McIntosh, 1995). Excluding these

5198   ~~info~~data, the number of changes between *Apatosaurus ajax* and *Brontosaurus amplus* + mdA

5199   drops to nine. At this stage, an assignment to two different species appears thus better

5200   supported than an erection of a different genus for the sister clade of *Apatosaurus ajax*.

5201   ***Eobrontosaurus + Amphicoelias.*** Both the pruned and reduced consensus trees of the equally

5202   weighted analysis recover these two genera as sister taxa within Apatosaurinae. If applying

5203   implied weighting, *Amphicoelias* results as the most basal diplodocid sauropod, sister taxon to

5204   Diplodocinae + Apatosaurinae, whereas *Eobrontosaurus* is still found well within

5205   Apatosaurinae. Two shared 'synapomorphies' are found for the clade *Eobrontosaurus*

5206   +*Amphicoelias* (Tab. S88). Whereas one does not occur in other apatosaurines (265-1), the

5207   other synapomorphy is shared with *Elosaurus parvus* CM 566 and the specimen UW 15556

5208   (279-0). The latter (longer than wide bases of the posterior dorsal neural spines) are recovered

5209   as autapomorphic for *Amphicoelias* in the trees obtained with implied weighting. The low

5210   overlap index of seven percent casts further doubts on the validity of the grouping of

5211   *Eobrontosaurus* and *Amphicoelias*. If confirmed, two changes would separate the two

5212   specimens, not justifying the erection of two different species.

5213   ***Eobrontosaurus + mdA.*** Such a clade is recovered in both main trees with implied weights,

5214   as well as the equally weighted reduced consensus tree. It always includes the clade with

5215   *Apatosaurus ajax* and *Apatosaurus louisae*, and excludes the specimens NSMT-PV 20375,

5216   SMA 0087, and WDC-FS001A. '*Atlantosaurus*' *immanis* YPM 1840 switches positions in the

5217   two analyses from *A. ajax* to a sister taxon arrangement with NSMT-PV 20375. When

5218   excluding *Australodocus bohetii* from the implied weights analysis a priori, *Eobrontosaurus* +

5219   mdA becomes more inclusive as compared to the complete implied weights trees. Without

5220 *Australodocus*, it also includes AMNH 460, as well as the clade including the holotype

5221 specimens of *Dystrophaeus viaemalae*, *Brontosaurus excelsus*, and *Elosaurus parvus*. The

5222 unstable taxa are thus *Eobrontosaurus* and AMNH 460, ~~as~~because the clade with

5223 *Brontosaurus* also results sister clade to *Apatosaurus ajax + Apatosaurus louisae* if excluding

5224 *Eobrontosaurus*. The result of the analysis without *Australodocus* ~~can be neither confirmed~~

5225 ~~nor rejected~~cannot be tested by the equally weighted reduced consensus tree, ~~as~~because none

5226 of the doubtful specimens are recovered there.

5227 Combining the information of the main trees, nine shared synapomorphies are found (Tab.

5228 S89). All but one of these synapomorphies are unique within Apatosaurinae: the single lamina

5229 supporting the hyposphene (238-1) is also present in AMNH 460. This character, as well as

5230 two more (400-1, 452-1) are also found as synapomorphies for the more inclusive clade

5231 *Eobrontosaurus* + mdA in the implied weights analysis excluding *Australodocus bohetii* a

5232 priori. Three more shared and one unambiguous synapomorphies are found in the tree without

5233 *Australodocus*. None of these were possible to code for AMNH 460, with the result that all of

5234 them are recovered as synapomorphies for *Brontosaurus* + mdA in the complete implied

5235 weights analyses.

5236 In the equally weighted reduced consensus tree, *Eobrontosaurus + Amphicoelias* and its sister

5237 clade are separated by five changes. The trees obtained by implied weighting yield distances

5238 of 15 (pruned) and 14 (reduced) changes from *Eobrontosaurus* to *Apatosaurus ajax* + mdA.

5239 The tree without *Australodocus* shows nine changes between *Eobrontosaurus* and AMNH

5240 460 + mdA. Whereas *Eobrontosaurus* or *Eobrontosaurus + Amphicoelias* can thus be

5241 confidently considered a new species, support for being a different genus is dubious. The

5242 taxonomic status of *Eobrontosaurus* and *Amphicoelias* will be assessed with further detail

5243 below.

5244 **Dystrophaeus viaemalae USNM 2364 + UW 15556.** The unity of these two specimens to the

5245 exclusion of any other is only seen in the reduced consensus tree applying implied weights.

5246 Support from the overlap index is extremely low, being only four percent. A single shared

5247 'synapomorphy' is recovered (Tab. S90). The addition of the single specimen FMNH P25112

5248 to the reduced consensus tree with implied weights results in a polytomy between

5249 *Dystrophaeus viaemalae*, *Elosaurus parvus*, UW 15556, and FMNH P25112. Six changes are

5250 found between *Dystrophaeus viaemalae* USNM 2364 and UW 15556, but the states of all five

5251 autapomorphies recovered for UW 15556 are not known in *D. viaemalae*. The apomorphy

5252   count thus drops to one, indicating that the two specimens would represent the same species if

5253   they truly are sister taxa.

5254   ***Elosaurus parvus* CM 566 + UW 15556.** In the equally weighted pruned tree, the specimen

5255   UW 15556 is recovered together with the holotype specimen of *Elosaurus parvus* (CM 566),

5256   to the exclusion of all other taxa. *Dystrophaeus viaemalae* was excluded from that tree. When

5257   added to the equally weighted pruned tree, *Dystrophaeus* creates a large polytomy close to the

5258   base of the tree, and the unity of the two specimens CM 566 and UW 15556 remains. This

5259   clade was also recovered by Upchurch et al. (2004b), and interpreted as its own species within

5260   *Apatosaurus*, introducing the new combination *Apatosaurus parvus*. Seven shared

5261   'synapomorphies' are recovered for this clade, but only supported by the equally weighted

5262   pruned tree (Tab. S91). Five of the seven 'synapomorphies' are shared with other

5263   apatosaurines (184-0, 238-0, 261-0, 279-0, 408-1); the greatly reduced sprl in posterior dorsal

5264   vertebrae (274-0) is unique within Diplodocoidea. The two specimens can be distinguished by

5265   a sum of four 'autapomorphies', which are all also observable in the other specimen.

5266   ***Elosaurus parvus* CM 566 + (*Dystrophaeus* + UW 15556).** This triplet ~~does~~ only occurs in

5267   the reduced implied weight trees, excluding the specimen FMNH P25112. In the pruned

5268   implied weight tree, where FMNH P25112 is present, the four specimens form a polytomy,

5269   with *Brontosaurus excelsus* YPM 1980 as sister taxon. Three shared 'synapomorphies' are

5270   found by the reduced consensus tree, and five more are added in the pruned consensus tree

5271   with FMNH P25112 (Tab. S92). Due to its incompleteness, *Dystrophaeus* cannot ~~can~~ be

5272   scored for any of these 'synapomorphies'. The three 'synapomorphies' found by the reduced

5273   implied weights tree are in fact also found by the equally weighted trees for the cluster *E.*

5274   *parvus* + UW 15556. In the reduced implied weight trees, *Elosaurus parvus* CM 566 is

5275   separated from the *Dystrophaeus* cluster by four changes, not justifying specific separation.

5276   ***Brontosaurus excelsus* YPM 1980 + (*Elosaurus* + *Dystrophaeus*).** A grouping of the

5277   holotype specimen of *Brontosaurus excelsus* with *Elosaurus* and other specimens, as sister

5278   clade to a clade including the type specimens of *Apatosaurus ajax* and *A. louisae*, is only

5279   found by applying implied weights. The clade always contains three holotype specimens (*B.*

5280   *excelsus* YPM 1980, *E. parvus* CM 566, and *D. viaemalae* USNM 2364), as well as UW

5281   15556. In the pruned consensus tree, also FMNH P25112 was recovered within this group.

5282   Five shared and one exclusive 'synapomorphies are recovered (Tab. S93). Two of the shared

5283   synapomorphies are also present in other apatosaurs (237-1, 272-1). The transition of fan-

shaped to normal caudal ribs between Cd 5 and 6 (300-2) does not appear to be shown in UW 15556, where it is between Cd 4 and 5, according to Gilmore (1936). However, the caudal vertebrae were found disarticulated, and the serial positions proposed by Gilmore (1936) were based on comparisons with the type specimen of *A. louisae* (Gilmore, 1936: p. 251). Therefore, it could be that an anterior-most caudal vertebra is missing, and it would thus probably be more accurate to score UW 15556 as unknown in this character. As with the previous clade, due to the fragmentary state of USNM 2364, it was not possible to score *Dystrophaeus* for any of the characters herein recovered as synapomorphies for *Brontosaurus* + (*Elosaurus* + *Dystrophaeus*). *Brontosaurus excelsus* is separated from the sister clade by twelve changes, justifying the use of two distinct genera (see below).

***Brontosaurus* + mdA.** This clade is found in the implied weights analysis only. Whereas the main trees show the *Brontosaurus* clade to be sister taxon to *Eobrontosaurus* + mdA, the reduced consensus tree obtained by excluding *Australodocus* a priori does show a more basal position for *Eobrontosaurus*. The clade is supported by eight shared and one unambiguous synapomorphies (Tab. S94). Six of the ~~present~~ synapomorphies describe features of appendicular elements, which are lacking in several specimens included in the present analysis. ~~They~~These characters diagnose the more inclusive *Eobrontosaurus* + mdA in the reduced consensus tree of the analysis excluding *Australodocus* a priori (380-2, 391-1, 395-2, 396-1, 400-1, 452-1). In the latter analysis, only one, but ~~an~~ unambiguous, synapomorphy is found for *Brontosaurus* + mdA: posterior cervical rib shafts are initially directed in the same direction but turn to run a little downwards toward the distal tip (223-1). Including *Australodocus* in the analysis, 15 changes are recovered between the *Brontosaurus* clade and the *Eobrontosaurus* clade, whereas in the other analysis, eleven changes separate *Brontosaurus* from *Apatosaurus ajax* + mdA. Both counts support the use of different genera for the two clades.

WDC-FS001A + SMA 0087. The clustering of these two specimens is only found when using implied weighting. They have a very low overlap, indicated by the index of seven percent. Two shared 'synapomorphies' describing tibial morphology characterize the clade (Tab. S95). None of these traits are seen in other apatosaur specimens preserving the tibia. Two changes ~~are separating~~separate the two specimens, indicating that they might belong to the same species. More detailed study of the material will be needed in order to definitely assess the systematic position of these two specimens.

SMA 0087 + mdA. As for the clades discussed above, also this arrangement is only recovered in the trees obtained with implied weighting. Whereas AMNH 460 is found as sister taxon to the present clade in the trees obtained by the complete analysis, this specimen is included into SMA 0087 + mdA when *Australodocus* is deleted from the matrix a priori. No valid synapomorphies are found with the analysis including *Australodocus*, but one unambiguous synapomorphy characterizes this clade when *Australodocus* is excluded a priori (403-1; Tab. S96). However, only two ingroup specimens (out of twelve) and 14.7 percent of the specimens in the entire analysis were scorable for this character. Support for such an arrangement is thus very low. Nonetheless, eleven changes separate the clade SMA 0087 + WDC-FS001A from *Brontosaurus* + mdA in the main implied weights trees, and eight in the case of the analysis without *Australodocus*. This relatively high number indicates the presence of a new, previously unrecognized taxon.

AMNH 460 + mdA. The composition of this clade as recovered by the implied weight analyses changes depending on in- or exclusion of *Australodocus*. The specimens changing their positions in respect to this clade are *Eobrontosaurus yahnahpin* Tate-001, SMA 0087, and WDC-FS001A. They are nested within the present clade in the main trees, but fall outside when excluding *Australodocus*. A single valid, shared synapomorphy is found with the main, pruned consensus tree (Tab. S97). This trait (174-1) is not identified as synapomorphic for AMNH 460 + mdA in the analysis without *Australodocus*, as it shows the same development in *Eobrontosaurus*, which is recovered as sister taxon to the present clade, instead of being nested within. No changes separate AMNH 460 from the more derived clade SMA 0087 + mdA in the main implied weights trees, and one single change is found between AMNH 460 and *Brontosaurus* + mdA in the implied weights reduced consensus tree without *Australodocus*. Neither specific nor generic separation of AMNH 460 from its sister groups is thus warranted. The taxonomic affinities of AMNH 460 will be addressed below.

'*Atlantosaurus*' *immanis* YPM 1840 + NSMT-PV 20375. The grouping of these two specimens is only recovered with implied weights. Both specimens are usually interpreted as belonging to *Apatosaurus ajax* (McIntosh, 1995; Upchurch et al., 2004b), but are here found as the most basal apatosaurines. Whereas NSMT-PV 20375 occupies the same position in the equally weighted trees, '*Atlantosaurus*' *immanis* YPM 1840 switches to a sister arrangement with the *Apatosaurus ajax* holotype YPM 1860. Overlap is low, as indicated by the index of 15%. Four valid, shared 'synapomorphies' are found (Tab. S98). All four 'synapomorphies' are

5348 shared with other apatosaurines, and would thus not qualify as species autapomorphies. Two

5349 traits are also present in *Apatosaurus ajax* YPM 1860 (168-0, 426-1), which supports the

5350 earlier identifications, and casts additional doubt on the position recovered herein. If a true

5351 phylogenetic signal, the two specimens would be separated by one single difference, not

5352 allowing specific separation.

5353 **Apatosaurinae.** Whereas an apatosaurine clade was recovered in all four main trees,

5354 composition of it changes. Five putative apatosaur specimens are found outside

5355 Apatosaurinae, in a polytomy with the latter clade and Diplodocinae in the equally weighted

5356 pruned consensus tree: WDC-FS001A, SMA 0087, FMNH P25112, AMNH 460, and NSMT-

5357 PV 20375. When adding them one by one to the reduced consensus, only WDC-FS001A and

5358 SMA 0087 result in such a position, indicating that they are the main cause for the large

5359 polytomy in the pruned tree. *Amphicoelias altus* is found within Apatosaurinae when applying

5360 equal weights, but remains outside when using implied weighting. Two unambiguous, one

5361 exclusive, 20 shared, and one ambiguous synapomorphies add to a total of 24 synapomorphies

5362 recovered for the clade (Tab. S99). Seven of these traits result as synapomorphic for

5363 Diplodocidae in the equally weighted pruned tree (135-1, 185-2, 186-1, 216-1, 220-1, 256-0,

5364 275-1), but this is because of the apatosaur specimens recovered outside Apatosaurinae in this

5365 tree (135-1, 186-1, 216-1, 220-1, 256-0, 275-1), or the changing positions of *Supersaurus*

5366 (185-2). Nine synapomorphies are recovered for the less inclusive *Brontosaurus* + mdA in the

5367 implied weight trees, and should thus not be used in diagnoses of Apatosaurinae (259-0, 358-

5368 0, 380-2, 391-1, 395-2, 396-1, 400-1, 452-1, 466-2). The reason for the discrepancy is that the

5369 specimens found basal to *Brontosaurus* are mostly the ones recovered outside Apatosaurinae

5370 in the equally weighted pruned tree. Of the latter nine, two result as synapomorphic for

5371 *Eobrontosaurus* + mdA in the equally weighted reduced tree (400-1, 452-1), and seven for the

5372 same clade in the implied weights analysis without *Australodocus* (380-2, 391-1, 395-2, 396-

5373 1, 400-1, 402-0, 452-1). The high number of synapomorphies for Apatosaurinae contrasts

5374 with the low number of generally accepted genera this clade includes (*Apatosaurus*, and

5375 possibly *Eobrontosaurus*). This is surprising, when compared to its sister clade Diplodocinae,

5376 which includes at least six different genera, but does not appear to be much more divers

5377 morphologically. An analysis of morphological disparity would probably be able to quantify

5378 the difference, but is outside of the scope of this paper. In any case, the numerical approach as

5379 chosen herein also indicates a higher generic diversity within Apatosaurinae, with at least

5380 three, possibly up to six valid genera.

5381 The most basal taxon as recovered by this analysis, would be represented by NSMT-PV

5382 20375 (equal weights) or 'Atlantosaurus' immanis YPM 1840 + NSMT-PV 20375. These

5383 specimens are separated from more derived apatosaurs by 14 changes in the case of the

5384 equally weighted reduced tree, five in the case of the main implied weights trees, as well as

5385 the one without *Australodocus*. This difference is mainly due to the fact that many specimens

5386 recovered between *Eobrontosaurus* and NSMT-PV 20375 in the implied weight trees, are not

5387 present in the equally weighted reduced consensus tree, in which the 14 changes were found.

5388 However, the true number also depends on the systematic position of YPM 1840, which will

5389 be discussed in more detail below.

5390 **Apatosaurinae + Diplodocinae.** The unity of these clades usually corresponds to

5391 Diplodocidae, but since the definitions of the two clades are stem-based, as is Diplodocidae

5392 (Taylor and Naish, 2005), additional taxa can be recovered basal to Apatosaurinae +

5393 Diplodocinae, but still within Diplodocidae. This is the case in the implied weights trees,

5394 where *Amphicoelias altus* AMNH 5764 is found to be the basal-most diplodocid. Two

5395 unambiguous, four exclusive, and two shared synapomorphies are found for this clade (Tab.

5396 S100). Seven of these are also recovered as synapomorphies of Diplodocidae (17-1, 23-1, 25-

5397 1, 224-2, 259-1, 263-0, 294-0, 314-1). Two traits are scored differently in *Amphicoelias*

5398 (characters 259 and 294), and should thus not be used to diagnose Diplodocidae. The sum of

5399 synapomorphies for Apatosaurinae and Diplodocinae is 34.

5400 **Diplodocidae.** As stated above, the implied weight trees recover *Amphicoelias* as sister taxon

5401 to Apatosaurinae + Diplodocinae, and thus as the most basal diplodocid genus. Sixteen

5402 synapomorphies are supported by the analysis, three unambiguous, six exclusive, five shared,

5403 and two ambiguous (Tab. S101). One of the stated synapomorphies actually only occurs in

5404 apatosaurine specimens (216-1), and is recovered as a synapomorphy for that clade by all but

5405 the equally weighted pruned tree. It is thus more carefully treated as a synapomorphy of

5406 Apatosaurinae, and should not be used in diagnoses of Diplodocidae. A similar case is

5407 character 259, where the derived state is recovered as diplodocid synapomorphy, but

5408 *Amphicoelias* is scored for the plesiomorphic state. If the basal position of *Amphicoelias* is

5409 confirmed, the derived state would only diagnose the clade Apatosaurinae + Diplodocinae, as

5410 already stated above. *Amphicoelias* – in such a position – is separated from more derived

5411 diplodocids by a sum of twelve changes, but only six are actually comparable due to the

incomplete condition of the type specimen of *Amphicoelias*.

Flagellicaudata. The node-based taxon Flagellicaudata includes Diplodocidae and Dicraeosauridae. It is recovered by all four main trees, and supported by eight unambiguous, three exclusive, eight shared, and three ambiguous synapomorphies (Tab. S102). One of the above mentioned synapomorphies was recovered as diagnosing Diplodocimorpha in the implied weight trees, instead (318-1), because the sprl also extends onto the lateral aspect of the caudal neural spines in rebbachisaurs. ~~Since~~Because *Cetiosauriscus* and *Haplocanthosaurus* are recovered as diplodocoid sauropods more derived than rebbachisaurs in the equally weighted analysis, but have reduced caudal sprl, it results in a shared synapomorphy of rebbachisaurs and flagellicaudatans. If – as in the trees found by using implied weighting – *Cetiosauriscus* and *Haplocanthosaurus* are found to be more basal to rebbachisaurs, the well-developed caudal sprl become a diagnosing feature for Diplodocimorpha as defined by Taylor and Naish (2005).

Proximally closed haemal arches (352-0) are present as well in *Cetiosauriscus stewarti* NHMUK R3078. In the equally weighted pruned tree, where *C. stewarti* is recovered as diplodocoid more than Rebbachisauridae⊟s feature thus appears synapomorphic for a clade *C. stewarti* + mdD. The same occurs in character 463 describing the presence of a posterolateral projection on the distal condyle of metatarsal I, which is also present in *C. stewarti* and thus becomes a synapomorphy for the slightly more inclusive clade *C. stewarti* + mdD. Within Flagellicaudata, Dicraeosauridae and Diplodocidae are separated by 56 changes.

***Cetiosauriscus* + mdD.** Such a clade is only found with equal weighting, where *Cetiosauriscus stewarti* NHMUK R3078 is recovered in a position between Rebbachisauridae and Flagellicaudata. Three shared synapomorphies support this grouping (Tab. S103). All of these synapomorphies are shared with more basal taxa, close to the position where *Cetiosauriscus* is recovered in the implied weights trees, and are thus not conclusive evidence for diplodocoid affinities of *Cetiosauriscus*. The sum of apomorphies between *Cetiosauriscus* and Flagellicaudata is 30.

***Haplocanthosaurus* + mdD.** This clade corresponds to Diplodocoidea in the implied weights trees, but is more restricted when applying equal weighting. In the latter analysis, *Haplocanthosaurus* is recovered more derived than Rebbachisauridae. Such an arrangement is supported by one exclusive synapomorphy (Tab. S104). However, this feature (324-1) ~~is~~ also ~~present~~occurs in *Cetiosauriscus*. If the true phylogenetic position of *Cetiosauriscus* would be

outside Diplodocoidea, it would thus not be useful anymore to define this clade, and indeed was not found as such in the implied weights analysis. *Haplocanthosaurus* is separated from *Cetiosauriscus* + mdD by 14 changes.

Diplodocimorpha. ~~The present~~This clade is often used in the same way as Diplodocoidea, but in fact has a node-based definition, whereas Diplodocoidea is stem-based (Taylor and Naish, 2005). In the present analyses, Diplodocimorpha is only different from Diplodocoidea when using implied weighting, where *Haplocanthosaurus* is recovered more basal to Rebbachisauridae. In these cases, even the complete strict consensus tree finds Diplodocimorpha. One unambiguous, two exclusive, and one ambiguous synapomorphies are found to be reliable in the implied weights trees (Tab. S105). The semicircular dorsal margin of the ilium (409-1) was the only characteristic also recovered as synapomorphic for Diplodocoidea by equal weighting. One of the synapomorphies was found to diagnose Rebbachisauridae in the equally weighted tree (294-1). The latter clade is distinct from Flagellicaudata (which is the sister taxon to Rebbachisauridae in the implied weight trees) by 27 changes.

Diplodocoidea. The clade Diplodocoidea is represented in all consensus trees ~~but~~except for the complete strict consensus tree with equal weighting. Due to the more derived position of *Haplocanthosaurus priscus* in the equally weighted analyses compared to the analysis with implied weights, Diplodocoidea is equivalent to Diplodocimorpha in the former analysis. Synapomorphies recovered include 14 unambiguous, five exclusive, five shared, and one ambiguous traits (Tab. S106). Twenty of the synapomorphies mentioned describe cranial features, which are rarely preserved, as exemplified by the low percentage of ingroup specimens scored: nine of them are only known from less than 20% of all specimens included in the analysis, five from less than 15%. Their assignment as synapomorphies should thus be regarded provisional. The distance between *Haplocanthosaurus* and Diplodocimorpha amounts to 17 changes.

Validity and taxonomic assessment of the holotype specimens

Discussion of the taxonomic affinities of the holotype specimens is ordered based on date of description. By doing so, possible synonymy of the species and genera can be assessed in a more intuitive way. The specimens are listed with the initially proposed name.

***Dystrophaeus viaemalae* USNM 2364.** The phylogenetic position of *Dystrophaeus*

viaemalae is dubious, mostly due to its fragmentary remains. In the present analysis, the holotype USNM 2364 was among the six most unstable taxa, and thus was pruned taxa in the equally weighted trees. The analysis using implied weighting recovered it consistently as sister taxon to UW 15556, closely related with the holotype of *Elosaurus parvus*. Validity and phylogenetic position of *Dystrophaeus viaemalae* is particularly important because it was the first sauropod to be described from North America, and would thus have priority over any possibly synonymous taxon. The present study is the first to include the specimen in a phylogenetic analysis. Earlier studies proposed diplodocid affinities (McIntosh, 1997), but that was mainly based on the plesiomorphically short and robust metacarpals (Upchurch et al., 2004a). The latter did not find any diagnostic feature in the fragmentary material, but refrained to classify *Dystrophaeus* as nomen dubium asbecause it was found very low in stratigraphy, possibly even below the Morrison Formation.

One single, ambiguous autapomorphy was recovered for USNM 2364 (Tab. S107), describing the morphology of the distal radius. The identification of the partial radius as distal is debatable, however, as proximal and distal ends of the radius can be highly similar. McIntosh (1997), for example, identified the same piece as proximal radius, which would render the autapomorphy invalid. As recovered herein, it is shared with specimens from all major taxonomic groups included in the analysis. The fact that two specimens of the same diplodocine genus (*Galeamopus*) are scored differently for this character casts further doubt on its validity as autapomorphy. A single character ties *D. viaemalae* to UW 15556 (Tab. S90). This trait (389-0) is shared with *Omeisaurus,* and possibly affected by deformation. Incompleteness of the specimen inhibits a scoring for any character providing synapomorphies of lower-level clades (below Apatosaurinae) recovered including *Dystrophaeus*. The holotype specimen can be scored for a single character producing a shared synapomorphy of Apatosaurinae (robust metacarpal III), but actually results in a controversial coding (intermediate robustness of metacarpal III), not shown in any other apatosaurine specimen. A differential scoring is also present in an ambiguous synapomorphy of Diplodocidae (posterior centroparapophyseal lamina absent instead of single or double in mid- and posterior dorsal neural arches). However, identification of laminae in the preserved partial dorsal vertebra of *Dystrophaeus* is challenging, because distinction of bone from the still adherent matrix is not made without difficulty. The plesiomorphic coding for this character is furthermore shared by the type specimen *Elosaurus*, which groups with

Dystrophaeus in the implied weights tree. No synapomorphy of higher-level clades such as Flagellicaudata, Diplodocimorpha, or Diplodocoidea can be identified in USNM 2364. This implies that either USNM 2364 is not diagnostic, or not a diplodocoid sauropod. ~~As~~Because a macronarian affinity appears to be improbable given the relatively short metacarpals (McIntosh, 1997; Upchurch et al., 2004a), the only reasonable identification would be a non-neosauropod eusauropod.

In order to test these interpretations, constrained tree searches with equal weights were performed forcing USNM 2364 into a position with *Elosaurus parvus* CM 566 and UW 15556 as found by the implied weight trees, as well as forcing it into a position outside Diplodocoidea. Minimum tree length obtained by imposing a grouping of USNM 2364 with CM 566 and UW 15556 is three steps higher (1900) than the most parsimonious trees (1897), and produces one synapomorphy recognizable in *Dystrophaeus* as well: distal end of the radius much wider than midshaft (394-1). The same trait has been identified as a synapomorphy for Apatosaurinae (equally weighted pruned tree) or *Jobaria* + mdE (equally weighted reduced tree). The shortest tree constraining *Dystrophaeus* to a taxon outside Diplodocoidea resulted from a grouping with *Lourinhasaurus* or *Omeisaurus*, both producing the same tree length as the most parsimonious trees (1897). A single synapomorphy supports the grouping with *Lourinhasaurus*: presence of a subtriangular process on the ventral edge of the scapular blade (370-1) – which is present as well in several diplodocid specimens. The sister group arrangement with *Omeisaurus* yielded three synapomorphies: 1) a flat or slightly convex area posterior to the acromial ridge and the distal blade of the scapula (365-1); 2) the right angle between the two arms of the ulnar proximal articular surface (389-0); and 3) a beveled distal articular surface of the radius (393-1). Any of these traits are shared with diplodocid specimens as well. Forcing USNM 2364 into a non-diplodocoid position by using implied weights yielded a minimal tree length of 188.00488 when grouping with *Lourinhasaurus*, which is an increase of 0.03274 steps, compared to the most parsimonious trees. If forced to group with *Omeisaurus*, tree length increases to 188.3466. The synapomorphy found for *Lourinhasaurus* + *Dystrophaeus* is the same as in the equally weighted tree (370-1). A length increase of 0.16% is thus needed in the equally weighted trees to force *Dystrophaeus* into the position recovered with implied weighting, whereas a position outside Diplodocoidea results in the same length. On the other hand, using implied weighting, a tree length increase of 0.02% already supports a grouping of *Dystrophaeus* with

5540 *Lourinhasaurus*. A position outside Diplodocoidea seems thus better supported. More detailed

5541 studies are needed including basal Macronaria, Neosauropoda, as well as derived, non-

5542 neosauropod Eusauropoda, in order to resolve phylogenetic relationships of *Dystrophaeus*

5543 *viaemalae* and definitively assess its taxonomic validity.

5544 ***Amphicoelias altus* AMNH 5764.** The holotype of *Amphicoelias altus* is found in two

5545 different positions in the present analysis. Both positions contrast with the position found by

5546 Rauhut et al. (2005), Whitlock (2011a), Mannion et al. (2012) or Tschopp and Mateus

5547 (2013b).: w Whereas it AMNH 5764 was found within Diplodocidae in the present analysis,

5548 all earlier assessments recovered it more basal than Dicraeosauridae, mostly even outside

5549 Diplodocimorpha (Rauhut et al., 2005; Whitlock, 2011a; Mannion et al., 2012). The strict

5550 interpretation of the holotype as used in the present analysis (only including the dorsal

5551 vertebrae and the femur) possibly increased the diplodocid affinities, even though preliminary

5552 analyses recovered them in the same position. The positions recovered herein are in a

5553 dichotomy with *Eobrontosaurus yahnahpin* within Apatosaurinae, or as basal-most

5554 diplodocid, neither apatosaurine nor diplodocine.

5555 Four ambiguous autapomorphies were considered valid for the holotype, two of them for the

5556 position within Apatosaurinae (with equal weighting), and two as a basal-most diplodocid

5557 (with implied weights; Tab. S108). Nearly horizontal postzygapophyses (275-0) are

5558 widespread among sauropods, and thus probably not a meaningful autapomorphy. The 'petal'

5559 shape in the posterior dorsal of *A. altus* (294-1) is less developed than in rebbachisaurs and

5560 dicraeosaurs, and an additional tree search was performed changing this single character state.

5561 In both equal and implied weights analyses, length of the MPTs was increased compared to

5562 the main trees (1900 and 188.32214 steps, respectively). The pPosition of *Amphicoelias*

5563 remained the same, the interpretation of the neural spine shape is thus without influence. The

5564 gracile femur, with its mediolateral width subequal to anteroposterior depth (427-0, 430-0)

5565 describes the stove-pipe shape of this element, most often used as the best way to distinguish

5566 *Amphicoelias* from other sauropods. In fact, these are the autapomorphies least shared with

5567 other taxa. On the other hand, the greatly deformed femur of SMA 0087 shows that ratios like

5568 transverse width to anteroposterior depth can be considerably distorted. However, in contrast

5569 to SMA 0087, the femur of AMNH 5764 does not show any sign of breakage, indicating that

5570 the preserved subcircular cross-section might at least approach the true shape in the living

5571 animal. The subcircular femoral cross-section, as well as the 'petal'-shaped posterior dorsal

5572 neural spines, and the horizontal posterior dorsal postzygapophyses are all traits shared with

5573 dicraeosaurids, whereas only one is shared with a single apatosaurine. In fact, the horizontal

5574 posterior dorsal postzygapophyses contrast with the state in all other Apatosaurinae, for which

5575 the implied weights analysis recovered a low angle as synapomorphy shared by all

5576 apatosaurine specimens. Moreover, *Amphicoelias* does not show an additional otherwise

5577 shared synapomorphy of Apatosaurinae: mid- and posterior dorsal parapophyses are not

5578 located above the centrum, but anteriorly displaced (256-1, instead of 256-0). One exclusive

5579 synapomorphy of Apatosaurinae + Diplodocinae, the accessory laminae in the region between

5580 the pcdl and the pcpl of mid- and posterior dorsal vertebrae (259-1) is absent in *Amphicoelias*,

5581 but also in *Brontosaurus* + mdA, and in *Eobrontosaurus*. *Amphicoelias* shares the diplodocid

5582 synapomorphies of short posterior dorsal transverse processes, and the presence of a lateral

5583 bulge on the femur, both of which are not present in any other sampled diplodocoid sauropod.

5584 A diplodocid affiliation is thus probable. This is also supported by constrained searches

5585 testing the position of *Amphicoelias altus* recovered in the alternative analysis. When

5586 inhibiting a grouping of *Amphicoelias* with *Eobrontosaurus* in the equally weighted analysis,

5587 a tree of one step longer than the original is found (0.05% length increase), but relationships

5588 of *Amphicoelias* cannot be established beyond Diplodocidae indet. Tree length for a grouping

5589 of *Amphicoelias* and *Eobrontosaurus* using implied weights is 188.13188, which corresponds

5590 to a tree length increase of 0.08%. Such a constrain pulls *Amphicoelias* into Apatosaurinae,

5591 into the position corresponding to the one found in the equally weighted reduced consensus

5592 tree. However, given that relative tree length increase is lower when inhibiting instead of

5593 forcing such an interrelationship, the two taxa are herein considered distinct. Based on the

5594 ~~lacking~~absence of apatosaurine synapomorphies ~~of~~for *Amphicoelias*, and given that previous

5595 analyses agreed in a more basal position within Diplodocoidea, the position outside

5596 Apatosaurinae + Diplodocinae is herein interpreted as more reasonable.

5597 ***Amphicoelias latus* AMNH 5765.** All analyses ~~performed~~ agreed in a position of AMNH

5598 5765 within Camarasauridae. *Amphicoelias latus* is generally synonymized with

5599 *Camarasaurus supremus*, following Osborn and Mook (1921).

5600 No autapomorphies are found for *Amphicoelias latus*. The synapomorphies of *Camarasaurus*

5601 + Turiasauria, not shared with AMNH 5765 are a maximum to minimum mediolateral width

5602 of anterior caudal neural spines of 2.0 or greater (327-1), and a fourth trochanter on the femur,

5603 which is visible in anterior view (436-1). The first of these synapomorphies has actually been

5604 shown to be variable within *Camarasaurus* by Ikejiri (2004). The second is somewhat

5605 dubious, ~~as~~because AMNH 5765 was only scored based on the drawings in Cope (1877b) and

5606 Osborn and Mook (1921). Of the four synapomorphies recovered for *Camarasaurus* (92-0,

5607 333-1, 392-1, 408-0), AMNH 5765 is not scorable for any of these. Furthermore, given that

5608 the present analysis is designed to resolve relationships within Diplodocidae, and that AMNH

5609 5765 is highly incomplete (see above), the more basal position compared to the other two

5610 *Camarasaurus* OTUs should not be considered significant. The present result can thus be

5611 regarded to corroborate the referral of Osborn and Mook (1921) of the holotype material of

5612 *Amphicoelias latus* to *Camarasaurus*.

5613 ***Apatosaurus ajax* YPM 1860.** As type specimen of the type species of *Apatosaurus*, YPM

5614 1860 has special taxonomic importance. It is herein always recovered in the same tree branch

5615 as *Apatosaurus louisae* CM 3018. This ~~is opposite to~~contrasts with the finding of Upchurch et

5616 al. (2004b), where *Apatosaurus louisae* formed the sister group to all other apatosaur

5617 specimens included.

5618 Six autapomorphies are found for YPM 1860, one of which unambiguous (Tab. S109). Even

5619 when excluding the information of the putatively assigned braincase, the unambiguous

5620 synapomorphy would warrant specific separation. The specimen YPM 1860 can thus be

5621 regarded diagnostic~~,~~ and the species *Apatosaurus ajax* valid. YPM 1860 is thus per definition

5622 an apatosaurine diplodocid.

5623 ***Apatosaurus grandis* YPM 1901.** The specimen YPM 1901 has long been known not to

5624 belong to *Apatosaurus*, but to typify its own species within *Camarasaurus* (Marsh, 1878;

5625 Osborn and Mook, 1921; McIntosh et al., 1996a, b; Ikejiri, 2004). It is herein consistently

5626 recovered as sister taxon to the genus-level OTU *Camarasaurus*, thereby confirming this

5627 identification.

5628 Four ambiguous autapomorphies are considered valid (Tab. S110). Specific separation from

5629 *Camarasaurus* appears thus well-founded, and more detailed work on camarasaur

5630 intrarelationships will definitely produce more differences. *Apatosaurus grandis* is thus

5631 referred to *Camarasaurus*, as *Camarasaurus grandis*, with the type specimen being YPM

5632 1901.

5633 ***Amphicoelias fragillimus* AMNH 5777.** This specimen was the only putative diplodocid

5634 holotype specimen not included into the present analysis. Given that it ~~has been~~was lost

5635 shortly after publication (Carpenter, 2006), and that no other material has yet been reported

reaching anywhere near the same size as proposed in the initial description (Cope, 1878), it seems unwise to speculate about its phylogenetic position solely based on the single drawing and inadequate description of this extremely fragmentary specimen. *Amphicoelias fragillimus* is thus herein considered a nomen dubium.

'*Atlantosaurus*' *immanis* YPM 1840. Generally considered synonymous to *Apatosaurus ajax* (McIntosh, 1995; Upchurch et al., 2004b), ☰ lings of this study are controversial (see above). No recovered autapomorphy for the specimen can be considered valid according to the guidelines established above (Tab. S111). Both sister group arrangements with *Apatosaurus ajax* YPM 1860 and the putative *Apatosaurus ajax* NSMT-PV 20375 do not yield any synapomorphy not shared with any other apatosaur specimen. '*Atlantosaurus*' *immanis* YPM 1840 furthermore could not be scored for the single unambiguous autapomorphy found for *Apatosaurus ajax* YPM 1860 (smooth medial face of bifid posterior cervical neural spines). From the eight shared synapomorphies recovered for the clade *Apatosaurus ajax* + mdA (Tab. S87), only one was scored in YPM 1840, but opposite to the remaining ingroup specimens (C208). YPM 1840 unambiguously classifies as Apatosaurinae due to the divided posterior cervical cprl (185-2), the pcdl and podl of mid- and posterior cervical vertebrae that do not meet anteriorly (186-1), the cervical ribs projecting well beneath centrum (216-1), the bump-like anterior process of cervical ribs (220-1), and the high ratio of the pubic articulation of the ischia to the anteroposterior length of the pubic pedicel (420-1). However, placement within Apatosaurinae remains controversial.

Forcing YPM 1840 to group with NSMT-PV 20375 (as recovered with implied weighting) in the equally weighted analysis yielded minimal tree lengths of 1 step more than the most parsimonious trees, or a relative length increase of 0.05%. The strict reduced consensus tree shows three more taxa compared to the main equally weighted reduced consensus tree. The most important changes are the following: *Dystrophaeus* is found as most basal titanosauriform, thus further corroborating its non-diplodocoid affinities stated above; and *Brontosaurus excelsus*, together with UW 15556, now form the sister clade to *Apatosaurus ajax* + *Apatosaurus louisae*, which is the same arrangement as seen in the implied weights reduced consensus tree. Synapomorphies found for the union of YPM 1840 and NSMT-PV 20375 are the same as in the main implied weight trees. A constrained search with implied weighting, imposing a sister arrangement of YPM 1840 with YPM 1860 (as found by the equally weighted trees) resulted in a minimal tree length of 188.16879, which corresponds to

5668 a relative length increase of 0.1%. Apatosaurine intrarelationships changed considerably:

5669 NSMT-PV 20375 was found as sister taxon to YPM 1840 + YPM 1860, and together they

5670 formed the sister clade to SMA 0087 + mdA. The specimen AMNH 460 was recovered as

5671 most basal apatosaurine. The *Elosaurus parvus* group was pulled out of its relationship with

5672 *Brontosaurus excelsus*, and recovered as sister taxon to *Brontosaurus* + mdA, including

5673 *Brontosaurus excelsus*, *Brontosaurus amplus*, and *Eobrontosaurus yahnahpin* + FMNH

5674 P25112 as successive sister groups to a trichotomy with *Apatosaurus louisae*, *A. laticollis*,

5675 and CM 3378. Traits uniting NSMT-PV 20375 with *Apatosaurus ajax* + '*Atlantosaurus*'

5676 *immanis* are the following: 1) cervical vertebrae that are much wider than high (128-2); 2)

5677 mid-cervical neural spines that are shorter than the neural arches (168-0); 3) posterior dorsal

5678 centra wider than high (269-1); 4) the posterior edge of anterior chevrons expands in a step-

5679 like fashion (355-1); 5) an almost right angle between the scapular blade and the coracoid

5680 articular surface (361-0); 6) a flat or slightly convex area posterior to the acromial ridge and

5681 distal scapular blade (365-1); and 7) dorsoventrally expanded distal ends of the ischia (426-1).

5682 The low mid-cervical neural spines would qualify as unambiguous synapomorphy, and the

5683 dorsoventrally expanded distal end of the ischium would be unique within Apatosaurinae. All

5684 other traits are shared with other apatosaur specimens.

5685 To summarize, concerning the phylogenetic position of YPM 1840, the present study best

5686 supports a grouping with NSMT-PV 20375, with or without participation of *Apatosaurus ajax*

5687 remains to be seen these uncertainties, as well as the lacking autapomorphies for the

5688 specimen suggest that YPM 1840 has to be treated as undiagnostic, and classified as an

5689 indeterminate Apatosaurinae. '*Atlantosaurus*' *immanis* is thus a nomen dubium. ~~As~~Because it

5690 has no taxonomic reference, and was usually synonymized with *Apatosaurus ajax*, such a

5691 treatment has no influence on apatosaur taxonomy.

5692 ***Diplodocus longus* YPM 1920.** Being the type specimen of the type species of the genus

5693 *Diplodocus*, validity of YPM 1920~~it~~ is of particular taxonomic importance. Nonetheless,

5694 results obtained herein raise considerable doubts about the diagnosability of the specimen.

5695 *Diplodocus longus* YPM 1920 consistently groups with the other included specimens of

5696 *Diplodocus* in both types of analyses (equal and implied weighting). It is found as sister taxon

5697 to *Diplodocus hallorum* in the reduced consensus tree obtained by implied weighting, and is

5698 recovered in the same position, when added to the equally weighted reduced consensus tree.

5699 In all cases, if the tree also includes one or both specimens of *Diplodocus carnegii* (CM 84 or

94), a polytomy is formed with YPM 1920, the included specimen(s) of *D. carnegii*, and the *D. hallorum* clade. If *D. longus* is excluded, but both *D. carnegii* specimens are added, they form the sister clade to *D. hallorum*. This shows that *D. longus* YPM 1920 switches position between the two specimens of *D. carnegii*, and a position closer to *D. hallorum*, indicating that it is not diagnosable on its own. A single autapomorphy (338-1) was recovered from the main trees, but considered invalid ~~as~~because it is shared with the *Diplodocus* specimen AMNH 223 (Tab. S112). Given that no tree recovers this as a synapomorphy for a clade uniting YPM 1920 and AMNH 223 to the exclusion of all other *Diplodocus* specimens, this feature has probably to be interpreted as individual variation. A constrained search uniting these two specimens yielded an equally weighted tree of 1899 steps, and an implied weights tree of 188.14357 steps. Relative length increase thus amounts to 0.11% and 0.09%, respectively.

Although confidently identifiable as belonging to the same genus as the type specimens of *D. carnegii* and *Seismosaurus hallorum*, YPM 1920 does not appear to be diagnosable to the species level. This would mean that *Diplodocus longus* would have to be considered a nomen dubium, and that consequently also the genus name *Diplodocus* would have to be abolished. ~~As~~Because *Diplodocus* is probably one of the most iconic dinosaurs, and generally considered to be one of the best known sauropod genera, based on numerous partly to nearly complete skeletons (McIntosh and Carpenter, 1998; Upchurch et al., 2004a), an abolition of the genus just for the sake of strictly following ICZN rules is not advisable. A case to ICZN is thus being prepared to suggest the suppression of *D. longus* as type species of *Diplodocus*, and its replacement by *D. carnegii*. *D. carnegii* is typified by the nearly complete, and articulated type specimen CM 84, which includes a complete vertebral column from the second cervical to the twelfth caudal vertebra, as well as articulated fore- and hindlimb material. CM 84 is the most famous specimen of *Diplodocus*, constituting the largest part of the *Diplodocus* cast sent by Andrew Carnegie to various museums around the world in order to promote the activities of the newly founded Carnegie Museum (Nieuwland, 2010). The greater scientific importance of this specimen compared to the holotype specimen of *D. longus*, YPM 1920, is also exemplified by the fact that important studies of diplodocoid interrelationships ~~do not base~~are not based on personal observations of YPM 1920, but mainly of CM 84 (e.g. Whitlock, 2011a). This shows that even if further studies would reveal YPM 1920 to be diagnosable, and that *D. longus* would therefore be valid, a suppression of the latter species in favor of CM

5732 84 and *D. carnegii* as type for *Diplodocus* would still make sense due to the wider availability

5733 for study, as well as the much higher degree of completeness of the specimen. Consequently,

5734 and pending a decision on the prepared case to ICZN, it is hereby suggested to use *D.*

5735 *carnegii* as type species for *Diplodocus*. YPM 1920 is considered not diagnostic at species

5736 level, and *Diplodocus longus* has therefore to be regarded a nomen dubium. A similar case

5737 was announced by Upchurch and Martin (2003) for the substitution of *Cetiosaurus medius* by

5738 *C. oxoniensis* as type species, and submitted in 2009 (Upchurch et al., 2009). Their reasoning

5739 leading to the case was almost identical to the one presented herein.

5740 **Brontosaurus excelsus YPM 1980.** Differences between YPM 1980 and *Apatosaurus ajax*

5741 YPM 1860 are usually considered not abundant enough to justify generic distinction (Riggs,

5742 1903), leading to a treatment of *Brontosaurus* as junior synonym of *Apatosaurus* (Riggs,

5743 1903; Gilmore, 1936; McIntosh, 1995; Upchurch et al., 2004a, b). The specimen YPM 1980

5744 is the genoholotype of *Brontosaurus*. Where recovered, it forms the sister taxon to a clade

5745 including *Apatosaurus ajax* YPM 1860 and *Apatosaurus louisae* CM 3018.

5746 Four ambiguous autapomorphies are found to be reliable (Tab. S113). One was found to be

5747 unique within Diplodocidae (443-1). Given the high number of differences with the

5748 *Elosaurus* clade, as well as with the *Apatosaurus ajax* clade, generic separation from both of

5749 these genera is herein regarded valid.

5750 Additional support for generic separation and thus a resurrection of *Brontosaurus* as a valid

5751 genus comes from the equally weighted tree, and the position recovered for *Amphicoelias*

5752 *altus* therein. *Amphicoelias altus* was described before any other putative apatosaurine genus

5753 (Cope 1877a), and would thus have priority over any genus recovered as sister taxon and

5754 considered to pertain to the same genus. In the equally weighted reduced consensus tree,

5755 *Amphicoelias altus* + *Eobrontosaurus yahnahpin* form the sister clade to *Apatosaurus ajax* +

5756 *Apatosaurus louisae*. When adding *Brontosaurus excelsus* to the tree, a trichotomy is formed

5757 between *Brontosaurus*, *Amphicoelias* + *Eobrontosaurus*, and *Apatosaurus*. If *Brontosaurus*

5758 would be considered synonymous to *Apatosaurus* in such an arrangement, *Apatosaurus* would

5759 have to be synonymized with *Amphicoelias* according to ICZN rules. The specimen YPM

5760 1980 is thus herein considered diagnosable, and distinct enough to justify generic separation

5761 from *Apatosaurus*.

5762 **Apatosaurus laticollis YPM 1861.** Based on a single, fragmentary, mid- to posterior cervical

5763 vertebra, this specimen is one of the least complete included in the analysis. McIntosh (1995)

suggested it to come from the same individual as YPM 1840, but evidence from two partial femur elements suggest that more than one individual was present in the quarry (McIntosh, 1995). The fact that no tree of the present analysis shows a sister taxon arrangement of YPM 1840 and 1861 casts further doubts on the proposal of McIntosh (1995). *A. laticollis* YPM 1861 is herein consistently found as most closely related to *A. louisae* CM 3018 and CM 3378. If true, and if YPM 1861 is considered diagnosable, this would indicate that the two species would be synonymous, and that *A. laticollis* would therefore have priority over *A. louisae*.

One ambiguous autapomorphy is found for *Apatosaurus laticollis* YPM 1861, which is unique within Apatosaurinae (Tab. S114). However, ~~as~~because only two traits distinguish *A. laticollis* from *A. louisae*, specific separation cannot be justified, and the two traits are more cautiously interpreted as individual variation, at least in the present species. The fact that the two shared synapomorphies for CM 3018 + CM 3378 (and thus YPM 1861 as well) could not be scored in YPM 1861 indicates that the latter specimen does not exhibit any taxonomically significant character for the species it forms together with CM 3018 and CM 3378.

Forcing *Apatosaurus laticollis* YPM 1861 into close relationship with YPM 1840 (following McIntosh, 1995), recovered tree lengths are 1898 (length increase of 0.05%) with equal weighting, and 188.34011 (relative increase of 0.2%) with implied weighting. In both analyses, YPM 1861 is pulled into the clade where YPM 1840 was found in the unconstrained search. The fact that YPM 1861 readily changes position further indicates that it is not diagnosable to species level~~,~~ and that *A. laticollis* has to be considered a nomen dubium. Pending further detailed studies of the specimens YPM 1840 and 1861, YPM 1861 is herein referred to *A. louisae*.

***Brontosaurus amplus* YPM 1981.** *Brontosaurus amplus* YPM 1981 is often considered synonymous ~~to~~with *Brontosaurus excelsus* (McIntosh, 1995; Upchurch et al., 2004b), although ~~mostly~~usually stating that further studies are needed in order to assess its taxonomic affinities. The present study does not allow a much more detailed assessment, mostly because of limited personal observations of the specimen due to time constraints during the collection visit at YPM. However, some conclusions can be drawn from the trees recovered. Although not present in the equally weighted reduced consensus tree, addition of the specimen results in a polytomy with *Apatosaurus louisae* + CM 3378, *Eobrontosaurus* + *Amphicoelias*, and *Apatosaurus ajax* + YPM 1840. In the implied weights trees, *Brontosaurus amplus* does not

5796 group with *Brontosaurus excelsus*, but with *Apatosaurus louisae*.

5797 Two ambiguous autapomorphies were recovered for YPM 1981 (Tab. S115). However, the

5798 four changes separating YPM 1981 from *Apatosaurus louisae* do not allow specific separation

5799 (see above). Also, the polytomy recovered when adding *A. laticollis* to the reduced consensus

5800 tree obtained by implied weights indicates that all four specimens (CM 3018, CM 3378, YPM

5801 1861, and YPM 1981) might belong to the same species. More detailed studies of YPM 1981

5802 would be needed in order to confirm presence or absence of the five synapomorphies found

5803 for the clade uniting these four specimens. Although no apatosaurine synapomorphies can be

5804 positively identified in YPM 1981 to date, the robust humerus (380-2) and astragalus (452-1)

5805 suggest that an identification of *B. amplus* as apatosaur more derived than *Eobrontosaurus* or

5806 *Brontosaurus* can be stated with some confidence.

5807 Constraining the search to trees recovering a clade with *Brontosaurus excelsus* and *B. amplus*

5808 ~~expulses~~expels ☰ h *Apatosaurus ajax* and *A. louisae* from the equally weighted reduced

5809 consensus tree. Tree length is 1898 steps, and three major clades are recovered within

5810 Apatosaurinae: the previously unrecognized combination of FMNH P25112 + (SMA 0087 +

5811 AMNH 460) forms the sister taxon to *Elosaurus + Brontosaurus*, which include CM 566 +

5812 UW 15556, and YPM 1980 + YPM 1981, respectively. When one of the *Apatosaurus*

5813 specimens is added, a large polytomy is formed including many diplodocine specimens as

5814 well. The same constraint in the implied weights analysis yields trees of a length of 187.98825

5815 steps, which is only 0.01% longer than the most parsimonious trees. Several changes are

5816 introduced to apatosaurine interrelationships: SMA 0087 forms a clade together with AMNH

5817 460, *Elosaurus parvus* CM 566 + UW 15556 are separated from *Brontosaurus*, and form the

5818 sister clade to *Apatosaurus ajax* + mdA, the two *Brontosaurus* type specimens form the sister

5819 group to *Apatosaurus ajax*, together forming the sister clade to *Eobrontosaurus* + (FMNH

5820 P25112 + (*Apatosaurus louisae* + CM 3378)). However, no valid synapomorphies unite YPM

5821 1980 with YPM 1981 in that tree, and only one of the four found synapomorphies for the

5822 clade uniting them with *Apatosaurus ajax* is found as well in YPM 1981: the presence of a

5823 ridge on the ventral side of the third sacral rib (288-1). The latter trait has been proposed by

5824 Mook (1917), but regarded as unreliable for species identification within *Apatosaurus* by

5825 Upchurch et al. (2004b). Given this, although tree length is not increased much by the current

5826 constraint, morphological support for the recovered arrangement appears low. A closer

5827 relationship with *Apatosaurus louisae* seems thus better supported by the present analysis, but

5828 ~~since~~because YPM 1981 cannot be scored for any of the recovered species autapomorphies, it

5829 has to be considered a nomen dubium, pending restudy. It is tentatively referred to

5830 *Apatosaurus louisae*.

5831 ***Diplodocus lacustris* YPM 1922.** Marsh (1884) established this species based on more

5832 slender teeth compared to the ones present in the skull USNM 2672. Whereas this appears to

5833 be true (Tab. S16), both specimens are within the minimum and maximum values of the teeth

5834 of the skull CM 11161, which was only found after Marsh's death (Holland, 1924). The

5835 specimen YPM 1922 was found to be the least stable in both main analyses, being mainly

5836 responsible for the large polytomy within Diplodocoidea in the complete strict consensus tree.

5837 Given that no characters are known that would allow an identification of diplodocid teeth at

5838 species level, and that both the premaxilla and maxilla referred to the type specimen are not

5839 diplodocid (see above), the teeth of the holotype specimen YPM 1922 can only be identified

5840 as Diplodocidae indet. *D. lacustris* should thus be regarded as a nomen dubium. It is thus also

5841 not available as type specimen for the substitution of the suppressed *D. longus* YPM 1920.

5842 The choice of *D. carnegii* and CM 84 to typify *Diplodocus* is thus further supported.

5843 ***Elosaurus parvus* CM 566.** The specimen CM 566 is a very juvenile individual, as

5844 exemplified by its small size and the lacking neurocentral fusion (Peterson and Gilmore,

5845 1902; McIntosh, 1995; Upchurch et al., 2004b; Schwarz et al., 2007c). Until recently, it was

5846 generally referred to *Brontosaurus excelsus*, together with the adult specimen UW 15556,

5847 with which it was found (Gilmore, 1936; McIntosh, 1995). By means of a specimen-based

5848 phylogenetic analysis, Upchurch et al. (2004b) showed that specific separation of CM 566 and

5849 UW 15556 from other apatosaur species is justifiable. Recovered autapomorphies for the

5850 species were also shown in the juvenile specimen CM 566, leading Upchurch et al. (2004b) to

5851 propose the new combination *Apatosaurus parvus*. The present analysis also consistently

5852 recovers CM 566 together with UW 15556, and confirms the validity of the species

5853 autapomorphies found by Upchurch et al. (2004b), as well as their presence in CM 566.

5854 Position in the trees is generally close to the holotype of *Brontosaurus excelsus* (YPM 1980).

5855 Whereas at first sight, this might corroborate synonymy of *Elosaurus parvus* with

5856 *Brontosaurus excelsus*, the high number of differences between the two taxa not only allows

5857 specific, but also generic distinction (see above). *Elosaurus* is thus considered a valid genus,

5858 with *Elosaurus parvus* as its type species, and CM 566 as its genoholotype.

5859 ***Gigantosaurus africanus* various specimen numbers.** The holotype specimen of

Gigantosaurus africanus consists of several bones excavated in the first expedition to Tendaguru, Tanzania, now housed at the Staatliches Museum für Naturkunde in Stuttgart, Germany. More elements from the same individual were found later and brought to the Museum für Naturkunde in Berlin, Germany (Remes, 2006). The taxon has a complex taxonomic history: *Gigantosaurus* being preoccupied, it was later renamed *Tornieria* (Sternfeld, 1911), and then synonymized with *Barosaurus* (Janensch, 1922). After a thorough redescription and study of all preserved material, Remes (2006) re-established it as the separate genus *Tornieria*, in the combination *Tornieria africana*, adapting the latinized species name to the female genus. Its generic distinction from *Barosaurus* has been shown to hold in phylogenetic analyses as well (Remes, 2006; Whitlock, 2011a; Mannion et al., 2012). The current study confirms this separation. Skeleton A, ~~from~~of which the holotype material is a part ~~of~~, consistently clusters with a second specimen referred to the same species by Remes (2006), skeleton k, also from Tendaguru. Both together form a relatively basal clade within Diplodocinae, in many ~~cases~~trees the most basal one. Five shared synapomorphies unite the two specimens (Tab. S77), although only one of these qualifies as a species autapomorphy (420-1), ~~as~~because all other four are shared with other diplodocine specimens. The holotype specimen is thus diagnosable at the species level, and *Tornieria africana* a valid species.

Apatosaurus louisae CM 3018. The type specimen of *A. louisae* is the most complete type specimen of the entire clade of Apatosaurinae. It is also one of the few diplodocid holotypes which has been ~~decently~~thoroughly described and figured (Gilmore, 1936). CM 3018 is thus probably the best known and most used reference~~d~~ specimen for *Apatosaurus*, even though it is not its genoholotype. In the recovered main trees, it consistently groups with CM 3378 and *A. laticollis* YPM 1861, with which it forms the sister clade to *A. ajax*. Even though it is so complete, only one ambiguous 'autapomorphy' was found for the single specimen (Tab. S116). This indicates that the other specimens grouping with CM 3018 belong to the same species. ~~As~~Because *Apatosaurus laticollis* is herein considered a nomen dubium, the only available species name for this group is *A. louisae*, as initially proposed for CM 3018 (Holland, 1915a). The specimen CM 3018 shows all ~~the~~ five 'synapomorphies' found for the clade with CM 3018, CM 3378, YPM 1861, and YPM 1981 (see above). Of these, three qualify as valid autapomorphies for the species, not shared with any other apatosaur specimen (see updated diagnosis below). Following the numerical approach, generic separation from *A. ajax* is not justified, corroborating previous referrals of CM 3018 to *Apatosaurus*, as *A.*

5892   *louisae*.

5893   ***Apatosaurus minimus* AMNH 675.** *Apatosaurus minimus* was described by Mook (1917),

5894   based on a sacrum and pelvic girdle. The specimen has generally been considered

5895   misidentified, and its diplodocoid affinities rejected (McIntosh, 1995; Upchurch et al.,

5896   2004b). Whereas pubis morphology strongly resembles *Camarasaurus*, the presence of six

5897   sacral vertebrae and widely splayed preacetabular lobes of the ilium are generally considered

5898   titanosauriform characteristics (McIntosh, 1990a; Upchurch et al., 2004a, b). Due to its

5899   incompleteness, the true identity of AMNH 675 still remains dubious. Other than confirming

5900   the non-flagellicaudatan (and probably non-diplodocoid) affinities of AMNH 675, the present

5901   study does not help much in resolving this issue. Whereas the equally weighted trees

5902   recovered AMNH 675 as one of the six most unstable taxa (thus deleted from the pruned

5903   consensus), implied weighting resolves AMNH 675 as somphospondylian titanosauriform,

5904   based on the two characteristics mentioned above. The three autapomorphies found for the

5905   specimen indicate that AMNH 675 probably shows a unique combination of features.

5906   Addition of AMNH 675 to the equally weighted reduced consensus tree results in a polytomy

5907   with *Cetiosauriscus stewarti*, SMA 0009, AMNH 5765, Titanosauriformes, *Camarasaurus* +

5908   Turiasauria, Rebbachisauridae, and Flagellicaudata.

5909   Forcing *Apatosaurus minimus* AMNH 675 into a titanosauriform position in the equally

5910   weighted analysis results in a tree three steps longer than the most parsimonious tree.

5911   *Dystrophaeus* is pulled into Titanosauriformes as well, and *Australodocus* is recovered as

5912   basal-most Diplodocinae. The same tree length is found when imposing apatosaurine

5913   affinities, with a completely unresolved clade as result. Camarasaurid affinities are much

5914   more probable, given that a forcing into this group yields the same tree length as the equally

5915   weighted most parsimonious trees (1897 steps). Furthermore, ~~also~~ the presence of six sacral

5916   vertebrae has already been reported in a camarasaur (Tidwell et al., 2005)~~,~~ and was interpreted

5917   as an ontogenetic feature. Tree length of the implied weight trees increase<u>s</u> to ~~188.23~~185

5918   steps, or by a percentage of 0.14%, when restricting AMNH 675 to Apatosaurinae (where it

5919   grouped with *Dystrophaeus* and *Elosaurus*), and to 188.18066 (0.11%) when forcing it into

5920   Camarasauridae. Camarasaurid or titanosauriform affinities are thus the most probable for

5921   AMNH 675, but more detailed studies of those clades are needed in order to identify AMNH

5922   675 properly.

5923   ***Diplodocus hayi* HMNS 175.** Described by Holland (1924) as *Diplodocus hayi*, HMNS 175

5924 (initially CM 662) was often thought not to belong to *Diplodocus* (e.g. McIntosh, 1990b;

5925 Foster, 1998; Harris, 2006c), due to its relatively robust forelimbs, and the widely diverging

5926 basipterygoid processes – both traits that are generally interpreted to diagnose apatosaurs

5927 (Berman and McIntosh, 1978; McIntosh, 1990a; Upchurch et al., 2004a). The specimen

5928 HMNS 175 is one of the most complete specimens known from Diplodocinae, but has never

5929 been completely described. It preserves cranial material, cervical, dorsal, sacral, and caudal

5930 vertebrae, as well as a nearly complete forelimb and hindlimb (McIntosh, 1981; ET, pers.

5931 obs., 2010). The current analysis supports a generic separation from *Diplodocus*, as HMNS

5932 175 consistently results in a clade more basal to *Diplodocus*, together with the specimens

5933 AMNH 969 and SMA 0011. It is therefore herein referred to the new genus *Galeamopus*, of

5934 which it is the genoholotype specimen.

5935 Autapomorphies for HMNS 175 amount to four (Tab. S117), one of which unique within

5936 Diplodocidae (392-0), and a second one within Diplodocoidea (387-2). Forcing *Galeamopus*

5937 *hayi* HMNS 175 to group with the classical *Diplodocus* specimens, equally weighted analysis

5938 recovers shortest trees of 1904 steps, a length increase of seven steps of 0.37% compared to

5939 the unconstrained most parsimonious trees. Applying implied weights, tree length counts

5940 188.70122 steps, corresponding to a relative increase of 0.39%. A generic separation from

5941 *Diplodocus* is thus well-supported.

5942 **'*Apatosaurus*' alenquerensis MIGM various numbers (lectotype).** As *Tornieria africana*,

5943 ~~also~~ '*Apatosaurus*' *alenquerensis* has had a complicated taxonomic history. After being

5944 referred to *Camarasaurus* (McIntosh, 1990b), Dantas et al. (1998) erected the new genus

5945 *Lourinhasaurus* for a number of specimens thought to belong to the same species. No specific

5946 type specimen was attributed to the name (only a skeleton was mentioned without specimen

5947 number; Dantas et al., 1998), until Antunes and Mateus (2003) established the first specimen

5948 found at Moinho do Carmo, Alenquer, Lourinhã, as lectotype specimen. In the meantime, the

5949 specimen on which Dantas et al. (1998) made most observations of differences between

5950 *Lourinhasaurus* and *Camarasaurus* was redescribed and referred to a new species and genus,

5951 *Dinheirosaurus lourinhanensis* (Bonaparte and Mateus, 1999). Even so, *Lourinhasaurus*

5952 remained accepted, and its generic separation subsequently justified by means of phylogenetic

5953 analyses, which did not recover the lectotype specimen in a position close to *Camarasaurus*

5954 or *Apatosaurus* (e.g. Upchurch et al., 2004a; Royo-Torres and Upchurch, 2012).

5955 Two ambiguous autapomorphies are found to diagnose *Lourinhasaurus* (Tab. S118). The fact

5956 that *Lourinhasaurus* consistently forms its own clade in any recovered tree indicates that it

5957 also exhibits a unique combination of traits. The lectotype specimen is thus considered

5958 diagnostic, and *Lourinhasaurus alenquerensis* valid.

5959 Forcing *Lourinhasaurus* into the Camarasauridae clade, equal weighting results in a tree only

5960 one step longer than the most parsimonious trees. *Lourinhasaurus* is found to be in the

5961 turiasaur clade, not supported by any synapomorphy. Implied weighting recovers

5962 *Lourinhasaurus* basal to *Camarasaurus* + Turiasauria, with a tree length of 188.03513, an

5963 increase of 0.03%. A close relationship with *Camarasaurus* can thus not be excluded,

5964 although generic separation is probably warranted. Although the precise phylogenetic position

5965 of *Lourinhasaurus* cannot be resolved herein, a position at the base of Neosauropoda appears

5966 the most supported.

5967 ***Cetiosauriscus stewarti* NHMUK R3078.** The pPhylogenetic position of *Cetiosauriscus*

5968 *stewarti* has been debated (Charig, 1980; McIntosh, 1990b; Heathcote and Upchurch, 2003;

5969 Upchurch et al., 2004a). Diplodocid affinities were purported several times (Charig, 1980;

5970 McIntosh, 1990b; Upchurch et al., 2004a), but mostly based on a second specimen containing

5971 a whip-lash tail, which has no overlapping bones with the holotype (Heathcote and Upchurch,

5972 2003; Upchurch et al., 2004a). Diplodocid affinities of the holotype specimen are thus

5973 questionable, and consequently, a closer relationship to *Mamenchisaurus* or *Omeisaurus* was

5974 found by Heathcote and Upchurch (2003). The current analysis recovers NHMUK R3078 in

5975 two different positions, depending on the weighting strategy applied. Equal weighting yields

5976 diplodocimorph affinities, more derived than Rebbachisauridae, whereas implied weighting

5977 recovers NHMUK R3078 as a non-neosauropod eusauropod, close to *Mamenchisaurus* or

5978 *Omeisaurus* as proposed by Heathcote and Upchurch (2003).

5979 No autapomorphies were found by the implied weights analysis, probably due to the sister

5980 relationship with *Barosaurus affinis* YPM 419. The incompleteness of the latter find inhibited

5981 the recovery of autapomorphies in its sister taxon *Cetiosauriscus*, asbecause for many features

5982 the two specimens are not comparable. However, the recovered autapomorphies from the

5983 equally weighted trees were assessed in two ways, and their validity was tested based on both

5984 diplodocoid as well as non-neosauropod eusauropod affinities. Three traits qualified as

5985 ambiguous autapomorphyies in both cases (Tab. S119). The fact that autapomorphies were

5986 found reliable independent from the phylogenetic position indicates that NHMUK R3078 is

5987 diagnosable, and *Cetiosauriscus stewarti* thus valid.

Imposing a sister arrangement of *Cetiosauriscus* and *Barosaurus affinis* YPM 419 in the equally weighted tree does not increase length, nor influence the position of *Cetiosauriscus*. Forced sister arrangements with *Omeisaurus* and *Mamenchisaurus* produced tree lengths of 1900 and 1903 steps or length increases of 0.16% and 0.32%, respectively. When forcing *Cetiosauriscus* into Apatosaurinae or Diplodocinae with implied weighting, tree lengths of 188.80886 or 189.29031 steps are recovered (length increase of 0.45% or 0.7%). Imposing dicraeosaurid or rebbachisaurid affinities results in tree lengths of 188.72199 or 188.99738, corresponding to an increase of 0.4% or 0.55%, respectively. Consequently, changing the position from diplodocoid to non-neosauropod eusauropod in the equally weighted tree (in particular close to *Omeisaurus*) is easier than imposing diplodocoid affinities of *Cetiosauriscus* in the implied weights analysis. *Cetiosauriscus stewarti* is thus herein interpreted as non-diplodocoid eusauropod, possibly closely related to *Omeisaurus*, as already proposed by Heathcote and Upchurch (2003).

***Supersaurus vivianae* BYU 12962.** The holotype specimen of *Supersaurus vivianae* is restricted to a scapula (Jensen, 1985), but other elements from the same quarry most probably belong to the same individual (Curtice and Stadtman, 2001; Lovelace et al., 2007). A scapula is not ~~present~~preesrved in the second specimen referred to *Supersaurus vivianae* by Lovelace et al. (2007; WDC DMJ-021), which inhibited recognition of autapomorphies on the scapula by TNT. However, the fact that both referred specimens consistently group together in all trees indicates that identification of additional elements as belonging to the same individual as the type specimen (Curtice and Stadtman, 2001; Lovelace et al., 2007) was right. Even though the holotype might not be diagnostic, the individual it is part of definitely is. No valid autapomorphies separate the type individual from the second specimen, WDC DMJ-021, indicating that they belong to the same species. Of the seven traits uniting the two specimens (Tab. S79), only three can be considered valid autapomorphies for the species (231-0, 296-1, 307-0), ~~as~~because the other four also occur in other diplodocine specimens. *Supersaurus vivianae* forms a clade together with *Dinheirosaurus* when applying equal weighting, whereas implied weighting recovers it together with *Australodocus*, in a position more basal to *Dinheirosaurus*, and even *Tornieria*. The fact that trees excluding *Australodocus* a priori, or restricting it to Titanosauriformes, show *Supersaurus* again as sister taxon to *Dinheirosaurus*, in its more derived position, indicates that the change is mainly due to the instability of *Australodocus*. Furthermore, when restricting *Supersaurus* to

6020   *Dinheirosaurus* in the implied weights trees, *Australodocus* is again recovered within

6021   Titanosauriformes. Tree length in this case is 188.02344, which is even shorter than the trees

6022   recovered when forcing *Australodocus* directly into Titanosauriformes (188.09844). The

6023   former tree length equals a length increase of 0.03%, which corresponds to less than a one-

6024   step increase in the equally weighted trees. The position more derived than *Tornieria* appears

6025   thus better supported by the present analysis, even though this is contrary to the findings of

6026   Whitlock (2011a), Mannion et al. (2012), or Tschopp and Mateus (2013b).

6027   ***Dystylosaurus edwini* BYU 4503.** The holotype specimen of *Dystylosaurus edwini* was

6028   previously proposed to belong to the same individual as the *Supersaurus vivianae* holotype

6029   scapula (Curtice and Stadtman, 2001), a view supported by Lovelace et al. (2007), as well as

6030   preliminary analyses of the present study (see above). Therefore, *Dystylosaurus edwini* is

6031   herein considered a junior synonym of *Supersaurus vivianae*. Its type specimen BYU 4503

6032   has thus not been included in the final analysis as separate slot, but was incorporated into the

6033   OTU called *Supersaurus vivianae* BYU+.

6034   ***Seismosaurus halli* NMMNH 3690.** Gillette (1991) named this new genus based on the

6035   specimen NMMNH 3690, and later changed to species name to *hallorum*, in order to correct it

6036   for wrongly applied latin grammar (Gillette, 1994). *Seismosaurus* was later synonymized with

6037   *Diplodocus* (Lucas et al., 2006; Lovelace et al., 2007), with uncertainties if it can be retained

6038   as separate species or if it should be regarded synonymous to *Diplodocus longus* (Lovelace et

6039   al., 2007). The latter statement was most probably based on previous identifications of the

6040   more complete specimens AMNH 223 and USNM 10865 as *Diplodocus longus* (Osborn,

6041   1899; Gilmore, 1932), which was herein showed to be erroneous, or at least questionable.

6042   *Seismosaurus hallorum* NMMNH 3690 is consistently recovered in a group with AMNH 223,

6043   USNM 10865, and DMNS 1494, which has been shown to constitute its own species.

6044   Showing four of the six shared traits of the group, *Seismosaurus hallorum* NMMNH 3690 can

6045   be considered diagnostic. ~~As~~Because it is the only type specimen in this cluster, and since the

6046   number of changes does not allow generic separation (see above), *Diplodocus hallorum* is the

6047   only valid, available name for this taxon.

6048   ***Dyslocosaurus polyonychius* AC 663.** *~~Being b~~*Based on very fragmentary appendicular

6049   material, assessment of the phylogenetic position is difficult for this taxon. Although initially

6050   described as diplodocid (McIntosh et al., 1992), the high number of probable pedal unguals

6051   resembles basal sauropods, ~~as~~because the loss of pedal phalanges and unguals is usually

considered typical for Eusauropoda and more derived forms (Wilson, 2002; Upchurch et al.,

2004a). However, almost no complete and articulated pes is known from any diplodocid, and

of the included specimens, only few preserve pedal material. A positive confirmation of the

absence of vestigial phalanges or unguals is very difficult, if not impossible. The true

distribution of a high number of pedal phalanges can thus not be assessed with the present

analysis.

Although reduced consensus trees omit *Dyslocosaurus polyonychius*, both pruned trees find it

as dicraeosaurid. Five synapomorphies found for Dicraeosauridae are present in

Dyslocosaurus, but four of them are only shared with one other dicraeosaurid taxon (431-1,

443-1, and 452-1 are shared with *Dicraeosaurus*; 477-1 is shared with *Suuwassea*; and 461-0

is shared with *Dicraeosaurus* and *Suuwassea*). None of these traits could be coded in

Amargasaurus or *Brachytrachelopan*, and all of them are also present in certain diplodocid

taxa. If *Dyslocosaurus* should not be a dicraeosaurid, only the gracility of the metatarsal I

(461-0) would possibly remain as dicraeosaurid synapomorphy, pending further finds of

dicraeosaurid hindlimb material.

Five ambiguous autapomorphies are found for AC 663 when considered a dicraeosaurid (Tab.

S120). Three of these autapomorphies are shared with apatosaur specimens (442-1, 468-1,

470-1), four also occur in diplodocines (442-1, 446-0, 456-1, 468-1). The fact that this

specimen appears to unite apatosaur, diplodocine, and dicraeosaurid traits indicates that AC

663 – even though highly incomplete – is diagnostic, and *Dyslocosaurus polyonychius* thus a

valid taxon.

Forcing *Dyslocosaurus* into a position within Apatosaurinae produced shortest trees of a

length of 1902 (equal weighting) and 188.17813 (implied weighting) steps, an increase of

0.26% and 0.11%, respectively. When imposing diplodocine affinities, tree lengths of 1910

and 189.51146 steps are recovered, corresponding to length increases of 0.69% and 0.82%.

Diplodocine affinities are thus the least parsimonious, followed by an identification as

Apatosaurinae, which still appears improbable. Despite the shared characters with both

diplodocid clades, an identification of *Dyslocosaurus* as dicraeosaurid diplodocoid is

considerably better supported.

***Apatosaurus yahnahpin* Tate-001.** *Apatosaurus yahnahpin* Tate-001 has been renamed

Eobrontosaurus yahnahpin (Bakker, 1998), but it was never included in any phylogenetic

analysis, and no detailed description has yet been published. Based on purportedly primitive

6084   conditions in the pectoral girdle and the cervical ribs, Bakker (1998) interpreted

6085   *Eobrontosaurus* as the basal-most apatosaurine. Upchurch et al. (2004a) stated that the

6086   specimen Tate-001 is practically indistinguishable from *Camarasaurus*, but personal

6087   comments of R. Wilhite (cited in Taylor et al., 2011) and P. Mannion (2012) implied that the

6088   taxon might be a valid diplodocid. The present analysis confirms this: Tate-001 is consistently

6089   recovered as apatosaurine diplodocid. Whereas it forms the sister taxon to *Amphicoelias altus*

6090   in the equally weighted tree, its position within the clade is less clear when applying implied

6091   weighting: *E. yahnahpin* is found as sister taxon to *Apatosaurus ajax* + mdA in the main trees,

6092   whereas an a priori deletion or forced titanosauriform affinities of *Australodocus* result in a

6093   more basal position of *E. yahnahpin*, as sister taxon to AMNH 460 + mdA.

6094   Eight ambiguous autapomorphies are considered valid for Tate-001 (Tab. S121). Whereas this

6095   already justifies specific separation, support for generic separation depends on the position

6096   where it is recovered (see above). The least support for generic distinction is found if

6097   recovered as sister taxon to *Amphicoelias* (five changes), followed by the tree without

6098   *Australodocus* (nine changes). As *Amphicoelias* is more parsimoniously considered the basal-

6099   most diplodocid genus, instead of an Apatosaurinae, distance between *Eobrontosaurus* and its

6100   sister clade *Apatosaurus ajax* + mdA in the equally weighted tree increases to 16. Given that

6101   it is generally found as single slot, *Eobrontosaurus* is herein accepted as valid genus within

6102   Apatosaurinae.

6103   Forcing *Eobrontosaurus* to lie outside AMNH 460 + mdA in the implied weight trees resulted

6104   in tree lengths of 188.00659 steps, an increase of 0.02%. The Pphylogenetic position of

6105   *Eobrontosaurus* is thus not very clear to date, and has to await publication of the promised

6106   detailed description.

6107   ***Dinheirosaurus lourinhanensis* ML 414.** *Dinheirosaurus lourinhanensis* ML 414 was first

6108   described as *Lourinhasaurus alenquerensis* (Dantas et al., 1998), but a more detailed

6109   redescription showed that it constitutes its own genus within Diplodocidae (Bonaparte and

6110   Mateus, 1999). Such a position was later confirmed by phylogenetic analyses, and refined to

6111   Diplodocinae (Rauhut et al., 2005; Whitlock, 2011a; Mannion et al., 2012). The present

6112   analysis supports this assignment, but recovered *Dinheirosaurus* in an even more derived

6113   position than Whitlock (2011a) or Mannion et al. (2012). Both analyses find *Dinheirosaurus*

6114   in a position within Diplodocinae, more derived than *Tornieria*. Differences occur in the

6115   relative position of *Supersaurus*, although a position as sister genus of *Dinheirosaurus*

6116 appears more probable, as discussed above.

6117 Four ambiguous autapomorphies are found for ML 414, and thus for *Dinheirosaurus*

6118 *lourinhanensis* (Tab. S122). The ten changes found between *Dinheirosaurus* and *Supersaurus*

6119 or (in the case of a more basal position of the latter) *Galeamopus* + mdD are considered

6120 enough to justify generic separation, especially given that *Dinheirosaurus* is a Portuguese

6121 taxon, and thus also geographically separated from its closest relatives.

6122 ***Losillasaurus giganteus*** MCNV Lo-5. Whereas the holotype is restricted to an anterior

6123 caudal vertebrae, it actually belongs to a more complete individual (Casanovas et al., 2001)

6124 and was included as such in the present analysis. Initially regarded a basal diplodocoid

6125 (Casanovas et al., 2001), *Losillasaurus* was soon found to represent a non-diplodocoid,

6126 probably non-neosauropod eusauropod (Rauhut et al., 2005; Harris, 2006c). With the

6127 description of *Turiasaurus* (Royo-Torres et al., 2006), which has since been consistently

6128 recovered as sister genus to *Losillasaurus* (Royo-Torres et al., 2006, 2009; Barco, 2009;

6129 Carballido et al., 2012b; Royo-Torres and Upchurch, 2012), the more basal position has been

6130 generally accepted. The present study supports this view as well.

6131 Two ambiguous autapomorphies are found (Tab. S123). Despite the low number of

6132 autapomorphies, the numerical approach is not applied here, as non-diplodocid OTUs have

6133 not been sampled with enough detail to apply the same standards as established for

6134 Diplodocidae. *Losillasaurus* is thus considered herein a valid, non-diplodocoid genus,

6135 probably a non-neosauropod eusauropod.

6136 *Suuwassea emilieae* ANS 21122. *Suuwassea emilieae* was initially described as

6137 indeterminate flagellicaudatan (Harris and Dodson, 2004). Whereas earlier studies showed

6138 more diplodocid affinities (Gallina and Apesteguia, 2005; Rauhut et al., 2005; Remes, 2006;

6139 Lovelace et al., 2007), the discovery of the dentary of the holotype specimen (Whitlock and

6140 Harris, 2010) subsequently resulted in an identification as dicraeosaurid (Whitlock, 2011a;

6141 Mannion et al., 2012; Tschopp and Mateus, 2013b). The present analysis supports the latter

6142 assignment: *Suuwassea emilieae* ANS 21122 is consistently found as the basal-most

6143 dicraeosaurid sauropod.

6144 *Suuwassea emilieae* ANS 21122 is herein diagnosed by 35 ambiguous autapomorphies (Tab.

6145 S124). The high number of autapomorphies for *Suuwassea emilieae* reflect not only its

6146 diagnosability, but also the fact that the main dicraeosaurid OTUs were not studied in the

6147 same detail as the diplodocid sauropods. Given that the majority of the found autapomorphies

6148 are shared with certain diplodocid specimens, the difficulties in determining its dicraeosaurid
6149 affinities are not surprising. However, forcing *Suuwassea* into an apatosaurine clade (as found
6150 by Lovelace et al., 2007) yields trees of 1907 or 189.58814 steps (relative length increases of
6151 0.53% and 0.86%, respectively). Diplodocine relationships are found in shortest trees of 1903
6152 and 189.21056 steps, corresponding to increases in tree length of 0.32% and 0.66%.
6153 Apatosaurine or diplodocine affinities are thus much less parsimonious than an identification
6154 as dicraeosaurid.
6155 ***Australodocus bohetii* MB.R.2455.** Whereas the holotype only includes the single cervical
6156 vertebra MB.R.2455, a second, probably adjacent, cervical vertebrae most ~~probably~~likely
6157 belongs to the same animal (MB.R.2454; Remes, 2007). *Australodocus* was first described as
6158 diplodocid (Remes, 2007), but later found to represent a titanosauriform (Whitlock, 2011a, c;
6159 Mannion et al., 2012, 2013). The present analysis shows ambiguous results, with the equal
6160 weights analysis recovering it as brachiosaurid titanosauriform, but implied weighting finding
6161 diplodocine affinities. The incompleteness of the type individual complicates the recovery of
6162 a stable position for *Australodocus*.
6163 Of the autapomorphies recovered for *Australodocus*, only two were found by both analyses
6164 (Tab. S125). Both of these autapomorphies are shared with diplodocine specimens. In general,
6165 autapomorphies recovered for a brachiosaurid position are shared with diplodocines, and
6166 autapomorphies found for a diplodocine position with titanosauriforms. This indicates that the
6167 combination of traits is unique in *Australodocus*, which is thus regarded valid.
6168 As mentioned in the discussion of *Supersaurus*, *Australodocus* pulls the former genus into a
6169 more basal position in the main implied weight trees. When forcing *Supersaurus* into a
6170 ~~monophyletic group~~sister relationship with *Dinheirosaurus*, *Australodocus* is recovered again
6171 as a brachiosaurid titanosauriform. The latter constrained search produced shortest trees of
6172 188.02344 (a 0.03% length increase), whereas diplodocine affinities for *Australodocus* in the
6173 equally weighted trees finds trees of a length of 1898 steps, one more ~~compared~~than
6174 recovered in ~~to~~ the most parsimonious trees (an increase of 0.05%). In this case, however,
6175 *Supersaurus* remains united with *Dinheirosaurus*, instead of grouping with *Australodocus* as
6176 in the most parsimonious implied weight trees. The low number of titanosauriform OTUs in
6177 the present specimen lowers the capability of the analysis to recover *Australodocus* as
6178 belonging to that taxon, such that convergences found with Diplodocinae tend to become
6179 more important. Given that *Australodocus* is still recovered as titanosauriform in many trees,

6180 and that relative tree length increase to impose diplodocine affinities is slightly higher than
6181 the inverse direction in the implied weight trees, indicates that an identification as
6182 titanosauriform is more probable. Addition of titanosauriform specimens preserving cervical
6183 vertebrae would help to resolve this problem, but is not the scope of this analysis.
6184 ***Kaatedocus siberi* SMA 0004.** *Kaatedocus siberi* was initially described as a diplodocine less
6185 derived than *Tornieria*, *Diplodocus*, and *Barosaurus* (Tschopp and Mateus, 2013b). In the
6186 present analysis, *Kaatedocus* is consistently recovered in a more derived position, as sister
6187 taxon to *Barosaurus lentus*.
6188 The type specimen SMA 0004 bears one ambiguous 'autapomorphy' (a transverse ridge on the
6189 basal tubera; Tab. S126). ~~As~~Because no 'synapomorphy' was found for the sister clade
6190 AMNH 7530 + SMA D16-3, only one change separates SMA 0004 from the latter. The
6191 presence of such a transverse ridge is thus better interpreted as individual variation. Four of
6192 the nine 'synapomorphies' found for the entire group of *Kaatedocus siberi* qualify as species
6193 autapomorphies, not shared with other diplodocine specimens (178-1, 202-1, 211-1, and 212-
6194 1; Tab. S64).
6195 ***Galeamopus*** ▉▉▉▉ **SMA 0011.** *Galeamopus* ▉▉▉▉ is herein reported and described
6196 for the first time, and thus no comparisons with earlier studies exist. The holotype specimen
6197 SMA 0011 consistently groups with the holotype of *Galeamopus hayi*, HMNS 175, and the
6198 skull previously identified as *Diplodocus*, AMNH 969 (Holland, 1906).
6199 The specimen SMA 0011 shows four ambiguous and three unambiguous autapomorphies,
6200 justifying specific separation from *Galeamopus hayi* (Tab. S127). One of these, the horizontal
6201 canal connecting the preantorbital and the antorbital fenestra (12-1) was not recovered by the
6202 analysis, ~~as~~because the state in AMNH 969 or HMNS 175 cannot be discerned due to
6203 incomplete preservation. The trait ~~could~~thus could ~~thus~~ also be diagnostic for a more inclusive
6204 taxon, possibly the genus *Galeamopus*.
6205
6206 **Taxonomic affinities and identification of diplodocid non-type specimens**
6207 **AMNH 223.** Described as *Diplodocus longus* (Osborn, 1899), AMNH 223 readily became
6208 the reference specimen for this species (Hatcher, 1901; Gilmore, 1932). However, the present
6209 analysis does not recover AMNH 223 together with the holotype specimen YPM 1920, but as
6210 most basal OTU of a clade including the holotype of *Seismosaurus hallorum*.
6211 Two ambiguous 'autapomorphies' are found for this specimen (Tab. S128), which describe

6212 scapular morphology. The fact that only one of the other three specimens in the same clade

6213 preserves a scapula, and the low number of differences between AMNH 223 and the

6214 remaining triplet, indicates that these might represent individual variation, and that AMNH

6215 223 is most parsimoniously identified as belonging to the same species, which would be

6216 *Diplodocus hallorum*.

6217 **AMNH 460.** The specimen AMNH 460 has never been described, but was included in the

6218 specimen-level phylogenetic analysis of Upchurch et al. (2004b). In the latter, it has been

6219 identified as *Apatosaurus ajax*, which is not supported by the most parsimonious trees of the

6220 present analysis. In the equally weighted pruned tree, AMNH 460 is pulled outside

6221 Apatosaurinae due to unresolved relationships with SMA 0087 and WDC-FS001A. When

6222 applying implied weights, AMNH 460 is found within Apatosaurinae, as a single slot between

6223 YPM 1840 + NSMT-PV 20375 and SMA 0087 + WDC-FS001A. When excluding

6224 *Australodocus* from Diplodocidae, AMNH 460 changes position within Apatosaurinae, and

6225 forms the sister taxon to *Brontosaurus* + *Apatosaurus*, still as single slot. The

6226 foundreconstructed positions would imply that AMNH 460 represent a different taxon, but the

6227 fact that no found 'autapomorphy' is unique within Apatosaurinae (Tab. S129) makes such an

6228 assignment questionable.

6229 A constrained search forcing AMNH 460 into the clade including *Apatosaurus ajax* YPM

6230 1860 yielded trees of a length of 1902 or 188.54847 steps, corresponding to relative length

6231 increases of 0.26% or 0.31%. AMNH 460 continues to be found as a single slot, more basal to

6232 *Apatosaurus ajax* YPM 1860. Imposed brontosaur affinities for AMNH 460 result in tree

6233 lengths of 1903 and 188.31076 steps, or relative increases of 0.32% and 0.18%. A sister clade

6234 arrangement with *Eobrontosaurus* produces tree lengths of 1900 and 188.10509 steps, relative

6235 increases of 0.16% and 0.07%. In both cases, the pair is recovered basal to the clade

6236 *Brontosaurus* + mdA. When forced into a triplet with SMA 0087 and WDC-FS001A, tree

6237 length stayed the same (1897) or increased by 0.01%, to 187.98825 steps. Equal weighting

6238 finds trees of 1903 steps (0.32% longer) if constrained by a unity of AMNH 460 with NSMT-

6239 PV 20375, whereas implied weighting results in trees 0.05% longer (188.06943 steps) if

6240 constraining the triplet AMNH 460, NSMT-PV 20375, and YPM 1840. A closer relationship

6241 with the specimens SMA 0087 and WDC-FS001A can thus cannot be excluded by the present

6242 analysis. Such a triplet would be supported by the following three ambiguous

6243 synapomorphies: 1) posterior dorsal centra longer than high (268-0, unique within

6244 Apatosaurinae); 2) a widely rounded cnemial crest of the tibia, in anterior view (444-0, unique

6245 within Apatosaurinae); and 3) the posterior surface of the tibial cnemial crest bears a distinct

6246 fibular trochanter (445-1, unique within Apatosaurinae). It thus possibly represents a yet

6247 ~~unknown~~unnamed, apatosaurine taxon. However, none of the specimens included have yet

6248 been completely described, and it thus refrained herein to establish a new name at the

6249 moment. Relative positions are considered too unstable to confidently suggest a new taxon.

6250 **AMNH 969.** This skull was generally considered to belong to *Diplodocus* (Holland, 1906,

6251 1924; Berman and McIntosh, 1978), probably due to strong resemblances with the purported

6252 skulls of *Diplodocus longus* USNM 2672 and 2673. However, the latter two specimens

6253 cannot be confidently referred to the type species, as there is no overlap with the type

6254 specimen YPM 1920 (McIntosh and Carpenter, 1998). Furthermore, given the few differences

6255 in skull morphology between diplodocine and apatosaurine species, even less can be expected

6256 within one of the two clades only. Indeed, the present analysis recovers AMNH 969

6257 consistently with the two type specimens of *Galeamopus hayi* and *G.* ███████ indicating

6258 that it belongs to this genus. Constrained searches support this assignment, as a forced

6259 inclusion in *Diplodocus* yields shortest trees of 1901 or 188.61461 steps, a relative increase of

6260 0.21% or 0.34%, respectively.
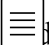
6261 One ambiguous 'autapomorphy' is found that distinguishes AMNH 969 from the other two

6262 specimens (Tab. S130). ~~As~~Because the clade formed by the other two *Galeamopus* specimens

6263 ~~does~~ only show~~s~~ one shared synapomorphy, differences between the species are not enough to

6264 justify erection of a third species. When forcing AMNH 969 to group with either of the two

6265 species of *Galeamopus*, tree lengths for a *G. hayi* assignment are 1900 (equal weighting) and

6266 188.21024 (implied weighting) steps, whereas affinities with *G.* ███████ are found with

6267 trees of a length of 1898 (equal weighting) and 188.1269 (implied weighting) steps. The skull

6268 and first two cervical vertebrae of AMNH 969 are thus herein tentatively referred to

6269 *Galeamopus* ██████ The more squared snout of AMNH 969, compared to SMA 0011

6270 might indicate a higher individual age of AMNH 969 (Whitlock et al., 2010).

6271 **AMNH 6341.** The specimen AMNH 6341 is the most complete specimen generally

6272 considered to be a *Barosaurus lentus*. ~~As~~Because it is completely prepared, and appears

6273 largely undeformed (in contrast to the type specimen YPM 429), AMNH 6341 has generally

6274 been used as reference specimen for the genus (see Whitlock, 2011a). Although it was found

6275 early after the discovery of the Carnegie Quarry at what was later to be named Dinosaur

6276 National Monument (McIntosh, 2005), it was only described by McIntosh (2005), but still not

6277 in a very detailed way.

6278 In the present analysis, AMNH 6341 was consistently found as sister taxon to the holotype

6279 specimen of *Barosaurus lentus*, YPM 429. Given that all the recovered 'autapomorphies'

6280 cannot be considered valid (Tab. S131), AMNH 6341 is most parsimoniously interpreted to

6281 belong to the same species as YPM 429. Previous assignments to *Barosaurus lentus* are thus

6282 corroborated by the current analysis.

6283 **AMNH 7530.** The specimen AMNH 7530 was never described but is labeled as *Barosaurus*

6284 sp. on display at AMNH. It is herein consistently recovered together with *Kaatedocus siberi*

6285 SMA 0004. No autapomorphies are found for the specimen, probably due to the fragmentary

6286 preservation of the specimen with which it forms a dichotomy (the partial skull SMA D16-3).

6287 Differences between AMNH 7530 and SMA 0004 exist in the shape of the dorsal edge of the

6288 parietal (C62), in the orientation of the longest axes of the basal tubera (C87), and in the

6289 development of the pre-epipophyseal anterior spur (C167). However, the sum of recovered

6290 'autapomorphies' between the specimens is too low to justify specific separation. The

6291 mentioned differences are thus interpreted as individual variation, contrary to the

6292 interpretation in Tschopp and Mateus (2013b), where the anterior spur of the pre-epipophysis

6293 was stated as autapomorphic for the species *Kaatedocus siberi*.

6294 Forcing AMNH 7530 in a position with the other sampled *Barosaurus* specimens increased

6295 tree length by 0.42% (equal weighting) and 0.4% (implied weighting), to 1905 ☰ 188.73208

6296 steps, respectively. Such an assignment is thus considerably less parsimonious than an referral

6297 to *Kaatedocus siberi*.

6298 **AMNH 7535.** As for AMNH 7530, ~~also~~ AMNH 7535 also was tentatively identified as

6299 *Barosaurus* in the AMNH data base, but ~~was~~ never described. In contrast to the specimen

6300 AMNH 7530, here identified as *Kaatedocus*, AMNH 7535 consistently groups with other

6301 *Barosaurus* specimens in the present analysis.

6302 No autapomorphies were recovered for the specimen, and as stated above, the sum of

6303 differences between AMNH 7535 and its sister clade CM 11984 + mdD is too low to establish

6304 specific separation. Obvious differences between AMNH 7535 and the holotype specimen

6305 YPM 429 (as transverse width, or size of the cervical vertebrae) are herein interpreted to

6306 represent a combination of ontogenetic variation, deformation, and serial variation within the

6307 cervical column. AMNH 7535 is thus referred to *Barosaurus lentus*.

CM 94. This specimen was designated the paratype of *Diplodocus carnegii* (Hatcher, 1901). It complements the knowledge of *Diplodocus carnegii* in crucial parts such as the mid-caudal vertebrae (thus allowing comparisons with the holotype specimen of *D. longus* YPM 1920), and appendicular elements. When pruning YPM 1920 from the complete consensus trees, CM 94 is consistently recovered as sister taxon to the holotype specimen of *D. carnegii*, CM 84. Three 'autapomorphies' are found reliable for the specimen CM 94 (Tab. S132). Of these, only one (366-1) can be compared with CM 84, ~~as~~because other two describe pedal morphology, and CM 84 does not preserve a pes. The sum of comparable differences thus amounts to one (no valid 'autapomorphies' were found for CM 84), and referral to the same species and thus an assignment of CM 94 as paratype for *Diplodocus carnegii* is justified.

CM 3378. The specimen CM 3378 was found together with the holotype of *Apatosaurus louisae* at Dinosaur National Monument~~,~~ and preserves the most complete vertebral column of any of the specimens included herein (McIntosh, 1981). Nonetheless, it has only been described and figured in parts (Holland, 1915b; Gilmore, 1936). It was included into the specimen-based phylogenetic analysis of Upchurch et al. (2004b), and ~~resulted~~identified there as specimen of *Apatosaurus louisae*. ~~As~~Because none of the recovered 'autapomorphies' for CM 3378 can be considered valid (Tab. S133), the present analysis confirms this interpretation.

CM 3452. The specimen CM 3452 is one of very few preserving an almost complete skull in articulation with the first few cervical vertebrae. It was reported as a juvenile to subadult *Diplodocus* specimen (Holland, 1924; McIntosh and Berman, 1975; Whitlock et al., 2010), but never described in detail. A referral to *Diplodocus* is questionable, ~~as~~because almost no overlapping material exists between CM 3452 and any type specimen of *Diplodocus*. Now that generic separation from *Diplodocus* is confirmed for *Galeamopus hayi*, the only *Diplodocus* type specimen preserving anterior cervical vertebrae is CM 84. With the description of two additional specimens preserving articulated skulls and cervical vertebrae (SMA 0004 and 0011), affinities of CM 3452 can be assessed more accurately. The present analysis consistently recovers CM 3452 as sister taxon to *Kaatedocus siberi + Barosaurus lentus*.

A single 'autapomorphy' was found valid for CM 3452 (Tab. S134). Summed differences between CM 3452 and its sister clade amount to four, not justifying specific separation. Constrained searches were thus performed in order to evaluate the most parsimonious

6340 identification. Forcing CM 3452 into *Diplodocus*, following earlier identifications, equal

6341 weighting finds shortest trees of 1905 steps, and implied weighting 188.82961 steps – relative

6342 length increases of 0.42% and 0.46%, respectively. Imposed affinities with *Kaatedocus* yield

6343 trees with a length of 1903 and 188.44375 steps, corresponding to an increase in length of

6344 0.32% and 0.25%. A forced inclusion into the *Barosaurus* clade results in length increases of

6345 0.11% and 0.04%, to 1899 and 188.04743 steps, respectively.

6346 In the case of affinities to *Barosaurus*, CM 3452 is recovered as the basal-most specimen,

6347 united with the remaining quartet by the presence of an accessory horizontal lamina in the

6348 center of the spinodiapophyseal fossa of mid- and posterior cervical vertebrae, not connected

6349 with any surrounding lamina (187-1). This trait is shared with all included *Barosaurus*

6350 specimens but AMNH 7535, which was not scorable for this character. The only other

6351 diplodocine specimen showing the same development is *Diplodocus carnegii* CM 94.

6352 Distance between CM 3452 and the more derived clade amounts to a single difference, which

6353 does not allow specific separation. Therefore, CM 3452 is herein tentatively referred to

6354 *Barosaurus lentus*.

6355 **CM 11161.** This skull-only specimen is generally referred to *Diplodocus* (Holland, 1915b,

6356 1924; McIntosh and Berman, 1975; Berman and McIntosh, 1978; Whitlock et al., 2010;

6357 Whitlock and Lamanna, 2012), and has been used in numerous publications as a model for

6358 feeding strategies or other ecological or behavioral studies concerning this genus (e.g. Haas,

6359 1963; Barrett and Upchurch, 1994; Calvo, 1994; Upchurch and Barrett, 2000; Whitlock,

6360 2011b; Young et al., 2012). However, ~~as~~because no overlap exists with any of the type

6361 specimens of *Diplodocus*, referral to that genus remains controversial. Given that all skulls

6362 with articulated vertebrae are herein identified as other diplodocine species (AMNH 969 and

6363 SMA 0011 as *Galeamopus* ▮▮▮▮▮▮ CM 3452 as *Barosaurus lentus*, SMA 0004 as

6364 *Kaatedocus siberi*), only indirect evidence can be used for such an assignment, as exemplified

6365 by the present analysis, which is not able to resolve the position of CM 11161 due to the

6366 lacking overlap.

6367 Two ambiguous 'autapomorphies' are found for the specimen (Tab. S135). One of these traits

6368 (61-0) was scored as unknown in the other putative *Diplodocus* skull, USNM 2672, due to

6369 ~~lacking~~missing measurements. In another skull not included in the present analysis, the mean

6370 ratio is 1.4 (USNM 2673), thus resembling CM 11161. The short posteroventral process of

6371 the jugal, however, is not present in USNM 2672 (ET, pers. obs., 2011) and CM 11255, a

6372 putative juvenile *Diplodocus* skull (Whitlock et al., 2010; but see above).

6373 Constrained searches were performed forcing CM 11161 to group with diplodocine taxa

6374 preserving articulated skull material. Imposed relationships with *Galeamopus* produced trees

6375 0.16% and 0.18% longer than the most parsimonious trees, with lengths of 1900 and

6376 188.31381 steps, respectively. A forced assignment to *Kaatedocus* yielded shortest trees of

6377 1911 and 189.77095 steps, a relative increase in length of 0.74% and 0.96%. When

6378 constraining CM 11161 to group with *Barosaurus*, tree length increases by 0.58% and 0.62%,

6379 reaching 1908 and 189.12979 steps. Given that all these alternative assignments increase tree

6380 length by at least three steps (or almost the equivalent to it in implied weight trees), a referral

6381 to *Diplodocus* still remains the most parsimonious identification. However, given that nearly

6382 complete specimens including articulated skulls, vertebrae from anterior cervical to distal

6383 caudal elements, as well as appendicular elements including manual and pedal material are

6384 known from *Galeamopus*, the latter genus appears more appropriate as representative of the

6385 diplodocine clade in phylogenetic analyses.

6386 **CM 11984.** The specimen CM 11984 was partly described as *Barosaurus lentus* by McIntosh

6387 (2005), but is largely unprepared. The present analysis finds CM 11984 in all most

6388 parsimonious trees as sister taxon to *Barosaurus lentus* YPM 429 + AMNH 6341.

6389 'Autapomorphies' recovered for the specimen were all shared with other diplodocine

6390 specimens, and thus not considered reliable (Tab. S136). The four 'synapomorphies' found for

6391 the sister clade *Barosaurus lentus* YPM 429 + AMNH 6341 (Tab. S61) are thus not enough to

6392 erect a new species within *Barosaurus*. Therefore, McIntosh's (2005) referral of this specimen

6393 to *Barosaurus lentus* is herein corroborated.

6394 **DMNS 1494.** Although undescribed, DMNS 1494 is often considered a *Diplodocus longus*

6395 (McIntosh, 1981; Gillette, 1991), probably based on similarities with AMNH 223, the

6396 specimen described as *D. longus* by Osborn (1899). ~~As~~Because the latter identification was

6397 herein rejected, ~~also~~ the referral of DMNS 1494 to *D. longus* also appears questionable. In the

6398 present analysis DMNS 1494 is consistently found as sister taxon to USNM 10865.

6399 A single ambiguous 'autapomorphy' was found for the specimen (Tab. S137). As this is the

6400 only valid difference between DMNS 1494 and USNM 10865 (Tab. S67), the two are

6401 considered to belong to the same species. Following the reasoning stated above, this species

6402 will be *Diplodocus hallorum*.

6403 **FMNH P25112.** The current specimens is one of the few non-type specimens~~, which~~that was

6404 described (Riggs, 1903). Riggs (1903) referred it to *Apatosaurus excelsus* (herein

6405 reinterpreted as *Brontosaurus excelsus*), an identification which was accepted by Gilmore

6406 (1936). Upchurch et al. (2004b) recovered FMNH P25112 as a single OTU, proposing that it

6407 might belong to its own species within *Apatosaurus*. In the present analysis, FMNH P25112 is

6408 recovered in the same position as *Brontosaurus excelsus* when adding it to the equally

6409 weighted reduced consensus tree, whereas it groups with *Elosaurus* and *Dystrophaeus* in the

6410 implied weights pruned consensus tree.

6411 Forcing FMNH P25112 into the clade with *Apatosaurus ajax* YPM 1860 (together with YPM

6412 1840 in the equally weighted analysis, but alone when using implied weighting), tree lengths

6413 increase by 0.47% with equal weighting and 0.19% in the analysis with implied weights, to

6414 1906 and 188.38266 steps, respectively. Imposing a dichotomy with *Brontosaurus excelsus*

6415 YPM 1980, shortest trees measure 1903 and 188.17315 steps, an increase of 0.32% and

6416 0.11%. A grouping with *Elosaurus parvus* as proposed by the implied weights trees increases

6417 equally weighted tree lengths by 0.11%, to 1899 steps. When restricting FMNH P25112 to

6418 *Eobrontosaurus*, trees lengthen by 0.16% or 0.02%, to a length of 1900 or 188.01343 steps. A

6419 forced relationship with the putative new taxon including AMNH 460, SMA 0087, and WDC-

6420 FS001A (see above) is supported by trees of a length of 1897 or 188.11135 steps, a relative

6421 increase of 0% or 0.07% compared to the most parsimonious trees. Finally, imposing a

6422 relationship with NSMT-PV 20375 in the equally weighted trees, or with NSMT-PV 20375

6423 and YPM 1840 in the implied weights trees, produces shortest trees of 1897 or 187.99160

6424 steps, respectively, corresponding to increases of 0 or 0.01%. According to these values,

6425 several different referrals appear similarly parsimonious: an identification as *Elosaurus*, as

6426 belonging to the same taxon as AMNH 460, SMA 0087, and WDC-FS001A, or as NSMT-PV

6427 20375, possibly together with YPM 1840.

6428 A single synapomorphy supports an assignment to *Elosaurus* (274-0). The quartet FMNH

6429 P25112, AMNH 460, SMA 0087, and WDC-FS001A would be united by the two

6430 synapomorphies diagnosing SMA 0087 + WDC-FS001A (444-0, 445-1). However, both

6431 FMNH P25112 and AMNH 460 could not have been scored for these two characters. The

6432 unity of FMNH P25112 with NSMT-PV 20375 in the equally weighted tree would yield one

6433 synapomorphy (420-0). The triplet FMNH P25112, NSMT-PV 20375, and YPM 1840 in the

6434 implied weight trees is not supported by any valid synapomorphy. Taking all this together, an

6435 assignment to *Elosaurus* appears to be the best supported. Therefore, pending further studies

6436 on the involved specimens, FMNH P25112 is tentatively referred to *Elosaurus parvus*.

6437 **MB.R. skeleton k.** Skeleton k is the second individual referred to *Tornieria africana* by

6438 Remes (2006). The individual includes a braincase (MB.R.2386), which was interpreted to

6439 not belong to that taxon by Harris (2006a). However, based on preserved quarry maps,

6440 referral to the same individual appears justified (Heinrich, 1999; Remes, 2006). The present

6441 analysis consistently recovers skeleton k with the holotype individual of *Tornieria africana*.

6442 ~~As~~Because no autapomorphy was found distinguishing skeleton k from skeleton A, Remes'

6443 (2006) referral to the same species is herein corroborated.

6444 **ML 418.** Consisting of very fragmentary material, ML 418 was identified as one of the six

6445 most unstable taxa in the equally weighted analysis. It was referred to *Dinheirosaurus* by

6446 Antunes and Mateus (2003), and later assigned to *Apatosaurus* sp. by Mateus (2005).

6447 Mannion et al. (2012) noted that it cannot be confidently identified as either of these two taxa,

6448 as it lacks their autapomorphic traits, and identified it as indeterminate diplodocid. When

6449 added to the equally weighted reduced consensus tree, ML 418 produces a polytomy at the

6450 base of Diplodocinae, together with SMA 0011, *Galeamopus hayi* HMNS 175, AMNH 969,

6451 the two *Tornieria* skeletons, the clade uniting *Dinheirosaurus* with *Supersaurus*, and

6452 *Diplodocus* + mdD. In the most parsimonious implied weights trees, ML 418 occupies the

6453 most basal position within Diplodocinae, but switches to a position within the clade of

6454 *Dinheirosaurus* and *Supersaurus* when excluding *Australodocus* or restricting it to

6455 Titanosauriformes.

6456 One ambiguous 'autapomorphy' is found for the specimen (Tab. S138). The fact that the sum

6457 of differences between ML 418 and the remaining diplodocines is just two does not allow an

6458 identification as separate species. Constrained searches forcing ML 418 into a dichotomy with

6459 *Dinheirosaurus* (as suggested by Antunes and Mateus, 2003) produce equally weighted trees

6460 of a length of 1900 steps, whereas implied weighting finds shortest trees of 188.09487 steps,

6461 corresponding to length increases of 0.16% and 0.07%, respectively. In both cases, no

6462 synapomorphies are found for the clade uniting them. This implies that Mannion et al. (2012)

6463 were right in considering it a possible second diplodocid taxon, although not diagnosable

6464 based on the preserved material. ~~As~~Because ML 418 shows two shared synapomorphies of

6465 Diplodocinae (218-1, 283-1) and does not exhibit any of Apatosaurinae (275-0 instead of 275-

6466 1), it is herein considered ~~an~~ indeterminate Diplodocinae.

6467 **NSMT-PV 20375.** The specimen NSMT-PV 20375 was described by Upchurch et al. (2004b)

and identified as *Apatosaurus ajax*, by means of a specimen-based phylogenetic analysis. In the present analysis, it is never found in close relationship with the holotype specimen of *Apatosaurus ajax*. In fact, NSMT-PV 20375 consistently occupies the most basal position within Apatosaurinae, alone in the equally weighted trees, or together with YPM 1840 in the implied weights trees. A single, ambiguous 'autapomorphy' is recovered for NSMT-PV 20375 (Tab. S139).

Forcing NSMT-PV 20375 into a dichotomy together with YPM 1840 with the equally weighted analysis yielded trees one step longer (1898; 0.05%) than the most parsimonious trees. The resulting reduced consensus tree recovered *Elosaurus parvus*, *Apatosaurus ajax*, and *Apatosaurus louisae* in the same relative positions as the shortest implied weights trees. Imposing a grouping with *Apatosaurus ajax*, as found by Upchurch et al. (2004b) produced trees of 1899 and 188.10818 steps, a relative increase of 0.11% and 0.07%. In both cases, it has YPM 1840 as sister taxon, and the triplet is positioned relatively basal within Apatosaurinae, detached from *Apatosaurus louisae*. The same results are obtained when forcing the entire triplet (NSMT-PV 20375, YPM 1840 and YPM 1860) to cluster together, thus not imposing a sister taxon relationship between NSMT-PV 20375 and YPM 1860 a priori. The most parsimonious interpretation thus seems the arrangement found by the implied weights trees, with NSMT-PV 20375 and YPM 1840 forming the basal-most taxon within Apatosaurinae. It thus seems that two more, previously unrecognized taxa are present within Apatosaurinae. However, support for such a separation is low, and more detailed studies are needed to confirm such a hypothesis. No additional taxa shall thus be named herein.

SMA 0087. The specimen SMA 0087, yet unreported, but from the same quarry as SMA 0011, forms a clade together with WDC-FS001A – in the cases when the analysis is able to resolve their position. In the equally weighted pruned tree, SMA 0087 is found outside Apatosaurinae, as also if added to the equally weighted reduced consensus tree. On the other hand, implied weighting finds SMA 0087 + WDC-FS001A within Apatosaurinae, more derived than NSMT-PV 20375 + YPM 1840.

No valid 'autapomorphy' is found by the present analysis (Tab. S140), but both shared synapomorphies between SMA 0087 and WDC-FS001A would qualify as species autapomorphies (444-0, 445-1), given that they are not shared with any other apatosaurine specimen. Apatosaurine affinities are indicated for SMA 0087 by the presence of two shared (256-0, 275-1) and two ambiguous synapomorphies (235-1, 250-0) of the clade. The absence

of one exclusive (307-0 instead of 1) and three shared synapomorphies of Diplodocinae (283-0, 330-0, 332-0 instead of 283-1, 330-1, and 332-1) implies that an identification as apatosaurine is more probable.

When forcing SMA 0087 into a dichotomy with WDC-FS001A in the equally weighted trees, tree length does not increase, but SMA 0087 + WDC-FS001A remains in a trichotomy with Apatosaurinae and Diplodocinae. Imposing apatosaurine affinities, two large polytomies are found to form the clade, with SMA 0087, WDC-FS001A, FMNH P25112, and AMNH 460 being the sister clade to a polytomy with all other apatosaurine specimens. Tree length is 1898, one step more than in the most parsimonious trees. When forcing SMA 0087 into Diplodocinae, tree length stays the same, and SMA 0087 is recovered together with WDC-FS001A as the most basal diplodocine taxon. Five synapomorphies are found for Diplodocinae in such a case, but only one of these would be shared by all diplodocines, and not be present in any apatosaurine specimen: a subtriangular proximal articular surface of the tibia. However, the latter trait is not recognizable in the badly distorted tibia of SMA 0087. Given that previously established synapomorphies of Apatosaurinae and Diplodocinae favor an apatosaurine identification of SMA 0087, the latter is herein preferred over an assignment to Diplodocinae.

SMA D16-3. This partial skull has not been described in detail yet. It is herein consistently found as *Kaatedocus siberi*. No autapomorphies were found in any of the trees. A referral to *Kaatedocus siberi* is thus warranted.

SMA O25-8. The second isolated partial skull (besides SMA D16-3) from Howe Quarry exhibits both internal and external differences in braincase morphology, compared with the *Kaatedocus siberi* specimens (Schmitt et al., 2013). Being identified as one of the four most unstable taxa, it was excluded from all most parsimonious pruned and reduced consensus trees. When added, it consistently groups within the *Kaatedocus + Barosaurus* clade, but outside *Kaatedocus siberi*.

The specimen SMA O25-8 can be confidently identified as Diplodocidae due to the hook-shaped posterior process of the prefrontal and the slightly concave posterior face of the basal tubera, and as Diplodocinae given the box-like basal tubera and the presence of a basipterygoid recess. It is included in the *Kaatedocus + Barosaurus* clade based on the distinct nuchal fossae on the parietal, and the ridge on the posterior face of the paroccipital process.

6532 Forcing SMA O25-8 into *Barosaurus lentus* does not increase tree length, but a confident

6533 assignment to this taxon is hampered by the lack of overlap with definitive *Barosaurus lentus*

6534 specimens. Indeed, recovered consensus trees show one large polytomy including all of the

6535 specimens. When further including CM 3452 into *Barosaurus lentus* (following the

6536 identification of CM 3452 above), tree lengths increase by 0.42% (equal weighting) and

6537 0.31% (implied weighting), to 1905 and 188.55338 steps, respectively. Imposing a clustering

6538 with *Kaatedocus siberi* also does not increase tree length, but no synapomorphies are found

6539 for an inclusion into *Kaatedocus siberi*. Taking all the information into account, SMA O25-8

6540 can be confidently identified as derived diplodocine, most closely related to either

6541 *Kaatedocus* or *Barosaurus*. The fact that a unity of CM 3452, SMA O25-8 and the definitive

6542 *Barosaurus* specimens is relatively unparsimonious indicates that a third taxon might be

6543 present, or that morphological variety within *Kaatedocus* might be higher than acknowledged

6544 at present. Pending further studies, and given the differences found between SMA O25-8 and

6545 the known *Kaatedocus* braincases, SMA O25-8 is herein still tentatively referred to

6546 *Barosaurus*.

6547 **USNM 2672.** The specimen USNM 2672 is the second skull usually identified as *Diplodocus*

6548 included in the study. It also preserves a partial atlas. The problem for a confident

6549 identification of USNM 2672 remains the same as in CM 11161, ~~as~~because no definitive

6550 *Diplodocus* specimen is known with either atlas or skull.

6551 No 'autapomorphy' was found in the equally weighted pruned consensus tree, the only tree to

6552 include USNM 2672. Nonetheless, the specimen can be confidently identified as diplodocid

6553 due to the broad contact between maxilla and quadratojugal, the large preantorbital fenestra,

6554 the concave dorsal margin of the antorbital fenestra, the medially curving anteromedial corner

6555 of the prefrontal, the hook-shaped posterior process of the prefrontal, the slightly concave

6556 posterior face of the basal tubera, the absence of a coronoid eminence, as well as absence of

6557 direct crown-to-crown occlusion in the teeth. Diplodocine affinities are confirmed by the box-

6558 like basal tubera.

6559 The same constrained searches ~~are~~were performed as for CM 11161, in order to test affinities

6560 with species for which cranial material is known. Affinities with *Galeamopus* are found in

6561 trees of a length of 1900 or 188.43524 steps (an increase of 0.16% or 0.25%). Forcing an

6562 inclusion into the *Kaatedocus* clade yields trees of a length of 1911 and 189.61024 steps,

6563 corresponding to a 0.74% and 0.87% length increase. When imposing an assignment to the

6564   clade uniting *Kaatedocus*, *Barosaurus*, and CM 3452, the trees are lengthened by 0.11% and

6565   0.13%, reaching 1899 and 188.21381 steps. Taking everything together, USNM 2672 appears

6566   to be most parsimoniously referred to *Diplodocus*, but it remains unknown as to what species.

6567   **USNM 10865.** On display at USNM, the specimen USNM 10865 is the second, relatively

6568   complete skeleton referred to *Diplodocus longus* after AMNH 223 (Osborn, 1899; Gilmore,

6569   1932). It has been partially described by Gilmore (1932). In the present analysis, USNM

6570   10865 consistently forms a dichotomy with DMNS 1494.

6571   No valid 'autapomorphy' is found for the present specimen (Tab. S141), and as stated above,

6572   specific distinction from DMNS 1494, AMNH 223, and most importantly the holotype of

6573   *Seismosaurus hallorum*, NMMNH 3690, is not warranted. ~~As~~Because *Seismosaurus* was

6574   synonymized with *Diplodocus*, the specimen USNM 10865 is herein referred to the species

6575   *Diplodocus hallorum*.

6576   **UW 15556.** Described in detail by Hatcher (1902) and Gilmore (1936), the specimen UW

6577   15556 (previously CM 563) is one of the best known apatosaur specimens. It was often

6578   referred to *Apatosaurus excelsus* (Hatcher, 1902; Gilmore, 1936; McIntosh, 1981, 1995), but

6579   recently found to constitute its own species within *Apatosaurus*, together with the holotype of

6580   *Elosaurus parvus*, CM 566 (Upchurch et al., 2004b). Upchurch et al. (2004) thus proposed the

6581   new combination *Apatosaurus parvus*. However, as showed earlier, generic separation of the

6582   two specimens can be justified due to several differences with the recovered sister taxon

6583   *Brontosaurus excelsus*. The specimen UW 15556 is thus herein referred to *Elosaurus parvus*.

6584   **WDC DMJ-021.** The specimen WDC DMJ-021 was described by Lovelace et al. (2007), and

6585   identified as *Supersaurus vivianae*. Herein, it is always found together with the BYU

6586   specimen of *Supersaurus vivianae*, thus confirming the assignment of Lovelace et al. (2007).

6587   No valid 'autapomorphies' for the specimen are found by any of the trees (Tab. S142), but

6588   seven shared synapomorphies unite the two specimens of *Supersaurus* (Tab. S79). Three of

6589   them are unique within Diplodocinae, and can be considered autapomorphies of the species.

6590   **WDC-FS001A.** Only the manus of the present specimen has been described in detail (Bedell

6591   and Trexler, 2005). The specimen was identified as *Diplodocus* cf. *c**arnegii*, based on

6592   morphology of a caudal vertebra, which was different from the specimens generally

6593   considered '*Diplodocus longus*', and the general slenderness of the appendicular bones (Bedell

6594   and Trexler, 2005). The implied weights analysis finds WDC-FS001A together with SMA

6595   0087, for which apatosaurine affinities are more probable than diplodocine (see above). On

6596 the other hand, equal weighting is not able to resolve the relationships of WDC-FS001A,

6597 finding affinities with both Apatosaurinae and Diplodocinae.

6598 Two ambiguous 'autapomorphies' are found for WDC-FS001A, both of them shared with

6599 *Diplodocus* specimens (Tab. S143). Apatosaurinae affinities are ambiguous, as WDC-

6600 FS001A shares one shared synapomorphy (476-1), but does not exhibit an ambiguous

6601 synapomorphy of the clade (402-1 instead of 0). The first of these is shared with *Diplodocus*

6602 *hallorum* USNM 10865, whereas the second is also present in the basal apatosaurine NSMT-

6603 PV 20375. Information is also ambiguous concerning diplodocine synapomorphies: whereas

6604 WDC-FS001A shows one shared synapomorphy (330-1), a second one is absent (332-0

6605 instead of 1). Here, the first trait also occurs in apatosaurine specimens, but the second one is

6606 not shared by any diplodocine. Morphological evidence therefore slightly favors an

6607 assignment to Apatosaurinae.

6608 A forced clustering with the two *Diplodocus carnegii* specimens (as proposed by Bedell and

6609 Trexler, 2005) produces tree lengths of 1903 and 188.65885 steps, an increase of 0.32% and

6610 0.37%. Diplodocine affinities are found with shortest trees of 1898 and 188.28028 steps,

6611 corresponding to a lengthening of 0.05% and 0.16%, respectively. Imposing a grouping

6612 within Apatosaurinae (as found by the implied weight analysis) did not result in longer trees.

6613 Both morphological evidence as well as constrained searches thus indicate that apatosaurine

6614 affinities are more parsimonious for WDC-FS001A. Therefore, and ~~following~~ also following

6615 the reasoning in the earlier paragraphs about the affinities of SMA 0087 and AMNH 460,

6616 WDC-FS001A is herein referred to one of the putative new apatosaurine taxa, together with

6617 the specimens mentioned before.

6618

6619 **Combined cladogram**

6620 Based on the identifications stated above, a combined cladogram was created to summarize

6621 the results (Fig. 154). The cladogram represents the most up-to-date species-level taxonomy

6622 of Diplodocidae. Diagnoses of the proposed clades, genera, and species are given below.

6623 Outgroup taxa are reduced considerably compared to the trees recovered by the main

6624 analyses, in order to increase the intended focus on Diplodocidae.

6625

6626 **Biostratigraphic and paleobiogeographical implications**

6627 The present analysis rejects diplodocid affinities of the only putative Middle Jurassic and

Cretaceous ≡lodocid species, i.e. *Cetiosauriscus stewarti*, *Losillasaurus giganteus*, *Dystrophaeus viaemalae*, and *Dyslocosaurus polyonychius*. A single anterior caudal vertebra previously identified as Cretaceous diplodocid (Upchurch and Mannion, 2009) was subsequently shown to belong to Titanosauriformes (Whitlock et al., 2011), and therefore not included in the present analysis. Diplodocidae thus appear restricted to the Late Jurassic, with a caudal vertebra from the Oxfordian of Georgia being the first representative of the clade (Gabunia et al., 1998; Mannion et al., 2012). Given the high diversity, such a temporal restriction is remarkable. The Morrison Formation, from where the majority of diplodocids are known, is interpreted to represent a time span of about seven (Swierc and Johnson, 1996; Kowallis et al., 1998) to eleven million years (Platt and Hasiotis, 2006). Therefore, even though morphologically similar, at least two diplodocid species appear to have lived contemporaneously throughout the entire duration of the sedimentation of the Morrison Formation, and besides non-diplodocid sauropods like *Camarasaurus*, *Haplocanthosaurus*, *Brachiosaurus*, or others. If precise stratigraphical levels and geological ages would be known for all the sites where diplodocids were found, the present analysis would provide a good phylogenetic foundation on which hypotheses of speciation or niche partitioning within diplodocids from the Morrison Formation could be based. However, exact geological dating was rarely done, or has provided controversial results (in particular for the Howe Ranch sites, Tschopp and Mateus, 2013b). Therefore, and because no reliable marker beds appear to be present throughout the entire extent of the Morrison Formation (Trujillo, 2006; contra Turner and Peterson, 1999), long distance correlation between Morrison Formation quarries is nearly impossible at present. Proposed biostratigraphical zones within the formation (Bakker, 1998; Turner and Peterson, 1999; Foster, 2003; Ikejiri, 2004) have thus to be regarded questionable and provisional. Their validity is furthermore debatable because they heavily rely on species and genus referrals that have not been tested by means of phylogenetic analyses. Given that diversity appears to have been underestimated, as indicated by the present analysis, these referrals will have to be reconsidered. Notwithstanding the lack of knowledge concerning such specific stratigraphy and phylogeny, Diplodocidae as a whole appears to be a good candidate to serve for relative geological dating. Their presence in at least three continents, and restriction in time to the Late Jurassic, and more precisely the period of the Oxfordian to Tithonian qualifies them as age index fossils.

Diplodocidae is most diverse in North America, but the earliest finds from Georgia suggest

that the origin of the clade lies in Europe (Mannion et al., 2012). As for the Georgian caudal vertebra, ~~also~~ the non-American diplodocid OTU included herein (ML 418, *Dinheirosaurus lourinhanensis*, *Tornieria africana*) *also* can be referred to Diplodocinae (Mannion et al., 2012; this study). The fact that the latter two species lie at the base of the diplodocine radiation (Fig. 154) furthermore corroborates a hypothesis of an extra-American origin of this clade. Interestingly, apatosaurine specimens have only been recovered from North America to date, so that interpretations of their origin are more dubious.

Diagnoses

Updated diagnoses of the main diplodocoid subclades

The following lists of synapomorphies only includes the named nodes and stems in the recovered phylogenetic tree, which directly lead to Diplodocidae, as well as its sister clade Dicraeosauridae (Fig. 154). Synapomorphies are divided into their qualitative states as defined above, and ordered based on anatomical regions. Where conflicting interpretations exist between the analyses using equal or implied weighting, the synapomorphy is attributed to the less inclusive clade. Additional synapomorphies are added to the diagnoses following earlier studies, if supported by the data set, also in cases where the analysis did not recognize them as such. References for the synapomorphies credit the first recognition of the respective trait as synapomorphic for the taxon in question. Finally, previously proposed synapomorphies are discussed in the light of the new analysis.

Diplodocoidea Marsh, 1884.

Definition: *Diplodocus*, not *Saltasaurus* (stem-based; Wilson and Sereno, 1998).

Unambiguous synapomorphies:

premaxilla is a single elongate unit with nearly no distinction between the body and the nasal process (3-1; Upchurch et al., 2004a);

posteroventral edge of the ascending process of the premaxilla is straight in lateral view, and directed posterodorsally (5-2; Upchurch, 1995);

the dorsal process of the maxilla extends posterior to the posterior process (13-1; Wilson, 2002)

maximum diameter of the antorbital fenestra is subequal (greater than 90%) to the orbital maximum diameter (18-1; Wilson, 2002);

the external nares are retracted to a position between the orbits, facing dorsally or

6692 dorsolaterally (21-1; Marsh, 1898);

6693 a large contribution of the jugal to the antorbital fenestra, bordering approximately one-third
6694   of its perimeter (40-1; Upchurch, 1995);

6695 the anterior terminus of the quadratojugal lies below the anterior margin of the orbit or
6696   beyond (45-1; Rauhut et al., 2005);

6697 angle between anterior and dorsal processes of the quadratojugal is greater than 90°,
6698   approaching 130°, so that the quadrate shaft slants posterodorsally (46-1; McIntosh,
6699   1990b);

6700 the basipterygoid processes are angled less than 75° to the skull roof (normally approximately
6701   45°) (93-1; Calvo and Salgado, 1995);

6702 the transverse flange (i.e. ectopterygoid process) of the pterygoid lies anterior to the antorbital
6703   fenestra (102-1; Upchurch, 1998);

6704 four or more replacement teeth per alveolus (115-1; Wilson, 2002);

6705 planar wear facets of the teeth (117-1);

6706 cylindrical cross-sectional shape of the teeth at midcrown (121-1; Marsh, 1884);

6707 the fibular facet of the astragalus faces posterolaterally, such that the anterior margin is visible
6708   in posterior view (454-1).

6709 **Exclusive synapomorphies:**

6710 external surface of the premaxilla is marked by vascular grooves (2-1);

6711 the anterior maxillary foramen lies on the medial edge of the maxilla, opening medially into
6712   the premaxillary-maxillary boundary (11-1);

6713 the articular surface of the quadrate is roughly triangular in shape (49-1);

6714 SI values for tooth crowns are 3.4 or greater (119-1; McIntosh, 1990b);

6715 short cervical ribs, not reaching the posterior end of the centrum (214-1; Berman and
6716   McIntosh, 1978).

6717 **Shared synapomorphies:**

6718 the posterolateral process of the premaxilla and the lateral process of the maxillary are
6719   without any midline contact (6-0; Wilson, 2002);

6720 maximum diameter of the external nares is shorter than the orbital maximum diameter (22-0);

6721 the articular surface of the occipital condyle is continuously grading into the condylar neck
6722   (77-1);

6723 cervical ribs overlap no more than the next cervical vertebra in sequence (215-1);

6724 the proximal expansion of the humerus is more or less symmetrical (384-0).

6725 **Ambiguous synapomorphies:**

6726 the dorsal transverse processes are inclined dorsally more than 30° from the horizontal (230-
6727 1).

6728 **Previously suggested synapomorphies:**

6729 A very acute angle between medial and lateral margins of the premaxilla (Upchurch et al.,
6730 2004a). The character describing the angle between medial and lateral borders of the
6731 premaxilla was redefined herein, and the numeric boundary changed as to be able to
6732 distinguish between Dicraeosauridae and Diplodocidae. An angle lower than 17° would thus
6733 be synapomorphic for both Rebbachisauridae and Diplodocidae, but not for Dicraeosauridae.
6734 The same character was further found by Whitlock (2011a) to diagnose Diplodocimorpha.

6735 An elongate subnarial foramen (Upchurch et al., 2004a). The character describing the
6736 elongation of the subnarial foramen was not included in the present analysis, as it is
6737 impossible to code in most specimens. Even when rostral skull elements are preserved, the
6738 fossa containing the subnarial and the anterior maxillary foramina is often obliterated with
6739 matrix (e.g. USNM 2672), and only CT scanning would reveal the true shape.

6740 A strongly reduced anteroposterior diameter of the supratemporal fenestra (Upchurch et al.,
6741 2004a). The relation of anteroposterior diameter of the supratemporal to occipital width was
6742 not included in the present analysis, as it was not well explained what was measured for
6743 obtaining a value for the occiput width (Upchurch et al., 2004a). Also, anteroposterior
6744 diameter of supratemporal fenestrae seems to be variable within diplodocids, and relatively
6745 easily deformed (compare the two putative *Diplodocus* skulls CM 11161 and 11255).

6746 Elongate basipterygoid processes (McIntosh, 1990b; Upchurch, 1998). This trait is recovered
6747 as diplodocimorph synapomorphy by Wilson (2002) and Whitlock (2011a). In fact, the
6748 difference is inexistent as Diplodocimorpha describes the same clade as Diplodocoidea in
6749 McIntosh (1990b) and Upchurch (1998). Whitlock (2011a) resolved it as diplodocimorph
6750 synapomorphy due to the basal diplodocoid position of *Haplocanthosaurus*, which does not
6751 preserve cranial bones, and applying the character state optimization strategy DELTRAN. In
6752 the present analysis, definition of the character was slightly changed, which lead to varying
6753 scores for diplodocid taxa. It can thus not be considered a synapomorphy for any clade herein.

6754 A rectangular snout (Upchurch et al., 2004a). The rectangular snout was herein included as
6755 diagnosing Diplodocimorpha, following Whitlock (2011a).

6756 Dentary with ventrally projecting 'chin' (Wilson and Sereno, 1998). At the time Wilson and
6757 Sereno's (1998) monograph was published, no dentary was known from diplodocoids more
6758 basal than Flagellicaudata. The recovery of *Nigersaurus* and *Demandasaurus* dentaries
6759 showed that such a 'chin' was absent in rebbachisaurids (Sereno et al., 1999; Sereno and
6760 Wilson, 2005; Torcida Fernández-Baldor et al., 2011). Consequently, its presence was later
6761 found as synapomorphy for Flagellicaudata (Whitlock 2011a; this study).
6762 The anterior restriction of the tooth row (McIntosh, 1990a). The length of the tooth row is
6763 recovered as diplodocimorph synapomorphy by Whitlock (2011a), applying DELTRAN. In
6764 the present analysis, the number of states has been increased, compared to the definition of
6765 Whitlock (2011a), due to the recognition of a higher diversity within diplodocids. Also,
6766 brachiosaurid skulls have anteriorly restricted tooth rows (Janensch, 1935; Wilson and
6767 Sereno, 1998), which shows that this feature is present in diplodocoid outgroups as well.
6768 Atlantal intercentrum with anteroventral lip (Wilson and Sereno, 1998). The same doubts
6769 apply here as for the presence of a 'chin' in the dentary (see above). The question is
6770 furthermore complicated as no rebbachisaurid atlas has been described to date. With the
6771 present dataset it is thus more cautious to add this trait as synapomorphy of Flagellicaudata.
6772 Cervical and anterior dorsal vertebrae opisthocoelous (McIntosh, 1990a). Opisthocoel cervical
6773 and anterior dorsal vertebrae are actually widespread among sauropod dinosaurs, and
6774 represent the plesiomorphic condition. No phylogenetic analysis was thus able to support this
6775 trait as a synapomorphy of Diplodocoidea.
6776 Deeply divided V-shaped posterior cervical and anterior dorsal neural spines (McIntosh,
6777 1990b). Subdivided cervical and dorsal neural spines are known from a variety of sauropod
6778 dinosaurs from different clades (Upchurch et al., 2004a; Wedel and Taylor, 2013). The shape
6779 of the subdivision was proposed as distinguishing feature between diplodocids and
6780 camarasaurs (V- versus U-shaped; McIntosh, 1990a), but has rarely been used in phylogenetic
6781 analyses. In the present analysis, a character is used to describe the base of the notch.
6782 Reducing the description to the base of the notch, occurrence of U-shaped notches is not
6783 restricted to camarasaurs, but also present in diplodocoid species (e.g. *Amargasaurus cazaui*
6784 or *Apatosaurus ajax* YPM 1860). It should thus not be used to diagnose Diplodocoidea.
6785 Dorsal junction of the spinoprezygapophyseal laminae of dorsal vertebra (Whitlock, 2011a).
6786 Here, this feature is recovered as diagnosing a more inclusive clade, SMA 0009 + mdE, in the
6787 equally weighted reduced consensus tree, as well as in both main implied weights trees. The

6788 difference is a result of the addition of the titanosauriform species *Giraffatitan brancai*,

6789 *Ligabuesaurus leanzai*, and *Isisaurus colberti*, where spinoprezygapophyseal and prespinal

6790 laminae join dorsally (Janensch, 1950; Jain and Bandyopadhyay, 1997; Bonaparte et al.,

6791 2006).

6792 Posterior dorsal centra are amphicoelous (McIntosh, 1990a). Detailed study of diplodocine

6793 posterior dorsal centra showed that most of them are actually slightly opisthocoelous (e.g.

6794 *Diplodocus carnegii* CM 84) to distinctly so (*Supersaurus vivianae*). The amphicoelous

6795 condition was thus herein recovered as synapomorphic for Apatosaurinae or less inclusive

6796 clades.

6797 Arches of dorsal and caudal vertebrae tall (more than two and one-half times length of

6798 dorsoventral centrum height) (Wilson and Sereno, 1998). The present synapomorphy actually

6799 includes two characters as used by Whitlock (2011a) as well as in this study. They were both

6800 interpreted to diagnose Diplodocimorpha by Whitlock (2011a). In the present study, state

6801 boundaries for the dorsal neural arch height were changed, leading to differently scored

6802 diplodocid specimens, which actually show variable ratios. A detailed study of the ratio of

6803 diplodocid caudal neural spines showed that many specimens do not have neural spines that

6804 are 1.5 times taller than the posterior articular surface. Therefore, neither of the two characters

6805 was recovered as diplodocid or diplodocimorph synapomorphy.

6806 Proximal caudal vertebrae with procoelous centra (McIntosh, 1990b). Procoelous centra were

6807 shown to have a much wider distribution than just Diplodocoidea (Carballido et al., 2012b;

6808 D'Emic, 2012; Mannion et al., 2013). Herein, the character describing caudal articular surface

6809 shape, is subdivided into four states, including slight and strong procoely (following

6810 Carballido et al., 2012b). Whereas most diplodocines have slightly procoelous anterior caudal

6811 centra, many other diplodocid specimens actually have flat posterior articular surfaces. To

6812 state that all diplodocoid taxa have procoelous centra would thus over simplify the variety of

6813 morphologies found.

6814 Caudal vertebrae with wing-like transverse processes (McIntosh, 1990b). The same trait was

6815 found to diagnose Diplodocimorpha by Whitlock (2011a). Many non-diplodocid sauropod

6816 species do have dorsally expanded caudal transverse processes on their first caudal vertebra.

6817 These are herein interpreted as wing-like, but they do not have the same shape as diplodocoid

6818 taxa. The problem is best exemplified by a putative diplodocid anterior caudal from the

6819 Cretaceous of China (PMU R263; Upchurch and Mannion, 2009), which was later

6820 reidentified as somphospondylan titanosauriform (Whitlock et al., 2011). A more precise

6821 definition of wing-like would be beneficial for future analyses.

6822 Presence of a whiplash tail (at least 30 elongate, biconvex posterior caudal vertebrae)

6823 (McIntosh, 1990a; Wilson and Sereno, 1998). Even though probably valid, the present

6824 analysis is not able to identify this feature as synapomorphic for any clade, due to the

6825 incompleteness of the included specimens. Only the two specimens of *Apatosaurus louisae*

6826 (CM 3018 and 3378) preserve a tail complete enough to confidently score them for this

6827 character. The trait was thus not included into any clade diagnosis.

6828 Presence of forked chevrons (McIntosh, 1990b). Although named for this peculiar

6829 morphology (Marsh, 1878), *Diplodocus*, as well as its higher-level clades are not the only taxa

6830 to have forked chevrons. In fact, recent studies and discovery of new basal sauropods show

6831 that it might actually be a retained plesiomorphy (Zhang et al., 1988; Ouyang and Ye, 2002;

6832 Remes et al., 2009).

6833 Short metacarpals (McIntosh, 1990a). The same as for the forked chevrons accounts here:

6834 relatively short metacarpals are plesiomorphic for Sauropoda, whereas the elongate

6835 metacarpals diagnose macronarian and titanosauriform taxa (Wilson, 2002; Upchurch et al.,

6836 2004a; Tschopp, 2008).

6837 Ischia have expanded distal ends (McIntosh, 1990b). The expanded distal ends of the ischia

6838 are in fact typical for all diplodocoid sauropods from which ischia were known in 1990. Now,

6839 rebbachisaurs are known to have distally unexpanded ischia, restricting this trait to diagnose

6840 Flagellicaudata.

6841 **Diplodocimorpha Calvo and Salgado, 1995.**

6842 **Definition:** *Diplodocus* + *Rebbachisaurus* (node-based; Taylor and Naish, 2005).

6843 **Unambiguous synapomorphies:**

6844 the anterior margin of the premaxilla does not have a step (1-0; Wilson, 2002. This

6845 synapomorphy was not found by the present analysis, but recovered as such by Wilson (2002)

6846 and Whitlock (2011a). As the data matrix indeed supports an identification of this trait as

6847 unambiguous synapomorphy for Diplocimorpha, it has been included in the present list);

6848 squared (111-2) or blunted snout (111-1; Berman and McIntosh, 1978. As the first

6849 synapomorphy, also this one was found by Whitlock (2011a), but not directly confirmed by

6850 the present analysis, although supported by the data matrix);

6851 sprl extend onto lateral aspect of anterior caudal neural spines (318-1).

Exclusive synapomorphies:

posterior dorsal, sacral and anterior caudal neural spines are 'petal' shaped in anterior/posterior view, expanding transversely through 75% of its length and then tapering (294-1); transition from 'fan'-shaped to 'normal' caudal ribs occurs between Cd4 and Cd5 (300-1).

Ambiguous synapomorphies:

a semicircular dorsal margin of the ilium (409-1).

Previously suggested synapomorphies:

the analysis of Whitlock (2011a) produced a high number of synapomorphies for Rebbachisauridae + Flagellicaudata. Several of these are herein recovered as synapomorphic for Diplodocoidea: the straight, and posterodorsally directed nasal process of the premaxilla, the absence of a sharp distinction between the premaxillary main body and the nasal process, the lacking midline contact of the posterolateral process of the premaxilla and the lateral process of the maxilla, the dorsal process of the maxilla that extends posterior to the posterior process, the subequal diameters of the antorbital and orbital fenestra, the retracted external nares, the large contribution of the jugal to the antorbital fenestra, the anterior ramus of the quadratojugal that reaches anterior to the orbit, the wide angle between the anterior and the dorsal process of the quadratojugal, the low angle between basipterygoid processes and skull roof, the transverse flange of the pterygoid that reaches anterior to the antorbital fenestra, and the four or more replacement teeth per alveolus. As no skull is known for *Haplocanthosaurus*, the recovery of these synapomorphies for Diplodocidea or Diplodocimorpha depends on the method used. With ACCTRAN, they result synapomorphic for Diplodocoidea, whereas DELTRAN recovers them diagnosing Diplodocimorpha. Additional synapomorphies previously recovered for Diplodocimorpha are the following:

parietal excluded from margin of posttemporal foramen (Calvo and Salgado, 1995; Upchurch, 1998; Wilson, 2002). The exclusion of the parietal from the posttemporal foramen is not recovered as synapomorphy for any clade herein, although the data set would support one for Flagellicaudata, as proposed by Whitlock (2011a) as well.

Squamosal extends anteriorly past posterior margin of orbit (Whitlock, 2011a). The anterior extension of the squamosal is restricted in *Kaatedocus* (Tschopp and Mateus, 2013b), which inhibited an identification of the anteriorly reaching squamosal as diplodocimorph synapomorphy in the present analysis.

Tooth crowns aligned along jaw axis, not overlapping (Wilson, 2002). Lacking overlap of

tooth crowns is not restricted to Diplodocoidea, but also present in *Giraffatitan brancai*, for example (Janensch, 1935; Wilson and Sereno, 1998). It was thus not recovered as synapomorphy of any clade in the present analysis.

Mid-caudal vertebral centra length at least twice its height (Upchurch et al., 2004a). The mid-caudal centra are generally more elongate in diplodocoids, compared to other taxa. However, they only reach ratios of two times centrum height in advanced diplodocines, as a more detailed assessment of this character shows. It can thus not be regarded synapomorphic for Diplodocimorpha.

Biconvex distal-most caudal centra (Upchurch, 1998). Biconvex distal caudal vertebrae are exclusive to Diplodocimorpha in the present analysis (but absent in *Suuwassea*, Harris 2006a), which would favor an identification as synapomorphy, as in Whitlock (2011a). However, biconvex caudal vertebrae also occur in titanosauriforms (Wilson et al., 1999), and would thus only qualify for an ambiguous synapomorphy. Therefore, it was not included as such in the present diagnosis.

Distal-most caudal centra at least five times longer than tall (Wilson et al., 1999). The elongation of these distal caudal vertebrae was coded differently in Whitlock (2011a) and here, which resulted in *Apatosaurus* specimens being scored different than *Diplodocus*. The value of greater than five, as proposed by Whitlock (2011a) might thus still be valid, but cannot be recovered as synapomorphic with the present analysis due to varying state boundaries.

Proximal margin of humerus expanded, lateral margin concave in anterior/posterior view (Janensch, 1961). The last diplodocimorph synapomorphy recovered by Whitlock (2011a) describes the concave lateral border of the humerus. This feature is actually present as well in most of the basal sauropods used as outgroups herein. It is thus a plesiomorphic trait and cannot be used as synapomorphy of Diplodocimorpha.

Flagellicaudata Harris and Dodson, 2004.

Definition: *Dicraeosaurus + Diplodocus* (node-based; Harris and Dodson, 2004).

Unambiguous synapomorphies:

subnarial foramen and anterior maxillary foramen are separated by a narrow bony isthmus (8-1; Wilson, 2002);

presence of a preantorbital fossa (15-1);

6916 an elongate and slender posterior end of the quadrate (posterior to posterior-most extension of

6917 pterygoid ramus) (54-1);

6918 the absence of any squamosal-quadratojugal contact (56-1);

6919 the absence of a parietal contribution to the post-temporal fenestra (59-1; Whitlock, 2011a);

6920 vomer articulates with maxilla (103-1; Wilson, 2002. The recovery of this trait as

6921 synapomorphy for Flagellicaudata is supported by the ~~present~~current analysis but not

6922 recovered as such, probably due to the very low percentage of specimens scorable for the

6923 character);

6924 the anteroventral margin of the dentary bears a sharply projecting triangular process or 'chin'

6925 (104-1; Wilson and Smith, 1996);

6926 anteriorly oriented, procumbent teeth (122-1);

6927 atlantal intercentrum bears an anteroventral lip (144-1. Recovered as diplodocoid

6928 synapomorphy by Wilson and Sereno (1998), the presence of the anteroventral lip can

6929 actually only be confirmed for Flagellicaudata, ~~as~~because no rebbachisaurid atlas has yet been

6930 reported. The data matrix supports an identification of the derived as diagnostic for

6931 Flagellicaudata, even though it was not recovered as such);

6932 the distal shaft of the ischium is triangular, with its depth increasing medially (423-1).

6933 **Exclusive synapomorphies:**

6934 the longest axes of the basal tubera are oriented in an angle to each other, pointing towards the

6935 occipital condyle (87-1);

6936 the lateral spinal lamina of anterior-most caudal neural spines expands anteroposteriorly

6937 towards its distal end, and becomes rugose (303-1);

6938 the posterior edge of the distal blade of anterior chevrons is posteriorly expanded in a step-

6939 like fashion (355-1).

6940 **Shared synapomorphies:**

6941 a shallow quadrate fossa (51-0);

6942 absence of longitudinal grooves on the lingual aspect of the teeth (123-0);

6943 anterior diapophyseal laminae (acdl, prdl) are well defined in in anterior caudal vertebrae

6944 (313-1);

6945 a 'crus' bridging the haemal canal is present in some chevrons (352-0; Wilson, 2002);

6946 the cross-sectional shape of ischial distal shafts is V-shaped, forming an angle of nearly 50°

6947 with each other (424-0; Upchurch, 1998);

6948   the ischial shaft is transversely expanded distally (425-1; Upchurch, 1998);

6949   the distal condyle of metatarsal I bears a posterolateral projection (463-1; Berman and

6950   McIntosh, 1978).

6951   **Ambiguous synapomorphies:**

6952   presacral neural spine bifurcation present (126-1; McIntosh, 1990b; this synapomorphy was

6953   not found by the main analyses, but included in the list as it readily distinguishes derived

6954   diplodocoids from more basal forms as rebbachisaurs or *Haplocanthosaurus*);

6955   mid- and posterior dorsal neural arches have divided centropostzygapophyseal lamina, with

6956   the lateral branch connecting to the pcdl (261-1);

6957   the hyposphene-hypantrum system is well developed in posterior dorsal vertebrae, having a

6958   rhomboid shape up to last element (276-0);

6959   the ventral surface is marked by irregular foramina on some anterior caudal centra (305-1).

6960   **Previously suggested synapomorphies:**

6961   qQuadrate articular surface roughly triangular in shape (Whitlock, 2011a). The triangular

6962   articular surface of the quadrate was recovered as exclusive diplodocoid synapomorphy

6963   herein, with rebbachisaurids developing crescent-shaped surfaces. This is most probably due

6964   to the fact that the character was herein treated as ordered, thus assuming that a common

6965   ancestor of rebbachisaurs and flagellicaudatans must have had triangular articular surfaces.

6966   Distance between supratemporal fenestrae twice the length of the longest axis of the

6967   supratemporal fenestrae (Salgado and Calvo, 1992). A detailed assessment of this ratio

6968   showed that most diplodocids do not reach a ratio of two. Even after redefining the state

6969   boundaries, variation between diplodocid specimens results in differential scorings. A high

6970   ratio, and thus wide distance between the supratemporal fenestrae can thus not be regarded

6971   synapomorphic for Flagellicaudata.

6972   Ventrally directed occipital condyle (Upchurch, 1998). The orientation of the occipital

6973   condyle was not included in the present analysis, as it was found to be very difficult to define

6974   a character in an unambiguous way.

6975   Single planar occlusal facet on teeth (Wilson, 2002). This synapomorphy includes two

6976   characters as used in the present analysis, the distinction between single and double occlusal

6977   facets, as well as the planar versus V-shaped facets. The planar facets were found herein as

6978   synapomorphy for Diplodocoidea, whereas the single facets are not found to be typical for

6979   any clade.

17 dentary teeth or fewer (Wilson, 2002). Whereas it is true that flagellicaudatans have ~~less~~fewer than 17 teeth, the same is true for basal macronarian dinosaurs (e.g. *Camarasaurus* or *Giraffatitan*; Gilmore, 1925; Janensch, 1935), as well as for the rebbachisaurid *Demandasaurus*. It thus seems more parsimonious to interpret the ~~less~~fewer than 17 dentary teeth state as ancestral to all neosauropods, with subsequent reversal to a higher number of teeth in *Nigersaurus* (Sereno and Wilson, 2005).

Low-angled, planar wear facets on the teeth (Calvo, 1994). The angulation of the wear facets was not included as character in the present analysis, as an acute angle only characterizes rebbachisaurids, and enough characters were already used to resolve the position and relationship of that clade. Low angles are not restricted to diplodocids either, being also present as late stages in the wear of camarasaur teeth (e.g. SMA 0002; Wiersma, 2013).

Anterior cervical neural spines bifid (McIntosh, 1990b). Anterior neural spines are rarely preserved in cervical vertebrae, even in nearly complete specimens like the holotypes of *Apatosaurus louisae* or *Diplodocus carnegii* (CM 3018 and 84, respectively; Wedel and Taylor, 2013). Diplodocid specimens preserving anterior neural spines actually all show the bifurcation to initiate posterior to CV 5 or 6, and thus not in the anterior elements. The only group positively confirming bifid neural spines in anterior cervical vertebrae are the Dicraeosauridae. Indeed, the present analysis recovered bifid anterior neural spines as synapomorphic for this taxon.

Presence of a median tubercle in bifurcated cervical and dorsal neural spines (Wilson, 2002). Although generally present in Flagellicaudata, some specimens do not show such a tubercle (e.g. *Amargasaurus cazaui*, or UW 15556). Also, the probable non-diplodocoid *Australodocus* does have a median tubercle, such that its presence could at most be interpreted as ambiguous synapomorphy. Since it was not recovered as such by the present analysis, it was not included in the diagnosis.

Anterior dorsal vertebrae with divided centropostzygapophyseal laminae (Wilson, 2002). A divided centropostzygapophyseal lamina was only positively identified in mid- and posterior dorsal vertebrae, but not in anterior ones. Therefore, the character was restricted to mid- and posterior elements.

Height of sacral neural spines nearly four times length of centrum (Wilson, 2002). This ratio was redefined, and posterior dorsal vertebrae were included into the description. The apomorphic state of the new character (282-1) was found to diagnose Dicraeosauridae in the

7012 present analysis.

7013 Anterior caudal neural arches with spinoprezygapophyseal lamina (sprl) on lateral aspect of

7014 neural spine (Wilson, 2002). The extension of the caudal spinoprezygapophyseal lamina onto

7015 the lateral side of the neural spine is actually a diplodocimorph synapomorphy, as it is also

7016 present in rebbachisaurids, but absent in *Haplocanthosaurus* (Hatcher, 1903; Sereno et al.,

7017 2007).

7018 Procoelous first caudal centrum (Wilson, 2002). The first caudal centrum is actually flat

7019 posteriorly in many flagellicaudatan specimens (e.g. CM 84, ET, pers. obs., 2011), and only

7020 more posterior elements develop a slight convexity, if at all. This trait is thus not included as

7021 synapomorphic for any clade herein.

7022 Pubis with prominent ambiens process (McIntosh, 1990b). In the present analysis, a

7023 distinction is made between the hook-like ambiens process as present in *Diplodocus* and

7024 *Dicraeosaurus* (Hatcher, 1901; Janensch, 1961), for example, and the less developed, but still

7025 prominent process of apatosaurines (Ostrom and McIntosh, 1966). The presence of a

7026 prominent ambiens process can thus still be confirmed as synapomorphic for Flagellicaudata,

7027 but ~~as~~because the morphology is different, it was not recovered as such in the present

7028 analysis.

7029

7030 **Dicraeosauridae Huene, 1927.**

7031 **Definition:** *Dicraeosaurus*, not *Diplodocus* (stem-based; Sereno, 1998).

7032 **Unambiguous synapomorphies:**

7033 the crista prootica is expanded laterally into dorsolateral process (76-1; Salgado and Calvo,

7034 1992);

7035 basipterygoid processes are narrowly diverging (< 31°) (92-2; Wilson, 2002);

7036 the area between the basipterygoid processes and parasphenoid rostrum forms a deep slot-like

7037 cavity that passes posteriorly between the bases of the basipterygoid processes (95-1;

7038 Upchurch et al., 2004a);

7039 subtriangular cross-sectional shape of the symphysis of the dentary, tapering sharply towards

7040 its ventral extreme (105-1; Whitlock and Harris, 2010);

7041 presence of a tuberosity on the labial surface of the dentary, near the symphysis (106-1;

7042 Whitlock and Harris, 2010);

7043 the first bifid cervical neural spine is in CV 3 (140-0).

Shared synapomorphies:

frontal symphysis is fused in adult individuals (26-1; Salgado and Calvo, 1992);

presence of a pineal (parietal) foramen between frontals and parietals (36-0);

presence of a postparietal foramen (66-1; Salgado and Calvo, 1992);

the sagittal nuchal crest of the supraoccipital is narrow, sharp, and distinct (74-1);

the supraoccipital bears a foramen close to its contact with the parietal (75-1);

absence of a basioccipital depression between foramen magnum and basal tubera (80-0);

the anterolateral corner of the tooth row is displaced labially (112-1);

the width to height ratio of cervical vertebrae is less than 0.5 (128-0; Upchurch et al., 2004a);

the total height to centrum length ratio of anterior cervical vertebrae is greater than 1.2

(usually around 1.5) (154-2);

the pleurocoels of anterior cervical centra are undivided (157-0);

presence of paired pneumatic fossae on the ventral surface of anterior cervical centra (160-1);

mid-cervical neural spines are anteriorly inclined (169-1; Rauhut et al., 2005);

posterior cervical and anterior dorsal bifid neural spines are parallel to converging (211-1;

Rauhut et al., 2005);

absence of an anterior, middle single fossa projected through the midline of single dorsal

neural spines (233-1);

the transition from bifid to single dorsal neural spines is abrupt (235-1);

mid-dorsal neural spines are bifid, inclusive of at least the fifth dorsal vertebrae (250-1);

lateral pleurocoels are absent in mid- and posterior dorsal centra (252-0; Janensch, 1929a);

posterior dorsal centra are amphicoelous (270-0);

the ratio of height above postzygapophyses (neural spine) of posterior dorsal neural arches to

height below (pedicel) is 3.1 or greater (272-1);

the height of posterior dorsal and/or sacral neural spines (not including arch) is more than 3

times centrum length (282-2; McIntosh, 1990a);

absence of pleurocoels in sacral vertebral centra (287-0);

the ventral surface of anterior caudal transverse processes is directed dorsally (312-1);

a ratio of blade height above pubic peduncle of the ilium to its anteroposterior length of 0.40

or more (405-1);

the position of the highest point of the femoral head is laterally shifted in anterior view, and

lies above the main portion of the shaft (431-1);

presence of a short transverse ridge on the anteromedial surface of the distal end of the tibia (443-1);

a ratio of mediolateral width of the astragalus to maximum anteroposterior length of less than 1.6 (452-1);

metatarsal I is relatively gracile, proximal transverse width to greatest length is less than 0.8 (461-0);

the groove on the lateral surface of pedal unguals extends straight horizontally (477-1).

Ambiguous synapomorphies:

postzygodiapophyseal and spinopostzygapophyseal laminae of mid-cervical vertebrae form a right angle (170-1);

mid- and posterior cervical neural arches bear lateral fossae on the prezygapophysis process (183-1);

absence of dorsal pneumatopores (pleurocoels) (227-0);

the base of the notch between the metapophyses of anterior, bifid dorsal vertebrae is narrow and V-shaped (244-1);

the parapophysis of DV 3 lies mid-way between the top of the centrum and the level of the prezygapophyses (246-1).

Previously suggested synapomorphies:

premaxilla with anteroventrally orientated vascular grooves originating from an opening in the maxillary contact (Wilson, 2002). The grooves are shown to be present as well in some diplodocid specimens (see above). An identification of this trait as dicraeosaurid synapomorphy is thus questionable.

Frontal contributes to margin of supratemporal fenestra (reversal; Wilson and Sereno, 1998). Although this is true for *Dicraeosaurus* and *Amargasaurus*, *Suuwassea* does not show any participation of the frontal in the supratemporal fenestra. Therefore, the present analysis was not able to recover this reversal as synapomorphic for the entire clade Dicraeosauridae.

Supratemporal fenestra smaller than foramen magnum (Salgado and Calvo, 1992). The reduced size of the supratemporal fenestra has been found as synapomorphic for *Amargasaurus + Dicraeosaurus* by the equally weighted reduced consensus tree. However, this trait is shared with *Limaysaurus*, and it remains thus unclear how to interpret it (diplodocoid or diplodocimorph synapomorphy with reversals, or as convergently acquired traits of Rebbachisauridae and Dicraeosauridae).

Ventrally directed prong on squamosal (Whitlock, 2011a). A ventrally directed process is present in some diplodocids as well, and very similar to the state in *Dicraeosaurus* (see above). An enlarged prong-like structure is only present in *Amargasaurus*, which does not allow an identification of this feature as synapomorphic for Dicraeosauridae.

Basal tubera narrower than occipital condyle (Wilson, 2002). As shown by Mannion (2011), the ratio between basal tubera and occipital condyle width is highly variable. The state boundaries used herein do not allow to identify the lowest ratio as synapomorphic for Dicraeosauridae, although the ratios themselves indicate that it might be taxonomically significant.

'Petal' shaped posterior dorsal neural spines (Wilson, 2002). The peculiar 'petal' shape of dorsal, and sacral neural spines of dicraeosaurids is also present in rebbachisaurids, which led to an identification of this feature as a diplodocimorph synapomorphy herein.

Cervical vertebrae with longitudinal ridge on ventral surface (Sereno et al., 2007). The presence of a longitudinal ridge is a plesiomorphic feature within sauropods, and present as well in some diplodocid specimens (e.g. SMA 0004, YPM 429; Lull, 1919; Tschopp and Mateus, 2013b). Dicraeosaurids have well-developed keels in anterior cervical centra, shared with *Shunosaurus*, but also with *Galeamopus* ▮▮▮▮▮ SMA 0011 (see above). The presence of ventral ridges and keels is thus too variable as that a reversal to the plesiomorphic state could be recovered as synapomorphic for any clade.

Anterior caudal centra with irregularly placed foramina on ventral surface (Harris, 2007). The presence of ventral foramina in anterior caudal vertebrae is herein recovered as flagellacaudatan synapomorphy, as it is shared with numerous diplodocid specimens.

Mid-caudal vertebral centra with mid-height longitudinal ridge on lateral surface, centra hexagonal in anterior/posterior view (Whitlock, 2011a). Longitudinal ridges also mark the mid-caudal vertebrae of *Camarasaurus*, as well as many apatosaurine specimens (Gilmore, 1925, 1936). Their presence could thus only be interpreted as shared synapomorphy for Dicraeosauridae. Since it was not recovered as such, it is not included in the diagnosis herein.

Humerus with pronounced proximolateral corner (Wilson, 2002). This trait was recovered as neosauropod synapomorphy in the implied weights trees. As definition of 'pronounced' is somewhat vague, interpretation of this character might have been different in Wilson (2002). The herein used definition is explained and figured above.

Diplodocidae Marsh, 1884.

Definition: *Diplodocus*, not *Dicraeosaurus* (stem-based; Sereno, 1998).

Unambiguous synapomorphies:

maxilla-quadratojugal contact broad (14-1; Rauhut et al., 2005; not recovered by the present analysis, it is still supported by the data matrix. The reason why it was not recovered is probably the low percentage of specimens preserving these two bones);

antorbital fenestra with concave dorsal margin (20-1; Wilson, 2002; also this trait was not recovered as diplodocid synapomorphy, although supported by the specimens for which a scoring was possible. The reason is probably the same as in the previous synapomorphy);

posterior process of the prefrontal is hooked (25-1; Berman and McIntosh, 1978);

mandible without strong coronoid eminence (108-1; Whitlock, 2011a; as in the previous characters, the low number of specimens preserving the mandible probably precluded an identification of this character as synapomorphy for Diplodocidae, although supported by the data set);

direct crown-to-crown occlusion absent (116-1; Wilson, 2002; yet another trait not found as synapoorphic, probably due to low percentage of preservation, but supported by the dataset);

14 to 15 cervical vertebrae (127-1; Huene, 1929);

anterior centrodiapophyseal lamina (acdl) of anterior caudal vertebrae is divided (314-1; Wilson, 2002).

Exclusive synapomorphies:

preantorbital fenestra occupies at least 50% of the preantorbital fossa (17-1);

medial margin of the prefrontal is curving distinctly medially at its anterior end to embrace the anterolateral corner of the frontal (23-1);

ten dorsal vertebrae (224-2; Huene, 1929);

anterior and mid-caudal vertebrae bear ventrolateral ridges (329-1).

Shared synapomorphies:

shape of the posterior face of the basal tubera flat (85-1) or slightly concave (85-2);

short mid- and posterior dorsal transverse processes (263-0);

posterior dorsal, sacral and anterior caudal neural spines rectangular through most of their length (294-0; Whitlock, 2011a; the current state represents a reversal to the plesiomorphic condition, and it was scored differently in *Amphicoelias altus* AMNH 5764, which has a dorsally expanded neural spine, somewhat resembling a 'petal' shape, although not to the

7172   extent as in dicraeosaurs or rebbachisaurs)

7173   anterior caudal transverse processes with anteroposteriorly expanded lateral extremities (316-

7174   1);

7175   spinoprezygapophyseal laminae (sprl) and spol contact each other on anterior caudal neural

7176   spines (319-1; Wilson, 1999);

7177   presence of a lateral bulge on the femur (428-1).

7178   **Ambiguous synapomorphies:**

7179   dorsal transverse processes horizontal or only slightly inclined dorsally (230-0);

7180   posterior centroparapophyseal lamina of mid- and posterior dorsal neural arches present as

7181   single lamina (258-1; Wilson, 2002).

7182   **Previously suggested synapomorphies:**

7183   antorbital fenestra subequal to orbital maximum diameter (Wilson, 2002). The large antorbital

7184   fenestrae are recovered as diplodocid synapomorphy herein, as *Nigersaurus* also shows the

7185   apomorphic state (Sereno et al., 1999, 2007).

7186   Prefrontal posterior process elongate (Wilson, 2002). Determination of the length of the

7187   posterior process of the prefrontal is highly influenced by the orientation of the skull roof, as

7188   shown previously. Taking this into account, elongated posterior processes of the prefrontal are

7189   not present in all diplodocid specimens. This trait was thus excluded from the diagnosis.

7190   No internarial bar (Upchurch et al., 2004a). An internarial bar also appears to be absent in di-

7191   craeosaurids (Janensch, 1935; Harris, 2006b). It would thus more appropriately be interpreted

7192   as flagellicaudatan synapomorphy, but was not included in the present analysis, because in

7193   most specimens it is difficult to distinguish true absence from incomplete preservation.

7194   Frontal contribution to dorsal margin of orbit roughly equal to contribution of prefrontal

7195   (Whitlock, 2011a). Remeasuring the contribution of the frontal and prefrontal in various

7196   diplodocid skulls showed that variation occurs both within but also outside Diplodocidae.

7197   Neither one nor the other state can thus be confidently considered synapomorphic for any

7198   clade.

7199   Quadrate fossa shallow (Wilson, 2002). A shallow quadrate fossa was later found in *Su-*

7200   *uwassea* as well (Harris, 2006a), showing that this trait is not restricted to Diplodocidae. Con-

7201   sequently, it has here been found as flagellicaudatan synapomorphy.

7202   Squamosal-quadratojugal contact absent (Wilson, 2002). Tschopp and Mateus (2013b)

7203   showed that a contact between the squamosal and the quadratojugal was also absent in *Su-*

7204 *uwassea* (contrary to Harris, 2006a). Therefore, the present trait was herein recovered as flag-

7205 ellicaudatan synapomorphy.

7206 The jugal forms a substantial part of the caudoventral margin of the antorbital fenestra (Up-

7207 church, 1998). The contribution of the jugal to the antorbital fenestra was recovered as

7208 diplodocoid synapomorphy, ~~as~~because *Nigersaurus* shows the same morphology (Sereno and

7209 Wilson, 2005).

7210 An angle between the rostra1 and dorsal quadratojugal processes of 130° (Upchurch et al.,

7211 2004a). A wide angle between rostral and dorsal processes of the quadratojugal also occurs in

7212 *Nigersaurus* (Sereno and Wilson, 2005), leading to a recovery of this feature as diplodocoid

7213 synapomorphy herein.

7214 The distal end of the paroccipital process rounded and tongue-like (Upchurch et al., 2004a).

7215 This character was not used in the present analysis ~~as~~because it was unclear what tongue-like

7216 precisely means. It was substituted by a character describing dorsoventral expansion towards

7217 the distal ends of the paroccipital processes, which varies within Diplodocidae and does thus

7218 not qualify as a reliable synapomorphy.

7219 The parasphenoid rostrum is a laterally compressed, thin spike lacking the longitudinal dorsal

7220 groove (Upchurch et al., 2004a). A dorsal groove is actually present on many diplodocid

7221 parasphenoid rostra (e.g. CM 11161, ET, pers. obs., 2011). Transverse compression of the

7222 parasphenoid rostrum is also apparent in *Camarasaurus* (Madsen et al., 1995). Generally,

7223 diplodocid parasphenoid rostra are more spike-like, or dorsoventrally compressed, compared

7224 to *Giraffatitan* or *Camarasaurus* (Janensch, 1935; Madsen et al., 1995), but that is difficult to

7225 translate into a valid phylogenetic character, and was thus not used as such herein.

7226 The ectopterygoid process of the pterygoid located below the antorbital fenestra (Upchurch et

7227 al., 2004a). Such an anterior position of the ectopterygoid process is shared with reb-

7228 bachisaurs (Whitlock, 2011a) , and thus recovered as diplodocoid synapomorphy herein.

7229 The ectopterygoid process of the pterygoid reduced, so that it cannot be seen below the ven-

7230 tral margin of the skull in lateral view (Upchurch et al., 2004a). No such character was includ-

7231 ed in the present analysis. However, given the rareness of palatal complexes preserved in their

7232 true position, it remains doubtful if the analysis would have been capable to confidently re-

7233 solve character state distributions.

7234 The breadth of the main body of the pterygoid at least 33% of pterygoid length (Upchurch et

7235 al., 2004a). Given that only one disarticulated diplodocid pterygoid was available for direct

7236   study (SMA 0011), no character was included in the present analysis to test the distribution of

7237   this trait. Generally, diplodocid pterygoids do appear more elongate compared to non-

7238   diplodocid taxa, but only rarely measurements can be taken directly from the specimen. It is

7239   thus not included in the diagnosis herein.

7240   Cervical vertebrae with longitudinal sulcus on ventral surface (Upchurch, 1998). Presence of

7241   a ventral longitudinal sulcus in cervical vertebrae is uncommon in apatosaurs, if one does not

7242   consider the concave area between the strongly ventrally projecting parapophyses. Conse-

7243   quently, the sulcus is herein recovered as diplodocine synapomorphy.

7244   Bifurcated centroprezygapophyseal lamina in cervical vertebrae, with a medial and a lateral

7245   ramus connecting to the zygapophysis (Wilson, 2002). As *Supersaurus* does not seem to have

7246   divided cprl, the current analysis recovered this trait as synapomorphic for both Apatosaurinae

7247   and Diplodocinae more derived than *Supersaurus*.

7248   70-80 caudal vertebrae (Upchurch et al., 2004a). The high number of caudal vertebrae is diffi-

7249   cult to score in a specimen-based phylogenetic analysis, because only very few specimens

7250   preserve reasonably complete caudal series. In the present analysis, only CM 3018 and 3378

7251   positively confirm such a statement. Indirect evidence for an elongated tail also comes from

7252   the rod-like distal caudal vertebrae in some dicraeosaurid specimens, as well as in *Li-*

7253   *maysaurus*. The number of caudal vertebrae is thus not included in the diagnosis here.

7254   Presence of diapophyseal laminae on anterior caudal vertebrae (Upchurch, 1998). This char-

7255   acter has been divided in the present analysis, distinguishing between anterior and posterior

7256   diapophyseal laminae. Apatosaurs, as well as *Supersaurus*, tend to have much broader posteri-

7257   or diapophyseal laminae compared to diplodocines, thus not qualifying to be scored as 'dis-

7258   tinct'. On the other hand, well-developed anterior diapophyseal laminae also occur in di-

7259   craeosaurs. Therefore, the latter were recovered as flagellicaudatan synapomorphy, whereas

7260   distinct posterior diapophyseal laminae were found to diagnose *Galeamopus* + mdD.

7261   Humero-femoral length ratio is approximately 0.66 (Huene, 1927). Due to the lack of speci-

7262   mens preserving both complete fore- and hindlimbs, the distribution of this character state

7263   cannot be assessed in enough detail with the present analysis. While generally supporting the

7264   identification as diplodocid synapomorphy, the low number of only two specimens positively

7265   confirming this ratio for the entire clade Diplodocidae does not allow a well-founded inclu-

7266   sion of the trait into a diagnosis.

Insertion of the M. iliofibularis on the fibula located above midshaft (Wilson and Sereno, 1998). In fact, insertion of this muscle on the fibula is located further distally in apatosaurines and *Tornieria* than in more derived diplodocines, as a detailed assessment showed (see above). The proximal location of the insertion is thus recovered as synapomorphic for *Supersaurus* + mdD herein.

An absence of a calcaneum (McIntosh, 1990b). The absence of a calcaneum as diplodocid synapomorphy is most probably a preservational artifact. As shown by Bonnan (2000), at least one pes of *Diplodocus* preserves a calcaneum, and personal observations in two putative apatosaur pedes (CM 30766 and NHMUK R3215) reveal the probable presence of such an element in apatosaurs as well. It is thus not included in the diagnosis of any clade.

Pedal phalanx I-1 having a proximoventral margin drawn out into a thin plate or heel that underlies the distal end of metatarsal I (Upchurch et al., 2004a). The distribution of this trait is more complicated: it is also present in the non-diplodocid *Turiasaurus* and *Cetiosauriscus stewarti*, and absent in *Apatosaurus louisae* CM 3018. Its presence would thus only qualify for an ambiguous synapomorphy, but was not recovered as such by the present analysis.

Pedal phalanx II-2 reduced in craniocaudal length and having an irregular shape (Upchurch et al., 2004a). Whereas all included diplodocid specimens preserving this element show a reduced craniocaudal length in php II-2, the same is also present in *Mamenchisaurus* (Ouyang and Ye, 2002). ~~As~~Because no complete pes is known from any dicraeosaur or rebbachisaur, true distribution of this trait cannot be assessed to date, and it is thus excluded from the updated diagnosis of Diplodocidae.

Apatosaurinae Huene, 1927.

Definition: *Apatosaurus*, not *Diplodocus* (stem-based; Taylor and Naish, 2005).

Unambiguous synapomorphies:

cervical ribs projecting well beneath centrum, such that the length of the posterior process is subequal in length to the fused diapophysis/tuberculum (216-1).

Exclusive synapomorphies:

posterior cervical rib shafts are initially directed in the same direction but turn to run a little downwards toward the distal tip (223-1).

Shared synapomorphies:

dorsoventral height of the occipital process of the parietal is low, subequal to less than the

diameter of the foramen magnum (63-0);

presence of a foramen in the notch that separates the two basal tubera (90-1);

centroprezygapophyseal lamina of mid- and posterior cervical neural arches is divided, resulting in the presence of a 'true' divided centroprezygapophyseal lamina, which is dorsally connected to the prezygapophysis (185-2);

posterior centrodiapophyseal lamina (pcdl) and postzygodiapophyseal laminae (podl) of mid- and posterior cervical transverse processes do not meet anteriorly, such that the postzygapophyseal centrodiapophyseal fossa extends onto the posterior face of the transverse process (186-1);

anterior process of posterior cervical ribs is reduced to a short bump-like process or absent (220-1);

mid- and posterior dorsal parapophyses lie posterior to the anterior edge of centrum (256-0);

posterior dorsal postzygapophyses are oblique, including an almost 90° angle (275-1);

ratio of the pubic articulation of the ischia to the anteroposterior length of the pubic pedicel of 1.5 or greater (420-1);

pedal phalanges III-1 and IV-1 are wider than long (476-1).

Ambiguous synapomorphies:

posterior centrodiapophyseal lamina in cervical vertebrae reaches below the posterior end of the neural canal (135-1);

abrupt transition from bifid to single dorsal neural spines (235-1);

bifid dorsal neural spines (if present) do not extend past the second or third dorsal (250-0);

ratio of metacarpal III length to distal transverse width of less than 2.9 (402-0).

Previously suggested synapomorphies:

To our knowledge, only one phylogenetic study is published recognizing an apatosaurine clade including more than just the genus *Apatosaurus*: Lovelace et al. (2007) also recover *Supersaurus* and *Suuwassea* as apatosaurine diplodocids, but do not provide a diagnosis for the clade. The current diagnosis is thus the first for Apatosaurinae based on a cladistic analysis.

Diplodocinae Marsh, 1884.

Definition: *Diplodocus*, not *Apatosaurus* (stem-based; Taylor and Naish, 2005).

Exclusive synapomorphies:

7331 cervical vertebrae bear a small, shallow, anteroposteriorly elongate fossa posteroventral to the

7332 pleurocoel (131-1);

7333 large coels mark the anterior caudal centra (307-1; Wilson, 2002).

7334 **Shared synapomorphies:**

7335 box-like basal tubera (82-1);

7336 presence of a basisphenoid/basipterygoid recess (91-1);

7337 a longitudinal sulcus marks the ventral surface of the cervical vertebrae (133-1);

7338 the tuberculum of anterior and mid-cervical ribs is directed upwards and backwards in lateral

7339 view (218-1);

7340 an oblique ridge connects the medial and lateral edges at the base of the rib head in dorsal ribs

7341 (283-1);

7342 presence of a ventral longitudinal hollow in anterior and mid-caudal centra (330-1; Marsh,

7343 1895);

7344 a ratio of centrum length to posterior height in mid-caudal vertebrae of 1.7 or greater (332-1);

7345 the scapular acromial process that lies nearly at midpoint of the scapular body (364-1).

7346 **Previously suggested synapomorphies:**

7347 EI of mid-cervical vertebrae greater than 4.0 (Upchurch, 1998). State boundaries were

7348 changed herein in comparison to Upchurch (1998). However, a mean value of four or more is

7349 not reached by several diplodocine specimens, but convergently acquired by various outgroup

7350 taxa (Tab. S22). It is thus excluded from the diagnosis of Diplodocinae.

7351 Quadrangular anterior articular surface of anterior caudal centra (Wilson, 2002). There is a

7352 wide range of articular surface shapes in these elements, and it is difficult to describe them

7353 qualitatively or divide them into only two categories, as was done by Wilson (2002: circular

7354 or quadrangular). Most of the diplodocine anterior caudal centra have a flat ventral edge (e.g.

7355 *Barosaurus lentus* YPM 429; Lull, 1919), but this is accounted for in other characters. The

7356 shape becomes gradually more quadrangular towards middle caudal vertebrae in *Diplodocus*

7357 (e.g. AMNH 223; Osborn, 1899), but not in *Barosaurus*, which keeps its rounded lateral

7358 edges (e.g. AMNH 6341; ET, pers. obs., 2011). Although anterior caudal centra with flat

7359 ventral border can still be confidently assigned to Diplodocinae, more rounded centra cannot

7360 be excluded just based on this morphology. The 'quadrangular' shape of the anterior face

7361 should thus not be regarded a true synapomorphy of Diplodocinae.

7362 Caudal centrum length doubles over first 20 vertebrae (Wilson, 2002). Caudal centra that are

nearly doubling their length within the first 20 elements is not restricted to Diplodocinae. It is shared by *Cetiosauriscus stewarti* (NHMUK R3078, ET, pers. obs., 2011), *Zapalasaurus bonapartei* (Salgado et al., 2006), as well as *Suuwassea emilieae* (Harris, 2006a) and the apatosaur FMNH P25112 (Gilmore, 1936). It is therefore not considered a diplodocine synapomorphy herein.

Middle caudal neural spines vertical (Wilson, 2002). Actually, the majority of diplodocine specimens preserving mid-caudal vertebrae have posterodorsally directed neural spines. The only species with vertical mid-caudal neural spines is *Diplodocus hallorum*.

Updated diagnoses of valid diplodocid genera and species

The following diagnoses include autapomorphies found by the analysis as well as additional traits found to be unique at least within the respective higher-level clade (Apatosaurinae or Diplodocinae). Autapomorphies found only in one specimen ☰ marked by an asterisk. Referred specimens as well as localities and horizons only include information from the present analysis. Specific or generic identification of other specimens is often not done with enough detail (i.e. without phylogenetic analysis or accurate description of the material), such that earlier referrals require a reappraisal before definitely including them in the species lists. Geographical and temporal distribution of the genera and species proposed herein have thus to be regarded as smallest possible ranges.

Systematic Paleontology

Dinosauria Owen, 1842.

Sauropoda Marsh, 1878.

Neosauropoda Bonaparte, 1986.

Diplodocoidea Marsh, 1884.

Flagellicaudata Harris and Dodson, 2004.

Diplodocidae Marsh, 1884.

***Amphicoelias* Cope, 1877a.**

Type and only referred species: *Amphicoelias altus* Cope, 1877a.

Invalid proposed species: *Amphicoelias latus* Cope, 1877a (= *Camarasaurus*); *Amphicoelias fragillimus* Cope, 1878 (nomen dubium).

Revised diagnosis: *Amphicoelias* is diagnosed by the following autapomorphies: posterior

dorsal postzygapophyses almost horizontal, such that the two articular facets include a wide angle (275-0*, shared with Diplodocinae); posterior dorsal neural spines 'petal' shaped, expanding transversely through 75% of its length and then tapering (294-1*, unique within Diplodocidae); a gracile femur, with a robustness index (sensu Wilson and Upchurch, 2003) of less than 0.22 (427-0*, only shared with USNM 10865 within Diplodocidae); and a mediolateral width of the femur which is subequal to the anteroposterior diameter (430-0*, only shared with CM 566 and *Dicraeosaurus* within Diplodocoidea).

Comments: The characters initially used by Cope (1877a) to diagnose the genus are now known to be more widespread among sauropods, such as the amphicoelous dorsal centra, or the weak development of the greater trochanter on the femur. Osborn and Mook (1921) first recognized the extreme slenderness of the femur of *Amphicoelias*, compared to other sauropods. Wilson and Smith (1996) reported two autapomorphies for the skull, based on a second specimen referred to the genus. However, no detailed description nor figures of the material have yet been published, such that the validity of these traits as autapomorphic features for *Amphicoelias* are herein regarded questionable. The assignment of the specimen to *Amphicoelias* was mainly based on the circular cross section of the femur midshaft (Wilson and Smith, 1996), which has been recovered as autapomorphic herein as well. Upchurch et al. (2004a) proposed the unusual, slightly posterodorsal orientation of the posterior dorsal neural spine as an autapomorphy of the genus. Although characters were included in the present analysis to code for this morphology (C265 and 280), none of them was found as autapomorphic for *Amphicoelias*, and both are shared with specimens from both Apatosaurinae and Diplodocinae.

Locality and horizon: Cope Quarry 12, Garden Park Area, Fremont County, Colorado. Upper-most Brushy Basin Member, Morrison Formation (probably Tithonian). Dinosaur zone 4 (Turner and Peterson, 1999), Zone 6 (Foster, 2003).

***Amphicoelias altus* Cope, 1877a.**

Type specimen: AMNH 5764.

Referred specimens: -

Diagnosis, locality, and horizon as for genus.

Apatosaurinae Huene, 1927.

***Apatosaurus* Marsh, 1877a.**

7427 Syn. *Brontosaurus amplus* Marsh, 1881.

7428 **Type species:** *Apatosaurus ajax* Marsh, 1877a.

7429 **Referred species:** *Apatosaurus louisae* Holland, 1915a.

7430 **Invalid proposed species:** *Apatosaurus grandis* Marsh, 1877a (= *Camarasaurus grandis*), *A.*

7431 *laticollis* Marsh, 1879 (nomen dubium; =*A. louisae*), *A. minimus* Mook, 1917 (non-

7432 diplodocoid neosauropod), *A. alenquerensis* Lapparent and Zbyzewski, 1957 (=

7433 *Lourinhasaurus alenquerensis*), *A. yahnahpin* Filla and Redman, 1994 (= *Eobrontosaurus*

7434 *yahnahpin*).

7435 **Revised diagnosis:** *Apatosaurus* is diagnosed by the following autapomorphies: presence of

7436 an accessory horizontal lamina in the spinodiapophyseal fossa of mid- and posterior cervical

7437 vertebrae, not connected to any surrounding lamina (187-1, unique within Apatosaurinae),

7438 vertical struts divide lateral pneumatic foramen of mid- and posterior dorsal centra (253-1,

7439 unique within Apatosaurinae); gradual transverse expansion of anterior caudal neural spines

7440 (328-0, unique within Diplodocidae); absence of ventrolateral ridges (329-0, unique within

7441 Apatosaurinae); and a straight scapular blade in lateral view (368-0, unique within

7442 Diplodocidae).

7443 **Comments:** Berman and McIntosh (1978) proposed the relative positions of ectopterygoid

7444 and pterygoid as distinguishing character between the skulls CM 11161 and 11162. It was

7445 used as a phylogenetic character by Wilson (2002). However, there are only very few

7446 diplodocid skulls available, with the palatal complex articulated and complete. One of these is

7447 the juvenile probable *Diplodocus* skull CM 11255, which was interpreted to have an

7448 morphology more similar to the state in *Apatosaurus* than to *Diplodocus* (Whitlock et al.,

7449 2010). However, recent studies appear to show that actually *Apatosaurus* CM 11162 has the

7450 same arrangement as *Diplodocus* CM 11161 (Whitlock and Lamanna, 2012). The distribution

7451 of this character thus seems very difficult to interpret. The fact that there are so few specimens

7452 preserving this area also decreases the phylogenetic value of this character. Therefore, until a

7453 more numerous sample of diplodocid skulls with articulated palatal complex is found, this

7454 feature should not be used in diagnoses. In general, autapomorphies previously proposed for

7455 the genus *Apatosaurus* most often describe a more inclusive clade in the present analysis, as

7456 many taxa previously included in the genus are actually forming their own genera (e.g.

7457 *Brontosaurus*, or *Elosaurus*). These traits are thus not further discussed here.

7458 **Locality and horizon:** various sites in Colorado, Wyoming, and Utah. Middle to upper part

of the Upper Jurassic Morrison Formation, Late Kimmeridgian to Early Tithonian. Apatosaurine intervals 2 and 3 (Bakker, 1998); Dinosaur zone 3B upper (Turner and Peterson, 1999); Zone 5 (Foster, 2003).

Apatosaurus ajax **Marsh, 1877a.**

Syn.? *Brontosaurus amplus* Marsh, 1881

Type specimen: YPM 1860.

Referred specimens: ?YPM 1981

Revised diagnosis: *A. ajax* is diagnosed by the following autapomorphies: a shallow, second fossa marks the quadrate shaft medially to the pterygoid flange (not the quadrate fossa) (52-1*, unique within Apatosaurinae), box-like basal tubera (81-1*, unique within Apatosaurinae), longest axes of the basal tubera oriented parallel to each other (87-0*, unique within Apatosaurinae), medial surface of posterior bifid, cervical neural spines is smooth (206-1*, unambiguous), presence of an accessory lamina linking the hyposphene of mid- and posterior dorsal vertebrae with the base of the posterior centrodiapophyseal lamina (260-1*, unique within Apatosaurinae), and presence of an elliptical depression between the lateral spinal lamina of caudal neural spines and the postspinal lamina (292-1*, unique within Apatosaurinae).

Comments: In the most recent revised diagnosis of the species, Upchurch et al. (2004b) proposed four more autapomorphies of the species, which are not found in the present analysis, due to the differing set of referred specimens to the species. Upchurch et al. (2004b) also recovered the specimens AMNH 460, NSMT-PV 20375, YPM 1840, and 1861 within *A. ajax*, whereas the present analysis finds the first three specimens as more basal, possibly new apatosaurine taxa, and YPM 1861 as *Apatosaurus louisae*. Wide cervical vertebrae, and low cervical neural spines are thus variable within Apatosaurinae. The dorsolateral process of the distal condyle of mt I, as well as the flange-like proximoventral process of php II-1might diagnose NSMT-PV 20375 instead.

Locality and horizon: Lakes' Quarry 10, Morrison, Gunnison County, Colorado (YPM 1860), and possibly Reed's Quarry 11, Como Bluff, Albany County, Wyoming (YPM 1981). Upper middle to upper-most Morrison Formation, Late Kimmeridgian to Early Tithonian. Apatosaurine intervals 2 and 3 (Bakker, 1998); Dinosaur zone 3B upper (Turner and Peterson, 1999); Zone 5 (Foster, 2003).

***Apatosaurus louisae* Holland, 1915a.**

Syn.? *Brontosaurus amplus* Marsh, 1881

Type specimen: CM 3018.

Referred specimens: CM 3378, CM 11162, YPM 1861, ?YPM 1981.

Revised diagnosis: *A. louisae* can be diagnosed by the following autapomorphies: presence of a dorsoventrally elongate coel on anterior and mid-cervical neural spines (165-1*, unique within Apatosauridae), posterior cervical prezygapophyses terminate well behind anterior ball (194-1, unique within Flagellicaudata), absence of a subvertical lamina in the postzygapophyseal centrodiapophyseal fossa of posterior cervical vertebrae, with the free edge facing posteriorly (199-0, unique within Apatosaurinae), presence of a rounded, subtriangular process on posterior cervical ribs, below the tuberculum (222-1, unambiguous), DV 2 is longer than DV 1 (239-1, unique within Diplodocoidea), pleurocoel on the first dorsal centra located posteriorly (240-1, unique within Apatosaurinae), parapophysis of DV 3 lies mid-way between centrum and prezygapophyses (246-1, unique among Diplodocidae), presence of an oblique ridge on the rib head of some dorsal ribs (283-1, unique within Apatosaurinae), slightly bifid anterior caudal neural spines (326-1*, unique within Apatosaurinae), and presence of a subtriangular projection on the ventral edge of the scapular blade (370-1*, unique among Apatosaurinae).

Comments: In their revised diagnosis, Upchurch et al. (2004b) also proposed the presence of pneumatopores in the dorsal ribs as autapomorphic for *A. louisae*. However, pneumatized dorsal ribs were already figured by Marsh (1896) from the holotype of *Brontosaurus excelsus*, YPM 1980, and are also present in YPM 1981 (ET, pers. obs., 2011). The anterior restriction of the sacral ribs as interpreted to be present in the holotype specimen by Upchurch et al. (2004b) is herein regarded a questionable autapomorphy, as original matrix was left filling the space between the sacral ribs, which might thus partly be obliterated. Two more autapomorphies put forward by Upchurch et al. (2004b) are actually also present in other apatosaurine specimens: the heart-shaped anterior caudal centra, and the medially beveled glenoid surface of the scapula.

Locality and horizon: Dinosaur National Monument, Jensen, Uintah County, Utah (CM 3018, 3378, and 11162), and Lakes' Quarry 10, Morrison, Gunnison County, Colorado (YPM 1861). Upper middle to upper-most Morrison Formation, Late Kimmeridgian to Early

7523 Tithonian. Apatosaurine intervals 2 and 3 (Bakker, 1998); Dinosaur zone 3B upper (Turner

7524 and Peterson, 1999); Zone 5 (Foster, 2003).

7525

7526 ***Brontosaurus* Marsh, 1879.**

7527 **Type and only species:** *Brontosaurus excelsus* Marsh, 1879.

7528 **Invalid proposed species:** *Brontosaurus amplus* Marsh, 1881 (= *Apatosaurus*).

7529 **Revised diagnosis:** *Brontosaurus* can be diagnosed by the following autapomorphies:

7530 orientation of the tuberculum of mid-dorsal ribs follows the straight direction of the rib shaft

7531 (285-1*, unique among Apatosaurinae), the posterior end of mid- and posterior caudal neural

7532 spine summits lies more or less straight above the postzygapophyses (343-1*, unique among

7533 Apatosaurinae); presence of a large nutrient foramen opening on midshaft anteriorly on the

7534 femur (434-1*, unique among Apatosaurinae); presence of a short transverse ridge on the

7535 anteromedial surface of the distal end of the tibia (443-1*, unique among Diplodocidae).

7536 **Comments:** The autapomorphies proposed for '*Apatosaurus*' *excelsus* by Upchurch et al.

7537 (2004b) are questionable. Cervical ribs that terminate in front of the posterior end of the

7538 centrum are widespread among Diplodocoidea, and are recovered as synapomorphic for that

7539 clade herein. The ventromedially projecting process on the anterior end of the cervical ribs is

7540 here reinterpreted as shortened anterior process of the cervical rib. The spine summits in

7541 anterior dorsal vertebrae are actually longer than wide (Ostrom and McIntosh, 1966: plates 17

7542 and 18), and the slight medial widening is due to the presence of a medial ridge on the

7543 metapophyses, which is also present on other apatosaurine specimens (e.g. CM 3018, UW

7544 15556; Gilmore, 1936).

7545 **Locality and horizon:** Reed's Quarry 10, Como Bluff, Albany County, Wyoming. Middle

7546 (Bakker, 1998) to upper (Foster, 1998) Morrison Formation, Late Kimmeridgian to ?Early

7547 Tithonian. Dinosaur zone 3B upper (Turner and Peterson, 1999), Zone 5 (Foster, 2003).

7548 ***Brontosaurus excelsus* Marsh, 1879.**

7549 **Type specimen:** YPM 1980.

7550 **Referred specimens:** -

7551 Diagnosis, locality, and horizon as genus.

7552

7553 ***Elosaurus* Peterson and Gilmore, 1902.**

7554 **Type and only species:** *Elosaurus parvus* Peterson and Gilmore, 1902.

Revised diagnosis: *Elosaurus* is diagnosed by the following autapomorphies: greatly reduced spinoprezygapophyseal laminae in posterior dorsal vertebrae (274-0, unique within Diplodocoidea), and absence of a shallow, but distinct rugose tubercle at the center of the concave proximal portion of the anterior surface of the humerus (386-0*, unique within Apatosaurinae).

Comments: In their revised diagnosis of '*Apatosaurus*' *parvus*, Upchurch et al. (2004b) further mentioned wider than high posterior dorsal centra, a right angle between acromial ridge and scapular blade, differences in length of the ulnar proximal branches, a constriction in the distal half of mc III, and subequal width and depth of the distal articular surface of mc V. Wider than high dorsal centra are also present in NSMT-PV 20375 (Upchurch et al., 2004b), an almost right angle between acromial ridge and distal blade can be seen in *Apatosaurus ajax* as well as in *Eobrontosaurus yahnahpin* (Filla and Redman, 1994), and different lengths of the ulnar branches also mark *Apatosaurus ajax* (Tab. S46). The characters from the manus could not have been positively identified in the specimens included, and were thus omitted from the revised diagnosis.

Locality and horizon: Sheep Creep Quarry E, Albany County, Wyoming, and possibly Riggs' Quarry 15, Dinosaur Hill, Mesa County, Colorado. Middle Morrison Formation, probably Late Kimmeridgian. Dinosaur zone 3B lower (Turner and Peterson, 1999), Zone 4 (Foster, 2003).

***Elosaurus parvus* Peterson and Gilmore, 1902.**

Type specimen: CM 566.

Referred specimens: UW 15556 (previously CM 563), FMNH P25112 (provisionally). Diagnosis, locality, and horizon as genus.

***Eobrontosaurus* Bakker, 1998.**

Type and only species: *Eobrontosaurus yahnahpin* (Filla and Redman, 1994). The species was initially described as belonging to *Apatosaurus*.

Revised diagnosis: *Eobrontosaurus* can be diagnosed by the following autapomorphies: presence of a longitudinal sulcus on the ventral surface of cervical vertebrae (133-1*, unique among Apatosaurinae), total height of anterior cervical vertebrae to centrum length ratio is greater than 1.2 (usually around 1.5) (154-2*, unique among Apatosaurinae), the medial surface of anterior dorsal, bifid neural spines is gently rounded transversely (245-0*, unique

within Apatosaurinae), mid- and posterior dorsal neural spines narrow dorsally to form a triangular shape in lateral view, with the base approximately twice the width of the dorsal tip (265-1*, unique among Apatosaurinae), absence of a thickened anterior rim of anterior caudal prespinal lamina (321-0*, unique among Apatosaurinae), a rounded anteroventral margin of the coracoid (372-0*, unique among Apatosaurinae), a ratio of the longest metacarpal to radius length of 0.40 or greater (399-1*, unique among Diplodocoidea), and the distal articular surface of the metatarsal I being perpendicular to the axis of the shaft (462-1*, unique among Flagellicaudata).

Comments: Bakker (1998) mentioned three more diagnosing features: long cervical ribs, distal scapular blade expanded, and coracoid suture at right angle with the long axis of the scapular blade. The presence of long cervical ribs could not have been confirmed based on the available pictures of the type specimen. The distally expanded scapular blade is actually shared with many apatosaur specimens (e.g. CM 3018, UW 15556, Gilmore, 1936). The unexpanded state is primarily based on the type specimen of *Apatosaurus ajax*, YPM 1860, but personal observations showed that the edges of the distal end are broken, and that the true expansion can therefore not be assessed in its entirety. The angle between the coracoid articulation and the distal blade, measured from photographs, is 74° (Tab. S41). Even if that should be wrong, the specimen described by Upchurch et al. (2004b), NSMT-PV 20375 shows an almost right angle, which would thus impede an interpretation as autapomorphy for *Eobrontosaurus*.

Locality and horizon: Bertha Quarry, Como Bluff, Albany County, Wyoming. Lower Morrison Formation, Kimmeridgian. Apatosaurine interval 1 (Bakker, 1998), Dinosaur zone 2 (Turner and Peterson, 1999), Zone 2 (Foster, 2003).

***Eobrontosaurus yahnahpin* (Filla and Redman, 1994).**

Type specimen: Tate-001.

Referred specimens: -

Diagnosis, locality, and horizon as genus.

⊟lodocinae Marsh, 1884.

***Diplodocus* Marsh, 1878.**

Syn. *Seismosaurus* Gillette, 1991

Type species: *Diplodocus carnegii* Hatcher, 1901 (suppressing the *D. longus* Marsh, 1878,

7619 see above).

7620 **Referred species:** *Diplodocus hallorum* (Gillette, 1991).

7621 **Invalid proposed species:** *Diplodocus longus* Marsh, 1878 (nomen dubium, previous type

7622 species, case to ICZN in preparation to propose *D. carnegii* as substitute), *D. lacustris* Marsh,

7623 1884 (nomen dubium), *D. hayi* Holland, 1924 (= *Galeamopus hayi*).

7624 **Revised diagnosis:** *Diplodocus* can be diagnosed by the following autapomorphies: base of

7625 posterior dorsal neural spines anteriorly inclined (280-1, unique within Diplodocinae),

7626 pneumatopores of anterior caudal centra persist until caudal 16 or more posteriorly (308-1,

7627 unambiguous), well-developed rugosity on dorsolateral margin of metatarsal II, near the distal

7628 end, extending to the center of the shaft (468-1, unique among Diplodocidae).

7629 **Comments:** Whitlock (2011a) proposes three cranial traits as autapomorphies of *Diplodocus*:

7630 a well-defined preantorbital fossa, the pterygoid that lies medial to the ectopterygoid, and the

7631 anteriorly inclined, procumbent teeth. As no skull can be definitely attributed to *Diplodocus*,

7632 these suggestions are questionable. Furthermore, distinct preantorbital fossae, and procumbent

7633 teeth are also present on other diplodocine taxa (e.g. *Galeamopus, Kaatedocus*), and the

7634 relative positions of the pterygoid and ectopterygoid are not established with enough certainty

7635 to use it as diagnostic character (see above). Upchurch et al. (2004a) also defines *Diplodocus*

7636 solely based on cranial traits, most of which are actually shared with other diplodocine species

7637 that were not described or recognized at the time (*Galeamopus, Kaatedocus*). Wilson (2002)

7638 proposed the anteriorly expanded femoral distal condyles as autapomorphic for *Diplodocus*,

7639 as shared characteristic with advanced titanosauriforms. However, although the distal

7640 condyles are accompanied anteriorly by two distinct vertical ridges, the articular surface does

7641 not extend onto them as in *Rapetosaurus krausei* FMNH PR 2209, for example (Curry

7642 Rogers, 2009).

7643 **Locality and horizon:** various sites in Colorado, New Mexico, Utah, and Wyoming. Middle

7644 Morrison Formation, probably Late Kimmeridgian. Apatosaurine interval 2 (Bakker, 1998),

7645 Dinosaur zones 3A to 3B upper (Turner and Peterson, 1999), Zones 3 to 5 (Foster, 2003).

7646

7647 *Diplodocus carnegii* **Hatcher, 1901.**

7648 **Type specimen:** CM 84.

7649 **Paratype:** CM 94.

7650 **Referred specimens:** -

7651 **Revised diagnosis:** *Diplodocus carnegii* is diagnosed by the following autapomorphies:
7652 spinopostzygapophyseal laminae (spol) of posterior dorsal neural arches divided near the
7653 postzygapophyses (277-1, unique among Flagellicaudata), and slender metatarsal II (mean
7654 proximal and distal transverse breadth/maximum length <0.53) (465-0*, unique among
7655 Diplodocoidea).
7656 **Comments:** Hatcher (1901) proposed two different characters to distinguish *D. carnegii* from
7657 *D. longus*: shorter cervical ribs, and more posteriorly directed caudal neural spines. However,
7658 comparisons were not based on the holotype of *D. longus*, but on two referred specimens
7659 (USNM 4712 and AMNH 223), which are now known not to belong to the species: the
7660 cervical vertebra Hatcher (1901) mentions (USNM 4712) actually has apatosaurine affinities
7661 (Hatcher, 1903), whereas the specimen AMNH 223, on which Hatcher (1901) based his
7662 comparisons, is herein interpreted to belong to *Diplodocus hallorum*. The short cervical ribs
7663 are widespread among Diplodocinae~~,~~ and ~~do~~ thus do not qualify as a species autapomorphy.
7664 Caudal neural spine orientation is one of the main features distinguishing *D. carnegii* from *D.*
7665 *hallorum*, but the vertical spines from the latter species are herein found to be the derived
7666 state, such that the more posteriorly inclined spines in *D. carnegii* cannot be used to diagnose
7667 the species.
7668 **Locality and horizon:** Sheep Creek Quarries D (CM 94) and D(3) (CM 84), Albany County,
7669 Wyoming. Middle Morrison Formation, Late Kimmeridgian. Dinosaur zone 3B lower (Turner
7670 and Peterson, 1999), Zone 4 (Foster, 2003).
7671
7672 ***Diplodocus hallorum* (Gillette, 1991).**
7673 Syn. *Seismosaurus hallorum*, *Seismosaurus halli*.
7674 **Type specimen:** NMMNH 3690.
7675 **Referred specimens:** AMNH 223, DMNS 1494, USNM 10865.
7676 **Revised diagnosis:** *Diplodocus hallorum* can be diagnosed by the following autapomorphies:
7677 dorsal end of the postspinal lamina of single dorsal neural spines concave transversely (234-1,
7678 unique among Diplodocoidea), mid-caudal neural arches are situated on the anterior half of
7679 the centrum (337-1, unique among Diplodocoidea), vertical mid-caudal neural spines (340-1,
7680 unambiguous), posterior end of mid- and posterior caudal neural spine summits lies more or
7681 less straight above the postzygapophyses (343-1, unique among Diplodocinae), presence of
7682 distinct fossae on the medial surfaces of the proximal branches of middle chevrons (357-1,

unique among Diplodocinae), a gracile femur (robustness index (sensu Wilson and Upchurch, 2003) <0.22) (427-0*, unique among Diplodocinae), and the groove on the lateral surface of pedal unguals extends straight horizontally (477-1*, unique among Diplodocinae).

Comments: Lucas et al. (2006) in their taxonomic reappraisal of *Seismosaurus hallorum* proposed two more characters that distinguish the type specimen of *D. hallorum* from other species of *Diplodocus*: a more robust pubis, and paddle-shaped distal blades of the chevrons. Whereas the first is difficult to quantify and is thus provisionally omitted from the present diagnosis, the paddle shape of the chevrons is partly included in the character coding the posterior expansion of the chevron blade (C355), which is not present in the other specimens referred to *D. hallorum*. The specific chevron shape of NMMNH 3690 is thus herein regarded as individual variation.

Locality and horizon: *Seismosaurus* Quarry, Sandoval County, New Mexico (NMMNH 3690), Dinosaur National Monument Quarry, Uintah County, Utah (DMNS 1494, USNM 10865), and AMNH 223 Quarry, Como Bluff, Albany County, Wyoming (AMNH 223). Middle Morrison Formation, Late Kimmeridgian. Apatosaurine interval 2 (Bakker, 1998), Dinosaur zones 3B lower to upper (Turner and Peterson, 1999), Zones 4 to 5 (Foster, 2003).

Barosaurus **Marsh, 1890.**

Type and only species: *Barosaurus lentus* Marsh, 1890.

Invalid proposed species: *Barosaurus affinis* Marsh, 1899 (nomen dubium), *Barosaurus gracilis* Russell et al., 1980 (nomen nudum).

Revised diagnosis: *Barosaurus* can be diagnosed by the following autapomorphies: pleurocoel not extending onto parapophysis in anterior cervical vertebrae (158-1*, unique among Diplodocidae), elongation index of posterior cervical vertebrae (without anterior condyle) greater than 2.6 (192-2*, unique among Diplodocoidea), an anterior projection on the prdl of posterior cervical, or anterior and mid-dorsal vertebrae, right lateral to the prezygapophysis (213-1, unique among Diplodocoidea), nine dorsal vertebrae (224-3*, unambiguous), transition from 'fan'-shaped to 'normal' caudal ribs occurs between Cd 6 and Cd 7 (300-3*, unique among Diplodocinae), pneumatopores of anterior caudal centra disappear by Cd 15 (308-0*, unique within Diplodocinae), depth of ventral hollow increasing from anterior to posterior caudal centra (the present trait could not have been assessed in the current analysis, but is provisionally included in the diagnosis of *Barosaurus* following

7715   Upchurch et al., 2004a).

7716   **Comments:** Whitlock (2011a) does not list any autapomorphies for *Barosaurus*. McIntosh

7717   (2005) states four more diagnosing features for the genus: bifurcation of cervical neural spines

7718   restricted to the posterior half of the neck, summits of caudal neural spines undivided, a

7719   proportionally shorter tail, and a less prominent ventral hollow in anterior and mid-caudal

7720   centra. However, all of these traits represent the basal diplodocid morphology, and are shared,

7721   e.g., with *Kaatedocus* or *Supersaurus* (Lovelace et al., 2007; Tschopp and Mateus, 2013b).

7722   Upchurch et al. (2004a) suggested an additional autapomorphy: the parapophysis of DV 2 is

7723   situated at the bottom of the centrum. Such a low position of the parapophysis is also present

7724   in DV 2 of *Galeamopus*   and can thus not be regarded diagnostic for *Barosaurus*.

7725   **Locality and horizon:** various sites in South Dakota, Utah, and Wyoming. Lower to middle

7726   Morrison Formation, Kimmeridgian. Apatosaurine intervals ?1 to 2 (Bakker, 1998), Dinosaur

7727   zones 2 to 3B upper (Turner and Peterson, 1999), Zones 2 to 5 (Foster, 2003).

7728

7729   ***Barosaurus lentus* Marsh, 1890.**

7730   **Type specimen:** YPM 429.

7731   **Referred specimens:** AMNH 6341, AMNH 7535, CM 11984.

7732   Diagnosis, locality, and horizon as genus.

7733

7734   *nieria* **Sternfeld, 1911.**

7735   **Type and only species:** *Tornieria africana* (Fraas, 1908). The species was originally assigned

7736   to *Gigantosaurus africanus* (Fraas, 1908).

7737   **Invalid proposed species:** *Tornieria robustus* (Fraas, 1908) (=*Janenschia robusta*).

7738   **Revised diagnosis:** *Tornieria* is diagnosed by the following autapomorphies: mid-caudal

7739   prezygapophyses terminate at or behind the anterior edge of the centrum (339-0*, unique

7740   among Diplodocinae), a straight posterior border of the sternal plate (377-1*, unique among

7741   Neosauropoda), and distal femoral condyles expand onto the anterior portion of the femoral

7742   shaft (439-1*, unambiguous).

7743   **Comments:** Whitlock (2011a) listed a single autapomorphy for the genus: the absence of a

7744   ventral hollow in anterior and mid-caudal centra. Contrary to Whitlock (2011a), a ventral

7745   hollow is present in the preserved caudal vertebrae of both specimens included herein

7746   (Remes, 2006). In his revision of *Tornieria*, Remes (2006) proposed additional

7747 autapomorphies: frontal forms the entire dorsal margin of the orbit, prefrontal with a short

7748 posterior process, elongate cervical vertebrae, relatively long anterior caudal vertebrae,

7749 pleurocoel located on the upper third of the caudal centra, caudal transverse processes situated

7750 high on the centrum, caudal neural spines single, and lacking lateral processes, the distal blade

7751 of the scapula is only slightly expanded, unequal lengths of the proximal ulnar processes,

7752 robust ischial shaft, and a low tibia to femur length ratio. The traits of the frontal and

7753 prefrontal were later shown to be present in *Kaatedocus* as well (Tschopp and Mateus,

7754 2013b). Elongate cervical vertebrae ~~were~~ developed several times within Diplodocinae (e.g.

7755 *Barosaurus*, *Supersaurus*; McIntosh, 2005; Lovelace et al., 2007). Centrum length increases

7756 from anterior-most towards middle caudal vertebrae in all diplodocines, making relative

7757 length a serially variable character. It was thus not included in the present analysis, and a

7758 detailed assessment of the relative position of the anterior caudal vertebrae in the *Tornieria*

7759 specimens would be needed before including relative centrum length as diagnosing trait for

7760 the genus. The position of the pleurocoel in the preserved anterior-most caudal vertebra of the

7761 holotype individual (SMNS 12141a) does not appear to be restricted to the upper third

7762 (Remes, 2006: fig. 4C). Pneumatic foramina are dorsally located in the referred caudal

7763 vertebrae from trench dd (MB.R.2956 to MB.R.2958; Remes, 2006), but as this trait appears

7764 different in the holotype, it should not be used in a diagnosis. The same accounts for the

7765 dorsal location of the transverse processes, which is most probably influenced by the position

7766 of the pleurocoel. Single caudal neural spines without lateral processes can only be observed

7767 in the referred caudal vertebrae, which were not included in the present analysis. However,

7768 these traits also occur in other diplodocine species, and are thus not reliable characters to

7769 distinguish *Tornieria*. A slight expansion of the scapular blade as well as robustness of the

7770 ischial shaft are difficult to quantify, but ratios do not appear to be significantly different from

7771 other diplodocine taxa. Unequally long ulnar proximal processes are shared with *Galeamopus*

7772 ███████ (Tab. S46), as is the low tibia to femur ratio (Tab. S54).

7773 **Locality and horizon:** localities A and k, Upper Saurian Beds, Tendaguru, District of Lindi,

7774 Tanzania. Tithonian.

7775

7776 *Tornieria africana* **(Fraas, 1908).**

7777 **Type specimen:** SMNS 12141a, 12145a, 12143, 12140, and 12142. The individual also

7778 contains the specimens SMNS 12145c, MB.R.2672, 2713, and 2728 (Remes, 2006).

7779 **Referred specimens:** MB.R.2386, 2572, 2586, 2669, 2673, 2726, 2730, 2733, 2913, and

7780 3816 (all belonging to a single individual; Heinrich, 1999; Remes, 2006).

7781 Diagnosis, locality, and horizon as genus.

7782

7783 *Supersaurus* **Jensen, 1985.**

7784 Syn. *Dystylosaurus* Jensen, 1985; *Ultrasauros* Olshevsky, 1991.

7785 **Type and only species:** *Supersaurus vivianae* Jensen, 1985.

7786 **Revised diagnosis:** *Supersaurus* can be diagnosed by the following autapomorphies:

7787 spinoprezygapophyseal laminae in single dorsal neural spines separate along their entire

7788 length (231-0, unique among Diplodocoidea), presence of an infradiapophyseal pneumatopore

7789 between the acdl and the pcdl of mid- and posterior dorsal neural arches (262-1*, unique

7790 among Diplodocinae), opisthocoelous posterior dorsal centra (270-2, unique among

7791 Diplodocoidea), 'heart'-shaped anterior-most caudal centra with an acute ventral ridge (296-1,

7792 unique among Diplodocinae), pneumatopores on anterior caudal centra restricted to foramina

7793 (307-0, unique among Diplodocinae), and an angle between the acromial ridge and the distal

7794 blade greater than 81° (362-2*, unique among Diplodocinae).

7795 **Comments:** Lovelace et al. (2007) listed several additional diagnosing traits for *Supersaurus*:

7796 elongate cervical vertebrae, an extreme narrowing of the ventral surface of cervical centra,

7797 well-developed parallel keels that mark the ventral surface of cervical centra, pneumatic

7798 foramina present on the ventral surface of cervical centra, lateral pneumatopores on cervical

7799 centra small, located within a shallow coel, anterior dorsal vertebrae with a ventral keel, tall

7800 posterior dorsal neural spines, relatively low posterior dorsal neural arch, pneumatized dorsal

7801 ribs, and a dorsally expanded scapular blade. Most of these traits are actually shared with

7802 other diplodocine species: the elongate cervical vertebrae (e.g. *Tornieria*), the well-developed

7803 parallel keels (herein called posteroventral flanges), the ventral pneumatic foramina (e.g. in

7804 *Dinheirosaurus*), the restricted and small lateral pneumatic foramina of cervical vertebrae

7805 (e.g. *Galeamopus* the ventral keel in anterior dorsal centra, the low dorsal neural

7806 arches, and the pneumatized dorsal ribs (e.g. *Dinheirosaurus*), the tall dorsal neural spines

7807 (typical for diplodocids in general), as well as the expanded scapular blade (e.g. *Galeamopus*).

7808 The extreme narrowing of the ventral surface of cervical centra is herein interpreted as a

7809 consequence of the centrum elongation, as a narrowing is generally seen relative to the

7810 centrum length.

7811 **Locality and horizon:** Dry Mesa Quarry, Montrose County, Colorado, and Jimbo Quarry,

7812 Converse County, Wyoming. Middle Morrison Formation, Late Kimmeridgian to ?Early

7813 Tithonian. Dinosaur zone 3B lower (Turner and Peterson, 1999), Zone 4 (Foster, 2003).

7814 *Supersaurus vivianae* Jensen, 1985.

7815 Syn. *Dystylosaurus edwini* Jensen, 1985; *Ultrasauros macintoshi* (Jensen, 1985).

7816 **Type specimen:** BYU 12962. The holotype Iindividual probably also ~~contains~~includes the

7817 specimens BYU 4503, 4839, 9024-25, 9044-45, 9085, 10612, 12424, 12555, 12639, 12819,

7818 12861, 12946, 13016, 13018, 13981, 16679, and 17462 (Lovelace et al., 2007).

7819 **Referred specimens:** WDC DMJ-021.

7820 Diagnosis, locality, and horizon as for the genus.

7821

7822 *Dinheirosaurus* Bonaparte and Mateus, 1999.

7823 **Type and only species:** *Dinheirosaurus lourinhanensis* Bonaparte and Mateus, 1999.

7824 **Revised diagnosis:** *Dinheirosaurus* can be diagnosed by the following autapomorphies:

7825 single posterior cervical and anterior dorsal neural spines (126-0*, unique among

7826 Flagellicaudata), the ventral keel is restricted to the posterior portion of the posterior cervical

7827 centrum (193-1*, unique within Flagellicaudata), three small fossae on the lateral face of the

7828 posterior cervical neural spine, posterior to the elongated coel (unambiguous; this trait was

7829 not included as character, as unambiguous autapomorphies of single OTUs do not bear any

7830 phylogenetic information), dorsal centrum length (excluding articular 'ball') remains

7831 approximately the same along the sequence (225-0*, unique among Diplodocinae), dorsal

7832 transverse processes are more than 30° inclined dorsally from the horizontal (230-1*, unique

7833 among Diplodocidae), and the ventral surface of anterior caudal centra is without irregularly

7834 placed foramina (305-0*, unique within Flagellicaudata).

7835 **Comments:** In their redescription of the species, Mannion et al. (2012) mention two

7836 additional autapomorphies: an accessory, subvertical lamina in the postzygapophyseal

7837 centrodiapophyseal fossa, and an accessory lamina linking the hyposphene to the posterior

7838 centrodiapophyseal lamina in mid- and posterior dorsal neural arches. A subvertical accessory

7839 lamina actually subdivides the pocdf in a variety of diplodocid and diplodocine taxa (e.g.

7840 *Galeamopus hayi*), whereas a lamina connecting hyposphene and pcdl is also present in

7841 posterior dorsal neural arches of *Supersaurus vivianae*.

7842 **Locality and horizon:** Praia de Porto Dinheiro, Lourinhã, Portugal. Amoreira-Porto Novo

7843   Member, Lourinhã Formation, Late Kimmeridgian.

7844   ***Dinheirosaurus lourinhanensis* Bonaparte and Mateus, 1999.**

7845   **Type specimen:** ML 414.

7846   **Referred specimens:** -None.

7847   Diagnosis, locality, and horizon as for the genus.

7848

7849   ***Kaatedocus* Tschopp and Mateus, 2012.**

7850   **Type and only species:** *Kaatedocus siberi* Tschopp and Mateus, 2012.

7851   **Revised diagnosis:** *Kaatedocus* can be diagnosed by the following autapomorphies:

7852   anteriorly restricted squamosals (55-0*, unique among Diplodocoidea), a rugosity on the

7853   anterodorsal corner of the lateral side of mid- and posterior cervical centra (178-1, unique

7854   among Diplodocidae), posterior cervical prezygapophyseal facets are posteriorly followed by

7855   a transverse sulcus (195-1*, unambiguous), posterior cervical epipophyses are dorsoventrally

7856   compressed (202-1, unique among Flagellicaudata), posterior cervical neural spines parallel to

7857   converging (211-1, unique among Diplodocidae), and the distance between the bifid posterior

7858   cervical neural spine summits is subequal to neural canal width (212-1, unique among

7859   Diplodocidae).

7860   **Comments:** The species and genus reference given above ('Tschopp and Mateus, 2012') does

7861   not refer to the publication listed in the references as Tschopp and Mateus (2012), but to

7862   Tschopp and Mateus (2013b). This is because the online version of the description of *K.*

7863   *siberi* was published in 2012, and thus the name is valid since that year. The printed version

7864   of the paper, however, was only published in 2013.

7865   Tschopp and Mateus (2013b) list several other autapomorphies as well: a U-shaped notch

7866   between the frontals, presence of a post-parietal foramen, a sharp, narrow sagittal nuchal

7867   crest, a straight anterior edge of the basal tubera, and the cervical pre-epipophysis that forms a

7868   distinct anterior spur. The notch is herein shown to be shared with *Galeamopus* █████████

7869   The presence of a post-parietal foramen is difficult to interpret in most diplodocid skulls, due

7870   to often fractured surfaces in this area of the skull. Moreover, it is present as well in another

7871   braincase from the Howe Quarry, SMA O25-8, which was tentatively referred to *Barosaurus*

7872   (Schmitt et al., 2013; this study). A relatively sharp sagittal nuchal crest also occursis present

7873   as well in the skull of *Galeamopus hayi* HMNS 175 (Holland, 1906). Straight to convex

7874   anterior margins of the basal tubera are shared with CM 3452 and *Galeamopus* █████████ The

development of the cervical pre-epiphysis is actually different in the holotype and the referred specimen AMNH 7530, where no distinct anterior spur is present. The presence or absence of a spur is thus better interpreted as individually variable within *Kaatedocus*, and thus not diagnostic for the present genus.

Locality and horizon: Howe Quarry, Shell, Bighorn County, Wyoming. Lower Morrison Formation, Kimmeridgian. Dinosaur zone 2 (Turner and Peterson, 1999), Zone 2 (Foster, 2003).

Kaatedocus siberi **Tschopp and Mateus, 2012.**

Type specimen: SMA 0004.

Referred specimens: AMNH 7530, SMA D16-3.

Diagnosis, locality, and horizon as genus.

Galeamopus **gen. nov.**

Type species: *Galeamopus hayi* (Holland, 1924). The type species was originally assigned to *Diplodocus hayi*.

Diagnosis: *Galeamopus* is diagnosed by the following autapomorphies: portion of the parietal contributing to the skull roof is practically inexistent (60-2, unique among Flagellicaudata), a foramen in the notch that separates the two basal tubera (90-1, unique among Diplodocinae), well-developed anteromedial processes on the atlantal neurapophyses, which are distinct from the posterior wing (146-1, unique among Diplodocoidea), the posterior wing of atlantal neurapophyses remains of subequal width along most of its length (148-1, unambiguous), and the axial prespinal lamina develops a transversely expanded, knob-like tuberosity at its anterior end (151-1, unambiguous).

Locality and horizon: ~~v~~Various sites in Wyoming. Lower to Middle Morrison Formation, Kimmeridgian. *Apatosaurus* interval 1 (Bakker, 1998), Dinosaur zone 2 to possibly 3 (Turner and Peterson, 1999), Zones 2 to possibly 3 or 4 (Foster, 2003).

Galeamopus hayi **(Holland, 1924).**

Type specimen: HMNS 175 (previously CM 662).

Referred specimens: -

Diagnosis: *Galeamopus hayi* is diagnosed by the following autapomorphies: dorsoventral height of the parietal occipital process is low, subequal to less than the diameter of the foramen magnum (63-0*, unique among Diplodocinae), basipterygoid processes widely

7907 diverging (> 60°; 92-0*, unique among Diplodocinae), an ulna to humerus length of more

7908 than 0.76 (387-2*, unique within Diplodocoidea), distal articular surface for the ulna on the

7909 radius is reduced and relatively smooth (392-0*, unique within Diplodocidae), and the distal

7910 condyle of the radius is beveled at least 15° to the long axis of the shaft (393-1*, unique

7911 within Diplodocinae).

7912 **Locality and horizon:** Quarry A, Red Fork of the Powder River, Johnson County, Wyoming.

7913 Lower Morrison Formation, Kimmeridgian. Apatosaurine interval 1 (Bakker, 1998).

7914 ███████ ██████ ██████

7915 ██████████

7916 ████████████

7917 ████████ █████ ██████████████████████

7918 ███████████████████████████████

7919 ████████████████████████████████

7920 █████████████████████████████████

7921 ███████████████████████████████

7922 ███████████████████████████████

7923 █████████████████████████████████

7924 █████████████████████████████████

7925 ███████████████

7926 █████████████████████████████████

7927 ██████████████████████████████████

7928 ████████████████████████████████

7929 ████████████████████████

7930

Conclusions

7932 The present paper increases knowledge about the morphology and the phylogenetic

7933 relationships of diplodocid sauropods. One new, partially complete specimen is described,

7934 including a nearly complete skull, and represents a new diplodocine species: *Galeamopus*

7935 ██████ In order to resolve its exact systematic position within Diplodocidae, a specimen-

7936 based phylogenetic analysis was performed, which included all holotypes that have been

7937 identified as belonging to a diplodocid sauropod at some point in history.

7938 By doing so, one of the main challenges was where to decide if specific or generic separation

7939 of the included specimens is warranted. Given that the only applicable species concept in
7940 paleontology is based on morphological differences, the sum of differences can be the only
7941 way how to approach this issue. Basing on the assumption that the rate of evolution was
7942 similar in the two temporally as well as spatially coexisting taxa Diplodocinae and
7943 Apatosaurinae, accumulation of individually varying traits is assumed to lead to speciation
7944 with the same speed in both taxa. Thus, a numerical approach was introduced, including a
7945 three-step approach to account for individual variation: first, phylogenetic software does not
7946 find all potential autapomorphies for single specimens or synapomorphies for recovered
7947 clades, because the sister clades (specimens or taxa in the case of a specimen-based analysis)
7948 often do not preserve the same bones, and are thus not comparable. Second, the quality and
7949 thus validity of found apomorphies was assessed based on the number of taxa they were
7950 shared with, as well as the relative phylogenetic positions of these taxa with the specimen or
7951 clade in question. Finally, the number of valid apomorphies was summed between sister
7952 clades (sometimes specimens). Based on the relationship between *Supersaurus* and
7953 *Dinheirosaurus*, which have been continuously found as sister taxa (Mannion et al., 2012;
7954 Tschopp and Mateus, 2013b; this study), and where generic separation is further supported by
7955 the geographical separation (North America versus Portugal), a sum of ten steps was
7956 considered enough for generic separation. By comparing the sum of differences between
7957 generally accepted species of the same genus with the sum of differences between specimens
7958 usually identified as belonging to the same species, a sum of five steps was established as
7959 being enough for specific separation. Given the three-step approach to reduce influence of
7960 individual variation, the true sum of differences between specimens or clades would even be
7961 higher in most cases. By applying these rules to all sister group arrangements found in the
7962 tree, validity of the included taxa was assessed in a more objective way.
7963 The numerical approach established in the present analysis allowed a reassessment of the
7964 validity of the numerous taxonomic names proposed within Diplodocidae. Thereby, it was
7965 found that apatosaurine diversity was particularly underestimated in the past. Two genera
7966 previously synonymized with *Apatosaurus* ~~resulted~~were recoered as valid based on the sum
7967 of differences with their recovered sister taxa: *Brontosaurus* and *Elosaurus,* which together
7968 form the sister clade to *Apatosaurus* in the present analysis. *Eobrontosaurus* was found to be
7969 valid as well, and two more clusters of specimens were recovered at the base of
7970 Apatosaurinae, which might even represent two additional apatosaurine genera. However,

more detailed work has to be done on the specimens forming these clades before being able to confirm such an extraordinary increase in the number of apatosaurine genera. *Apatosaurus* was found to be the only apatosaurine genus with more than one species: *A. ajax*, and *A. louisae*. This results in four to six genera and five to seven species belonging to Apatosaurinae. In a less inclusive and less detailed specimen-based analysis of *Apatosaurus*, Upchurch et al. (2004b) found five species as probably valid, but did not include *Eobrontosaurus yahnahpin*. The species count thus remained more or less the same in the two analyses.

The intrarelationships of Diplodocinae were already well established before (Whitlock, 2011a; Mannion et al., 2012; Tschopp and Mateus, 2013b). However, by including single specimens, it became possible to furthermore assess the validity of the various species proposed in *Diplodocus*. Thereby, the type species *D. longus* was considered a nomen dubium, given the undiagnostic, fragmentary holotype specimen. This would lead to an abolishment of the famous and popular generic name *Diplodocus*. ~~As~~Because this was not considered reasonable, a case is being prepared for submission to ICZN proposing *D. carnegii* as the new type species, and suppressing *D. longus*. Furthermore, the holotype specimen of '*Diplodocus*' *hayi*, often mentioned to probably not belong to *Diplodocus* (Holland, 1924; McIntosh, 1990a; Curtice, 1996; Foster, 2003), was found to form its own genus (herein named *Galeamopus*), together with the newly described specimen SMA 0011, and the diplodocine skull AMNH 969 – ~~also~~ the latter also having previously been identified as *Diplodocus* (Holland, 1906, 1924; McIntosh and Berman, 1978). Interestingly, no diplodocine specimen preserving articulated skulls and postcranial elements was herein found to group with *Diplodocus*: AMNH 969 and '*Diplodocus*' **hayi** are referred to *Galeamopus*, and CM 3452, on which Holland (1924), McIntosh and Berman (1975), and Berman and McIntosh (1978) based their identification of the skull-only specimens as *Diplodocus*, is recovered as more closely related to *Barosaurus* and *Kaatedocus*, and provisionally referred to *Barosaurus*. Although essentially complete and well-preserved, skulls such as~~like~~ CM 11161~~,~~ or USNM 2672 can thus not be definitely identified as *Diplodocus*. However, their recovered intermediate position between *Galeamopus* and *Kaatedocus* + *Barosaurus* indicates that a referral to *Diplodocus* might be justifiable, even though direct evidence ~~for it~~ is lacking. In any case, given the completeness and articulation of the two *Galeamopus* specimens HMNS 175 and SMA 0011, as well as the presence of at least an additional, referred skull, the

8003 morphology of *Galeamopus* can be considered better preserved than *Diplodocus*, where

8004 information on skull, forelimb, or distal tail morphology is not available from type specimens.

8005 In total, nine different species in seven genera are recognized within Diplodocinae. Together

8006 with the probable non-apatosaurine, non-diplodocine diplodocid *Amphicoelias altus*, this

8007 ~~amounts to a total of~~totals 15 to 17 valid diplodocid species, 13 to 15 of which are from the

8008 Morrison Formation of the Western United States.

Acknowledgment

References

Antunes, M. T., and O. Mateus. 2003. Dinosaurs of Portugal. Comptes Rendus Palevol 2:77–95.

Apesteguía, S. 2005. Evolution of the titanosaur metacarpus; pp. 321–346 in V. Tidwell and K. Carpenter (eds.), Thunder-Lizards: The Sauropodomorph Dinosaurs. Indiana University Press, Bloomington.

Arbour, V. M., and P. J. Currie. 2012. Analyzing taphonomic deformation of ankylosaur skulls using retrodeformation and Finite Element Analysis. PLoS ONE 7:e39323.

Ayer, J. 2000. The Howe Ranch Dinosaurs. Sauriermuseum Aathal, Aathal, Switzerland, 96

pp.

Bakker, R. T. 1998. Dinosaur mid-life crisis; the Jurassic-Cretaceous transition in Wyoming and Colorado. Bulletin of the New Mexico Museum of Natural History and Science 14:67–77.

Balanoff, A. M., G. S. Bever, and T. Ikejiri. 2010. The braincase of *Apatosaurus* (Dinosauria: Sauropoda) based on Computed Tomography of a new specimen with comments on variation and evolution in sauropod neuroanatomy. American Museum Novitates 3677:1–32.

Barco, J. 2009. Sistemática e implicaciones filogenéticas y paleobiogeográficas del saurópodo *Galvesaurus herreroi* (Formación Villar del Arzobispo, Galve, España). 405 pp.

Barrett, P. M., and P. Upchurch. 1994. Feeding mechanisms of *Diplodocus*. Gaia 10:195–203.

Barrett, P. M., G. W. Storrs, M. T. Young, and L. M. Witmer. 2011. A new skull of *Apatosaurus* and its taxonomic and palaeobiological implications. 1606.

Bedell, M. W. J., and D. L. Trexler. 2005. First articulated manus of *Diplodocus carnegii*; pp. 302–320 in V. Tidwell and K. Carpenter (eds.), Thunder-Lizards: The Sauropodomorph Dinosaurs. Indiana University Press, Bloomington.

Berman, D. S., and J. S. McIntosh. 1978. Skull and relationships of the Upper Jurassic sauropod *Apatosaurus* (Reptilia, Saurischia). Bulletin of the Carnegie Museum of Natural History 8:1–35.

Bird, R. T. 1985. Bones for Barnum Brown: Adventures of a Dinosaur Hunter. Texas Christian University Press, Fort Worth, 225 pp.

Birkemeier, T. 2011. Neurocentral suture closure in *Allosaurus* (Saurischia: Theropoda): sequence and timing. Journal of Vertebrate Paleontology, Program and Abstracts 2011:72A.

Bonaparte, J. F. 1986. The early radiation and phylogenetic relationships of the Jurassic sauropod dinosaurs, based on vertebral anatomy; pp. 247–258 in K. Padian (ed.), The Beginning of the Age of Dinosaurs. Cambridge University Press, Cambridge.

Bonaparte, J. F., and O. Mateus. 1999. A new diplodocid, *Dinheirosaurus lourinhanensis* gen. et sp. nov., from the Late Jurassic beds of Portugal. Revista Del Museo Argentino de Ciencias Naturales 5:13–29.

Bonaparte, J. F., B. J. González Riga, and S. Apesteguía. 2006. *Ligabuesaurus leanzai* gen. et sp. nov. (Dinosauria, Sauropoda), a new titanosaur from the Lohan Cura Formation

8098   (Aptian, Lower Cretaceous) of Neuquén, Patagonia, Argentina. Cretaceous Research

8099   27:364–376.

8100 Bonaparte, J. F., W.-D. Heinrich, and R. Wild. 2000. Review of *Janenschia* Wild, with the

8101   description of a new sauropod from the Tendaguru beds of Tanzania and a discussion on

8102   the systematic value of procoelous caudal vertebrae in the Sauropoda.

8103   Palaeontographica Abteilung A 256:25–76.

8104 Bonnan, M. F. 2000. The presence of a calcaneum in a diplodocid sauropod. Journal of

8105   Vertebrate Paleontology 20:317–323.

8106 Bonnan, M. F. 2001. The evolution and functional morphology of sauropod dinosaur

8107   locomotion. Ph.D. dissertation, Northern Illinois University., Dekalb, Illinois, 759 pp.

8108 Bonnan, M. F. 2003. The evolution of manus shape in sauropod dinosaurs: implications for

8109   functional morphology, forelimb orientation, and phylogeny. Journal of Vertebrate

8110   Paleontology 23:595–613.

8111 Bonnan, M. F. 2005. Pes anatomy in sauropod dinosaurs: Implications for functional

8112   morphology, evolution, and phylogeny; pp. 346–380 in V. Tidwell and K. Carpenter

8113   (eds.), Thunder-lizards: the Sauropodomorph dinosaurs. Indiana University Press,

8114   Bloomington.

8115 Bonnan, M. F. 2007. Linear and geometric morphometric analysis of long bone scaling

8116   patterns in Jurassic neosauropod dinosaurs: their functional and paleobiological

8117   implications. The Anatomical Record: Advances in Integrative Anatomy and

8118   Evolutionary Biology 290:1089–1111.

8119 Bonnan, M. F., and M. J. Wedel. 2004. First occurrence of *Brachiosaurus* (Dinosauria:

8120   Sauropoda) from the Upper Jurassic Morrison Formation of Oklahoma. PaleoBios

8121   24:13–21.

8122 Brinkmann, W., and H.-J. Siber. 1992. Dinosaurier in Aathal. Sauriermuseum Aathal, Aathal,

8123   37 pp.

8124 Brochu, C. A. 1996. Closure of neurocentral sutures during crocodilian ontogeny:

8125   Implications for maturity assessment in fossil archosaurs. Journal of Vertebrate

8126   Paleontology 16:49–62.

8127 Brown, B. 1935. Sinclair dinosaur expedition, 1934. Natural History 36:2–15.

8128 Calvo, J. O. 1994. Jaw mechanics in sauropod dinosaurs. Gaia 10:183–193.

8129 Calvo, J. O., and L. Salgado. 1995. *Rebbachisaurus tessonei* sp. nov. A new sauropod from

8130   the Albian-Cenomanian of Argentina; new evidence on the origin of the Diplodocidae.

8131   Gaia 11:13–33.

8132   Canudo, J. I., R. Royo-Torres, and G. Cuenca-Bescós. 2008. A new sauropod: *Tastavinsaurus*

8133   *sanzi* gen. et sp. nov. from the Early Cretaceous (Aptian) of Spain. Journal of Vertebrate

8134   Paleontology 28:712–731.

8135   Carballido, J. L., and P. M. Sander. 2013. Postcranial axial skeleton of *Europasaurus holgeri*

8136   (Dinosauria, Sauropoda) from the Upper Jurassic of Germany: implications for

8137   sauropod ontogeny and phylogenetic relationships of basal Macronaria. Journal of

8138   Systematic Palaeontology. 1–53.

8139   Carballido, J. L., J. S. Marpmann, D. Schwarz-Wings, and B. Pabst. 2012a. New information

8140   on a juvenile sauropod specimen from the Morrison Formation and the reassessment of

8141   its systematic position. Palaeontology 55:567–582.

8142   Carballido, J. L., L. Salgado, D. Pol, J. I. Canudo, and A. Garrido. 2012b. A new basal

8143   rebbachisaurid (Sauropoda, Diplodocoidea) from the Early Cretaceous of the Neuquén

8144   Basin; evolution and biogeography of the group. Historical Biology 24:631–654.

8145   Carballido, J. L., O. W. M. Rauhut, D. Pol, and L. Salgado. 2011. Osteology and phylogenetic

8146   relationships of *Tehuelchesaurus benitezii* (Dinosauria, Sauropoda) from the Upper

8147   Jurassic of Patagonia. Zoological Journal of the Linnean Society 163:605–662.

8148   Carpenter, K. 2010. Species concept in North American stegosaurs. Swiss Journal of

8149   Geosciences 103:155–162.

8150   Carpenter, K., and J. McIntosh. 1994. Upper Jurassic sauropod babies from the Morrison

8151   Formation. Dinosaur Eggs and Babies 265–278.

8152   Carpenter, K., and V. Tidwell. 1998. Preliminary description of a *Brachiosaurus* skull from

8153   Felch quarry 1, Garden Park, Colorado. Modern Geology 23:69–84.

8154   Casanovas, M. L., J. V. Santafé, and J. L. Sanz. 2001. *Losillasaurus giganteus* , un nuevo

8155   saurópodo del tránsito Jurásico-Cretácico de la cuenca de" Los Serranos"(Valencia,

8156   España). Paleontologia i Evolució 99–122.

8157   Charig, A. J. 1980. A diplodocid sauropod from the Lower Cretaceous of England; pp. 231–

8158   244 in L. L. Jacobs (ed.), Aspects of Vertebrate History. Essays in Honor of Edwin

8159   Harris Colbert. Museum of Northern Arizona Press, Flagstaff.

8160   Chatterjee, S., and Z. Zheng. 2002. Cranial anatomy of *Shunosaurus*, a basal sauropod

8161   dinosaur from the Middle Jurassic of China. Zoological Journal of the Linnean Society

136:145–169.

Chatterjee, S., and Z. Zheng. 2005. Neuroanatomy and dentition of *Camarasaurus lentus*; pp. 199–211 in V. Tidwell and K. Carpenter (eds.), Thunder-lizards. The sauropodomorph dinosaurs. Indiana University Press, Bloomington.

Christiansen, N. A., and E. Tschopp. 2010. Exceptional stegosaur integument impressions from the Upper Jurassic Morrison Formation of Wyoming. Swiss Journal of Geosciences 103:163–171.

Chure, D. J., R. Litwin, S. T. Hasiotis, E. Evanoff, and K. Carpenter. 2006. The fauna and flora of the Morrison Formation: 2006. Paleontology and Geology of the Upper Jurassic Morrison Formation. New Mexico Museum of Natural History and Science Bulletin 36:233–249.

Chure, D., B. Britt, J. Whitlock, and J. Wilson. 2010. First complete sauropod dinosaur skull from the Cretaceous of the Americas and the evolution of sauropod dentition. Naturwissenschaften 97:379–391.

Claessens, L. P. A. M. 2004. Dinosaur gastralia; origin, morphology, and function. Journal of Vertebrate Paleontology 24:89–106.

Cooper, M. R. 1984. A reassessment of *Vulcanodon karibaensis* Raath (Dinosauria: Saurischia) and the origin of the Sauropoda. Palaeontologia Africana 25:203–231.

Cope, E. D. 1877a. On *Amphicoelias*, a genus of saurians from the Dakota Epoch of Colorado. Paleontology Bulletin 27:1–5.

Cope, E. D. 1877b. On a dinosaurian from the Trias of Utah. Proceedings of the American Philosophical Society 16:579–584.

Cope, E. D. 1878. A new species of *Amphicoelias*. American Naturalist 12:563–564.

Curry, K. A. 1999. Ontogenetic histology of *Apatosaurus* (Dinosauria: Sauropoda): new insights on growth rates and longevity. Journal of Vertebrate Paleontology 19:654–665.

Curry Rogers, K. A. 2005. Titanosauria: a phylogenetic overview; pp. 51–103 in K. A. Curry Rogers and J. A. Wilson (eds.), The Sauropods: Evolution and Paleobiology. University of California Press, Berkeley, CA.

Curry Rogers, K. A. 2009. The postcranial osteology of *Rapetosaurus krausei* (Sauropoda: Titanosauria) from the Late Cretaceous of Madagascar. Journal of Vertebrate Paleontology 29:1046–1086.

Curry Rogers, K. A., and C. A. Forster. 2001. The last of the dinosaur titans: a new sauropod

from Madagascar. Nature 412:530–534.

Curry Rogers, K. A., and C. A. Forster. 2004. The skull of *Rapetosaurus krausei* (Sauropoda: Titanosauria) from the Late Cretaceous of Madagascar. Journal of Vertebrate Paleontology 24:121–144.

Curtice, B. 1996. Codex of diplodocid caudal vertebrae from the Dry Mesa dinosaur quarry. Master Thesis, Brigham Young University. Department of Geology., 156 pp.

Curtice, B. D., and K. L. Stadtman. 2001. The demise of *Dystylosaurus edwini* and a revision of *Supersaurus vivianae*. Mesa Southwest Museum Bulletin 8:33–39.

Curtice, B. D., K. L. Stadtman, and L. J. Curtice. 1996. A reassessment of *Ultrasauros macintoshi* (Jensen, 1985). Museum of Northern Arizona Bulletin 60:87–95.

D'Emic, M. D. 2012. The early evolution of titanosauriform sauropod dinosaurs. Zoological Journal of the Linnean Society 166:624–671.

D'Emic, M. D., P. D. Mannion, P. Upchurch, R. B. J. Benson, Q. Pang, and C. Zhengwu. 2013. Osteology of *Huabeisaurus allocotus* (Sauropoda: Titanosauriformes) from the Upper Cretaceous of China. PLoS ONE 8:e69375.

Dantas, P., J. Sanz, C. Marques da Silva, F. Ortega, V. Santos, and M. Cachão. 1998. *Lourinhasaurus* n. gen. novo dinossáurio saurópode do Jurássico superior (Kimeridgiano superior-Titoniano inferior) de Portugal. Actas Do V Congresso Nacional de Geologia.-Com. Inst. Geol. Mineiro 84:91–94.

Filla, J., and P. D. Redman. 1994. *Apatosaurus yahnahpin*: a preliminary description of a new species of diplodocid dinosaur from the Late Jurassic Morrison Formation of Southern Wyoming, the first sauropod dinosaur found with a complete set of "belly ribs."159–178.

Foster, J. R. 1998. Aspects of vertebrate paleoecology, taphonomy, and biostratigraphy of the Morrison Formation (Upper Jurassic), Rocky Mountain region, western United States. University of Colorado, 466 pp.

Foster, J. R. 2003. Paleoecological analysis of the vertebrate fauna of the Morrison Formation (Upper Jurassic), Rocky Mountain Region, U.S.A. New Mexico Museum of Natural History and Science Bulletin 23:2–100.

Fraas, E. 1908. Ostafrikanische Dinosaurier. Palaeontographica 15:105–144.

Gabunia, L. K., G. Mchedlidze, V. M. Chkhikvadze, and S. G. Lucas. 1998. Jurassic sauropod dinosaur from the Republic of Georgia. Journal of Vertebrate Paleontology 18:233–236.

8226 Galiano, H., and R. Albersdörfer. 2010. *Amphicoelias* "Brontodiplodocus", a New Sauropod,
8227   from the Morrison Formation, Big Horn Basin, Wyoming, with Taxonomic
8228   Reevaluation of *Diplodocus*, *Apatosaurus*, *Barosaurus* and Other Genera. Dinosauria
8229   International, LLC, 50 pp.

8230 Gallina, P. A. 2011. Notes on the axial skeleton of the titanosaur *Bonitasaura salgadoi*
8231   (Dinosauria-Sauropoda). Anais Da Academia Brasileira de Ciências 83:235–246.

8232 Gallina, P. A. 2012. Histología ósea del titanosaurio *Bonitasaura salgadoi*(Dinosauria:
8233   Sauropoda) del Cretácico Superior de Patagonia. Ameghiniana 49:289–302.

8234 Gallina, P. A., and S. Apesteguía. 2005. *Cathartesaura anaerobica* gen. et sp. nov., a new
8235   rebbachisaurid (Dinosauria, Sauropoda) from the Huincul Formation (Upper
8236   Cretaceous), Río Negro, Argentina. Revista Museo Argentino Ciencias Naturales Nueva
8237   Serie 7:153–166.

8238 Gauthier, J. 1986. Saurischian monophyly and the origin of birds. Memoirs of the California
8239   Academy of Sciences 8:55.

8240 Gillette, D. D. 1991. *Seismosaurus halli*, gen. et sp. nov., a new sauropod dinosaur from the
8241   Morrison Formation (Upper Jurassic/Lower Cretaceous) of New Mexico, USA. Journal
8242   of Vertebrate Paleontology 11:417–433.

8243 Gillette, D. D. 1994. *Seismosaurus*: The Earth Shaker. Columbia University Press, New York,
8244   205 pp.

8245 Gillette, D. D. 1996a. Origin and early evolution of the sauropod dinosaurs of North America:
8246   the type locality and stratigraphic position of *Dystrophaeus viaemalae* Cope 1877. Utah
8247   Geological Association Guidebook 25:313–324.

8248 Gillette, D. D. 1996b. Stratigraphic position of the sauropod *Dystrophaeus viaemalae* Cope
8249   1877 and its evolutionary implications. Museum of Northern Arizona, Bulletin 60:59–
8250   68.

8251 Gilmore, C. W. 1925. A nearly complete articulated skeleton of *Camarasaurus*, a saurischian
8252   dinosaur from the Dinosaur National Monument, Utah. Memoirs of the Carnegie
8253   Museum 10:347–384.

8254 Gilmore, C. W. 1932. On a newly mounted skeleton of *Diplodocus* in the United States
8255   National Museum. Proceedings of the United States National Museum 81:1–21.

8256 Gilmore, C. W. 1936. Osteology of *Apatosaurus*: with special reference to specimens in the
8257   Carnegie Museum. Memoirs of the Carnegie Museum 11:175–300.

8258   Goloboff, P. A. 1993. Estimating character weights during tree search. Cladistics 9:83–91.

8259   Goloboff, P. A., J. S. Farris, and K. C. Nixon. 2008. TNT, a free program for phylogenetic
8260   analysis. Cladistics 24:774–786.

8261   Goloboff, P. A., J. S. Farris, M. Källersjö, B. Oxelman, M. J. Ramírez, and C. A. Szumik.
8262   2003. Improvements to resampling measures of group support. Cladistics 19:324–332.

8263   González Riga, B. J. 2002. Estratigrafía y Dinosaurios del Cretácico Tardío en el extremo sur
8264   de la provincia de Mendoza, Argentina. Ph.D. dissertation, National University of
8265   Córdoba, Argentina, 280 pp.

8266   González Riga, B. J., E. Previtera, and C. A. Pirrone. 2009. *Malarguesaurus florenciae* gen. et
8267   sp. nov., a new titanosauriform (Dinosauria, Sauropoda) from the Upper Cretaceous of
8268   Mendoza, Argentina. Cretaceous Research 30:135–148.

8269   Haas, G. 1963. A proposed reconstruction of the jaw musculature of *Diplodocus*. Annals of
8270   Carnegie Museum 36:139–157.

8271   Harris, J. D. 2006a. Cranial osteology of *Suuwassea emilieae* (Sauropoda: Diplodocoidea:
8272   Flagellicaudata) from the Upper Jurassic Morrison Formation of Montana, USA.
8273   Journal of Vertebrate Paleontology 26:88–102.

8274   Harris, J. D. 2006b. The axial skeleton of the dinosaur *Suuwassea emilieae* (Sauropoda:
8275   Flagellicaudata) from the Upper Jurassic Morrison Formation of Montana, USA.
8276   Palaeontology 49:1091–1121.

8277   Harris, J. D. 2006c. The significance of *Suuwassea emilieae* (Dinosauria: Sauropoda) for
8278   flagellicaudatan intrarelationships and evolution. Journal of Systematic Palaeontology
8279   4:185–198.

8280   Harris, J. D. 2007. The appendicular skeleton of *Suuwassea emilieae* (Sauropoda:
8281   Flagellicaudata) from the Upper Jurassic Morrison Formation of Montana (USA).
8282   Geobios 40:501–522.

8283   Harris, J. D., and P. Dodson. 2004. A new diplodocoid sauropod dinosaur from the Upper
8284   Jurassic Morrison Formation of Montana, USA. Acta Palaeontologica Polonica 49:197–
8285   210.

8286   Hatcher, J. B. 1901. *Diplodocus* (Marsh): its osteology, taxonomy, and probable habits, with a
8287   restoration of the skeleton. Memoirs of the Carnegie Museum 1:1–63.

8288   Hatcher, J. B. 1902. Structure of the forelimb and manus of *Brontosaurus*. Annals of the
8289   Carnegie Museum 1:356–376.

Hatcher, J. B. 1903. Osteology of *Haplocanthosaurus*, with description of a new species and remarks on the probable habits of the Sauropoda and the age and origin of the *Atlantosaurus* beds: Additional remarks on *Diplodocus*. Memoirs of the Carnegie Museum 2:1–72.

He, X., K. Li, and K. Cai. 1988. The Middle Jurassic Dinosaur Fauna from Dashanpu, Zigong, Sichuan. Vol. IV. Sauropod Dinosaurs (2) *Omeisaurus tianfuensis*. Sichuan Publishing House of Science and Technology, Chengdu, China, 143 pp.

He, X., K. Li, K. Cai, and Y. Gao. 1984. *Omeisaurus tianfuensis*—a new species of *Omeisaurus* from Dashanpu, Zigong, Sichuan. Journal of Chengdu College Geology, Supplement 2:13–32.

He, X., S. Yang, K. Cai, K. Li, and Z. Liu. 1996. A new species of sauropod, *Mamenchisaurus anyuensis* sp. nov. Proceedings of the 30th International Geological Congress 12:83–86.

Heathcote, J., and P. Upchurch. 2003. The relationships of *Cetiosauriscus stewarti* (Dinosauria; Sauropoda): implications for sauropod phylogeny. Journal of Vertebrate Paleontology 23:60A.

Hedrick, B., A. R. Tumarkin-Deratzian, and P. Dodson. 2012. Bone microstructure and relative age of the holotype specimen of the diplodocoid sauropod dinosaur *Suuwassea emilieae*. Acta Palaeontologica Polonica.

Heinrich, W.-D. 1999. The taphonomy of dinosaurs from the Upper Jurassic of Tendaguru (Tanzania) based on field sketches of the German Tendaguru Expedition (1909-1913). Fossil Record 2:25–61.

Herne, M. C., and S. G. Lucas. 2006. *Seismosaurus hallorum*: osteological reconstruction from the holotype. Bulletin of the New Mexico Museum of Natural History and Science 36:139–148.

Hohn, B. 2011. Walking with the shoulder of giants: biomechanical conditions in the tetrapod shoulder girdle as a basis for sauropod shoulder reconstruction; pp. 182–196 in N. Klein, K. Remes, C. T. Gee, and P. M. Sander (eds.), Biology of the Sauropod Dinosaurs: Understanding the Life of Giants., Life of the Past Indiana University Press, Bloomington.

Hohn-Schulte, B. 2010. Form and function of the shoulder girdle in sauropod dinosaurs: a biomechanical investigation with the aid of finite elements. Ruhr-Universität Bochum,

Universitätsbibliothek, Bochum, 233 pp.

Holland, W. J. 1906. The osteology of *Diplodocus* Marsh. Memoirs of the Carnegie Museum 2:225–264.

Holland, W. J. 1915a. A new species of *Apatosaurus*. Annals of the Carnegie Museum 10:143–145.

Holland, W. J. 1915b. Heads and tails: a few notes relating to the structure of the sauropod dinosaurs. Annals of the Carnegie Museum 9:272–278.

Holland, W. J. 1924. The skull of *Diplodocus*. Memoirs of the Carnegie Museum 9:378–403.

Holliday, C. M., and L. M. Witmer. 2008. Cranial kinesis in dinosaurs: intracranial joints, protractor muscles, and their significance for cranial evolution and function in diapsids. Journal of Vertebrate Paleontology 28:1073–1088.

Huene, F. 1904. *Dystrophaeus viaemalae* Cope in neuer Beleuchtung. Separat-Abdruck Aus Dee Neuen Jahrbuch Fur Mineralogie, Geologie Und Palaeontologie, Stuttgart, Germany.

Huene, F. 1927. Sichtung der Grundlagen der jetzigen Kenntnis der Sauropoden. Eclogae Geologicae Helvetiae 20:444–470.

Huene, F. 1929. Los Saurisquios y Ornithisquios de Cretaceo Argentine. Annales de Museo de La Plata 3 (Series 2):1–196.

Ikejiri, T. 2004. Anatomy of *Camarasaurus lentus* (Dinosauria: Sauropoda) from the Morrison Formation (Late Jurassic), Thermopolis, central Wyoming, with determination and interpretation of ontogenetic, sexual dimorphic, and individual variation in the genus. Master Thesis, Fort Hays State University, Kansas, UMI pp.

Ikejiri, T. 2012. Histology-based morphology of the neurocentral synchondrosis in *Alligator mississippiensis* (Archosauria, Crocodylia). Anatomical Record 295:18–31.

Ikejiri, T., V. Tidwell, and D. L. Trexler. 2005. New adult specimens of *Camarasaurus lentus* highlight ontogenetic variation within the species; pp. 154–179 in Thunder-lizards: the Sauropodomorph dinosaurs. Indiana University Press, Bloomington.

Irmis, R. B. 2007. Axial skeleton ontogeny in the Parasuchia (Archosauria: Pseudosuchia) and its implications for ontogenetic determination in archosaurs. Journal of Vertebrate Paleontology 27:350–361.

Jain, S. L., and S. Bandyopadhyay. 1997. New titanosaurid (Dinosauria: Sauropoda) from the Late Cretaceous of Central India. Journal of Vertebrate Paleontology 17:114–136.

Janensch, W. 1922. Das Handskelett von *Gigantosaurus robustus* und *Brachiosaurus brancai* aus den Tendaguru-Schichten Deutsch-Ostafrikas. Centralblatt Für Mineralogie, Geologie Und Paläontologie 15:464–480.

Janensch, W. 1929a. Die Wirbelsäule der Gattung *Dicraeosaurus*. Palaeontographica Supplement 7:38–133.

Janensch, W. 1929b. Material und Formengehalt der Sauropoden in der Ausbeute der Tendaguru-Expedition. Palaeontographica-Supplementbände 1–34.

Janensch, W. 1935. Die Schädel der Sauropoden *Brachiosaurus*, *Barosaurus* und *Dicraeosaurus* aus den Tendaguruschichten Deutsch-Ostafrikas. Palaeontographica Supplement 7:145–298.

Janensch, W. 1950. Die Wirbelsäule von *Brachiosaurus brancai*. Palaeontographica Supplement 7:27–93.

Janensch, W. 1961. Die Gliedmassen und Gliedmassengürtel der Sauropoden der Tendaguru-Schichten. Palaeontographica-Supplementbände 177–235.

Jensen, J. A. 1985. Three new sauropod dinosaurs from the Upper Jurassic of Colorado. Western North American Naturalist 45:697–709.

Jensen, J. A. 1987. New brachiosaur material from the Late Jurassic of Utah and Colorado. Western North American Naturalist 47:592–608.

Jensen, J. A. 1988. A fourth new sauropod dinosaur from the Upper Jurassic pf the Colorado Plateau and sauropod bipedalism. Western North American Naturalist 48:121–145.

Klein, N., and M. Sander. 2008. Ontogenetic stages in the long bone histology of sauropod dinosaurs. Paleobiology 34:247-263.

Klein, N., A. Christian, and P. M. Sander. 2012. Histology shows that elongated neck ribs in sauropod dinosaurs are ossified tendons. Biology Letters 8:1032–1035.

Knoll, F., L. M. Witmer, F. Ortega, R. C. Ridgely, and D. Schwarz-Wings. 2012. The braincase of the basal sauropod dinosaur *Spinophorosaurus* and 3D reconstructions of the cranial endocast and inner ear. PLoS ONE 7:e30060.

Kowallis, B. J., E. H. Christiansen, A. L. Deino, F. Peterson, C. E. Turner, M. J. Kunk, and J. D. Obradovich. 1998. The age of the Morrison Formation. Modern Geology 22:235–260.

Ksepka, D. T., and M. A. Norell. 2006. *Erketu ellisoni*, a long-necked sauropod from Bor Guvé (Dornogov Aimag, Mongolia). American Museum Novitates 3508:1–16.

8386   Lapparent, A. F. de, and G. Zbyszewski. 1957. Les dinosauriens du Portugal. Memoires Des
8387   Services Géologiques Du Portugal 2:1–63.

8388   Lovelace, D. M., S. A. Hartman, and W. R. Wahl. 2007. Morphology of a specimen of
8389   *Supersaurus* (Dinosauria, Sauropoda) from the Morrison Formation of Wyoming, and a
8390   re-evaluation of diplodocid phylogeny. Arquivos Do Museu Nacional 65:527–544.

8391   Lucas, S. G., J. A. Spielman, L. A. Rinehart, A. B. Heckert, M. C. Herne, A. P. Hunt, J. R.
8392   Foster, and R. M. Sullivan. 2006. Taxonomic status of *Seismosaurus hallorum*, a Late
8393   Jurassic sauropod dinosaur from New Mexico. New Mexico Museum of Natural History
8394   and Science Bulletin 36:149–162.

8395   Lull, R. S. 1919. The sauropodous dinosaur *Barosaurus* Marsh. Memoirs of the Connecticut
8396   Academy of Arts and Sciences 6:1–42.

8397   Madsen, J. H., J. S. McIntosh, and D. S. Berman. 1995. Skull and atlas-axis complex of the
8398   Upper Jurassic sauropod *Camarasaurus* Cope (Reptilia: Saurischia). Bulletin of
8399   Carnegie Museum of Natural History 31:1–115.

8400   Mannion, P. D. 2009. A rebbachisaurid sauropod from the Lower Cretaceous of the Isle of
8401   Wight, England. Cretaceous Research 30:521–526.

8402   Mannion, P. D. 2010. Environmental and geological controls on the diversity and distribution
8403   of the sauropodomorpha. Ph.D. Dissertation, University College London, London, 349
8404   pp.

8405   Mannion, P. D. 2011. A reassessment of *Mongolosaurus haplodon* Gilmore, 1933, a
8406   titanosaurian sauropod dinosaur from the Early Cretaceous of Inner Mongolia, People's
8407   Republic of China. Journal of Systematic Palaeontology 9:355–378.

8408   Mannion, P. D., and J. O. Calvo. 2011. Anatomy of the basal titanosaur (Dinosauria,
8409   Sauropoda) *Andesaurus delgadoi* from the mid-Cretaceous (Albian–early Cenomanian)
8410   Río Limay Formation, Neuquén Province, Argentina: implications for titanosaur
8411   systematics. Zoological Journal of the Linnean Society.

8412   Mannion, P. D., P. Upchurch, O. Mateus, R. N. Barnes, and M. E. H. Jones. 2012. New
8413   information on the anatomy and systematic position of *Dinheirosaurus lourinhanensis*
8414   (Sauropoda: Diplodocoidea) from the Late Jurassic of Portugal, with a review of
8415   European diplodocoids. Journal of Systematic Palaeontology 10:521–551.

8416   Mannion, P. D., P. Upchurch, R. N. Barnes, and O. Mateus. 2013. Osteology of the Late
8417   Jurassic Portuguese sauropod dinosaur *Lusotitan atalaiensis* (Macronaria) and the

evolutionary history of basal titanosauriforms. Zoological Journal of the Linnean Society 168:98–206.

Marsh, O. C. 1877a. Notice of some new dinosaurian reptiles from the Jurassic Formation. American Journal of Science (series 3) 14:514–516.

Marsh, O. C. 1877b. A new order of extinct Reptilia (Stegosauria) from the Jurassic of the Rocky Mountains. American Journal of Science, 3rd Series 14:34–35.

Marsh, O. C. 1878. Principal characters of American Jurassic dinosaurs, Part I. American Journal of Science (series 3) 16:411–416.

Marsh, O. C. 1879. Notice of new Jurassic reptiles. American Journal of Science (series 3) 18:510–505.

Marsh, O. 1880. The sternum in dinosaurian reptiles. American Journal of Science (Series 3) 19:395–396.

Marsh, O. C. 1881. Principle characters of American Jurassic dinosaurs. Part V. American Journal of Science (Series 3) 21:417–437.

Marsh, O. C. 1883. Principal characters of American Jurassic dinosaurs. Restoration of *Brontosaurus*. Geological Magazine (Decade II) 10:385–388.

Marsh, O. C. 1884. Principal characters of American Jurassic dinosaurs. Part VII. On the Diplodocidae, a new family of the Sauropoda. American Journal of Science (series 3) 27:160–168.

Marsh, O. C. 1890. Description of new dinosaurian reptiles. American Journal of Science (series 3) 39:81–86.

Marsh, O. C. 1895. On the affinities and classification of the dinosaurian reptiles. American Journal of Science 483–498.

Marsh, O. C. 1896. The dinosaurs of North America. US Geological Survey Annual Report 16:142–230.

Marsh, O. C. 1898. On the families of sauropodous Dinosauria. American Journal of Science 6:487–488.

Marsh, O. C. 1899. Footprints of Jurassic dinosaurs. American Journal of Science s4-7:227–232.

Mateus, O. 2005. Dinossauros do Jurássico Superior de Portugal, com destaque para os saurísquios. Ph.D. dissertation, Universidade Nova de Lisboa, Lisboa 381 pp.

Mateus, O. and E. Tschopp. 2013. *Cathetosaurus* as a valid sauropod genus and comparisons

8450   with *Camarasaurus*. Journal of Vertebrate Paleontology, Programs and Abstracts: 173.

8451 Mateus, O., L. L. Jacobs, A. S. Schulp, M. J. Polcyn, T. S. Tavares, A. Buta Neto, M. L.

8452   Morais, and M. T. Antunes. 2011. *Angolatitan adamastor*, a new sauropod dinosaur and

8453   the first record from Angola. Anais Da Academia Brasileira de Ciências 83:221–233.

8454 Matthew, W. D. 1905. The mounted skeleton of *Brontosaurus*. American Museum Journal

8455   5:63–71.

8456 McIntosh, J. S. 1981. Annotated catalogue of the dinosaurs (Reptilia, Archosauria) in the

8457   collections of Carnegie Museum of Natural History. Bulletin of Carnegie Museum of

8458   Natural History 18:1–67.

8459 McIntosh, J. S. 1989. The sauropod dinosaurs: a brief survey; pp. 85–99 in K. Padian and D.

8460   J. Chure (eds.), The Age of Dinosaurs., Short Courses in Paleontology Paleontological

8461   Society, Saint-Louis.

8462 McIntosh, J. S. 1990a. Species determination in sauropod dinosaurs with tentative suggestions

8463   for their classification; pp. 53–69 in K. Carpenter and P. J. Currie (eds.), Dinosaur

8464   Systematics: Perspectives and Approaches. Cambridge University Press, New York.

8465 McIntosh, J. S. 1990b. Sauropoda; pp. 345–401 in D. B. Weishampel, P. Dodson, and H.

8466   Osmólska (eds.), The Dinosauria. University of California Press, Berkeley, CA.

8467 McIntosh, J. S. 1995. Remarks on the North American sauropod *Apatosaurus* Marsh. Short

8468   Papers 119–123.

8469 McIntosh, J. S. 1997. The saga of a forgotten sauropod dinosaur. Dinofest International

8470   Proceedings 7–12.

8471 McIntosh, J. S. 2005. The genus *Barosaurus* Marsh (Sauropoda, Diplodocidae); pp. 38–77 in

8472   V. Tidwell and K. Carpenter (eds.), Thunder-lizards: the Sauropodomorph dinosaurs.

8473   Indiana University Press, Bloomington.

8474 McIntosh, J. S., and D. S. Berman. 1975. Description of the palate and lower jaw of the

8475   sauropod dinosaur *Diplodocus* (Reptilia: Saurischia) with remarks on the nature of the

8476   skull of *Apatosaurus*. Journal of Paleontology 49:187–199.

8477 McIntosh, J. S., and K. Carpenter. 1998. The holotype of *Diplodocus longus*, with comments

8478   on other specimens of the genus. Modern Geology 23:85–110.

8479 McIntosh, J. S., C. A. Miles, K. A. Cloward, and J. R. Parker. 1996a. A new nearly complete

8480   skeleton of *Camarasaurus*. Bulletin of the Gunma Museum of Natural History 1:1–87.

8481 McIntosh, J. S., W. E. Miller, K. L. Stadtman, and D. D. Gillette. 1996b. The osteology of

Camarasaurus lewisi (Jensen, 1988). Brigham Young University Geology Studies 41:73–116.

McIntosh, J. S., W. P. Coombs, and D. A. Russell. 1992. A new diplodocid sauropod (Dinosauria) from Wyoming, USA. Journal of Vertebrate Paleontology 12:158–167.

Michelis, I. 2004. Taphonomie des Howe Quarry's (Morrison-Formation, Oberer Jura), Bighorn County, Wyoming, USA. Ph.D. dissertation, Institute of Palaeontology, University of Bonn, Bonn, Germany, 41 pp.

Mocho, P., R. Royo-Torres, and F. Ortega. 2014. Phylogenetic reassessment of *Lourinhasaurus alenquerensis*, a basal Macronaria (Sauropoda) from the Upper Jurassic of Portugal. Zoological Journal of the Linnean Society.

Mook, C. C. 1917. Criteria for the determination of species in the Sauropoda, with description of a new species of *Apatosaurus*. Bulletin of the American Museum of Natural History 37:355–358.

Mossbrucker, M. T., and R. T. Bakker. 2013. Missing muzzle found: new skull material referrable to *Apatosaurus ajax* (Marsh 1877) from the Morrison Formation of Morrison, Colorado. Geological Society of America Abstracts with Programs 45:111.

Nair, J. P., and S. W. Salisbury. 2012. New anatomical information on *Rhoetosaurus brownei* Longman, 1926, a gravisaurian sauropodomorph dinosaur from the Middle Jurassic of Queensland, Australia. Journal of Vertebrate Paleontology 32:369–394.

Nieuwland, I. 2010. The colossal stranger. Andrew Carnegie and *Diplodocus* intrude European culture, 1904–1912. Endeavour 34:61–68.

Nopcsa, F. B. 1902. Notizen über die Cretacischen Dinosaurier. Pt. 3. Wirbel eines südamerikanischen Sauropoden. Sitzungsberichte der Berliner Akademie der Wissenschaften 3:108–114.

Olshevsky, G. 1991. A revision of the parainfraclass Archosauria Cope, 1869, excluding the advanced Crocodylia. Mesozoic Meanderings 2:1–196.

Osborn, H. F. 1898. Additional characters of the great herbivorous dinosaur *Camarasaurus*. Bulletin of the American Museum of Natural History 10:219–233.

Osborn, H. F. 1899. A skeleton of *Diplodocus*. Memoirs of the American Museum of Natural History 5:191–214.

Osborn, H. F. 1904. Manus, sacrum, and caudals of Sauropoda. Bulletin of the American Museum of Natural History 20:181–190.

Osborn, H. F., and C. C. Mook. 1921. *Camarasaurus*, *Amphicoelias*, and other sauropods of Cope. Memoirs of the American Museum of Natural History, New Series 3:249–387.

Ostrom, J. O., and J. S. McIntosh. 1966. Marsh's Dinosaurs: The Collection from Como Bluff. Vol. 1. Yale University Press, New Haven, 388 pp.

Ouyang, H., and Y. Ye. 2002. The First Mamenchisaurian Skeleton with Complete Skull, *Mamenchisaurus youngi*. Sichuan Publishing House of Science and Technology, Chengdu, China, 138 pp.

Owen, R. 1842. Report on British Fossil Reptiles Pt. II. Report of the British Association for the Advancement of Science 1841:60–204.

Paul, G. S. 1988. The brachiosaur giants of the Morrison and Tendaguru with a description of a new subgenus, *Giraffatitan*, and a comparison of the world's largest dinosaurs. Hunteria 2 (3):1–14.

Pereda Suberbiola, X., F. Torcida, L. A. Izquierdo, P. Huerta, D. Montero, and G. Pérez. 2003. First rebbachisaurid dinosaur (Sauropoda, Diplodocoidea) from the early Cretaceous of Spain: paleobiogeographical implications. Bulletin de La Societe Geologique de France 174:471–479.

Peterson, O. A., and C. W. Gilmore. 1902. *Elosaurus parvus*; a new genus and species of the Sauropoda. Annals of the Carnegie Museum 1:490–499.

Platt, B. F., and S. T. Hasiotis. 2006. Newly discovered sauropod dinosaur tracks with skin and foot-pad impressions from the Upper Jurassic Morrison Formation, Bighorn Basin, Wyoming, U.S.A. PALAIOS 21:249–261.

Raath, M. A., and J. S. McIntosh. 1987. Sauropod dinosaurs from the central Zambezi Valley, Zimbabwe, and the age of the Kadzi Formation. South African Journal of Geology 90:107–119.

Rauhut, O. W. M., K. Remes, R. Fechner, G. Cladera, and P. Puerta. 2005. Discovery of a short-necked sauropod dinosaur from the Late Jurassic period of Patagonia. Nature 435:670–672.

Remes, K. 2006. Revision of the Tendaguru sauropod dinosaur *Tornieria africana* (Fraas) and its relevance for sauropod paleobiogeography. Journal of Vertebrate Paleontology 26:651–669.

Remes, K. 2007. A second Gondwanan diplodocid dinosaur from the Upper Jurassic Tendaguru beds of Tanzania, East Africa. Palaeontology 50:653–667.

8546 Remes, K. 2008. Evolution of the pectoral girdle and forelimb in Sauropodomorpha
8547   (Dinosauria, Saurischia). Ph.D. dissertation, Fakultät für Geowissenschaften, LMU
8548   München, München, 355 pp.
8549 Remes, K. 2009. Taxonomy of Late Jurassic diplodocid sauropods from Tendaguru
8550   (Tanzania). Fossil Record 12:23–46.
8551 Remes, K., F. Ortega, I. Fierro, U. Joger, R. Kosma, J. M. M. Ferrer, O. A. Ide, and A. Maga.
8552   2009. A new basal sauropod dinosaur from the Middle Jurassic of Niger and the early
8553   evolution of Sauropoda. PLoS ONE 4:e6924.
8554 Riggs, E. S. 1901. The fore leg and pectoral girdle of *Morosaurus*: with a note on the genus
8555   *Camarosaurus*. Field Columbian Museum, Geological Series 2 275–281.
8556 Riggs, E. S. 1903. Structure and relationships of opisthocoelian dinosaurs: *Apatosaurus*
8557   Marsh. Field Columbian Museum, Geological Series 2 4:165–196.
8558 Riggs, E. S. 1904. Structure and relationships of opisthocoelian dinosaurs: the
8559   Brachiosauridae. Field Columbian Museum, Geological Series 2 2:229–247.
8560 Royo-Torres, R., A. Cobos, L. Lurque, A. Aberasturi, E. Espílez, I. Fierro, A. González, L.
8561   Mampel, and L. Alcalá. 2009. High European sauropod dinosaur diversity during
8562   Jurassic–Cretaceous transition in Riodeva (Teruel, Spain). Palaeontology 52:1009–
8563   1027.
8564 Royo-Torres, R., A. Cobos, and L. Alcalá. 2006. A giant European dinosaur and a new
8565   sauropod clade. Science 314:1925–1927.
8566 Royo-Torres, R., and A. Cobos. 2004. Estudio sistemático de un ilion de Sauropoda del
8567   yacimiento Pino de Jarque 2 en Riodeva (Teruel). Geo-Temas 6:59–62.
8568 Royo-Torres, R., and P. Upchurch. 2012. The cranial anatomy of the sauropod *Turiasaurus*
8569   *riodevensis* and implications for its phylogenetic relationships. Journal of Systematic
8570   Palaeontology 1–31.
8571 Russell, D. A., and Z. Zheng. 1993. A large mamenchisaurid from the Junggar Basin,
8572   Xinjiang, People's Republic of China. Canadian Journal of Earth Sciences 30:2082–
8573   2095.
8574 Russell, D. A., P. Béland, and J. S. McIntosh. 1980. Paleoecology of the dinosaurs of
8575   Tendaguru (Tanzania). Mémoires de La Société Géologique de France 139:169–175.
8576 Salgado, L. 1999. The macroevolution of the Diplodocimorpha (Dinosauria; Sauropoda): a
8577   developmental model. Ameghiniana 36:203–216.

8578   Salgado, L., and J. Calvo. 1992. Cranial osteology of *Amargasurus cazaui* Salgado &
8579   Bonaparte (Sauropoda, Dicraeosuridae) from the Neocomian of Patagonia.
8580   Ameghiniana 29:337–346.

8581   Salgado, L., and J. F. Bonaparte. 1991. Un nuevo saurópodo Dicraeosauridae, *Amargasaurus*
8582   *cazaui* gen. et sp. nov., de la Formación La Amarga, Neocomiano de la provincia del
8583   Neuquén, Argentina. Ameghiniana 28:333–346.

8584   Salgado, L., I. S. Carvalho, and A. C. Garrido. 2006. *Zapalasaurus bonapartei*, un nuevo
8585   dinosaurio saurópodo de la Formación La Amarga (Cretácico Inferior), noroeste de
8586   Patagonia, Provincia de Neuquén, Argentina. Geobios 39:695–707.

8587   Salgado, L., J. I. Canudo, A. C. Garrido, and J. L. Carballido. 2012. Evidence of
8588   gregariousness in rebbachisaurids (Dinosauria, Sauropoda, Diplodocoidea) from the
8589   Early Cretaceous of Neuquén (Rayoso Formation), Patagonia, Argentina. Journal of
8590   Vertebrate Paleontology 32:603–613.

8591   Salgado, L., R. A. Coria, and J. O. Calvo. 1997. Evolution of titanosaurid sauropods:
8592   Phylogenetic analysis based on the postcranial evidence. Ameghiniana 34:3–32.

8593   Sander, P. M., and C. Tückmantel. 2003. Bone lamina thickness, bone apposition rates, and
8594   age estimates in sauropod humeri and femora. Paläontologische Zeitschrift 77:161–172.

8595   Sander, P. M., O. Mateus, T. Laven, and N. Knötschke. 2006. Bone histology indicates
8596   insular dwarfism in a new Late Jurassic sauropod dinosaur. Nature 441:739–741.

8597   Schmitt, A., D. 2012. The inner ear of diplodocoid and basal macronarian sauropods:
8598   vestibular adaptations and paleobiological implications. Master, Rheinische Friedrich-
8599   Wilhelms-Universität, Bonn, Germany, 82 pp.

8600   Schmitt, A., D., E. Tschopp, F. Knoll, and P. M. Sander. 2013. Paleoneuroanatomy and
8601   braincase morphology indicate the presence of at least two diplodocine taxa
8602   (Dinosauria: Sauropoda) at the Howe Ranch (Wyoming, USA). Journal of Vertebrate
8603   Paleontology, Program and Abstracts 206.

8604   Schwarz, D., E. Frey, and C. A. Meyer. 2007a. Novel reconstruction of the orientation of the
8605   pectoral girdle in sauropods. The Anatomical Record: Advances in Integrative Anatomy
8606   and Evolutionary Biology 290:32–47.

8607   Schwarz, D., E. Frey, and C. A. Meyer. 2007b. Pneumaticity and soft-tissue reconstructions in
8608   the neck of diplodocid and dicraeosaurid sauropods. Acta Palaeontologica Polonica
8609   52:167–188.

Schwarz, D., T. Ikejiri, B. H. Breithaupt, P. M. Sander, and N. Klein. 2007c. A nearly complete skeleton of an early juvenile diplodocid (Dinosauria: Sauropoda) from the Lower Morrison Formation (Late Jurassic) of north central Wyoming and its implications for early ontogeny and pneumaticity in sauropods. Historical Biology 19:225–253.

Schwarz-Wings, D. 2009. Reconstruction of the thoracic epaxial musculature of diplodocid and dicraeosaurid sauropods. Journal of Vertebrate Paleontology 29:517–534.

Schwarz-Wings, D., and N. Böhm. 2012. A morphometric approach to the specific separation of the humeri and femora of *Dicraeosaurus* from the Late Jurassic of Tendaguru,Tanzania. Acta Palaeontologica Polonica.

Sereno, P. C. 1998. A rationale for phylogenetic definitions, with application to the higher-level taxonomy of Dinosauria. Neues Jahrbuch Für Geologie Und Paläontologie Abhandlungen 210:41–83.

Sereno, P. C., A. L. Beck, D. B. Dutheil, H. C. . Larsson, G. H. Lyon, B. Moussa, R. W. Sadleir, C. A. Sidor, D. J. Varricchio, and G. P. Wilson. 1999. Cretaceous sauropods from the Sahara and the uneven rate of skeletal evolution among dinosaurs. Science 286:1342–1347.

Sereno, P. C., and J. A. Wilson. 2005. Structure and evolution of a sauropod tooth battery; pp. 157–177 in K. Curry Rogers and J. A. Wilson (eds.), The Sauropods: Evolution and Paleobiology. University of California Press, Berkeley, CA.

Sereno, P. C., J. A. Wilson, L. M. Witmer, J. A. Whitlock, A. Maga, O. Ide, and T. A. Rowe. 2007. Structural extremes in a Cretaceous dinosaur. PLoS ONE 2:e1230.

Siber, H. J., and U. Möckli. 2009. The Stegosaurs of the Sauriermuseum Aathal. Sauriermuseum Aathal, Aathal, 56 pp.

Sternfeld, R. 1911. Zur Nomenklatur der Gattung *Gigantosaurus* Fraas. Sitzungsberichte Der Gesellschaft Naturforschender Freunde Zu Berlin 8:398.

Swierc, J. E., and G. D. Johnson. 1996. A local chronostratigraphy for the Morrison Formation, Northeastern Bighorn Basin, Wyoming. Wyoming Geological Association, 47th Annual Field Conference Guidebook 47:315–327.

Taylor, M. P. 2009. A re-evaluation of *Brachiosaurus altithorax* Riggs 1903 (Dinosauria, Sauropoda) and its generic separation from *Giraffatitan brancai* (Janensch 1914). Journal of Vertebrate Paleontology 29:787–806.

8642 Taylor, M. P. 2010. Sauropod dinosaur research: a historical review. Geological Society,

8643   London, Special Publications 343:361.

8644 Taylor, M. P., and D. Naish. 2005. The phylogenetic taxonomy of Diplodocoidea (Dinosauria:

8645   Sauropoda). PaleoBios 25:1–7.

8646 Taylor, M. P., and M. J. Wedel. 2013. Why sauropods had long necks; and why giraffes have

8647   short necks. PeerJ 1:e36.

8648 Taylor, M. P., M. J. Wedel, and R. L. Cifelli. 2011. A new sauropod dinosaur from the Lower

8649   Cretaceous Cedar Mountain Formation, Utah, USA. Acta Palaeontologica Polonica

8650   56:75–98.

8651 Tidwell, V., K. L. Stadtman, and A. Shaw. 2005. Age-related characteristics found in a partial

8652   pelvis of *Camarasaurus*; pp. 180–186 in V. Tidwell and K. Carpenter (eds.), Thunder-

8653   Lizards: The Sauropodomorph Dinosaurs. Indiana University Press, Bloomington.

8654 Torcida Fernández-Baldor, F., J. I. Canudo, P. Huerta, D. Montero, and X. Pereda Suberbiola.

8655   2011. *Demandasaurus darwini*, a new rebbachisaurid sauropod from the Early

8656   Cretaceous of the Iberian Peninsula. Acta Palaeontologica Polonica 56:535–552.

8657 Trujillo, K. C. 2006. Clay mineralogy of the Morrison Formation (Upper Jurassic-? Lower

8658   Cretaceous), and its use in long distance correlation and paleoenvironmental analysis.

8659   New Mexico Museum of Natural History and Science Bulletin 36:17–23.

8660 Trujillo, K., D. Demar, J. Foster, and S. A. Bilbey. 2011. An exceptionally large juvenile

8661   *Camarasaurus* from the Morrison Formation (Upper Jurassic) of Albany County, WY,

8662   USA. Journal of Vertebrate Paleontology, Program and Abstracts Suppl. 2:205.

8663 Tschopp, E. 2008. The complete set of autopodia of the *Camarasaurus* SMA 0002 and what it

8664   can tell about systematics, taphonomy, ontogeny, and footprint shape. Master Thesis,

8665   Paläontologisches Institut und Museum, Zürich, 185 pp.

8666 Tschopp, E., and G. Dzemski. 2012. 3-dimensional reproduction techniques to preserve and

8667   spread paleontological material – a case study with a diplodocid sauropod neck. Journal

8668   of Paleontological Techniques 10:1–8.

8669 Tschopp, E., and O. Mateus. 2012. A sternal plate of a large-sized sauropod dinosaur from the

8670   Late Jurassic of Portugal. ¡Fundamental! 20:263–266.

8671 Tschopp, E., and O. Mateus. 2013a. Clavicles, interclavicles, gastralia, and sternal ribs in

8672   sauropod dinosaurs: new reports from Diplodocidae and their morphological, functional

8673   and evolutionary implications. Journal of Anatomy 222:321–340.

8674 Tschopp, E., and O. Mateus. 2013b. The skull and neck of a new flagellicaudatan sauropod
8675   from the Morrison Formation and its implication for the evolution and ontogeny of
8676   diplodocid dinosaurs. Journal of Systematic Palaeontology 11:853–888.

8677 Tschopp, E., J. Russo, and G. Dzemski. 2013. Retrodeformation as a test for the validity of
8678   phylogenetic characters: an example from diplodocid sauropod vertebrae.
8679   Palaeontologia Electronica 16:1–23.

8680 Turner, C. E., and F. Peterson. 1999. Biostratigraphy of dinosaurs in the Upper Jurassic
8681   Morrison Formation of the Western Interior, USA; pp. 77–114 in Vertebrate
8682   Paleontology in Utah., Utah Geological Survey Miscellaneous Publication Salt Lake
8683   City.

8684 Upchurch, P. 1995. The evolutionary history of sauropod dinosaurs. Philosophical
8685   Transactions of the Royal Society of London. Series B: Biological Sciences 349:365.

8686 Upchurch, P. 1998. The phylogenetic relationships of sauropod dinosaurs. Zoological Journal
8687   of the Linnean Society 124:43–103.

8688 Upchurch, P. 1999. The phylogenetic relationships of the Nemegtosauridae (Saurischia,
8689   Sauropoda). Journal of Vertebrate Paleontology 19:106–125.

8690 Upchurch, P. 2009. The sauropodomorph supermatrix: towards a global phylogeny of the
8691   largest terrestrial animals. Journal of Vertebrate Paleontology Suppl 1:194A.

8692 Upchurch, P., and J. Martin. 2002. The Rutland *Cetiosaurus*: the anatomy and relationships of
8693   a Middle Jurassic British sauropod dinosaur. Palaeontology 45:1049–1074.

8694 Upchurch, P., and P. D. Mannion. 2009. The first diplodocid from Asia and its implications
8695   for the evolutionary history of sauropod dinosaurs. Palaeontology 52:1195–1207.

8696 Upchurch, P., and P. M. Barrett. 2000. The evolution of sauropod feeding mechanisms; pp.
8697   79–122 in Evolution of herbivory in terrestrial vertebrates: perspectives from the fossil
8698   record., Cambridge University Press. Sues, H.-D., Cambridge.

8699 Upchurch, P., P. M. Barrett, and P. Dodson. 2004a. Sauropoda; pp. 259–322 in D. B.
8700   Weishampel, P. Dodson, and H. Osmólska (eds.), The Dinosauria. Second edition.
8701   University of California Press, Berkeley, CA.

8702 Upchurch, P., P. M. Barrett, and P. M. Galton. 2007. A phylogenetic analysis of basal
8703   sauropodomorph relationships: implications for the origin of sauropod dinosaurs.
8704   Evolution and Palaeobiology of Early Sauropodomorph Dinosaurs 57–90.

8705 Upchurch, P., Y. Tomida, and P. M. Barrett. 2004b. A new specimen of *Apatosaurus ajax*

8706   (Sauropoda: Diplodocidae) from the Morrison Formation (Upper Jurassic) of Wyoming,

8707   USA. National Science Museum Monographs 26:1–118.

8708 Varricchio, D. J. 1997. Growth and embryology; pp. 282–288 in Encyclopedia of Dinosaurs.

8709   Academic Press, London.

8710 Wedel, M. J. 2003. The evolution of vertebral pneumaticity in sauropod dinosaurs. Journal of

8711   Vertebrate Paleontology 23:344–357.

8712 Wedel, M. J. 2009. Another mystery: embossed laminae and "unfossae." Sauropod Vertebra

8713   Picture of the Week. http://svpow.com/2009/12/07/another-mystery-embossed-laminae-

8714   and-unfossae/

8715 Wedel, M. J., and M. P. Taylor. 2013. Neural spine bifurcation in sauropod dinosaurs of the

8716   Morrison Formation: ontogenetic and phylogenetic implications. PalArch's Journal of

8717   Vertebrate Palaeontology 10:1–34.

8718 Wedel, M. J., and R. K. Sanders. 2002. Osteological correlates of cervical musculature in

8719   Aves and Sauropoda (Dinosauria: Saurischia), with comments on the cervical ribs of

8720   *Apatosaurus*. PaleoBios 22:1–12.

8721 Wedel, M. J., R. L. Cifelli, and R. K. Sanders. 2000. Osteology, paleobiology, and

8722   relationships of the sauropod dinosaur Sauroposeidon. Acta Palaeontologica Polonica

8723   45:343–388.

8724 Wellik, D. M., and M. R. Capecchi. 2003. Hox10 and Hox11 genes are required to globally

8725   pattern the mammalian skeleton. Science 301:363–367.

8726 Whitlock, J. A. 2011a. A phylogenetic analysis of Diplodocoidea (Saurischia: Sauropoda).

8727   Zoological Journal of the Linnean Society 161:872–915.

8728 Whitlock, J. A. 2011b. Inferences of diplodocoid (Sauropoda: Dinosauria) feeding behavior

8729   from snout shape and microwear analyses. PLoS ONE 6:e18304.

8730 Whitlock, J. A. 2011c. Re-evaluation of *Australodocus bohetii*, a putative diplodocoid sauro-

8731   pod from the Tendaguru Formation of Tanzania, with comment on Late Jurassic sauro-

8732   pod faunal diversity and palaeoecology. Palaeogeography, Palaeoclimatology, Palaeoe-

8733   cology 309:333–341.

8734 Whitlock, J. A., and J. D. Harris. 2010. The dentary of *Suuwassea emilieae* (Sauropoda:

8735   Diplodocoidea). Journal of Vertebrate Paleontology 30:1637–1641.

8736 Whitlock, J. A., and M. C. Lamanna. 2012. A reanalysis of CM 11162, a skull of *Apatosaurus*

8737   (Sauropoda: Diplodocidae). Journal of Vertebrate Paleontology Program and

8738   Abstracts:192.

8739   Whitlock, J. A., J. A. Wilson, and M. C. Lamanna. 2010. Description of a nearly complete
8740   juvenile skull of *Diplodocus* (Sauropoda: Diplodocoidea) from the Late Jurassic of
8741   North America. Journal of Vertebrate Paleontology 30:442–457.

8742   Whitlock, J. A., M. D. D'Emic, and J. A. Wilson. 2011. Cretaceous diplodocids in Asia? Re-
8743   evaluating the phylogenetic affinities of a fragmentary specimen. Palaeontology
8744   54:351–364.

8745   Wiersma, K. 2013. Morphology and function of the dentition of *Camarasaurus*. Bachelor
8746   Thesis, Universität Bonn, Bonn, Germany, 66 pp.

8747   Wilhite, D. R. 2003. Biomechanical reconstruction of the appendicular skeleton in three North
8748   American Jurassic sauropods. Ph.D. dissertation, Graduate Faculty of the Louisiana
8749   State University and Agricultural and Mechanical College 232 pp.

8750   Wilhite, D. R. 2005. Variation in the appendicular skeleton of North American sauropod
8751   dinosaurs: taxonomic implications; pp. 268–301 in V. Tidwell and K. Carpenter (eds.),
8752   Thunder-lizards: the Sauropodomorph dinosaurs. Indiana University Press,
8753   Bloomington.

8754   Wilson, J. A. 1999. A nomenclature for vertebral laminae in sauropods and other saurischian
8755   dinosaurs. Journal of Vertebrate Paleontology 19:639–653.

8756   Wilson, J. A. 2002. Sauropod dinosaur phylogeny: critique and cladistic analysis. Zoological
8757   Journal of the Linnean Society 136:215–275.

8758   Wilson, J. A. 2005. Overview of sauropod phylogeny and evolution; pp. 15–49 in K. A. Curry
8759   Rogers and J. A. Wilson (eds.), The Sauropods: Evolution and Paleobiology. University
8760   of California Press, Berkeley, CA.

8761   Wilson, J. A. 2012. New vertebral laminae and patterns of serial variation in vertebral laminae
8762   of sauropod dinosaurs. Contributions from the Museum of Paleontology, University of
8763   Michigan 32:91–110.

8764   Wilson, J. A., and M. B. Smith. 1996. New remains of *Amphicoelias* Cope (Dinosauria:
8765   Sauropoda) from the Upper Jurassic of Montana and diplodocoid phylogeny. Journal of
8766   Vertebrate Paleontology 16:73A.

8767   Wilson, J. A., and M. T. Carrano. 1999. Titanosaurs and the origin of "wide-gauge"
8768   trackways: a biomechanical and systematic perspective on sauropod locomotion.
8769   Paleobiology 25:252–267.

8770 Wilson, J. A., and P. C. Sereno. 1998. Early evolution and higher-level phylogeny of
8771   sauropod dinosaurs. Journal of Vertebrate Paleontology 18:1–79.

8772 Wilson, J. A., and P. Upchurch. 2003. A revision of *Titanosaurus* Lydekker (Dinosauria-
8773   Sauropoda), the first dinosaur genus with a "Gondwanan"distribution. Journal of
8774   Systematic Palaeontology 1:125–160.

8775 Wilson, J. A., and P. Upchurch. 2009. Redescription and reassessment of the phylogenetic
8776   affinities of *Euhelopus zdanskyi* (Dinosauria: Sauropoda) from the Early Cretaceous of
8777   China. Journal of Systematic Palaeontology 7:199–239.

8778 Wilson, J. A., R. N. Martinez, and O. Alcober. 1999. Distal tail segment of a titanosaur
8779   (Dinosauria: Sauropoda) from the Upper Cretaceous of Mendoza, Argentina. Journal of
8780   Vertebrate Paleontology 19:591–594.

8781 Wilson, J. A., M. D. D'Emic, T. Ikejiri, E. M. Moacdieh, and J. A. Whitlock. 2011. A
8782   nomenclature for vertebral fossae in sauropods and other saurischian dinosaurs. PLoS
8783   ONE 6:e17114.

8784 Witmer, L. M., R. C. Ridgely, D. L. Dufeau, and M. C. Semones. 2008. Using CT to Peer into
8785   the Past: 3D Visualization of the Brain and Ear Regions of Birds, Crocodiles, and
8786   Nonavian Dinosaurs; pp. 67–87 in H. Endo and R. Frey (eds.), Anatomical Imaging.
8787   Springer Japan, Tokyo.

8788 Woodruff, D. C., and D. W. Fowler. 2012. Ontogenetic influence on neural spine bifurcation
8789   in Diplodocoidea (Dinosauria: Sauropoda): a critical phylogenetic character. Journal of
8790   Morphology 273:754–764.

8791 Woodward, A. S. 1905. On parts of the skeleton of *Cetiosaurus leedsi*, a sauropodous
8792   dinosaur from the Oxford Clay of Peterborough. Proceedings of the Zoological Society
8793   of London 1:232–243.

8794 Young, C.-C. 1939. On a new sauropoda, with notes on other fragmentary reptiles from
8795   Szechuan. Bulletin of the Geological Society of China 19:279–315.

8796 Young, C.-C. 1958. New sauropods from China. Vertebrata PalAsiatica 2:1–28.

8797 Young, C.-C., and X. Zhao. 1972. Description of the type material of *Mamenchisaurus*
8798   *hochuanensis*. Institute of Vertebrate Paleontology and Paleoanthropology Monograph
8799   Series I 8:1–30.

8800 Young, M. T., E. J. Rayfield, C. M. Holliday, L. M. Witmer, D. J. Button, P. Upchurch, and
8801   P. M. Barrett. 2012. Cranial biomechanics of *Diplodocus* (Dinosauria, Sauropoda):

8802   testing hypotheses of feeding behaviour in an extinct megaherbivore.

8803   Naturwissenschaften 1–7.

8804 Yu, C. 1993. The skull of *Diplodocus* and the phylogeny of the Diplodocidae. Ph.D.

8805   dissertation, Faculty of the Division of Biological Sciences and the Pritzker School of

8806   Medicine, University of Chicago, Chicago, 154 pp.

8807 Zaher, H., D. Pol, A. B. Carvalho, P. M. Nascimento, C. Riccomini, P. Larson, R. Juarez-

8808   Valieri, R. Pires-Domingues, N. J. da Silva, and C. D. de Almeida. 2011. A complete

8809   skull of an Early Cretaceous sauropod and the evolution of advanced titanosaurians.

8810   PLoS ONE 6:e16663.

8811 Zhang, Y. 1988. The Middle Jurassic Dinosaur Fauna from Dashanpu, Zigong, Sichuan, Vol.

8812   1: Sauropod Dinosaur (I): *Shunosaurus*. Sichuan Publishing House of Science and

8813   Technology, Chengdu, China, 114 pp.

8814 Zheng, Z. 1996. Cranial anatomy of *Shunosaurus* and *Camarasaurus* (Dinosauria:

8815   Sauropoda) and the phylogeny of the Sauropoda. Ph. D. dissertation, Texas Tech

8816   University, Lubbock, TX, USA, 208 pp.